Control Methods for Energy Management of Refrigeration Systems

Shafiei, Seyed Ehsan

Publication date:
2015

Document Version
Publisher's PDF, also known as Version of record

Seyed Ehsan Shafiei

Control Methods for Energy Management of Refrigeration Systems

AALBORG UNIVERSITY
DENMARK

Control Methods for Energy Management of Refrigeration Systems
PhD thesis

ISBN: 978-87-7152-061-3
March 2015

Title:
Control Methods for Energy Management of Refrigeration Systems

Author:
Seyed Ehsan Shafiei

Supervisors:
Professor Jakob Stoustrup (2012 and 2013)
External Lecturer Henrik Rasmussen (2013 and 2014)
Professor Rafael Wisniewski (2014)
Associate Professor Palle Andersen (2014)
Lead Expert, PhD, Roozbeh Izadi-Zamanabadi (2012-2014)

List of Publications:
Enclosed journal papers

- Seyed Ehsan Shafiei, Henrik Rasmussen and Jakob Stoustrup, "Modeling Supermarket Refrigeration Systems for Demand-Side Management," *Energies, Special issue: Smart grid and the future electrical network*, 6(2), pp. 900-920, 2013.

- Seyed Ehsan Shafiei, Torben Knudsen, Rafael Wisniewski and Palle Andersen, "Data-Driven Predictive Direct Load Control of Refrigeration Systems," *IET Control Theory & Applications, Special issue: Data-based control and process monitoring with industrial applications*, DOI: 10.1049/iet-cta.2014.0666, Online ISSN 1751-8652, Available online: 23 March 2015.

- Seyed Ehsan Shafiei and Andrew Alleyne, "Model Predictive Control of Hybrid Thermal Energy Systems in Transport Refrigeration," *Applied Thermal Engineering*, vol. 82, pp. 264-280, 2015.

Enclosed conference papers

- Seyed Ehsan Shafiei, Jakob Stoustrup and Henrik Rasmussen, "A Supervisory Control Approach in Economic MPC Design for Refrigeration Systems," *Proceedings of the European Control Conference*, Zurich, Switzerland, July, 2013.

- Seyed Ehsan Shafiei, Henrik Rasmussen and Jakob Stoustrup, "Model Predictive Control for a Thermostatic Controlled System," *Proceedings of the European Control Conference*, Zurich, Switzerland, July 2013.

- Seyed Ehsan Shafiei, Roozbeh Izadi-Zamanabadi, Henrik Rasmussen and Jakob Stoustrup, "A Decentralized Control Method for Direct Smart Grid Control of Refrigeration Systems," *Proceedings of the 52nd IEEE Conference on Decision and Control*, Firenze, Italy, December 2013.

- Seyed Ehsan Shafiei, Jakob Stoustrup and Henrik Rasmussen, "Model Predictive Control for Flexible Power Consumption of Large-Scale Refrigeration Systems," *Proceedings of the American Control Conference*, Portland, OR, USA, June, 2014.

Additional conference papers, not enclosed

- Rasmus Pedersen, John Schwensen, Senthuran Sivabalan, Chiara Corazzol, Seyed Ehsan Shafiei, Kasper Vinther and jakob Stoustrup, "Direct Control Implementation of a Refrigeration System in Smart Grid," *Proceedings of the American Control Conference*, Washington, DC, USA, June, 2013.

- Seyed Ehsan Shafiei, Henrik Rasmussen and J. Stoustrup, "Modeling Supermarket Refrigeration Systems for Supervisory Control in Smart Grid," *Proceedings of the American Control Conference*, Washington, DC, USA, June, 2013.

- Morten Juelsgaard, Luminita C. Totu, Seyed Ehsan Shafiei, Rafael Wisniewski and Jakob Stoustrup, "Control Structures for Smart Grid Balancing," *Proceedings of the 4th European Innovative Smart Grid Technologies* (IEEE PES ISGT), Copenhagen, Denmark, October, 2013.

- Harm H. M. Weerts, Seyed Ehsan Shafiei, Jakob Stoustrup and Roozbeh Izadi-Zamanabadi, "Model-Based Predictive Control Scheme for Cost Optimization and Balancing Services for Supermarket Refrigeration Systems," *Proceedings of the 19th IFAC World Congress*, Cape Town, South Africa, August, 2014.

- Samira Rahnama, Seyed Ehsan Shafiei, Jakob Stoustrup, Henrik Rasmussen and Jan D. Bendtsen, "Evaluation of Aggregators for Integration of Large-scale Consumers in Smart Grid," *Proceedings of the 19th IFAC World Congress*, Cape Town, South Africa, August, 2014.

Patent Applications, not enclosed

- Seyed Ehsan Shafiei, Roozbeh Izadi-Zamanabadi, Henrik Rasmussen and Jakob Stoustrup, "A Method for Controlling a Vapor Compression Cycle System Connected to a Smart Grid," *Submitted patent application*.

- Seyed Ehsan Shafiei and Roozbeh Izadi-Zamanabadi, "A Method for Estimating of Thermal Capacity of Food in Display Cases/Freezers," *Submitted patent application*.

This thesis has been submitted for assessment in partial fulfillment of the PhD degree. The thesis is based on the submitted or published scientific papers which are listed above. Parts of the papers are used directly or indirectly in the extended summary of the thesis. As part of the assessment, co-author statements have been made available to the assessment committee and are also available at the Faculty. The thesis is not in its present form acceptable for open publication but only in limited and closed circulation as copyright may not be ensured.

Contents

Contents V

Preface IX

Abstract XI

Synopsis XIII

1 Introduction 1
- 1.1 Motivation . . . 1
- 1.2 State-of-the-Art and Background . . . 5
- 1.3 Research Objectives and Hypotheses . . . 20
- 1.4 Outline of the Thesis . . . 22

2 Summary of Contributions 25
- 2.1 Modeling for Control and Simulations . . . 26
- 2.2 Indirect Load Control . . . 32
- 2.3 Direct Load Control . . . 37
- 2.4 Control of Hybrid Thermal Systems . . . 52

3 Concluding Remarks 65
- 3.1 Conclusions . . . 65
- 3.2 Perspectives . . . 66

References 69

Contributions 81

Paper A: Modeling Supermarket Refrigeration Systems for Demand-Side Management 83
- 1 Introduction . . . 85
- 2 System Description . . . 88
- 3 Modeling . . . 90
- 4 Parameter Estimation . . . 93
- 5 System Integration and Simulation Benchmark . . . 98
- 6 Demand-Side Management . . . 102

7 Conclusions . . . 105
References . . . 105

Paper B: A Supervisory Control Approach in Economic MPC Design for Refrigeration Systems 109
1 Introduction . . . 111
2 Refrigeration System . . . 112
3 Supervisory Control . . . 114
4 Simulation Results . . . 118
5 Discussions . . . 122
6 Conclusions . . . 122
References . . . 123

Paper C: Model Predictive Control for a Thermostatic Controlled System 125
1 Introduction . . . 127
2 Refrigeration System . . . 128
3 Set-Point Control . . . 130
4 Simulation Study . . . 134
5 Conclusions . . . 139
References . . . 139

Paper D: A Decentralized Control Method for Direct Smart Grid Control of Refrigeration Systems 141
1 Introduction . . . 143
2 System Description and Problem Statement . . . 144
3 Design of Control Structure . . . 147
4 Simulation Results . . . 151
5 Discussions . . . 154
6 Conclusion . . . 154
References . . . 155

Paper E: Model Predictive Control for Flexible Power Consumption of Large-Scale Refrigeration Systems 157
1 Introduction . . . 159
2 System Description and Problem Statement . . . 160
3 MPC Formulation . . . 163
4 Simulation Results . . . 167
5 Conclusions . . . 170
References . . . 171

Paper F: Data-Driven Predictive Direct Load Control of Refrigeration Systems 173
1 Introduction . . . 175
2 System Description and Problem Statement . . . 177
3 Control Strategy . . . 179
4 Subspace Identification Method . . . 179
5 Data-Driven Predictive Control . . . 182
6 Simulation Results . . . 185

7 Conclusion 193
References 194

Paper G: Model Predictive Control of Hybrid Thermal Energy Systems in Transport Refrigeration **197**
1 Introduction 200
2 System Description and Problem Statement 202
3 Control Strategy 204
4 Gray-Box Modeling 206
5 Control System Design 212
6 Simulation Results 216
7 Conclusion 226
A Simulation Parameters 227
References 229

Preface and Acknowledgements

This thesis is submitted as a collection of papers in partial fulfillment of the requirements for the degree of Doctor of Philosophy at the Section of Automation and Control, Department of Electronic Systems, Aalborg University, Denmark. The research has been supported by the Southern Denmark Growth Forum and the European Regional Development Fund, under the project "Smart & Cool". It has been carried out in the period from December 2011 to December 2014. The work has been supervised by Professor Jakob Stoustrup and Associate Professor Henrik Rasmussen until December 2013, and thereafter by Professor Rafael Wisniewski and Associate Professor Palle Andersen.

I would like to thank all my supervisors, Jakob for his great inspiration and support and for incredible discussions, Henrik for his remarkable industrial standpoints, Rafael for his invaluable know-how in theoretical and academic research, and finally Palle for his precious advice. I would also like to express my gratitude to all nice colleagues in our section of Automation and Control who made it a joyful atmosphere. Especially I appreciate Associate Professor Torben Knudsen's advice in system identification theory and his contribution to this research.

Throughout the work, I visited Danfoss Air-Conditioning & Refrigeration for a period of three months.Their supports are indeed appreciated. I would like to especially thank Roozbeh Izadi-Zamanabadi who wholeheartedly supported my stay at Danfoss where we had an enjoyable and productive collaboration. Thanks also goes to Torben Green who provided valuable data required for this research through ESO2 project.

Apart from the industrial visit, I also had the opportunity to visit Mechanical Engineering and Science Laboratory at the University of Illinois at Urbana-Champaign, USA, for a period of four months. I stayed at the Alleyne Research Group under supervision of Professor Andrew Alleyne. I am truly thankful to Andrew for his exceptional guidance. It might have not been a long term visit, but it added a remarkable value to this research. I would like to thank all friendly persons in that group who were indeed welcoming.

Last but not least, my greatest and heartily thanks goes to my lovely wife Solmaz for her patience, love, supports and encouragements. I am really indebted this achievement to her.

December 2014, Aalborg, Denmark
S. Ehsan Shafiei

Abstract

In order to improve the efficiency, reliability, economics, and sustainability of electricity services, a state-of-the-art electrical grid is needed to gather, process, and distribute information about the behavior of all participants including both suppliers and consumers. This has led to a new concept which is called smart grid where both the consumption and the generation are coordinated to ensure that the power generation and consumption will maintain balanced. Demand-side management (DSM) is a promising technology to improve the energy system at the side of consumption. The main advantage of DSM is that it is less expensive than the alternative solutions which may require building a new power plant or installation some electric storage devices.

In Denmark, with around 5.5 million inhabitants, there are about 4,500 supermarkets consuming approximately 550 GWh annually that means around 62.8 MWh in average. This is a significant potential that can be released by taking advantage of the flexibility of the consumption using advanced control strategies. The flexibility can be defined as the ability to shift the cooling load across the time or as the ability to follow a specific load profile to help the power grid maintain balanced. The main idea is to utilize the thermal capacity of refrigerated goods for storage and delivery of thermal energy. In a broader perspective, the methods proposed in this thesis can be applied to other similar applications, like building cooling systems with some degree of modifications.

The main objective of the existing control for refrigeration systems is to maintain the foodstuff temperatures within the desired limits imposed by the legislative requirements. The major challenge in energy management of refrigeration systems is to respect those limitations. For this purpose, advanced control methods are required depending on the type of balancing services that should be provided by supermarkets. Another important factor that needs to be taken into account is to preserve the energy efficiency of the system in any demand response scenario. The latter may make the control design even more challenging. Model predictive control (MPC) is a favorable model-based control scheme by which it is possible to deal with the multiple-input multiple-output refrigeration systems. Furthermore, inclusion of the temperature constraints in an MPC formulation is quite straightforward.

We face the control challenge by first developing a simulation model for supermarket refrigeration systems. The model is validated against real data obtained from a supermarket in Denmark. Then we look into two different demand-side management schemes: indirect and direct load control. The former is based on the electricity price incentive, and in the latter the consumption is directly managed by a third party based on a contract. For the indirect load control, we propose two different supervisory control approaches using MPC to address the problem of electricity cost minimization. For the direct load control, three different control methods are proposed. The first method is the least com-

plex one including decentralized proportional-integral control loops that can be applied to a general class of supermarket refrigeration systems. The second method uses MPC requiring a high fidelity model specific for each supermarket system which makes the practical implementation of the method highly complex. The advantage is that the higher performance – in terms of the reference load following – is achieved. In the third method, we utilize a data-driven approach using the subspace method. It has the advantages of the formers such that it does not need an explicit model of the system and the desired load following performance is attained.

Often overlooked in the broader discussion is the energy consumption for various transport refrigeration applications which are also very important. Recent research findings indicate that the refrigeration system commonly employed in food transportation can account for 40% of the total greenhouse gas emissions from the corresponding vehicle engines. As the final contribution of this thesis, the problem of the optimization of a hybrid transport refrigeration system is addressed. The hybrid refrigeration system is made by the integration of conventional refrigeration technology with thermal energy storage.

Synopsis

For at forbedre effektivitet, pålidelighed, økonomi og bæredygtighed af forsyning med elektrisk energi er der behov for at el-produktion -distribution og -forbrug koordineres ved hjælp af state-of-the-art metoder til indsamling, behandling og fordeling af information om opførslen af både elproducenter og elforbrugere.

Dette har ført til det nye koncept, smart grid, hvor både forbrug og produktion bliver koordineret for at sikre at øjeblikkelig produktion og forbrug hele tiden holdes i balance. Demand-side management (DSM), altså aktiv påvirkning af forbruget, er en lovende teknik til at forbedre energisystemet på forbrugssiden. Fordelen ved DSM er at det er mindre dyrt end alternative løsninger, som kan kræve bygning af et nyt kraftværk eller installation af elektriske lagerenheder

I Danmark, med omkring 5.5 millioner indbyggere, er der omkring 4500 supermarkeder, som forbruger cirka 550 GWh om året svarende til en middeleffekt på 62.8 MW. Der er et betydeligt potentiale i at udnytte fleksibilitet i dette forbrug ved hjælp af avancerede control strategier. Fleksibilitet kan i denne forbindelse defineres som evnen til at tidsforskyde elforbruget til køling eller som evnen til følge en specifik belastningsprofil som hjælp til at holde balance i produktion og forbrug i elnettet. Hovedideen er at udnytte termisk kapacitet i nedkølede varer til at oplagre, henholdsvis frigive termisk energi. I bredere perspektiv kan de metode,r der foreslås i afhandlingen med nogen grad af modifikation anvendes i lignende forbrugsenheder, for eksempel systemer til køling af bygninger. Hovedformålet med den eksisterende regulering af kølesystemet er at holde temperaturen af de nedkølede fødevarer indenfor ønskede grænser bestemt i overensstemmelse med lovgivningskrav. Den største udfordring med energy-management i kølesystemer er at sikre at disse begrænsninger respekteres. Til dette formål kræves avancerede styring og regulerings metoder indrettet efter hvilken type balanceringsydelse der ønskes leveret af supemarkedet. En anden vigtig faktor der skal tages i betragtning er opretholdelse af kølesystemets effektivitet i alle demand response scenarier. Det sidste giver endnu en udfordring til regulatordesignet. Model prædiktiv regulering (Model Predictive Control, MPC) er en fordelagtig modelbaseret reguleringsmetode som giver mulighed for at håndtere kølesystemer med multiple inputs og multiple outputs og indrage prognoser om fremtidige driftsbetingelser. Endvidere giver MPC mulighed for at håndtere temperaturbegrænsninger på en ligefrem og systematisk måde.

I afhandlingen er reguleringsudfordringerne imødegået ved først at udvikle en simuleringsmodel for kølesystemer i supermarkeder. Modellen er valideret imod målte data fra et dansk supermarked. Derefter behandles to forskellige Demand-side management ordninger: indirekte og direkte styring af elforbruget. Den første ordning er baseret på tilskyndelse gennem elprisen og i den sidste bliver elforbruget styret direkte af en tredje part på betingelser fastlagt i en kontrakt. Til indirekte forbrugsstyring foreslås to forskellige

tilgange til regulering på overordnet niveau, begge bruger MPC som tilgang til det problem at minimere omkostningerne til elektricitet med varierende elektricitetspriser. Til direkte styring af belastning foreslås tre forskellige regulerings metoder. Den første metode, som er den mindst komplicerede og er baseret på decentraliserede reguleringssløjfer med proportional- og integral-regulering, kan anvendes på en bred klasse af supermarkedskølesystemer. Den anden metode bruger MPC og kræver en nøjagtig model tilpasset hvert enkelt supermarkedssystem, hvilket gør den kompliceret at implementere i praksis. Fordelen er at der opnås bedre ydelse i form af evnen til at følge forskellige forløb af ønsket elforbrug. I den tredje metode bruges en data drevet tilgang med udnyttelse af underrum til at uddrage den ønskede informationen af data. Metoden omgår nogen af ulemperne ved den anden metode idet den ikke behøver en explicit model af systemet og kan opnå samme ydelse i form af evnen til at følge et ønsket forbrugs forløb.

I den brede diskussion bliver energiforbruget til køling i forbindelse med forskellige transportanvendelser ofte overset skønt det også udgør en vigtig andel. Undersøgelser indikerer at de kølesystemer der anvendes i forbindelse med fødevaretransport giver anledning til 40% af den samlede udledning af drivhusgasser fra transporten. Et sidste bidrag i afhandlingen behandler optimering af et hybrid system til køling under transport. I det hybride kølesystem er konventionel køleteknik integreret med et termisk energilager.

1 | Introduction

This chapter begins with explaining the motivation behind doing the present PhD study. Research background and state-of-the-art are presented next. The research objectives are then introduced and the scientific hypotheses are stated. Finally, the thesis will be outlined.

1.1 Motivation

The modern life, especially in developed countries, are increasingly relying on availability of electricity, almost everywhere. In Europe (Eu27+), the electricity use would increase by 1.2% per year from 3,043 TWh in 2008 to 4,300 TWh in 2050 [EUREL, 2013]. Similarly in US, it would increase by 0.9% per year, from 3,826 TWh in 2012 to 4,954 TWh in 2040 [EIA, 2014]. The huge energy use all around the world has resulted in tremendous CO_2 emissions and consequently the problem of global warming that threats our planet.

One solution to respond to the energy demand in a clean way is to integrate the renewable energy resources such as wind and solar energy into the electricity generation sector. In Europe, the target is that 20% of EU energy consumption should come from renewable recourses by 2020 [EUREL, 2013]. On the other hand, the volatility nature of the renewable recourses may affect the stability of the electricity power grid in terms of the imbalance between the power generation and consumption. The Smart & Cool project aims at addressing this problem by coordination of the power generation and consumption, such that the balance of energy in the grid is preserved. The focus of the work package 1 which is the subject of this PhD study is on the energy management at the consumer side, specifically for supermarket refrigeration systems. Fig. 1.1 shows a typical layout of a smart grid in which the energy consumption of the consumers are managed as well as the power generation to maintain the balance between the energy demand and supply.

From research point of view, this project is in line with the Danish strategic research towards green and smart energy systems. It can help Denmark keep going as one of the leading countries using renewable resources within a stable power grid providing high quality electricity to the energy consumers. Collaborating with industrial partners who support the project, especially Danfoss for this work package, would keep the Danish industry on the track of innovation. The latter is particularly important as can open up new possibilities for future investments that may lead to new opportunities for researchers, job seekers and entrepreneurs.

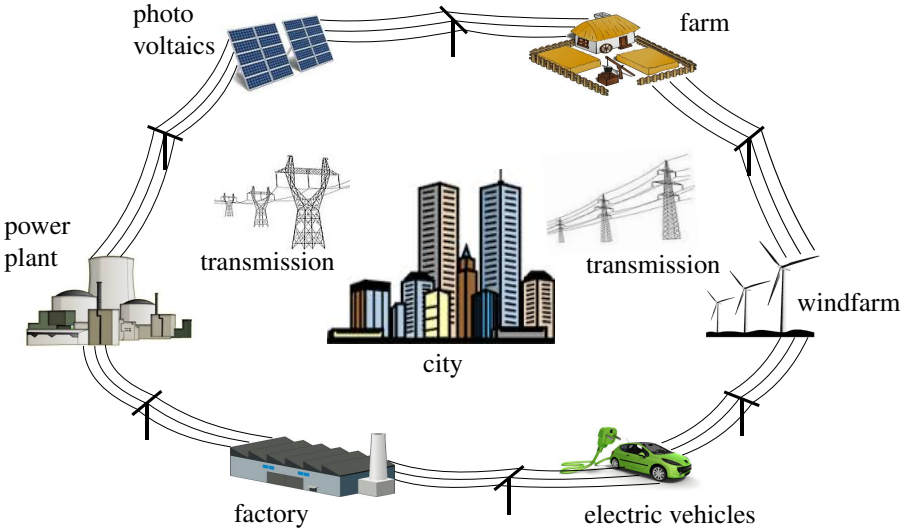

Figure 1.1: In the smart grid the energy consumption of the consumers are managed as well as the power generation to maintain the balance between the energy demand and supply.

1.1.1 Demand Response

Demand response (DR) is defined as [Balijepalli et al., 2011]: "Changes in electric usage by end-use customers from their normal consumption patterns in response to changes in the price of electricity over time, or to incentive payments designed to induce lower electricity use at times of high wholesale market prices or when system reliability is jeopardized". Under a demand response program, energy consumers would have the opportunity to play a significant role in the electric grid operation by energy/power management in terms of reducing or shifting their electricity usage in response to incentive-based schemes or time-based rates. The main purpose is to maintain supply and demand balanced which allows for more integration of renewable resources into the power grid. It can also lower the cost of electricity in wholesale markets.

Demand response implementation for refrigeration systems lies under the framework of smart buildings for which there is a great potential to participate in DR programs by managing their loads. For example in US, the energy consumption in residential and commercial buildings accounts for around 40% of the total energy consumption [EIA, 2014]. Implementation of energy management strategies is not limited to developed countries inside Europe or USA; there are also several practices in developing countries like India [Harish and Kumar, 2014], Brazil [Macedo et al., 2015], China [Zheng et al., 2014], Turkey [Tascikaraoglu et al., 2014], etc that shows the world-wide acceptance of the concept.

1.1.2 Refrigeration System

The main objective of the existing control for refrigeration systems is to maintain the foodstuff temperatures within the desired limits imposed by the legislative requirements.

The major challenge in demand response implementation for refrigeration systems is to respect the food safety while managing the energy consumption for grid balancing services. For this purpose, advanced control methods are required depending on the type of balancing services that should be provided by the refrigeration systems. Another important factor that needs to be taken into account is to preserve the energy efficiency of the consumer units in any demand response scenario.

Vapor Compression Cycle

Vapor compression cycle (VCC) system, shown in Fig. 1.2, is the most common refrigeration system in use due to its high coefficient of performance compared to alternative solutions [Tassou et al., 2009].

Starting at the low pressure side (see Fig. 1.2), the refrigerant in a nominal vapor compression cycle flows through the evaporator where an expansion valve (EV) at the inlet controls the refrigerant mass flow rate to ensure superheated refrigerant exits the evaporator. Superheat is desirable to avoid liquid ingestion by the compressor. The evaporator (EVAP) is equipped with a fan that provides air circulation inside the refrigerated container. The air from the cold reservoir is forced over the evaporator coil and cooled down as the heat is absorbed by the cold low-pressure refrigerant. After passing over the evaporator, the air is returned to the cold reservoir. The superheated refrigerant flows into the suction line where a liquid accumulator (ACC) is placed to buffer any liquid that may exit the evaporator and ensure vapor ingestion by the compressor. The compressor (COMP) raises the pressure and enthalpy of the refrigerant by performing work on it. The high pressure refrigerant enters the condenser (COND) where another fan circulates ambient air across the coil. Heat is transferred from the hot refrigerant to the ambient air and the refrigerant condenses from a vapor to a multiphase liquid/gas mixture. As the refrigerant loses enthalpy, it exits the condenser, possibly in a subcooled state, and flows into a liquid receiver (REC). From the receiver, it enters the expansion valve where the cycle starts again.

Supermarket Refrigeration Systems

In Denmark, with around 5.5 million inhabitants, there are about 4,500 supermarkets consuming approximately 550 GWh annually [Hovgaard et al., 2013] that means around 62.8 MWh in average. This is a significant potential that can be released by taking advantage of the flexibility of the consumption using advanced control strategies. The flexibility can be defined as the ability to shift the cooling load across the time or as the ability to follow a specific load profile to help the power grid maintain balanced. In a broader perspective, the methods proposed in this thesis can be applied to other similar applications like building cooling systems with some degree of modifications.

Transport Refrigeration

Apart from energy management and demand response, the energy efficiency is in itself a great matter. The target set by the EU Heads of State and Government demands a 20% reduction in primary energy use compared with projected levels in 2020 to be achieved by improving energy efficiency [EUREL, 2013]. The energy usage of heating, ventilation,

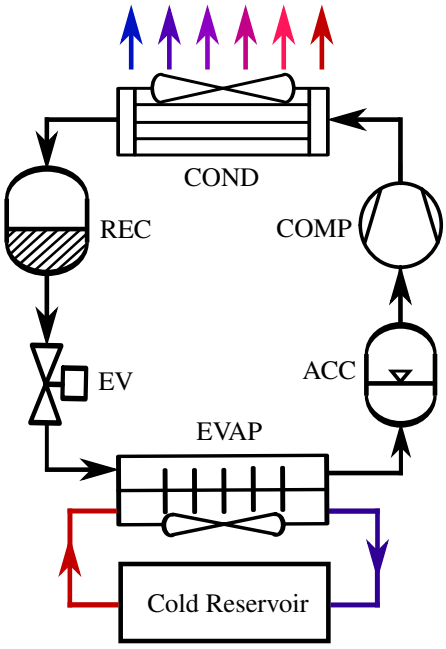

Figure 1.2: The layout of a vapor compression cycle system.

Figure 1.3: In Denmark around 4500 supermarkets consume 550 GWh/year that means around 62.8 MWh in average.

air-conditioning and refrigeration (HVAC&R) systems accounts for a significant amount of the total energy consumption in residential and commercial buildings.

Often overlooked in the broader discussion is the energy consumption for various transport refrigeration applications which are also very important. The analysis provided by [Tassou et al., 2009] indicates that the refrigeration system commonly employed in food transportation can account for 40% of the total greenhouse gas emissions from the

corresponding vehicle engines. The VCC system is widely used in transport refrigeration. In the thermal system literature, the integration of conventional refrigeration technology with thermal energy storage (TES) results in a hybrid refrigeration system. Optimization of these hybrid systems is another focus of the present work since the optimization of the individual VCC process has been previously addressed in the literature.

1.2 State-of-the-Art and Background

Energy management of refrigeration systems is a multidisciplinary research area requiring various knowledge about thermodynamics, mathematical modeling, system identification, control theory, etc. Each of those is a well-developed filed of research from theoretical point of view. However, when the combination of them is required for exploring new applications such as demand-side management, smart grid integration and transport refrigeration is quite challenging and needs tremendous research effort.

1.2.1 Modeling for Control and Simulation

The model development is influenced by the purpose of modeling and the application at hand. In the model-based control design, the models can be employed by the control system to predict the future behavior of the plant and accordingly apply the appropriate control effort. Individual components, like compressor [Pérez-Segarra et al., 2005], condenser [Corradi et al., 2006], evaporator [Willatzen et al., 1998], etc. are modeled for performing optimization of the mechanical design, dynamical analysis and performance and efficiency improvements at the local control levels. Those models are usually too detailed to be employed directly by the control system due to the increase of the computational burden and the complexity which might be consequent on. Therefore, low order and simplified models are usually used in the control design like the evaporator model utilized in [Vinther et al., 2013], which is also validated in a refrigeration lab.

A mathematical model for industrial refrigeration plants is proposed by [Cleland, 1985] for simulation of food refrigeration processes. The air temperature of the cold rooms are estimated by the model. However, there is a discrepancy between the predicted and measured air temperatures. The development of a Modelica library for CO_2 refrigeration systems is accomplished by Pfafferott and Schmitz, [Pfafferott and Schmitz, 2002]. The heat exchangers model is explained, and the steady-state conditions are validated by experimental data. An extension of the model for transient simulation and validation is given by [Pfafferott and Schmitz, 2004]. The pressures are well estimated, but the air temperature of cold rooms are not reported. Investigation of a thermodynamic model supported by experimental analysis is accomplished by [Aprea and Renno, 2004]. The method is proposed to improve the COP by matching the compressor capacity to the load, replacing the classical thermostatic control. A similar work is accomplished to provide an excellent transient characteristics by using a decoupling model [Li et al., 2008]. Although the latter two methods can be applied to a single vapor compression cycle, they are not applicable to the multi-evaporator systems used in supermarkets. [Wang et al., 2007a] presents a dynamic mathematical model for coupling the refrigeration system and phase change materials. The model can predict the refrigerant states and dynamic COP.

A more generalized model is introduced in [Shao et al., 2008a] based on a two-phase fluid network. The proposed model can simulate different kinds of complex refrigeration

systems in different operating modes and conditions. It can estimate the steady-state values in different operating modes. Applications of the developed model to estimate the different operating points of the multi-unit inverter air conditioner, heat pump with domestic hot water and multi-unit heat pump dehumidifier are demonstrated in [Shao et al., 2008b]. It should be noted that the steady-state models without considering cold room dynamics cannot be employed for demand-side managements, in which playing with the cold room temperatures is required for energy solutions. Another example of an steady-state model is presented in [Zhou et al., 2010].

The model presented in [Petre et al., 2009] provides an analytical method for COP optimization. Although the model does not simulate the system operation, it can be employed for commissioning the refrigerating machines in terms of the selection, design and optimization of the main parameters. With focus on local controls, [Schurt et al., 2010] proposes a model-driven linear controller as well as giving an assessment for a single vapor compression cycle [Schurt et al., 2009]. A dynamic model of a transcritical CO_2 system is developed by using the equation-based modeling language, Modelica, which can be simulated e.g. in Dymola [Shi et al., 2010]. Only gas cooler equations and model validation are provided in that paper. With a different perspective, a numerical model are developed for evaluation of the use of thermoeconomic diagnosis in transcritical refrigeration [Ommen and Elmegaard, 2012]. In order to simulate the energy use in supermarket refrigeration systems, a model is developed in [Ge and Tassou, 2011a]. Nevertheless, the cold room dynamics are not given by the model and the map-based routing proposed for estimating the compressor power consumption is not quite accurate. Considering power consumption in refrigeration systems, [Hovgaard et al., 2011] proposes a modeling for optimization purposes.

In an industrial PhD project supported by Danfoss, [Larsen, 2005], a static model is developed for set-point optimizing control of refrigeration systems. Since the objective is to find the optimum operating point in terms of the energy efficiency in the steady-state condition, there is no dynamical model required. On the contrary, in the second part of that thesis, a low order nonlinear continuous-time dynamical model of the supermarket refrigeration system is presented where the relevant dynamics of the suction manifold and the display cases are captured. The model is used for improving the dynamic behavior of the thermostatic control system by preventing the simultaneous ON/OFF operation of the cooling power in all display cases which is known as synchronization problem. The dynamical model developed by [Larsen, 2005] is slightly modified by [Petersen et al., 2012] and extended to include some static nonlinearities to model a high pressure CO_2 refrigeration system with booster configuration. A gray-box method using lumped parameter modeling approach is taken and parameter estimation and model validation are performed using the data obtained from a medium-size supermarket in Denmark. The detailed thermodynamic analysis of such CO_2 systems as well as explanation of the transcritical cycle are given by [Ge and Tassou, 2011b].

Supermarket refrigeration systems are seen as large-scale systems including several components that makes the laboratory set-up of such systems very expensive. Moreover, such thermal systems have very slow dynamic response such that some experiments may need couple of weeks or even months to be accomplished. Consequently, simulation tools are needed to speed up the development of control algorithms and accomplishment of the performance analysis for these systems. A nonlinear continuous model of the VCC systems was developed by [Rasmussen, 2002] based on which the Thermosys toolbox for

Matlab/Simulink environment has been created [CU Aerospace, 2013]. It is a nonlinear simulation tool capturing a broad range of dynamics of the air-conditioning and refrigeration systems. It also has the capability to simulate the transient behavior including the startup and shutdown dynamics. Although it is a powerful tool for simulation of the thermal systems with different configurations and refrigerant in use, it is too slow to be used for long run simulations of the supermarket refrigeration systems including several cold reservoirs. A comprehensive survey in dynamic modeling and simulation of the VCC systems is given by [Rasmussen, 2012a] and [Rasmussen, 2012b]. Depending on the application in mind, there is a trade-off between the model accuracy and the simulation speed.

Fig. 10.16 shows how the dynamical models can be used in a simulation environment for control system developments. A higher order nonlinear model can be used for simulation of the plant dynamics. But those kind of models might be to detailed to be employed directly by the control system. Instead, a lower order simplified or even linearized model can be used for control design. In spite of that, in order to evaluate the control performance, it is a good idea to apply the control algorithm to the full model of the plant which mismatches the model used in the control algorithm.

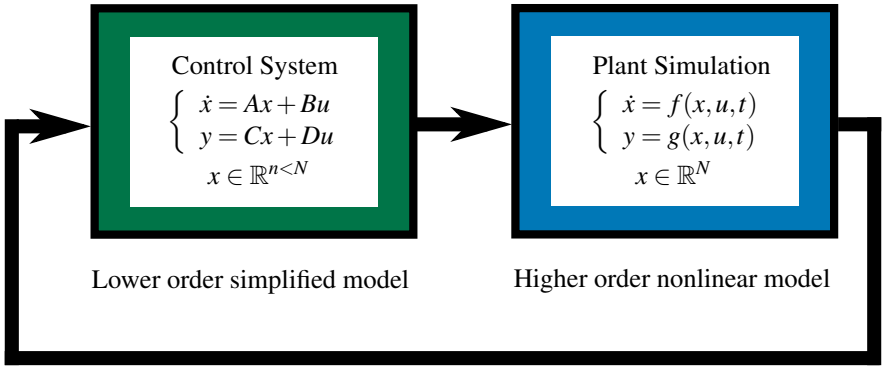

Figure 1.4: Simulation environment for development of the control algorithms. A higher order nonlinear model is used for simulation of the plant dynamics, and a lower order simplified model is employed by the control system.

1.2.2 Model Predictive Control

Model predictive control (MPC) is a technique for digital implementation of optimal control formulations. Different constraints in the system such as input saturation limits and state or output constraints are handled using this method which also accommodates systems with multiple inputs and outputs [Maciejowski, 2002]. Fig. 10.4 shows the basic idea of the MPC implementation for set-point regulation problems. At time instant k, an optimization problem is solved for the next N_p samples — known as the prediction horizon — where the future output is predicted using a model. The future inputs can freely move within the next N_c samples — known as the control horizon — to minimize the output deviation from the set-point. The first move in the predicted inputs is applied as

the control signal to the system. In the next time instant the optimization problem will be solved again by updating the output measurements and moving the prediction and control horizon one step forward.

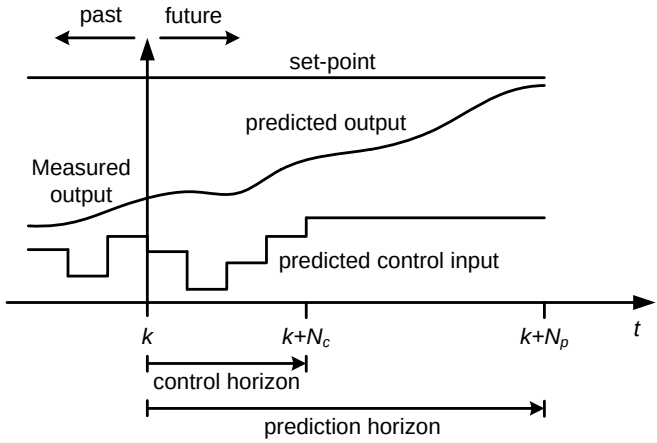

Figure 1.5: A typical MPC implementation for set-point regulation problems which is also known as receding horizon optimal control.

MPC has been widely used in HVAC&R applications as an advanced control technique for effectively accommodating input (e.g compressor) and output (temperature range) constraints. Several different studies have successfully applied MPC to building HVAC&R systems. A simplified linear thermal model is developed in [Candanedo et al., 2013] to predict the required cooling power which is utilized as the primary manipulated variable for the MPC formulation in the control of a building. The problem of model uncertainty in different operating conditions is considered in [Kim, 2013] where multiple local models are used in the MPC formulation to make it responsive to the entire operation regime. The results show the superior performance comparing to the traditional logic based control. Regarding the smart grid applications, in [Chen et al., 2013] and [Ma et al., 2014] the total cost of electricity is minimized using the MPC which systematically takes the electricity price prediction into account. [Chen et al., 2013] proposes the formulation of a finite horizon optimization problem for scheduling the thermal appliances. In [Ma et al., 2014] a dynamic thermal process as well as power model of the building thermal mass are incorporated by the MPC to shift the peak demand to off-peak hours under the time-of-use price policy. Regarding the efficiency improvement and energy optimization, MPC is employed in [Aswani et al., 2012], [Hu and Karava, 2014], [Zakula et al., 2015] and [Castilla et al., 2015] to minimize the total energy consumption of the cooling systems. A novel learning-based MPC algorithm, [Aswani et al., 2013], is implemented by [Aswani et al., 2012] in an air-conditioning laboratory set-up which results in 30%-70% reduction of the energy consumption compared to the typical thermostatic control. An application to a complex mixed-mode cooling system (window opening position, fan assist, and night cooling schedule) is investigated by [Hu and Karava, 2014]. Because of the model complexity, the MPC could only be implemented off-line. The simulation results show a significant reduction in the cooling requirements while maintaining

the temperature limits compared to a heuristic rule-based algorithm typically used for the window opening position which may even cause overcooling with lower thermal comfort acceptability. Another advanced cooling system, known as low-lift cooling system, is analyzed by [Zakula et al., 2015]. It comprises thermally activated building surfaces and a parallel dedicated outdoor air system for dehumidification and ventilation. Compared with the variable air volume system, 24% electricity saving is achieved by the low-lift cooling when MPC is used in both cases. A two-layer hierarchical control structure is proposed by [Castilla et al., 2015]. A nonlinear MPC is used in the upper layer to guarantee the thermal comfort conditions, and the lower layer contains a PI controller combined with a split-range controller to obtain energy saving. The two objectives of the electricity cost reduction and efficiency improvement are achieved in [Ma et al., 2012b] where an MPC for the chilling system operation is proposes for optimal usage of the water tank in the system.

Several MPC formulations have successfully been applied for various improvements in refrigeration systems. With hybrid system formulation, MPC is employed in [Ricker, 2010, Sarabia et al., 2009] and [Sonntag et al., 2007] to solve the synchronization problem in display cases that causes wearing of the compressors. [Fallahsohi et al., 2010] applies predictive functional control to minimize the superheat in an evaporator. For multi-evaporator systems, a decentralized MPC is proposed to control the cooling capacity of each evaporator [Elliott and Rasmussen, 2008]. A nonlinear predictive control scheme is designed in [Leducq et al., 2006] to reduce the total power consumption of the compressor in a vapor compression cycle. The cooling capacity is regulated by a variable speed compressor. But this method cannot be applied directly to the refrigeration systems with different cooling units in which the cooling capacity is regulated by expansion valves as well. As a thorough study that proposes an MPC to reduce the operating cost of such systems, one can refer to [Hovgaard et al., 2012].

1.2.3 Demand-Side Management

In order to have a high quality electricity (in terms of frequency and voltage stability) available by the power system, it is crucial that the power generation and consumption maintain balanced. In an extreme case the imbalance may even cause a black out in the system. Demand-side management (DSM) is a promising technology to improve the energy system at the side of consumption. The main advantage of DSM is that it is less expensive than the alternative solutions which may need to build a new power plant or install some electric storage devices. The following taxonomy of DSM is given by [Palensky and Dietrich, 2011] depending on the timing and the impact of the applied measures on the costumer process.

a) *Energy Efficiency*: It results in immediate and permanent energy and emissions saving and is evaluated as the most welcome method.

b) *Time of use*: Thereby electricity prices are scheduled to be higher for certain periods of time on an advance or forward basis, typically not changing so often.

c) *Demand response*: It is categorized into incentive-based DR and time-based rates DR [Han and Piette, 2008].

d) *Spinning reserve*: This term is used in [Palensky and Dietrich, 2011] for the loads that can act as virtual spinning reserve in an autonomous way (similar to primary control)[1] or in a coordinated way (similar to secondary control)[2].

The problem of peak shaving is addressed by [Mahmood et al., 2014] using an energy consumption scheduling scheme. It considers the case where each subscriber has a smart meter equipped with an energy consumption controller. A distributed algorithm is run in each local controller and the users can interact with each other through a local area network. [Hayes et al., 2014] analyzes the role of network operators in encouraging and adding value to the implementation of specific DSM schemes. The results show that by the optimum network locations, it is possible to maximize the total benefit from DSM. Focusing on demand response and user engagement techniques, [Gelazanskas and Gamage, 2014] gives an overview of DSM technologies. All of the discussed techniques are based on load shifting strategy.

Whatever strategy is used, control and optimization methods play the key role in the energy management ranging from a simple scheduling method to sophisticated model-based approaches. DSM control policies for distributed energy resources (DER) are classified into four categories [Kosek et al., 2013]:

a) *Direct control*: Controllable DER receives specific commands from an external controller which has detailed information about the DER operation.

b) *Indirect control*: A control signal which is not a must followed command is issued and it is up to DERs to make their own decision regarding the issued signal.

c) *Transactional control*: It is based on negotiations in a bid-based market where DERs are competing for resources. Each DER puts a bid amount independently and can have its own control method according to the finalized bid.

d) *Autonomous control*: Here each DER is equipped with local controllers by which it can participate in frequency and voltage regulation as a virtual spinning reserve that was mentioned earlier in this section.

The first two methods are used for implementation of control strategies for supermarket refrigeration systems in this thesis. Consequently, there are explained in more details in the succeeding subsections.

Direct Load Control

In the direct control scheme, the consumer energy consumption is directly managed by an external utility[3] and may require one-way or two-way communication for information exchange. Four different types of direct control schemes are defined by [Gehrke and Isleifsson, 2010] for energy management of the consumers as:

[1] Primary control is the local, automatic control action that adjusts the active power output of the generation units in direct response to measured frequency variations.

[2] Secondary control is responsible for removing any steady-state error introduced by the primary control.

[3] An electric utility, or simply utility, is an electric power company that operates in a power/energy regulated market.

1) *Deferred consumption*: A certain amount of energy usage is shifted in time such that the amount of power consumption as well as the duration of the consumption are remained unchanged. Here the control command is a time shift Δt.

2) *Delta consumption*: The consumption is increased or decreased by an offset issued as a power difference signal ΔP.

3) *Scheduled operation*: The unit receives an operation schedule consisting of series of power set-point and time stamp pairs as $(t_i, P_i),\ i = 1 \ldots N$.

4) *Direct power control*: At runtime, a power set-point, P, is assigned to the unit.

The definitions has been extended by [Kosek et al., 2013] to cover DER operation control. The last scheme (*i.e.,* direct power control) is employed for the direct load control (DLC) implementation in this thesis. It is the most flexible scheme in terms of shaping the consumption profile.

[Ng and Sheblé, 1998] explains how load management may benefit both utilities and customers. It introduces profit-based management and differentiates it from cost-based approach. Furthermore, a linear programming algorithm is proposed for solving a load scheduling problem. [Battegay et al., 2015] presents a method to quantify the benefits of load control for reducing the reinforcement costs of power distribution networks. For this purpose, a linear model is developed to estimate the impact of DLC on the modification of electric demand. A hierarchical direct control structure in smart grid is proposed by [Trangbaek et al., 2012]. The structure consists of a higher level control system balancing the production and consumption, a second level of aggretaors each aggregating several loads, and the lowest level autonomous consumers. It is shown how power and energy constraints of different consumers can be incorporated into the aggregated loads to achieve the full consumer flexibility. [Petersen et al., 2013] presents a taxonomy for modeling of the consumers flexibilities based on the power and energy constraints. Three different models are presented and denoted as *Bucket*, *Battery* and *Bakery*. The bucket model is a power and energy constraint integrator and represents consumers with energy storage capabilities. The battery model also describes a power and energy constraint integrator but with a further limitation on the charging duration. Consumers with further constraints to the extent that the process must run in one specified continuous time slot at constant power consumption level, those are identified by the bakery model.

[Molina et al., 2000] presents a DLC algorithm using constrained predictive control to shape the overall load demand by controlling a group of residential HVAC systems. A thermal comfort controller of air-conditioning systems is proposed by [Chu et al., 2005] to the energy saving efficiency such that it can be employed by a DLC program to prolong the load shedding time duration. This method is later extended to a group DLC concept that enables the load management program to take account of the direct controller as an aggregated load [Chu and Jong, 2008]. [Callaway and Hiskens, 2011] reviews different load control programs initiated for the provision of power system services. It argues that direct load control is required to achieve full responsiveness defined as enabling high-resolution system-level control across multiple time scales. The load following problem for aggregated thermostatically control loads, such as refrigerators, air-conditioners, and electric water heaters, is investigated by [Mathieu and Callaway, 2012] considering the situation in which measured state information are not available. [babar et al., 2013] proposes a DLC algorithm for an incentive-based program in the form of demand reduction

bidding. It utilizes a dynamic programming technique for design of a consumer selection method. Thermal environments and thermal comfort impacts of DLC events on a university building are explored by [Zhang and Dear, 2015] by investigating the influences of various off cycle fractions, cycling periods, cooling set-point temperatures, thermal performance of the building envelope, and ventilation rates. It concludes that to maintain acceptable thermal comfort, DLC algorithms must be applied judiciously and customized to the specific building.

Refrigeration systems in particular have also been subject of research for DLC implementations. The bucket model introduced by [Petersen et al., 2013] can be extended to a leaking bucket model describing the energy storage in refrigerated goods in the presence of thermal disturbances [Pedersen et al., 2013]. Subsequently, the leaking bucket model can be used by an MPC algorithm in a direct smart grid control scheme [Pedersen et al., 2013]. DLC implementation for aggregation of a large number of supermarket refrigeration systems is investigated by [Pedersen et al., 2014]. Therein simulation results show that a peak reduction of 24.7% is achieved at a cost of 13.5% increase in the overall energy consumption. The problem of additional energy consumption due the provision of balancing services is handled in a contract between the supermarket owners and the aggregator company.

Indirect Load Control

A conceptual understanding and classification of indirect control strategies are given by [Heussen et al., 2012]. Therein, two central characteristics of *indirectness* are defined: (i) the relationship between control objective and observables is indirect in a sense that the actual response to the demand control signal is not observed and/or the signal is an incentive instead of being a direct command; and (ii) the decision is made independently of demand side resource objectives at the local consumer level. The most common approach is indirect control via price signals where electricity usage by end-use customers is altered in response to changes in the price of electricity over time. [Albadi and El-Saadany, 2007] highlights different demand response programs including classical, new marker-based and dynamic pricing scenarios. It classifies price-based programs into time of use, critical peak pricing, extreme day critical peak pricing, extreme day pricing, and real time pricing. A review of pilot studies given in [Newsham and Bowker, 2010] indicates that a peak load reduction of at least 30% can be achieved in a critical peak pricing program, in contrast to an alternative simple time of use program which can only expect to realize 5% reduction. The price-based DSM not only can reduce the electricity cost at the consumption side, but also can facilitate integration of more renewable resources into the power system. The significance of the load flexibility in Irish electricity market in order to minimize the curtailment of wind energy is illustrated in [Newsham and Bowker, 2010]. Following the same goal as the previous study, the impact of indirect control of two industrial electricity consumers on increasing the share of wind energy in their consumption is analyzed in [Finn and Fitzpatrick, 2014]. The results indicate that for every 10% reduction in a consumer's average unit price of electricity, the consumer's consumption of wind generation increases by approximately 5.8%.

In the previous paragraph, we mentioned the studies which show the significance and benefits of indirect load control for the power system. Implementation of indirect control for various types of consumers in different markets demands a tremendous effort

of designing appropriate control strategies at the consumer side. A widely used control strategy for building DSM is temperature set-point control for shifting the thermal load from a peak pricing period to the time when the electricity price is cheaper. Prediction of the building required thermal load and the peak price hours plays a key role in indirect load control implementations. The effectiveness of the set-point control using thermostatic control strategies for saving peak energy consumption and overall cost is evaluated by [Surles and Henze, 2012]. It turns out that the peak energy saving using thermostatic control extremely depends on the climate conditions. It is also found that, in a time-of-use tariff, there might be more saving in electricity cost for building owners than for utility companies. When price and weather forecast are taken into account for indirect control, MPC is a suitable control candidate. It provides a strong tool for formulation of the economic objective using the price prediction while incorporating the weather forecast into process dynamics. When MPC is used for priced-based control purposes, it is usually referred as economic model predictive control (EMPC) [Ma et al., 2012a]. Set-point optimization using economic MPC is employed in [Ma et al., 2014] for energy cost saving in building HVAC systems under a time-of-use rate structure. Taking into account the extended forecast of disturbances (*e.g.,* weather and electricity price) requires longer prediction horizon for MPC implementation which imposes heavy computational burden. It will be even more demanding if there is nonlinearities in the control algorithm. [Touretzky and Baldea, 2014] faces this challenge by proposing a hierarchical EMPC for buildings such that the nonlinearity arises from the discrete operation of a thermal energy storage unit is handled by a dynamic scheduling algorithm in a slower time scale, and an MPC scheme is in charge of the comfort temperature control in a fast pace.

There are also some research focusing on indirect load control for refrigeration systems. Potential of refrigerated warehouses for load shedding and shifting from baseline electricity use in critical peak pricing programs is investigated by [Goli et al., 2011]. The results confirm the abilities of refrigerated warehouse for those DR implementations, but it varies depending on the facilities in use. An extended research reveals the impact of control technology on the DR potential of industrial refrigerated facilities [Scott et al., 2012]. Taking advantage of variation of electricity price and weather temperature, it is possible to formulate an optimization problem for minimizing the cost of operation. Using this possibility, an optimizing control scheme is presented in [Hovgaard et al., 2011] in which a linear approximation model for prediction of the electric power consumption of refrigeration system is introduced. [Hovgaard et al., 2013] proposes a method to tackle with a nonconvex cost function in the optimization formulation. The method is supported by a full year simulation of operation of a commercial refrigeration system showing that 30% cost saving can be achieved in case of real-time variation in electricity prices. Two different objectives are formulated under EMPC design in [Hovgaard et al., 2012]. One objective takes the electricity price signal into account for cost minimization, and the other one aims at power regulation in regard with a balancing power market. Due to the nonlinearity introduced in the optimization problem, a nonlinear optimization tool is employed resulting in significant saving chiefly because of incorporation of the second objective into the EMPC scheme.

1.2.4 Data-Driven Control

Developing a high fidelity model for an industrial process is a time-consuming task requiring tremendous efforts. Those models are usually not generally applicable and need to be tuned carefully for each specific process. In some cases, the model order and structure should be changed to fit a new system configuration. From control perspective, there might also be some priors and assumptions on the model that need to be satisfied in order for the control system to operate with the expected performance. Fig. 1.6 illustrates the model-based control concept.

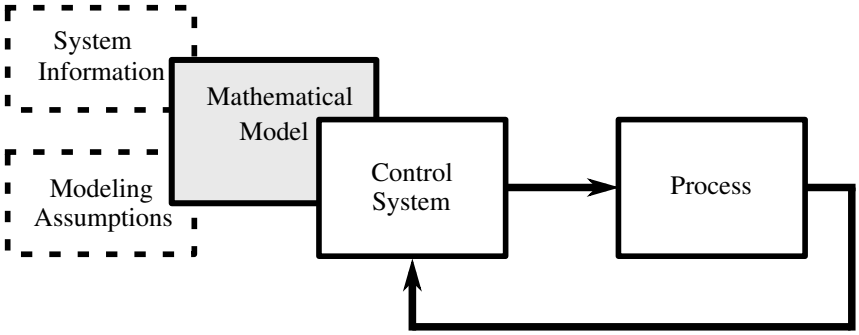

Figure 1.6: In model-based control, the control system utilizes a mathematical model of the process. The model is developed using system information (*e.g.,* physical parameters and input/output data) and modeling assumptions (*e.g.,* model structure and order).

On the other hand, *data-driven control* methods use measured data from the process input and output to optimize the control objective without any explicit information from a mathematical model. A simplified concept of the data-driven control is shown in Fig. 1.7.

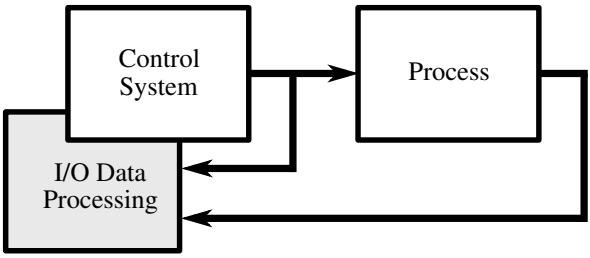

Figure 1.7: In data-driven control, the control objective is optimized using measured data from the process input and output.

A survey on different data-driven control methods is given by [Hou and Wang, 2013]. It presents different classifications of the methods in accordance with the use of measured input-output data and controller structure. We briefly list the main data-driven control strategies in the following disregarding the class which each method may belong to.

- *Approximate dynamic programming*: It is used for control of nonlinear processes

using input-output data. This approach provides approximate solutions for stochastic control problems through dynamic programming [Lee and Lee, 2005]. It includes four main schemes [Hou and Wang, 2013]: heuristic dynamic programming, dual heuristic dynamic programming, action dependent heuristic dynamic programming, and action-dependent dual heuristic dynamic programming.

- *Simultaneous perturbation stochastic approximation*: In this approach, the controller is parametrized to approximate the nonlinear dynamics of the process from the closed-loop input-output data. Optimal controller parameters are obtained by utilizing an stochastic search algorithm in which all of the parameters in the problem are varied simultaneously (and randomly) [Spall, 2000].

- *Virtual reference feedback tuning*: The controller is directly obtained from a database through an optimization procedure where the optimization variables are the controller parameters. A reference model is assigned, and a virtual reference signal is constructed using the inverse of the reference model which is a (nonlinear) function of the output data [Campi and Savaresi, 2006]. This virtual reference is then utilized to formulate the optimization problem.

- *Model free adaptive control*: As opposed to the model-based nonlinear control, in this method, an equivalent dynamical linearization model replaces the general discrete-time nonlinear system. A dynamic linearization technique with a novel concept called pseudo-partial derivative is used to build the equivalent linearization model along the dynamic operating points [Hou and Jin, 2011]. Then the time varying pseudo-partial derivative is estimated on-line merely using the input-output measurement data.

- *Unfalsified control*: It is an adaptive switching control scheme which recursively falsifies control parameter sets that are found inconsistent with performance objectives and past experimental data [Safonov and Tsao, 1997]. A controller candidate may be falsified ever before inserted in the feedback loop which results in a superior transient performance compared with the other adaptive methods which require inserting controller in the loop one-at-a-time to determine if they are suitable.

- *Iterative feedback tuning*: In this approach, the parameters of a fixed controller (*e.g.,* PID) are optimized using an iterative gradient-based method. The gradient of the control performance criterion is estimated from measured closed-loop data [Hjalmarsson et al., 1998].

- *Subspace approach*: Here (linear) system dynamics are represented as a subspace of a finite-dimensional vector space using subspace matrices which are directly identified from input-output data [Overschee and Moor, 1996]. These subspace matrices can be utilized to either identify a state-space linear model of the process or to be directly employed by the controller [Huang and Kadali, 2008].

- *Correlation-based tuning*: This method attempts to decorrelate the output error between the achieved and designed closed-loop systems by iteratively tuning the controller parameters [Karimi et al., 2004].

- *Iterative learning control*: For systems that execute the same task multiple times, this approach can improve the closed-loop performance by learning from the input-output data of the process obtained from the previous executions [Bristow et al., 2006]. Two design components are placed: One in the feedforward path which uses the past information from the control signals, and another in the feedback path which uses the output data from the previous trials.

As mentioned earlier, model predictive control is the main control strategy for energy management of HVAC&R systems. Among the above list of data-driven control methods, subspace approach can be used for predictive control design and would have the key features of generalized predictive control [Clarke et al., 1987] such as prediction over a finite horizon, inclusion of the trade-off weighting between the output signal and control moves in the optimization cost function, and the choice of the prediction and control horizons [Kadali et al., 2003]. Because of higher relevance of the subspace approach to the present research – it is actually part of the contributions of this thesis – its state-of-the-art and background are explained in more details in the succeeding section.

Subspace Approach to Predictive Control Design

Dynamics of the linear multivariable processes can be described by the discrete-time state-space equations in innovation form as:

$$x_{k+1} = Ax_k + Bu_k + Ke_k, \tag{1.1}$$

$$y_k = Cx_k + Du_k + e_k, \tag{1.2}$$

where $u_k \in \mathbb{R}^l$, $y_k \in \mathbb{R}^m$, and $x_k \in \mathbb{R}^n$ are the process inputs, outputs and states, respectively; $e_k \in \mathbb{R}^m$ is a white noise (innovation) sequence with zero mean and covariance $E[e_k e_k^T] = S$. The parameters A, B, C, and D are state-space matrices with appropriate dimensions, and K is the Kalman filter gain. Subspace identification begins with partitioning input and output measurement data into two parts and then forming block Hankel matrices which are labeled as past and future (input/output) data as $\{U_p, Y_p\}$ and $\{U_f, Y_f\}$ [Overschee and Moor, 1996, Ch. 2]. The underlying idea is to reformulate (9.4) and (9.5) into the matrix forms (9.6), (9.7) and (9.11) thereby estimating subspace matrices which form the basis for the state-space model [Huang and Kadali, 2008, Ch. 3].

$$Y_f = \Gamma X_f + H^d U_f + H^s E_f, \tag{1.3}$$

$$Y_p = \Gamma X_p + H^d U_p + H^s E_p, \tag{1.4}$$

$$X_f = A^i X_p + \Delta^d U_p + \Delta^s E_p, \tag{1.5}$$

where Γ, H and Δ are subspace matrices with appropriate dimensions, the superscripts d and s indicates the correspondence to deterministic and stochastic inputs u_k and e_k, and the subscript i denotes the number of block columns. Several subspace identification methods differ depending on the numerical tools used in the estimation of the basis [Overschee and Moor, 1996, Ch. 3] such as singular value decomposition (used in [Moonen et al., 1989] and N4SID [Overschee and Moor, 1994]), QR-decomposition (used in MOESP [Verhaegen, 1994]), canonical variable analysis (used in CVA [Larimore, 1996]), etc.

The last step in subspace identification is to estimate state-space matrices from the subspace ones. The data-driven state-space model can then for example be used in model

predictive control design. It turns out that the derivation of the state-space model is not necessary and the subspace matrices can be directly used in predictive control design which is called subspace predictive control (SPC). In many cases the following linear predictor is identified for SPC design [Favoreel et al., 1998]:

$$Y_f = L_w W_p + L_u U_f + L_e E_f, \tag{1.6}$$

where $W_p = \begin{bmatrix} Y_p^T & U_p^T \end{bmatrix}^T$, and L_w, L_u, and L_e are subspace matrices corresponding to the past inputs and outputs (states), the deterministic future inputs, and the stochastic future inputs, respectively.

Utilization of subspace methods for predictive control design has been investigated for several applications such as buildings [Cigler and Privara, 2010], [Prívara et al., 2011], a turbo-generator pilot plant [Gambier and Unbehauen, 1999], solid oxide fuel cells [Wang et al., 2007c], a blast furnace ironmaking process [Zeng et al., 2010], a boiler-turbine unit [Wu et al., 2013], wind turbines [Navalkar et al., 2014], etc.

The linear predictor is identified using the data obtained from open-loop or closed-loop experiment. The performance of the data-driven control depends on the extent which the information – contained in the identification data – is rich. For stable plants like refrigeration systems, the open-loop experiments are of more interest since they are optimal especially when the system inputs are constrained [Agüero and Goodwin, 2007]. But special care should be taken regarding the input and output constraints that makes the experiment design more complicated.

When the identification part in SPC implementation is based on a method for which there exist fast and robust numerical computation algorithms (*e.g.,* QR-decomposition), it provides an opportunity for adaptation of the method by on-line updating the subspace matrices [Lovera et al., 2000]. The online adaptation can improve the control performance in case of variation of the system parameters, which is likely to happen in the large-scale thermal systems.

1.2.5 Thermal Energy Storage

In some thermal processes (*e.g.,* HVAC&R and heat pumps), it is possible to store energy in a thermal energy storage (TES) device by cooling or heating a material. Then the device can retain the thermal energy for a later use. The storage is charged by being supplied by the energy through a thermodynamic process and discharged later on by supplying the process with the stored energy. TES systems can be classified into the following three main categories [Arteconi et al., 2012]:

1) *Sensible TES*: The energy is stored by changing the temperature of the storage material. The types of devices vary depending on the storage medium in use. In thermally stratified TES tanks, the storage medium is water and they are characterized by separate volumes of water in the tank at different temperatures (see Fig. 1.8). The main application is in heating and air-conditioning systems. Another storage medium is concrete. As an smart grid application, it is shown in [Tahersima et al., 2011] that concrete can be employed for energy storage in an underfloor heating system to manage the electric power consumption of heat pumps in order to compensate power imbalance in the grid. In applications with higher temperature (above 100 °C) where

water temperature cannot raise to that point, rock TES can be used. However, it has a lower volumetric thermal capacity. Rock TES is utilized for instance in home air-conditioning systems and domestic hot water production, coupled with solar collector [Arteconi et al., 2012].

2) *Latent TES*: In latent TES, phase change materials (PCMs) are used where the state of the medium is changed by releasing or absorbing energy. As apposed to the sensible TES, the process of energy storage happens in nearly constant temperature. In general, the energy stored in form of latent heat is higher than that of sensible heat for a given mass consequently a smaller storage volume is required. Typical PCMs used are water, salt hydrates and certain polymers [Arteconi et al., 2012]. A geometrical layout of a latent TES constructed by fins and tubes are shown in Fig. 1.9.

3) *Thermochemical energy storage*: Reversible chemical reaction can also be used to store thermal energy. The advantages are high storage energy density and long duration of detaining the storage. A particular application is in absorption heat pumps where energy is accumulated in a chamber containing vapor absorbing salt and heat is exchanged through condenser/evaporator containing the working fluid.

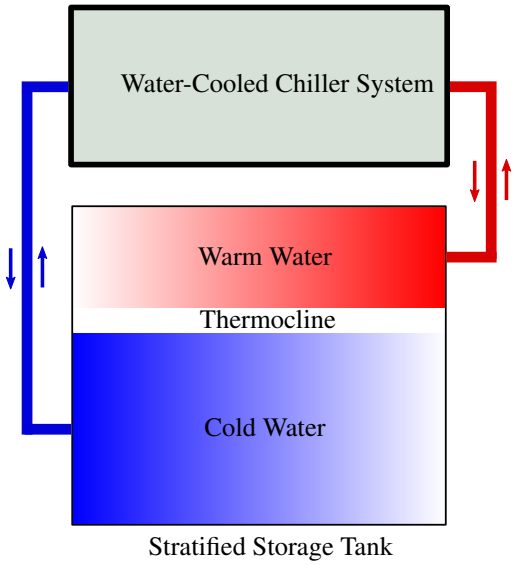

Figure 1.8: Stratified storage tank in a water-cooled chiller system. When the chiller is turned on, the cold water flows into (warm water flow out of) the tank, hence charging the storage. The reverse cycle can discharge the storage when the chiller system is turned off. A boundary layer or thermocline is established to separate the two zones.

Control technology plays a key role in increasing the efficiency of HVAC&R systems in buildings by active utilization of TES units. In [Ma et al., 2012b] a simple switching nonlinear model of a storage tank is developed and weather prediction is included in an MPC scheme for optimization of a chiller's operation. A novel configuration of a TES in

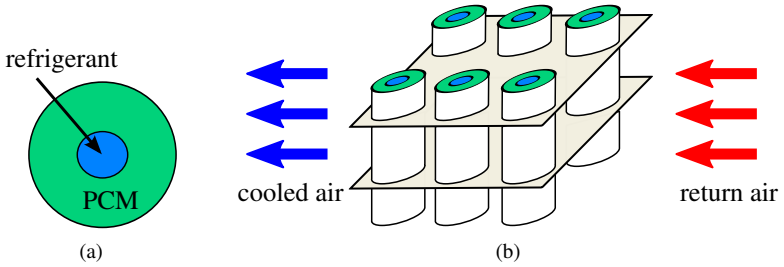

Figure 1.9: Geometry of a latent TES constructed by fins and tubes: (a) interior view of a cylinder: the PCM is placed inside the tubes being cooled by the refrigerant flow through the tube center thereby charging the TES; (b) exterior view of the device: when discharging, the TES can operate like an evaporator to cool the return air coming from the cooling medium.

a water chiller system is presented in [Cole et al., 2012] where the MPC is proposed to optimize the charge and discharge of the TES for minimizing both the energy consumption and operation cost. A simplified linear thermal model is developed in [Candanedo et al., 2013] to predict the required cooling power. The problem of model uncertainty in different operating conditions is considered in [Kim, 2013] where multiple local models are used in the MPC formulation to make it responsive to the entire operation regime. The results show the superior performance comparing to the traditional logic based control.

Thermal energy storages can be employed for demand-side management purposes using MPC as the dominant control scheme. A range of operational strategies for a TES in a heating system are investigated in [Fischer et al., 2014]. Therein the effect of different price signals as well as the storage size are analyzed and the results show that the heat pump efficiency can be improved by increasing the size of the storage, but on the other hand it would lead to additional losses in the storage unit hence limit the profitability in terms of the annual saving in energy costs. In [Mendoza-Serrano and Chmielewski, 2014] TES is employed for shifting power consumption of HVAC systems to low energy cost periods under an economic MPC scheme, and the impact of weather and electricity price forecasts on the cost reduction is shown. The switching nature in scheduling the TES challenges the MPC implementations by incorporating an integer decision variable into the optimization problem which results in computation difficulties for long horizon implementation. This problem is addressed in [Touretzky and Baldea, 2014] by designing a separated dynamic scheduling loop for a chilled water TES in the HVAC systems in a slower time scale than that of the HVAC control loop. Under the concept of zero energy buildings where the building has its own distributed power generation, [Zhao et al., 2015] proposes an MPC based strategy to optimize the power generation and consumption as well as scheduling of the TES utilization. The type of TES in that study is a stratified chilled water storage tank and the considered market policy is time-sensitive electricity pricing.

The application of TES in transport refrigeration systems is not quite as mature as in the building HVAC case [Walsh et al., 2013]; primarily because the constraints (size, weight, etc.) are more stringent. Nonetheless, there is a significant potential for different improvements in transport refrigeration sector by using of thermal storage technology.

For instance, an exergy analysis in [Javani et al., 2014] shows that the overall exergy efficiency of cooling systems in hybrid electric vehicles can be increased when TES is used. Depending on the application, different configurations have been proposed. Three different placements of the TES, for passive use of PCM in contact with the suction and liquid lines, are investigated in [Wang et al., 2007b]. The proposed layouts in [Wang et al., 2007b] can all be framed as a series configuration as explained in [Fasl, 2013]. Series arrangements have benefits and drawbacks, as explained in [Fasl, 2013]. For transportation applications with highly transient loadings, a parallel configuration may provide more rapid response to load disturbances. In [Fasl et al., 2014], a detailed nonlinear thermal model of a refrigeration system is presented with a parallel configuration for an active TES unit. The TES is configured in parallel with the evaporator heat exchanger and a heuristic switching control logic is proposed to deal with the different modes of operations like charging, discharging, etc.

1.3 Research Objectives and Hypotheses

The main and broad goal of the present research outlined in this thesis is to develop energy management methods for refrigeration systems in regard with the state-of-the-arts mentioned in the previous section. In the following the broad perspective is divided into several objectives and the challenges associated with each of them is stated.

a) *To enable supermarket refrigeration systems to participate in smart grid energy balancing.*

   This is made based on the idea that the thermal mass of refrigerated goods inside the supermarket display cases and freezing rooms can be employed for storing energy in form of coldness. Here the objective is to design a suitable control system enabling demand-side management for supermarket refrigeration systems under realistic smart grid balancing scenarios. The major challenge is that the designed control should provide high quality services (in terms of response time, power regulations, load predictions, etc) as well as ensuring the food temperature requirements.

b) *To reduce operation cost of large-scale refrigeration systems using model predictive control strategies.*

   As explained in the state-of-the-art section, the dominant control strategy for demand-response implementation of the buildings HVAC&R is MPC. Here we would like to design an MPC scheme by taking into account the forecast of different disturbances such as price variation and weather temperature. Having those predictions, the control system should be able to manage the energy use of the system such that the overall energy cost is minimized. The companies like Danfoss, they have their own local controllers that operate robustly and have been in the product for quite a long time. Therefore it is preferable if we design a control strategy which does not require having them replaced.

c) *To improve energy efficiency of the refrigeration systems using advanced control methods.*

In some demand response scenarios like indirect and direct load control, the major objective is to either reduce the operation cost (previous objective) or follow a certain reference load. It may result in an increase in the overall energy usage. In any probable scenario, it is very important to ensure the high efficiency of the system. On the other hand, it may conflict with the primary objective of the demand response and the trade-off needs to be handled within the control design.

d) *To unleash the full potential of energy management of the state-of-the-art hybrid refrigeration systems using advanced control strategies.*

The energy management of the advanced hybrid thermal systems is part of the goal of this research. Although the energy management regarding the smart grid problems might not be the case for transport refrigerations, but the similar idea of active utilization of TES devices can be utilized for energy optimization and performance improvement in hybrid refrigeration systems. It takes the prediction of disturbances into account under an MPC scheme that has been used for building applications. Compared to building HVAC&R systems, here the restrictions on TES (*e.g.,* size, weight, etc.) are more strict and variation of the disturbances happens in shorter time, consequently applying more rapid changes in the system dynamics.

The present research which is intended to reach the above objectives is established based on the following hypotheses:

H1) *Electrical power consumption of the compressor racks in supermarket refrigeration systems can be estimated and predicted using the thermodynamic states of the system.*

The compressor device in VCC systems is the main electricity using device. It provides the refrigerant mass circulation required for heat exchanges in the thermodynamic cycle. Knowing the thermodynamic states like enthalpies, temperatures and pressures and also the flow of the mass, it can be possible to estimate the electrical power consumption of the compressor. This hypothesis has already been justified in previous research for a single VCC cycle. The same seems to be valid for a large-scale supermarket refrigeration system. It is especially important when we want to predict the future electricity usage by changing the temperature or pressure set-points in the system.

H2) *Overall electricity cost of supermarket refrigeration systems can be reduced by employing model predictive control technique and taking the disturbance and price previews into account.*

If we have a good preview of the future price variations and the environmental disturbances, then we might know the periods in which the system performance is higher and/or the electricity price is cheaper. Then we can use the MPC technique to shift the load to those periods thereby reducing the total cost of operation.

H3) *Electricity usage of refrigeration systems can be directly controlled by tailoring the thermal load of the system.*

According to H1 there is a relationship between the thermodynamic states of the system and the electricity usage. The thermal load can be tailored by changing the temperature and pressure set-points. Therefore, the electricity usage can be directly controlled to follow a desired trajectory by designing a set-point control system.

H4) *Optimal direct load control of refrigeration systems can be achieved by only using the available input and output measured data.*

If there is no high fidelity model available for estimating the refrigeration load and electricity usage, then they can be estimated directly from the measured data. In that case a data-driven control approach which only uses the measured data from the process inputs and outputs can be applied for direct load control of refrigeration systems. By incorporating an optimization scheme into the control design we can also optimized the direct control objectives.

H5) *Total energy consumption of hybrid refrigeration systems can be reduced by active utilization of thermal energy storages.*

In Section 1.2.5 we explained that the energy consumption of the building HVAC systems can be reduced by active utilization of TES devices. We hypothesize that the same concept is valid for transport refrigeration systems which are equipped with TES devices.

H6) *Performance of the hybrid thermal energy systems in transport refrigeration can be improved by applying advanced control strategies and using the disturbance previews.*

The logic-based control methods that are proposed for control of TES devices in transport refrigeration systems cannot release the full potential of the TES for efficiency/performance improvement. There are different disturbances affect the system performance. The full potential of the TES device for performance improvement can be unleashed if we use an advanced model-based control strategy which can take the disturbance previews into account of the performance optimization.

1.4 Outline of the Thesis

So far we have presented the motivation behind this research in Section 1.1, the state-of-the-art and background in Section 1.2, and research objectives and hypotheses in Section 1.3. This PhD dissertation has been written in a format which includes a collection of papers. Those papers have either been published or been accepted and put in the waiting lists for publication. Only the papers which include the main contributions relevant to the previously mentioned hypotheses have been enclosed to this note. The remainder of the thesis is as follows. Chapter 2 presents a summary of contributions. They have been divided into for categories: (i) modeling for control and simulations; (ii) indirect load control; (iii) direct load control; and (iv) control of hybrid thermal systems. Chapter 3 concludes the thesis as well as giving a perspective for future research.

In order to have a quick overview of the contributions, they have been listed in the following where for each of them a short abstract is provided.

Paper A [Shafiei et al., 2013c]

Modeling Supermarket Refrigeration Systems for Demand-Side Management

In this paper, a nonlinear gray-box model of a supermarket refrigeration system is presented. Both the thermodynamic states such as cold unit temperatures, suction line pressures, etc. and the electricity usage of the compressors racks can be predicted by the model. The whole system is divided into several modules each is modeled separately. Individual models as well as the integration of them are validated against real data obtained from a supermarket in Denmark. Moreover, a simulation benchmark is created based on the produced model for developing and examining the demand-side management methods in smart grid.

Paper B [Shafiei et al., 2013e]

A Supervisory Control Approach in Economic MPC Design for Refrigeration Systems

In this paper, a supervisory model predictive control strategy is proposed for minimization of electricity cost for supermarket refrigeration systems. The forecasts of electricity price signal and weather temperature are employed under the MPC scheme. The pressure and temperature set-point control loops are separated in the control structure that can facilitate formulation of a convex optimization problem.

Paper C [Shafiei et al., 2013b]

Model Predictive Control for a Thermostatic Controlled System

In this paper, once again the problem of energy cost minimization for supermarket refrigeration systems is addressed by taking into account the forecasts of electricity price and weather temperature. Temperature of the cooling units are governed by thermostatic controllers. The nonlinearity arises from the hysteresis behavior of the local controllers makes the MPC objective nonconvex. An MPC algorithm is proposed which still allows for formulating a convex optimization problem.

Paper D [Shafiei et al., 2013a]

A Decentralized Control Method for Direct Smart Grid Control of Refrigeration Systems

In this paper, a decentralized supervisory control method is proposed for direct load control of supermarket refrigeration systems. No model information is required in this method. The temperature limits/constraints are respected. A novel adaptive saturation filter is also proposed to increase the system flexibility in storing and delivering the energy.

Paper E [Shafiei et al., 2014]

Model Predictive Control for Flexible Power Consumption of Large- Scale Refrigeration Systems

In this paper, an MPC scheme is proposed for direct load control of refrigeration systems. The proposed approach contains the control of cooling capacity as well as optimizing the efficiency factor of the system. A convex optimization problem is formulated under the MPC scheme by introducing a fictitious manipulated variable, and novel incorporation of the evaporation temperature set-point into the optimization problem.

Paper F [Shafiei et al., 2015]

Data-Driven Predictive Direct Load Control of Refrigeration Systems

In this paper, a predictive control using subspace identification is applied for the smart grid integration of refrigeration systems under a direct load control scheme. Two important objectives are fulfilled: To secure high coefficient of performance, and to participate in power consumption management. The control method is fully data-driven without an explicit use of model in the control implementation. As an important practical consideration, the control design relies on a cheap solution with available measurements than using the expensive mass flow meters.

Paper G [Shafiei and Alleyne, 2015]

Model Predictive Control of Hybrid Thermal Energy Systems in Transport Refrigeration

In this paper, a predictive control scheme is designed to control a transport refrigeration system, such as a delivery truck, that includes a vapor compression cycle configured in parallel with a thermal energy storage (TES) unit. A novel approach to TES utilization is introduced and is based on the current and future estimate of the vehicle driving state and load prediction. A cascade control structure is proposed consisting of (i) an outer loop controller that schedules the TES charging profile using a receding horizon optimization, and (ii) an inner loop model predictive controller (MPC) which regulates the TES state of charge while maximizing a derived efficiency factor.

2 | Summary of Contributions

This section summarizes different contributions given by seven papers enclosed in this thesis (Papers A to G). For the time being, Papers A to E have been published through pear review processes, Paper F has been accepted and will be appeared in an special issue of *IET Control Theory and Applications* and Paper G is under the second review for a journal publication. The papers appear in a chronological order in accordance with the progress of the research in the present PhD study. The contributions are divided into four categories:

1) *Modeling for control and simulations*: As it might be the case for many control engineering researches, this research started by developing a mathematical model for the system under the study (*i.e.,* supermarket refrigeration systems). The primary results has been presented in [Shafiei et al., 2013d], and the final results as well as more detailed explanations of the system operation and dynamics has been published in [Shafiei et al., 2013c] which the latter is enclosed as Paper A. A simulation tool based on the model obtained in this study has been developed in Matlab that can be accessed through the refrigeration lab homepage at Aalborg University [SRSim, 2013].

2) *Indirect load control*: The results of control design for demand-side management under indirect load control scheme for supermarket refrigeration systems have been presented in Paper B [Shafiei et al., 2013e] and Paper C [Shafiei et al., 2013b].

3) *Direct load control*: Three different control methods have been applied for demand-side management under indirect load control scheme for supermarket refrigeration systems and the results have been presented in Paper D [Shafiei et al., 2013a], Paper E [Shafiei et al., 2014] and Paper F [Shafiei et al., 2015].

4) *Control of Hybrid Thermal Systems*: The last part of this research has been dedicated to design an advanced control strategy for an state-of-the-art hybrid refrigeration system. The results have been submitted for a journal publication which is presented in Paper G [Shafiei and Alleyne, 2015].

The author also contributed to several other works through supervision of master students' projects and collaboration with other PhD students at Aalborg University. An implementation of direct load control in a laboratory test setup of a water chiller system is presented in [Pedersen et al., 2013]. It was our first attempt to examine an smart grid concept for refrigeration systems. In [Juelsgaard et al., 2013] the connection between a

coordination algorithm for smart grid balancing services and optimal control algorithms for consumer demand response has been analyzed. An evaluation of using simplified models for aggregator design has been given in [Rahnama et al., 2014] where the model developed in Paper A [Shafiei et al., 2013c] together with the direct load controller proposed in Paper E [Shafiei et al., 2014] have been used for simulation study. In another work, two different objectives, one for energy cost optimization and another for regulatory power services have been formulated in one MPC scheme and the results has been presented in [Hermanus et al., 2014].

2.1 Modeling for Control and Simulations

Developing a model for supermarket refrigeration systems seeks two goals within this study. The first one is that the model is required for model-based control design (*i.e.,* MPC), and the second goal is to create a simulation benchmark to examine the smart grid control algorithms devised for refrigeration systems. The modeling results are presented in Paper A [Shafiei et al., 2013c].

The model proposed in Paper A [Shafiei et al., 2013c] possesses most advantages of the preceding researches such as (i) simplifying the behavior of supermarket refrigeration systems as a simulation benchmark for supervisory control; (ii) being very accurate despite its simplicity; (iii) having modularity and reconfigurability; and (iv) being validated by real data. The first principle method is chosen for modeling in which the physical insight is used to define the model structure.

The modeling exercise is performed by a modular approach in which the system is separated into different subsystems (modules), each is modeled and validated separately. This modularity leaves open the possibility of modeling refrigeration systems with different configurations that are adopted in various supermarkets.

2.1.1 Description of CO_2 Booster Configuration System

Danfoss provided real data collected from normal operation of a supermarket refrigeration system in Denmark. The data collection was performed under a separated project [Petersen et al., 2012]. Those data have been used for parameter estimation and model validation in Paper A [Shafiei et al., 2013c].

For refrigeration systems with two temperature zones, medium temperature (MT) and low temperature (LT), the LT zone suction line can be separated from that of the MT by its own rack of compressors. A second rack of compressors is placed at the MT side which further boosts the pressure in the thermodynamic cycle. A basic layout of the booster configuration system is shown in Fig. 2.1. This system has 7 MT and 4 LT display cases.

Due to the fact that the CO_2 refrigeration system described in Paper A [Shafiei et al., 2013c] has been the case of study for control design in Papers B to F, it is described in more details here which help the reader to understand the contribution summaries provided in this part of the thesis. The similar description of the system is given in any of those papers that the reader can easily skip them when going through the papers.

Basically, the whole cycle is based on the vapor-compression cycle explained in Section 1.1.2. The thermodynamic cycle associated with the system in Fig. 2.1 is illustrated by the pressure-enthalpy (P-H) diagram in Fig. 2.2. Starting from the receiver (REC), two-phase refrigerant (mix of liquid and vapor) at point “8” is split out into saturated

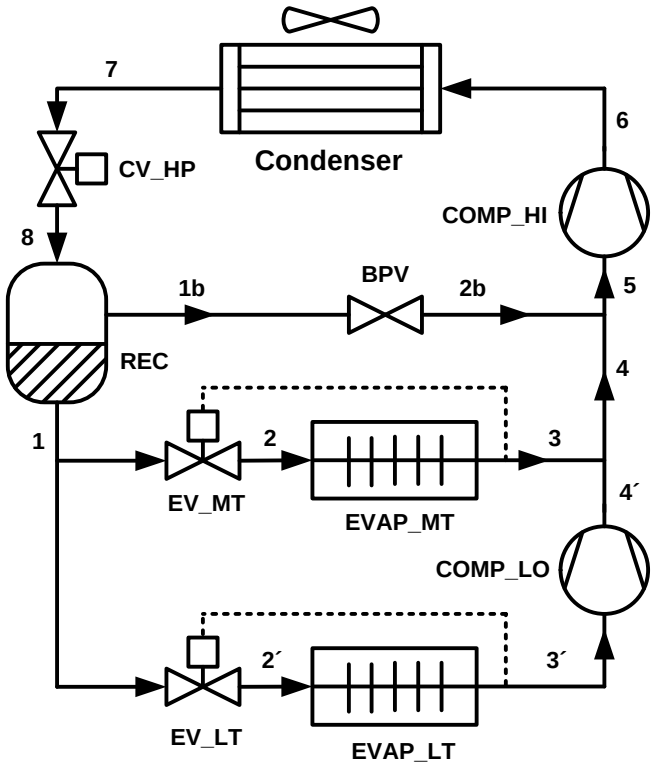

Figure 2.1: Basic layout of a CO2 booster configuration refrigeration system.

liquid (“1”) and saturated gas (“1b”). The latter is bypassed by BPV, and the former flows into expansion valves where the refrigerant pressure drops to the medium (“2”) and low (“2′”) pressures. The expansion valves EV_MT and EV_LT are driven by hysteresis ON/OFF controllers to regulate the temperatures of the MT and LT display cases, respectively. Flowing through medium and low temperature evaporators (EVAP_MT and EVAP_LT), the refrigerant absorbs heat from the cooling medium while a superheat controller is also operating on the valves. That is to make sure the refrigerant leaving the evaporators toward compressors is completely vaporized (only in gas phase). Both pressure and enthalpy of the refrigerant are increased by the low stage compressor rack (COMP_LO) from “3′” to “4′”. All mass flows at the outlet of COMP_LO, EVAP_MT and BPV are collected by the suction manifold at point “5” where the pressure and enthalpy are increased again to the highest point, “6”, by the high stage compressors (COMP_HI). Afterward, the gas phase refrigerant enters the condenser to deliver the absorbed heat from cooling mediums to the surrounding where its enthalpy decreased significantly from “6” to “7” accompanied by a small pressure drop. At the outlet of the high pressure control valve (CV_HP), the pressure drops to an intermediate level and the refrigerant, which is now in two-phase, flows into the receiver and the cycle is completed.

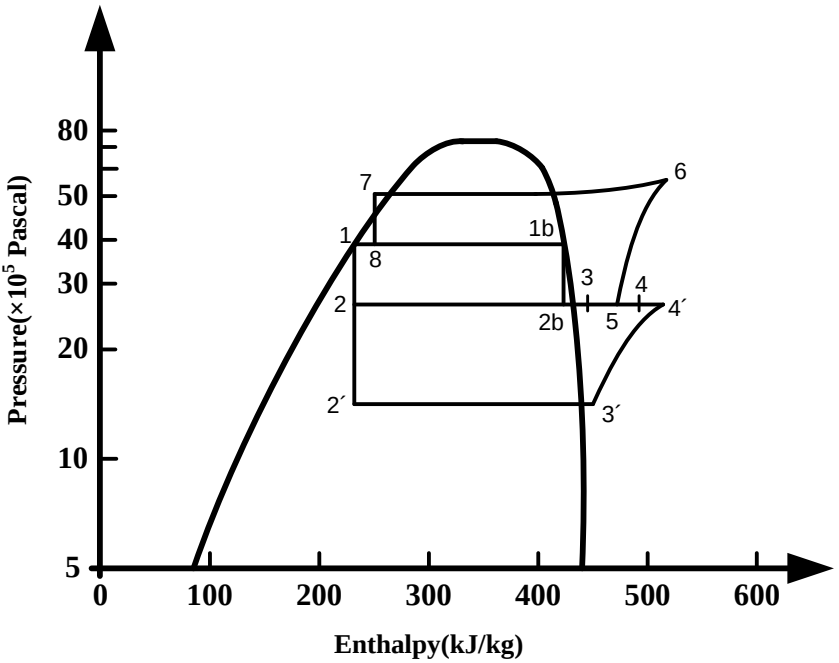

Figure 2.2: P-H diagram of (subcritical) thermodynamic cycle associated with the booster system shown in Fig. 2.1.

2.1.2 Modeling and Validation

The required dynamics that should be modeled are dictated by the modeling purpose. For smart grid control intentions, three types of output variables are of great importance to be predicted by the model: display cases temperatures, suction line pressures and electrical power consumptions of the compressor racks. Estimation of the display cases temperatures are needed to ensure the food temperature constraints. Suction line pressures affects both the evaporation temperatures (accordingly the air temperatures) and the system COP. Estimation of the electric power consumption is required for energy management objectives. The gray-box model presented in Paper A [Shafiei et al., 2013c] only captures the necessary dynamics which are essential for estimation of those three variables, and some other dynamics needed for simulation of the overall cycle. The essential parts of the model is presented in this section, and more details are found in Paper A [Shafiei et al., 2013c].

An off-line identification is performed to estimate the constant parameters and coefficients. The modeling error, computed by dividing the maximum absolute error over the maximum amplitude of variation of the measured signal, is provided on each plot. We use two sets of data:

a) *Training set*: This contains the measured input/output data required for the estimations. The data are selected from an interval during the day time when no defrost cycle takes place.

b) *Validation set*: This contains the measured input/output data required for validating the model after estimation. The data are selected in the same hours of interval as the previous one but from a different working day.

A modular parameter estimation approach is introduced in which the parameters of each subsystem are identified by providing related input-output pairs from measurement data.

Display Cases

In display cases, heat is transferred from foodstuffs to evaporator, $\dot{Q}_{foods/dc}$, and then from evaporator to circulated refrigerant, $\dot{Q}_e$, also known as the cooling capacity. There is however heat load from the environment, $\dot{Q}_{load}$, formulated as a variable disturbance. Here, we consider the measured air temperature at the evaporator outlet as the display case temperature, T_{dc}. Assuming a lumped temperature model, the following dynamical equations are derived based on energy balances for the foregoing heat transfers.

$$MCp_{foods}\frac{dT_{foods}}{dt} = -\dot{Q}_{foods/dc} \tag{2.1}$$

$$MCp_{dc}\frac{dT_{dc}}{dt} = \dot{Q}_{load} + \dot{Q}_{foods/dc} - \dot{Q}_e \tag{2.2}$$

where MCp denotes the corresponding mass multiplied by the heat capacity. The energy flows are

$$\dot{Q}_{foods/dc} = UA_{foods/dc}(T_{foods} - T_{dc}), \tag{2.3}$$

$$\dot{Q}_{load} = UA_{load}(T_{indoor} - T_{dc}) \tag{2.4}$$

and

$$\dot{Q}_e = UA_e(T_{dc} - T_e) \tag{2.5}$$

where UA is the overall heat transfer coefficient, h_{oe} and h_{ie} are enthalpies at the outlet and inlet of the evaporators and are nonlinear functions of the evaporation temperature, and T_{indoor} is the supermarket indoor temperature.

Identification results for the display case temperatures are illustrated in Fig. 2.3. For a fair comparison, all temperature plots have the same scale. The value of the modeling error provided on each plot shows the best fit for the 5th and the worst fit for the 7th display case. The result for the LT display cases are given in Paper A [Shafiei et al., 2013c].

Suction Manifold

The suction manifold is modeled by a dynamical equation by using the suction pressure as the state variable and employing the mass balance as [Sarabia et al., 2009],

$$\frac{dP_{suc}}{dt} = \frac{\dot{m}_{dc} + \dot{m}_{dist} - \dot{V}_{comp}\rho_{suc}}{V_{suc}\, d\rho_{suc}/dP_{suc}}, \tag{2.6}$$

where the compressor bank is treated as a big *virtual compressor*, $\dot{m}_{dc}$ is the total mass flow of the display cases, $\dot{m}_{dist}$ is the disturbance mass flow including the mass flow from

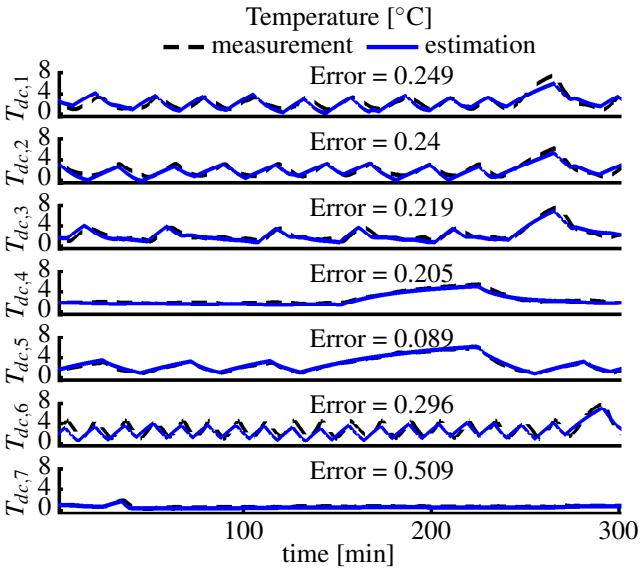

(a)

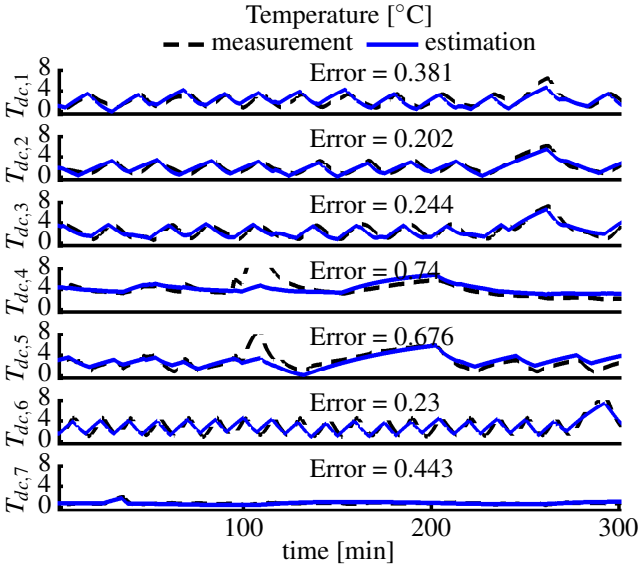

(b)

Figure 2.3: Estimation of display case temperatures. The 5th display case shows the best fit and the worst fit is related to 7th display case, which is still a good estimation. (a) Estimation using training data; (b) Estimation using validation data.

the freezing rooms and the bypass valve, and V_{suc} is the volume of the suction manifold.

$\dot{V}_{comp}$ is the volume flow out of the suction manifold,

$$\dot{V}_{comp} = f_{comp}\eta_{vol}V_d, \tag{2.7}$$

where f_{comp} is the virtual compressor frequency (total capacity) of the high stage compressor rack in percentage, V_d denotes the displacement volume, and η_{vol} is clearance volumetric efficiency. The following equation is used for calculation of the electrical power consumption:

$$\dot{W}_{comp} = \frac{1}{\eta_{me}}\dot{m}_{ref}(h_{o,comp} - h_{i,comp}), \tag{2.8}$$

where $\dot{m}_{ref}$ is the total mass flow into suction manifold, and $h_{o,comp}$ and $h_{i,comp}$ are the enthalpies at the outlet and inlet of the compressor bank. These enthalpies are nonlinear functions of the refrigerant pressure and temperature at the calculation point. The constant η_{me} indicates overall mechanical/electrical efficiency considering mechanical friction losses and electrical losses [Pérez-Segarra et al., 2005]. The enthalpy of refrigerant at the manifold inlet is bigger than that of the evaporator outlet ($h_{i,comp} > h_{oe}$) due to disturbance mass flows.

Fig. 2.4 shows the result of identification practice for estimating the suction line pressure and the power consumption of the higher stage compressor rack. The result for the LT zone are given in Paper A [Shafiei et al., 2013c].

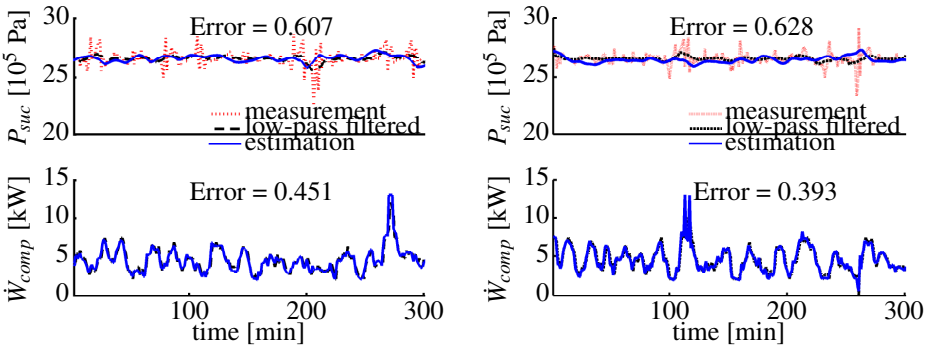

Figure 2.4: Suction pressure and power consumption estimations. Variation of consumption is mainly because of changing mass flow due to hysteresis and superheat control of expansion valves. Mechanical-electrical efficiency is obtained as $\eta_{me} = 0.65$. (a) Estimation using training data; (b) Estimation using validation data.

Even though the simple first order model introduced for suction manifold cannot generate the high frequency parts of the pressure signal, it can fairly estimate a low pass filtered version of the suction pressure. The bottom plots show the estimation of the power consumption.

2.2 Indirect Load Control

In this sections the problem of energy cost minimization for supermarket refrigeration systems is considered assuming that the forecast of disturbances like electricity price and weather temperature are available. This problem is addressed in Papers B and C [Shafiei et al., 2013e, Shafiei et al., 2013b]. The following aspects are the same in both of them:

- The refrigeration system is the booster system presented in Section 2.1.1.
- The cost optimizing control is placed in a supervisory level and the local controllers are remained unchanged.
- The supervisory controller is an MPC.
- A heuristic algorithm is designed for set-point control of the suction pressures
- A linear estimation of the system COP is presented.

Due to the nonlinearities present in calculation of the power consumption, the problem of cost minimization is in this case a nonconvex problem that is not computationally efficient for real-time implementations. It is shown in Papers B and C [Shafiei et al., 2013e, Shafiei et al., 2013b] that how a convex optimization problem can be formulated in a supervisory control level under an MPC scheme. Contributions of the two papers are different in terms of the type of the local controllers which are in operation. Consequently two different MPC algorithms are used for the supervisory control design. In Paper B [Shafiei et al., 2013e] the local controllers are linear (PI) in contrast to the nonlinear (Hysteresis) local controllers considered in Paper C [Shafiei et al., 2013b].

Supervisory Control Strategy

Fig. 2.23 shows the control system structure consists of two control loops, the local controllers are placed in an inner loop and the supervisory controller is located in the outer loop. The local controllers are responsible for regulation of the pressures and temperatures to the required set-points, and the supervisory controller should decide optimal set-points by which the total energy cost is minimized.

The compressors are responsible for regulating the suction pressure to a usually fixed set-point. Due to the different timescales between the dynamics of the compressors and the display case (The suction pressures can be regulated much faster than the display cases temperatures), the static model (2.7) is used for the compressors.

In Paper B [Shafiei et al., 2013e] the display case temperatures are regulated by distributed PI controllers using pulse width modulation techniques for expansion valves available in Danfoss products. Using linear local controllers gives the possibility of applying the supervisory MPC formulation proposed in [Balbis et al., 2006]. If nonlinear hysteresis (thermostatic) local controllers were used, it makes the MPC formulation more difficult. Paper C [Shafiei et al., 2013b] addresses this difficulty by proposing a new MPC formulation for thermostatic control systems. The set-point control structure in this case is shown in Fig. 2.6.

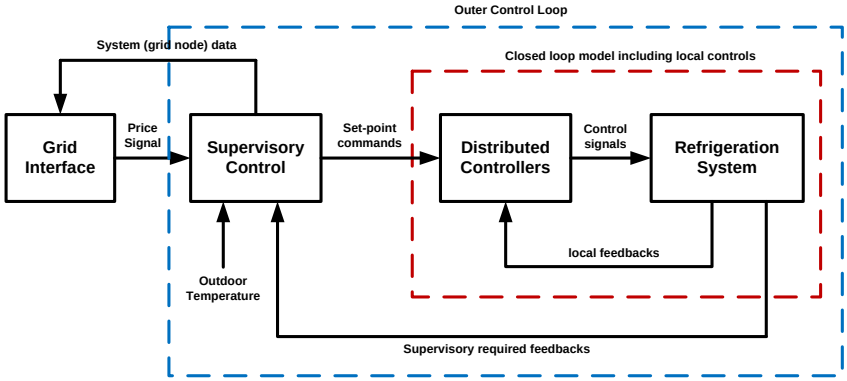

Figure 2.5: A supervisory control structure for refrigeration systems.

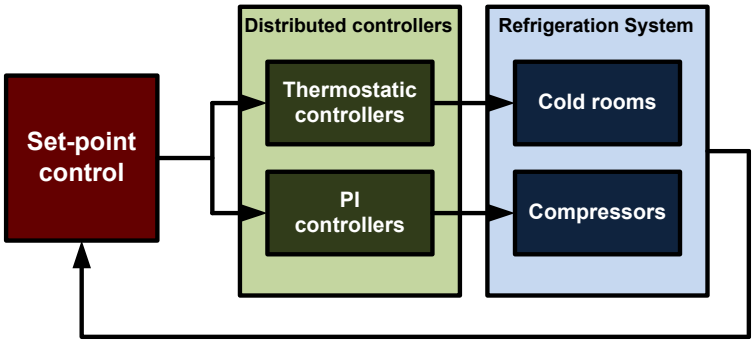

Figure 2.6: Set-point control structure for refrigeration systems with thermostatic temperature controllers.

Intuitive Pressure Control

We have proposed the following heuristic algorithm for the pressure set-point control using the fact that the near optimal pressure value will be achieved by increasing the suction pressure until one of the expansion valves is kept almost fully open, Paper B [Shafiei et al., 2013e]. A sampling time equal to one minute for the set-point controller ensures that the compressor speed is regulated to its steady-state value. Moreover, an upper limit $P_{suc,max}$ is put to keep a safety margin for pressure difference required for circulating the refrigerant. The lower limit $P_{suc,min}$ is put due to the limitations of compressor total capacities, and also the safety issues regarding the high pressure difference.

Because of the ON and OFF states of the valves in case of using thermostatic temperature controllers, the algorithm has been slightly modified in Paper C [Shafiei et al., 2013b] by applying moving average of the opening degrees for calculating the maximum state between the valves.

Algorithm 1 Calculation of the set-point value for the suction pressure

if $P_{suc} < P_{suc,max}$ and $\max(OD_i) < \delta_{max}$ **then**
    Increase the pressure set-point
else if $P_{suc} > P_{suc,min}$ and $\max(OD_i) > \delta_{min}$ **then**
    Decrease the pressure set-point
else
    Keep the previous set-point

Supervisory MPC

Here, the control objective is to minimize the operating cost. The economic objective function is achieved by multiplication of the real-time electricity price $e_p(t)$ by the power consumption $\dot{W}_{c,tot}$ at given time t. So, the energy cost, J_{ec} is computed over the specified time interval $[T_0 \;\; T_N]$ as

$$J_{ec} = \int_{T_0}^{T_N} e_p \dot{W}_{c,tot} dt. \tag{2.9}$$

Replacement of (2.8) for power calculation in (2.9) results in a nonconvex objective function (The details are given in Paper B [Shafiei et al., 2013e]). The nonconexity can be avoided by recovering the power calculation from the COP definition. The total COP is defined as ratio of the total cooling capacity over the total power consumption of the compressors.

$$COP = \frac{\dot{Q}_{e,tot}}{\dot{W}_{c,tot}} \tag{2.10}$$

The cost function (2.9) is rewritten using (2.10) as

$$J_{ec} = \sum_{k=0}^{N-1} \left\| e_p \frac{\dot{Q}_{e,tot}}{COP} \right\|_2^2, \tag{2.11}$$

where the COP calculation based on the mass flow and thermodynamic states is given in Paper B [Shafiei et al., 2013e], and $\dot{Q}_{e,tot} = \sum_{i=1}^{m} \dot{Q}_{e,i}$ with m indicating the number of cooling units. As shown in Fig. 2.7a, the COP is linearly estimated from the outdoor temperature. Fig. 2.7b shows the COP prediction for the next horizon based on the linear fit estimation obtained from the previous 24 hours of the historical data, and the prediction of the outdoor temperature for the next 24 hours. Since the pressure may change during the operation and also the outdoor temperature varies during the day, the linear fit is updated in each time step to avoid the significant bias in predictions.

The temperature dynamics (2.1)-(2.4) for each display case can be expressed by the following linear discrete-time state-space equation:

$$\begin{cases} x[k+1] = Ax[k] + B_1 u[k] + B_2 d[k] \\ y[k] = Cx[k] \end{cases} \tag{2.12}$$

with the states $x = \begin{bmatrix} T_{foods} & T_{cr} \end{bmatrix}^T$, the input $u = \dot{Q}_e$, and the disturbance $d = T_{indoor}$. The food temperature in Paper C [Shafiei et al., 2013b] is estimated using a reduced order

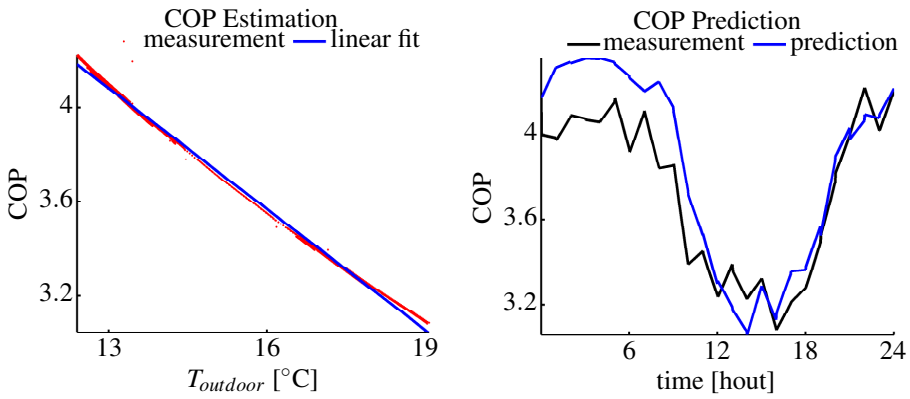

Figure 2.7: COP estimation and prediction. (a): Estimation of the system COP as a linear function of the outdoor temperature. (b): Prediction of the system COP using the obtained linear estimation and prediction of the outdoor temperature.

linear observer and is subject to the following constraint:

$$\begin{aligned} T_{min} - \varepsilon \Delta T_{foods} \leq T_{foods} \leq T_{max} + \varepsilon \Delta T_{foods}, \\ \varepsilon \geq 0, \end{aligned} \tag{2.13}$$

where ε is a slack variable used to soften the constraint and ensure the feasibility of soliving the optimization problem. The violations from temperature limits are penalized by adding the term $\rho_\varepsilon \varepsilon$ to the objective function. ΔT_{foods} and ρ_ε should be defined such that the violation occurs rarely. The input is also constrained as

$$0 \leq u \leq \dot{Q}_{e,max}. \tag{2.14}$$

Linear local controllers — In the case where linear local controllers are placed, the MPC formulation proposed in [Balbis et al., 2006] can be applied which results in the following optimization problem. The state-space equation in (2.15) includes both the system and local controller dynamics where r is the temperature set-point. The derivation of this equation is given in Paper B [Shafiei et al., 2013e].

$$\begin{aligned} \underset{r,\varepsilon}{minimize} \quad & J_{ec} + J_{\Delta u} + \rho_\varepsilon \varepsilon \\ subject\ to \quad & \begin{cases} X_s[k+1] = AX_s[k] + B_1 r[k] + B_2 d[k] \\ Y_s[k] = CX_s[k] + Dr[k] \end{cases} \\ & T_{min} - \varepsilon \Delta T_{foods} \leq T_{foods} \leq T_{max} + \varepsilon \Delta T_{foods} \\ & \varepsilon \geq 0 \\ & 0 \leq u \leq 1 \end{aligned}, \tag{2.15}$$

with

$$J_{\Delta u} = \sum_{k=1}^{N-1} \| R_{\Delta u} (r[k] - r[k-1]) \|_2^2 . \tag{2.16}$$

where $R_{\Delta u}$ is a diagonal matrix of tuning weights. The above objective function penalizes the rate of change of the set-point to avoid the oscillatory behavior in control commands. In this control design the input is the opening degree of the expansion valve $u - OD$ assuming

$$\dot{Q}_e = \beta_k OD, \tag{2.17}$$

where β_k is a time varying parameter updated at each time instant when the next move for MPC is calculated. The power consumption resulted from applying the MPC scheme using (2.15) is depicted in Fig. 2.9. An cost reduction of 32% is achieved compared with a low-energy simple scenario where the temperature set-points are fixed to highest levels (only 0.5 °C below the maximum limits).

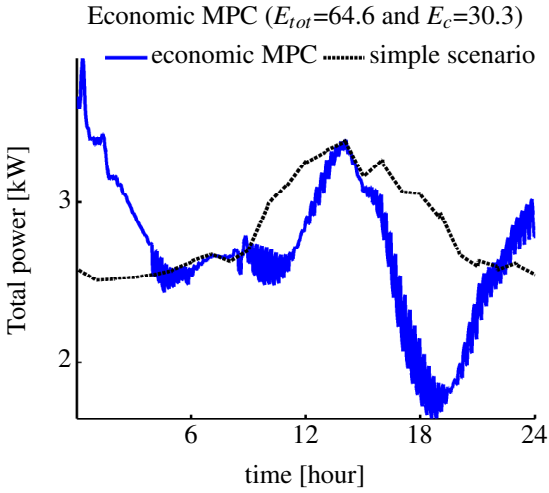

Figure 2.8: Power consumptions resulted from applying economic MPC and a low-energy operation.

Thermostatic local controllers — If thermostatic local controllers are used, the MPC scheme presented in Paper B [Shafiei et al., 2013e] cannot be applied due the nonlinearity imposed by the hysteresis behavior of the local control system. Instead, we have proposed a new MPC algorithm in Paper C [Shafiei et al., 2013b] which is provided in Algorithm 2. At each MPC trial the optimal cooling capacity $u = \dot{Q}_e$ is calculated. Then the linear dynamics (2.12) is used to predict the future display case temperature at the next time instant ($x_2[k+1]$). Finally this temperature is applied as the set-point T_{sp} to the thermostatic controllers. Note that $x = \begin{bmatrix} \hat{x}_1 & x_2 \end{bmatrix}^T$ where $\hat{x}_1$ is the estimation of the food temperature.

Fig. 2.9 shows the power consumption after applying the designed MPC together with Algorithm 1. An economic saving of 34% is achieved that is very close to the achievement when using the supervisory control in Paper B [Shafiei et al., 2013e].

Algorithm 2 Supervisory MPC algorithm for set-point control with economic objective.

Prediction

Load

COP and $T_{outdoor}$ from previous horizon

e_p and $T_{outdoor}$ predictions

Compute

COP prediction based on its previous horizon values and $T_{outdoor}$

Solve

$$\begin{aligned} \underset{u,\varepsilon}{\text{minimize}} \quad & J_{ec} + J_{\Delta u} + \rho_\varepsilon \varepsilon \quad \text{(over the horizon)} \\ \text{subject to} \quad & x[k+1] = A_d x[k] + B_{d,1} u[k] + B_{d,2} d[k] \\ & \hat{x}_1 \geq T_{min} - \varepsilon \Delta T_{foods} \\ & \hat{x}_1 \leq T_{max} + \varepsilon \Delta T_{foods} \\ & \varepsilon \geq 0 \\ & 0 \leq u \leq \dot{Q}_{e,max} \end{aligned}$$

Update

$u[k]$ = first move in obtained u

$x[k+1] = A_d x[k] + B_{d,1} u[k] + B_{d,2} d[k]$

$T_{sp} = x_2[k+1]$ where $x = \begin{bmatrix} \hat{x}_1 & x_2 \end{bmatrix}^T$

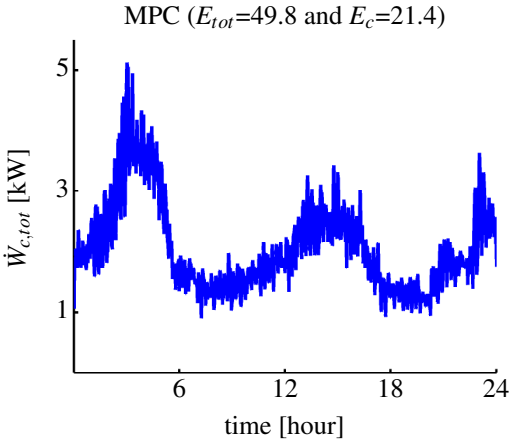

Figure 2.9: Power consumption after applying MPC (Algorithm 2) together with intuitive suction pressure control (Algorithm 1).

2.3 Direct Load Control

In this contribution, the refrigeration system undertakes both upward and downward power consumption management under the direct load control framework for a specific

period of time in response to an activation signal. An independent service operator aggregates a large number of loads for this purpose and sends the activation signals in accordance with the contingency conditions [Heffner et al., 2007]. During the activation period, refrigeration systems should follow the power reference assigned by the aggregator which operates within a hierarchical structure shown in Fig. 2.10.

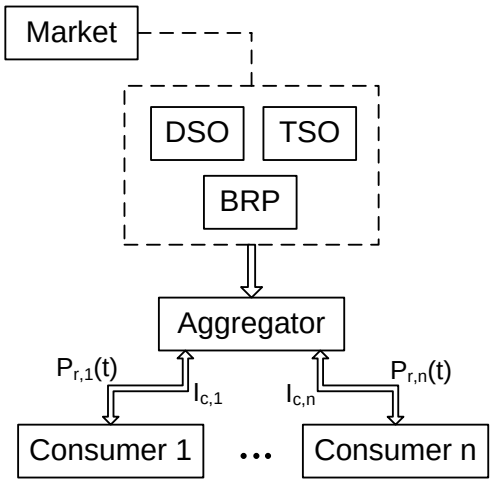

Figure 2.10: Hierarchical direct smart grid control layout. The higher level parties trade the flexibility, in terms of the energy management, with the aggregators according to the market conditions. The aggregators, on other hand, are in the two-way communication with the energy consumers. They receive the consumer information I_c and send the power reference signal P_r during the DR event.

This set-up enables the aggregator to offer flexibility, in terms of the energy management, to the higher level operators like TSO (Transmission System Operator), DSO (Distribution System Operator) or BRP (Balance Responsible Party). The problem of aggregator design, information flow and grid side strategies is outside the scope of this work, but the general and specific relevances can for example be found in [Trangbaek et al., 2011] and [Rahnama et al., 2014].

We have employed three different control strategy for the direct load control of supermarket refrigeration systems:

1) *Decentralized control*: This is a simple approach using decentralized P and PI controllers for regulation of the power consumption by manipulating the temperature setpoints. The contribution has been presented in Paper D [Shafiei et al., 2013a].

2) *Model predictive control*: This method requires a high fidelity model of the refrigeration system specific for the system under control. The control performance in terms of the power regulation is higher than the first method, but on the other hand the complexity in terms of the real-life implementation is also increased due to the fact that for each specific supermarket with a certain configuration, the dynamic model needs to be obtained. Paper E [Shafiei et al., 2014] presents this method.

3) *Data-driven predictive control*: This approach has been adopted to take the advantage of having high performance using prediction of the system dynamics, and at the same time to facilitate the real-life implementation by making the method generally applicable for a broad range of supermarket refrigeration systems. This method has been presented in Paper F [Shafiei et al., 2015].

2.3.1 Decentralized Control Approach

In Paper D [Shafiei et al., 2013a], we have proposed a simple but efficient supervisory control structure including P and PI controllers that enable balancing services of supermarket refrigeration systems in the smart grid. The heuristic algorithm proposed in Paper B [Shafiei et al., 2013e] for the pressure set-point control is replaced by a proportional controller. Similar to the control strategy adopted in Paper B [Shafiei et al., 2013e], the supervisory controller (which is now simply a PI) assigns set-points to the air temperatures inside the cooling units. No model information is required for the control implementation. The food temperatures should be constrained within the permissible limits. So we put a saturation filter at the control output that restricts the air temperature and consequently the food temperature. To handle integrator windup because of using the saturation filter, a decentralized structure equipped with anti-windup features is designed. In contrast to the MPC schemes, the model free controller cannot predict the future temperatures of the air and of the foodstuffs. To conclude the food safety, the same limits for the food temperatures should be considered for saturation limits applying to the air temperature. This however limits the range of control effort, and consequently decreases the control system flexibility in governing the power consumption. We have proposed an *adaptive saturation filter* that can effectively remove this restriction as well as respecting the food temperatures.

Practical considerations for facilitating industrial implementations are, first, we do not use any model information in our control practice, and second, we do not replace the existing local distributed controllers in the system.

Pressure Set-Point Control

Recalling from Section 2.2, Algorithm 1 is based on the optimality hypothesis that the optimum suction pressure is achieved by increasing the suction pressure such that one the expansion valves (corresponding to the most loaded cooling medium) needs to be almost fully open. Here we apply the same optimality condition by designing a simple proportional controller with saturation limits (to respect the pressure constraints). In order to prevent a large proportional gain and consequently a large variation of the set-point, the control command is considered as the change of the set-point,

$$\Delta P_{ref} = K_p(r_{OD} - \overline{OD}_{max}) \tag{2.18}$$

where K_p is the proportional gain, $\overline{OD}$ is the vector of opening degree of the valves, $\overline{OD}_{max}$ is the maximum value between the opening degrees, $r_{OD} = 1 - \varepsilon$ is the reference value that the mostly opened valve should follow. Note that r_{OD} should be a little bit smaller than 1 to ensure that only one valve is almost fully open at the same time thereby ensuring the minimum cooling capacity required for maintaining the temperature limits. The pressure set-point control structure is shown in Fig. 2.11.

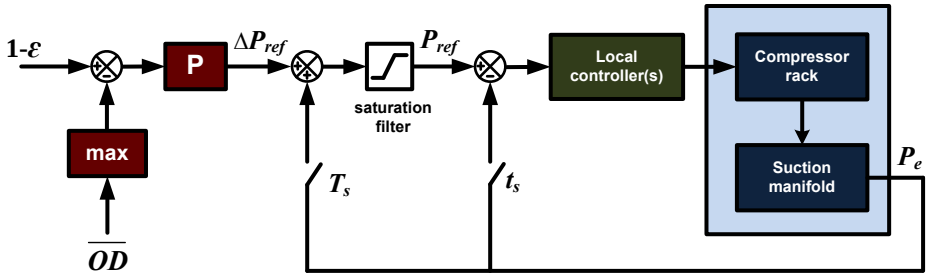

Figure 2.11: Control structure for set-point control of the suction pressure. The local controllers use a very shorter sampling period (t_s) than that of the supervisory P controller (T_s). More details are given in Remark 2 in Paper D [Shafiei et al., 2013a].

Temperature Set-Point Control

The electrical power consumption of the compressors is regulated by changing the temperature set-points. This approach is appropriate for the situation where the power reference ramps up/down from the baseline with an slow rate. Temperature set-point control structure is presented in Fig. 2.12. The temperature constraints are applied by putting the saturation filters with the following saturation bounds at the output of the ith PI controller.

$$\overline{U}_i = (\overline{T}_i - T_{0,i}), \tag{2.19}$$

and

$$\underline{U}_i = (\underline{T}_i - T_{0,i}), \tag{2.20}$$

where $\overline{T}$ and $\underline{T}$ are respectively the upper and lower limits of the food temperature, and T_0 is the fixed set-point for normal operation (that is when the system is not under the direct control feedback loop).

Using the decentralized structure we can add an anti-windup block to each PI controller. This might not be possible to apply in the same way when a centralized PI controller (with distributed gains) is used. The input error feedbacks $e_{s,i}$ in Fig. 2.12 are used for avoiding the integrator windups [Åström and Hägglund, 2006]. A sample PI unit including the anti-windup block is shown in Fig. 2.13.

Adaptive Saturation Filter

Putting the same temperature limits as required for the foods on the air temperatures inside the cooling units is quite restrictive. The air temperature can go beyond the limits for some time before the food temperature can reach the limit point. The adaptive saturation filter designed in Paper D [Shafiei et al., 2013a] provides more freedom to change the air temperature while ensuring the food temperature to be within the limits. In the proposed filter, saturation limits are adaptively updated based on the current value of the food temperature. Each PI unit in the control structure of Fig. 7.3 should be updated to the one shown in Fig. 2.14.

The adaptive algorithm for updating the saturation limits is described by

$$u_{max,i}(t) = \overline{U}_i + K_{u,i}(\overline{T}_i - T_{foods,i}(t)), \tag{2.21}$$

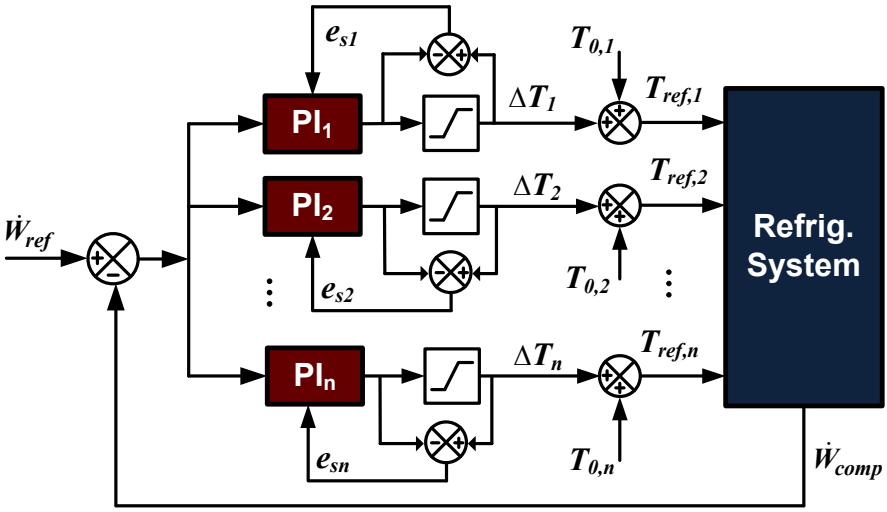

Figure 2.12: Control structure for set-point control of the air temperatures in cooling sites.

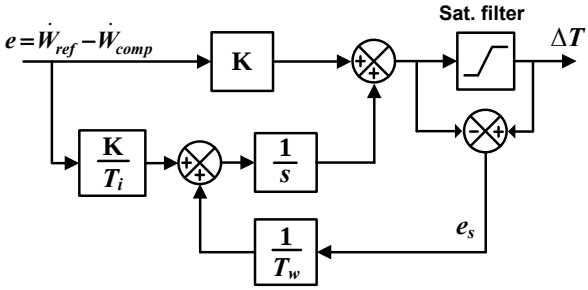

Figure 2.13: PI controller with anti-windup.

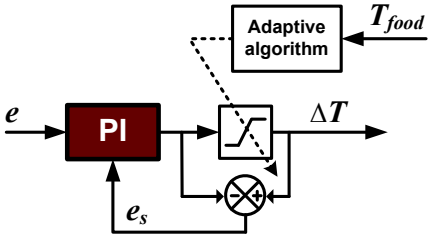

Figure 2.14: PI controller with anti-windup and adaptive saturation filter.

and

$$u_{min,i}(t) = \underline{U}_i + K_{l,i}(\underline{T}_i - T_{foods,i}(t)), \tag{2.22}$$

where $K_{u,i}$ and $K_{l,i}$ are constant parameters defined as *saturation limit gains*. The right-

hand side of the above equations are the adaptive terms added to (2.19) and (2.20). Analyses about the filter tuning and functioning are given in Paper D [Shafiei et al., 2013a].

Power Regulation Service

In a period of 24 hours, the power reference scenario is such that the aggregator demands the base-line power consumption until 5:00 AM. Following that, it demands an increase up to 20% over the base-line for 5:00-15:00, and a reduction down to 20% below the base-line for 15:00-20:00. Finally the reference gets back to the base-line from 20:00-24:00 to be ready for demand response for the next day. The power regulation results are shown in Fig. 2.15. Three cases of using different controllers are illustrated for the sake of comparison, one using a centralized PI, another using the decentralized PIs including anti-windups, and the last one using the decentralized PIs equipped with adaptive saturation filters. All three methods perform the same when increasing the power consumption (5:00-15:00), but the last method outperforms the other two for the decreasing period (15:00-20:00). The reason is that for this power reduction period the air temperatures reach the limit values that can be effectively handled by the adaptive saturation filter. The centralized controller cannot govern the power consumption back to the baseline after 20:00 h because of the integrator windup.

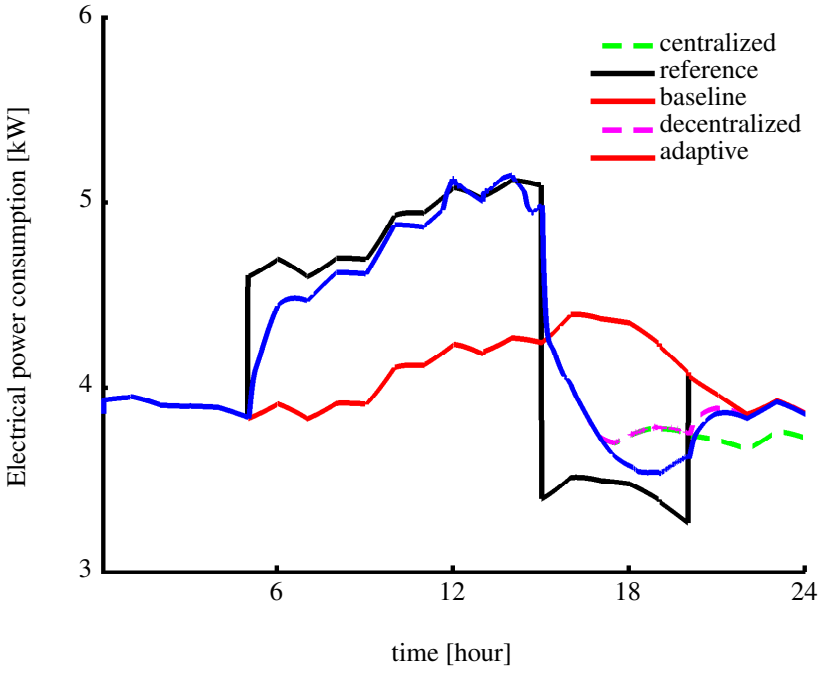

Figure 2.15: Electrical power consumption of the compressor racks in case of centralized control (dotted), decentralized control (dashed), and decentralized control with adaptive saturation filter (solid).

2.3.2 Model Predictive Control Approach

It is shown in Paper E [Shafiei et al., 2014] that by virtue of the faster dynamics of the flow change inside the evaporator comparing to the thermal dynamics, it is possible to describe the cooling capacity by static nonlinearity in terms of the valve opening degree and the evaporation temperature. It is simply achieved by choosing an appropriate sampling time for the MPC. At this point, the model would look like a Hammerstein model. Then, by taking the cooling capacity as fictitious manipulated variable, a model predictive control is formulated using a novel incorporation of the evaporation temperature into the optimization problem. It leads to 22% higher system coefficient of performance (COP).

Problem Statement

Here we would like to design a control algorithm for large-scale refrigeration systems such that their power consumptions would follow the references assigned by an aggregator while their coefficient of performances being optimized as a secondary objective. The system COP is highly influenced by the evaporation temperature (see Paper E [Shafiei et al., 2014] for detailed explanations) and its maximum value can be achieved by maximizing the evaporation temperature.

The objective function for a power following optimization problem is defined as:

$$J_{Pow} = \sum_{k=1}^{N} \|Pow_c[k] - Pow_{ref}[k]\|_2^2, \tag{2.23}$$

where Pow_{ref} is the power reference, k denotes the current time instant, and N is the prediction horizon in terms of number of time steps (samples). Manipulated variables are the opening degrees of the expansion valves (OD) and the evaporation temperature set-point ($\hat{T}$). As previously discussed in Section 2.2 the power consumption can be calculated from (2.10) as

$$Pow_c = \frac{\dot{Q}_{e,tot}}{COP}. \tag{2.24}$$

Due to the nonlinearities associated with the COP calculation, replacing (2.24) into (2.23) give a nonconvex cost function. In the sequel it is shown that how a convex optimization problem can be formulated by (i) introducing a fictitious manipulated variable; (ii) novel incorporation of T_e into the MPC scheme; and (iii) choosing appropriate sampling time and prediction horizon.

Problem Convexification using Synthetic Input

Considering $u = \dot{Q}_e$ as a fictitious manipulated variable, the temperature dynamics can be described linear system (2.12). The cooling capacity $\dot{Q}_e$ is given by

$$\dot{Q}_e = UA_e(T_{air} - T_e), \tag{2.25}$$

where UA is the overall heat transfer coefficient, T_e is the evaporation temperature, and T_{indoor} is the supermarket indoor temperature. The heat transfer coefficient between the refrigerant and the display case temperature, UA_e, is described as a linear function of the mass of the liquefied refrigerant in the evaporator [Sarabia et al., 2009],

$$UA_e = k_m M_r, \tag{2.26}$$

where k_m is a constant parameter. The refrigerant mass, $0 \leq M_r \leq M_{r,max}$, is subject to the following dynamic [Petersen et al., 2012],

$$\frac{dM_r}{dt} = \dot{m}_{r,in} - \dot{m}_{r,out}, \tag{2.27}$$

where $\dot{m}_{r,in}$ and $\dot{m}_{r,out}$ are the mass flow rate of refrigerant into and out of the evaporator, respectively. The entering mass flow is determined by the opening degree of the expansion valve and is described by the following equation:

$$\dot{m}_{r,in} = OD\ KvA\sqrt{\rho_{suc}(P_{rec} - P_e)} \tag{2.28}$$

where OD is the opening degree of the valve with a value between 0 (closed) to 1 (fully opened), P_{rec} and P_e are receiver and suction manifold (evaporating) pressures, ρ_{suc} is the density of the circulating refrigerant, and KvA denotes a constant characterizing the valve. The leaving mass flow is given by

$$\dot{m}_{r,out} = \frac{\dot{Q}_e}{\Delta h_{lg}} \tag{2.29}$$

where Δh_{lg} is the specific latent heat of the refrigerant in the evaporator, which is a non-linear function of the suction pressure (or equivalently evaporation temperature). When the mass of refrigerant in the evaporator reaches its maximum value ($M_{r,max}$), the entering mass flow is equal to the leaving one. The input constraints are

$$0 \leq u \leq u_{max}, \tag{2.30}$$

with $u_{max} = UA_{e,max}(T_{air} - T_e)$ where $UA_{e,max} = k_m M_{r,max}$. Now the convex cost function can be formulated using (2.24) and sum of the fictitious control inputs as

$$J_{Pow} = \sum_{k=1}^{N} \left\| \frac{\sum_{i=1}^{m} u_i[k]}{COP} - Pow_{ref}[k] \right\|_2^2. \tag{2.31}$$

Novel Incorporation of T_e into MPC Scheme

Note that evaporation temperature ($\hat{T}_e$) of the MT section is different from of the LT section, and remind the fact that several cooling units at each section have the same corresponding evaporation temperature. The COP can be preserved at the highest point by maintaining T_e as high as possible up to the point that enough cooling capacity is provided to cold reservoirs to preserve the required temperatures. This can be achieved by adding the following cost to the objective function.

$$J_{T_e} = \sum_{k=1}^{N} \|\hat{T}_e[k] - T_{e,max}\|_2^2 \tag{2.32}$$

where $T_{e,max}$ is the maximum value that T_e is allowed to rise to. Thus the MPC pushes the evaporation temperature up to the highest value. It should also be constrained as $\hat{T}_e \leq T_{e,max}$. Moreover, in order to make sure that the resulted cooling capacity from the optimization problem is coincide with the evaporation temperature, the upper limit of the input constraint (2.30) is modified to

$$u_{max} = UA_{e,max}(x_2 - \hat{T}_e) \tag{2.33}$$

with $x_2 = T_{air}$.

MPC Algorithm

In the proposed MPC provided in Algorithm 3 the objective function consists of the power tracking cost (2.31), cost of the input change (2.17), performance objective (2.32) and the term for penalizing the slack variable ε. The outcomes of solving the optimization problem are the fictitious inputs $\mathbf{u}$ and the evaporation temperature set-point $\hat{T}_e$. The latter can be applied as the set-point control signal, but $\mathbf{u}$ is used in (2.34) to calculate the opening degrees $\mathbf{O}D$ to be applied as the control inputs to the expansion valves.

$$OD = K_e(\hat{T}_e)u, \tag{2.34}$$

where $K_e(\hat{T}_e) = \left[\Delta h_{lg} K v A \sqrt{\rho_{suc}(P_{rec} - P_e)}\right]^{-1}$ is updated at each sample time k (note that P_e is a nonlinear function of T_e).

Algorithm 3 MPC implementation

Prediction

Load

Pow_{ref} from higher level aggregator

Compute

COP and keep it fixed all over the horizon

Solve

$$\begin{aligned} \min_{\mathbf{u},\hat{T}_e,\varepsilon} \quad & J_{pow} + W_{\mathbf{u}} J_{\Delta\mathbf{u}} + W_e J_{T_e} + W_r \|\varepsilon\|_2^2 \\ \text{subject to} \quad & \mathbf{x}[k+1] = \mathbf{A}x[k] + \mathbf{B}u[k] + \mathbf{B}_d d[k] \\ & \mathbf{x}_{1,min} - \varepsilon \le \mathbf{x}_1[k] \le \mathbf{x}_{1,max} + \varepsilon \\ & \varepsilon \ge 0 \\ & 0 \le \mathbf{u}[k] \le \mathbf{U}A_{e,max}(\mathbf{x}_2 - \hat{T}_e) \\ & \hat{T}_e \le T_{e,max} \end{aligned}$$

Update

$\mathbf{u}[k]$ = first move in obtained $\mathbf{u}$

$\hat{T}_e[k]$ = first move in obtained $\hat{T}_e$

$\mathbf{O}D[k] = \mathbf{K}_e(\hat{T}_e)\mathbf{u}[k]$

Control inputs

$\mathbf{O}D[k],\ \hat{T}_e[k]$

A simulation experiment is performed which illustrates the capability of the proposed control algorithm in performing the direct power control in case of significant changes in the power reference when undertaking upward and downward regulation services. The result is shown in Fig. 2.16. The power reference is increased 75% at 12 PM up to 13 PM for downward regulation services. For upward regulation, the refrigeration system needs to store thermal energy sometime ahead of the service start time. Consequently, at 15 PM the power reference is increased 12.5% for energy storage, and then is dropped significantly (87.5%) at 18 PM up to 19 PM.

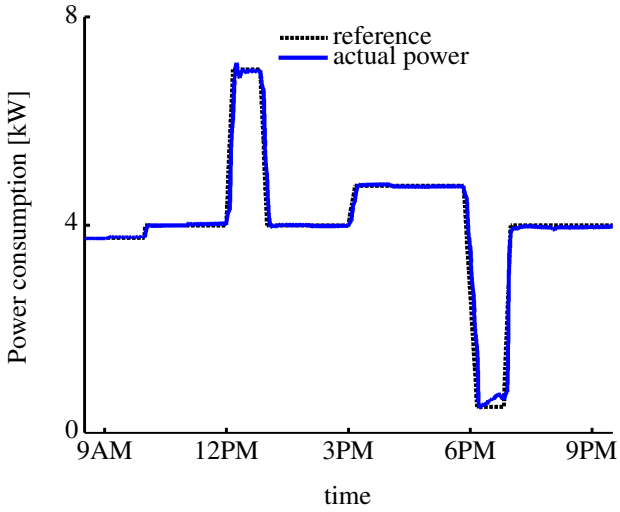

Figure 2.16: Power reference following for energy balancing services.

2.3.3 Data-Driven Predictive Control Approach

So far we have presented two different contributions toward direct load control of refrigeration systems. We saw that the decentralized approach proposed in Paper D [Shafiei et al., 2013a] is easy to be implemented but has some difficulties in following the quick and significant load changes. On the contrary, the MPC approach presented in Paper E [Shafiei et al., 2014] shows a superior performance but it may lead to significant performance degradation in case of model mismatches. Another issue is that such a model based approach is not generally applicable to different supermarket systems and, consequently, a comprehensive modeling effort should be accomplished for each specific refrigeration system before control system design.

A variation of data-driven control approach using the subspace method presented in Section 1.2.4 has been adopted in Paper F [Shafiei et al., 2015] for predictive direct load control design for refrigeration systems. It improves the load following performance comparing to Paper D [Shafiei et al., 2013a] and, at the same time, overcomes the mentioned disadvantages associated with the model based design proposed in Paper E [Shafiei et al., 2014].

Moreover, an open-loop experiment based on uncorrelated random input sequences is presented. A new method based on tuning the average duty cycle of the input signals is proposed. As a practical consideration, the control design does not rely on the mass flow measurements which is of great interest because these costly measurements are usually not available in commercial refrigeration applications. But, on the other hand, a flow measurement could enhance the performance of the suction pressure estimation. As an alternative, a feedforward inclusion of the condensation pressure into the SPC formulation is suggested in oder to regain similar performance with a cheaper measurement.

The nonlinear simulation tool [SRSim, 2013] — created based on th model developed in [**?**] — is employed for verification of the proposed approach.

For the rest of this section where we are presenting the data-driven approach, the specific notation of $(x_1, \cdots, x_n) = \begin{bmatrix} x_1^T & \cdots & x_n^T \end{bmatrix}^T$ is used.

Design of Experiment

In order to make the approach generic, we need to design a data collection experiment which is intuitive and applicable to various supermarket refrigeration systems. Here we explain the design of excitation signals required for identification practice and propose a new method for tuning those signals.

The input signal should be persistently exciting with an appropriate order. For this purpose, pseudo-random binary signals (PRBSs) are usually applied for identification of MIMO systems. There are two degrees of freedom for designing such input signals, *i.e.,* the bandwidth and the amplitude. The data required for tuning the input signal is obtained from the regular thermostatic control of the cooling units. Fig. 2.17 shows an example of variation of the air and the food temperatures due to applying the relay feedback test or thermostatic control effort.

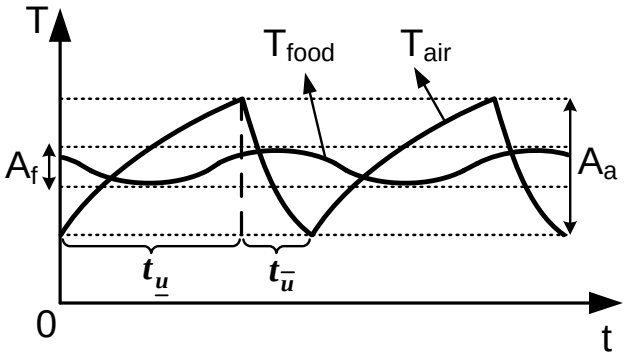

Figure 2.17: Periodic temperature change obtained from applying the relay feedback to the expansion valve. The time spans $t_{\bar{u}}$ and $t_{\underline{u}}$ correspond to the ON and OFF cycle of the expansion device, respectively.

Bandwidth of the input sequences — In order for food temperatures to vary as much as possible within the constrained range, bandwidth of the input frequency should be limited. The low frequency signal is realized by changing the switching probability up to α_{bw} times of the normalized Nyquist frequency, where $0 < \alpha_{bw} < 1$. The details can be found in [Soderstrom and Stoica, 1989, Ch. 5, Example 5.11].

In the relay feedback test, the frequency of the air temperature variation is the same as the input signal and its amplitude varies within the full range, but the food temperature amplitude is attenuated with the gain of $G_r = A_f/A_a$ at the frequency of $\omega_r = 2\pi/T_r$ with $T_r = t_{\underline{u}} + t_{\bar{u}}$ as depicted in Fig. 2.17. Having ω_r and G_r known, the following low pass filter transfer function from the air to the food temperature is computed

$$H_{af} = \frac{1}{\tau s + 1}. \tag{2.35}$$

The filtering effect from the air to the food temperature has a dominant pole comparing to the envisaged transfer function from the input signal to the air temperature. The attenuation gain below 5%, *i.e.,* $|H_{af}| < 0.05$, causes the variation of food temperature to be within the range of the measurement noise. Let the frequency corresponding to this gain be denoted by ω_{bw}. Thus, the bandwidth of the input sequences should be limited by

$$\alpha_{bw} = \omega_{bw}/\pi \tag{2.36}$$

Magnitude of the input sequences — For constrained and/or ill-conditioned systems, the dominant approach to respect the constraints is to limit the amplitude of the excitation signal by the so called rotated input method [Darby and Nikolaou, 2014]. Yet larger input amplitudes are more favorable to have a better signal to noise ratio. Here, we suggest to tune the average duty cycle of the PRBS. It is much more intuitive and simpler than the rotated input approach, [Conner and Seborg, 2004], as well as providing the largest possible amplitudes for input signals.

The difference between the time span values $t_{\underline{u}}$ and $t_{\overline{u}}$ in Fig. 2.17 is because of the difference in the gain directionality. In order to excite all directions with the same strength, the average duty cycle of the PRBS, $\overline{D}$, is proposed to be designed as

$$\overline{D} = \frac{t_{\overline{u}}}{t_{\underline{u}} + t_{\overline{u}}} \tag{2.37}$$

An example of the PRBS applied to the expansion valve is shown in Fig. 2.18a, where the first 1000 sequences of the signal used to excite the 6th MT cooling unit dynamics are illustrated. The temperature of the foodstuff in that unit is shown in Fig. 2.18b.

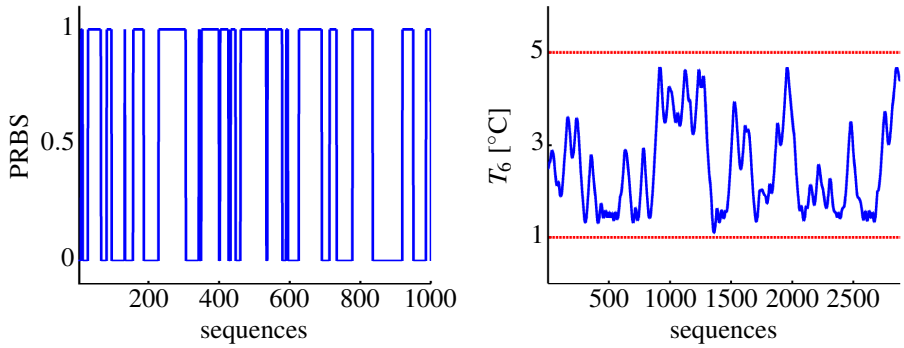

Figure 2.18: Identification experiment: (a) The firs 1000 sequences of the PRBS applied to the expansion valve of the 6th MT cold reservoir; (b) Corresponding food temperature.

Subspace Identification

The deterministic part of (1.6) can be estimated by the following linear predictor:

$$\hat{Y}_f = L_w W_p + L_u U_f. \tag{2.38}$$

Under some conditions (stated in Paper F [Shafiei et al., 2015]), the subspaces matrices can be consistently identified as the arguments of the following least squares problem, [Knudsen, 2001]:

$$\min_{L_w, L_u} \left\| Y_f - \begin{pmatrix} L_w & L_u \end{pmatrix} \begin{pmatrix} W_p \\ U_f \end{pmatrix} \right\|_F^2 . \tag{2.39}$$

where $\|\cdot\|_F$ stands for the Frobenius norm. An efficient and robust method for numerical implementation of the above problem is QR-decomposition of $(W_p,\ U_f,\ Y_f)$ as:

$$\begin{bmatrix} W_p \\ U_f \\ Y_f \end{bmatrix} = \begin{bmatrix} R_{11} & 0 & 0 \\ R_{21} & R_{22} & 0 \\ R_{31} & R_{32} & R_{33} \end{bmatrix} \begin{bmatrix} Q_1^T \\ Q_2^T \\ Q_3^T \end{bmatrix}, \tag{2.40}$$

in which the subspace matrices $L = \begin{bmatrix} L_w & L_u \end{bmatrix}$ can be calculated as

$$L = \begin{bmatrix} R_{31} & R_{32} \end{bmatrix} \begin{bmatrix} R_{11} & 0 \\ R_{21} & R_{22} \end{bmatrix}^{\dagger} \tag{2.41}$$

where † represents the Moore-Penrose pseudo-inverse. The subspace matrices are identified as:

$$L_w = L(p,q), \quad p = 1,\ldots,im \ \text{ and } \ q = 1,\ldots,i(l+m) \tag{2.42}$$

$$L_u = L(p,k), \quad p = 1,\ldots,im \ \text{ and } \ k = i(l+m)+1,\ldots,i(2l+m). \tag{2.43}$$

The future outputs of the plant are predicted by (2.38) using the subspace matrices and future moves in the control signals. This predictor can conveniently be utilized for predictive control formulation without identifying a state-space model [Favoreel et al., 1998].

The controlled outputs are the electrical power consumption of the compressor rack and the suction pressure. The measured outputs are the air and the food temperatures. The MT and LT compressor capacities and the opening degree of the electronic expansion valves are chosen as the vectors of manipulated input variables for the specific case considered in this work. Identification results for the food temperature of the 5th MT cooling unit and the suction pressure is shown in Fig. 2.19. More results and discussions are given in Paper F [Shafiei et al., 2015]. The goodness of fit between the nonlinear simulation model and the linear data-driven subspace predictor is calculated by

$$\text{fit} = \left(1 - \frac{\|y - \hat{y}\|_2}{\|y - \bar{y}\|_2} \right) \times 100\% \tag{2.44}$$

where y is the measured output, $\hat{y}$ is the one-step-ahead predicted output, and $\bar{y}$ denotes the average of the measured output data [Ljung, 1987].

2.3.4 Subspace Predictive Control

In subspace predictive control, the following objective function should be minimized at each time instant for the receding horizon implementation:

$$J = \sum_{k=1}^{N_f} (r_{k+1} - \hat{y}_{k+1})^T Q_k (r_{k+1} - \hat{y}_{k+1}) + \sum_{k=1}^{N_c} \Delta u_k^T R_k \Delta u_k, \tag{2.45}$$

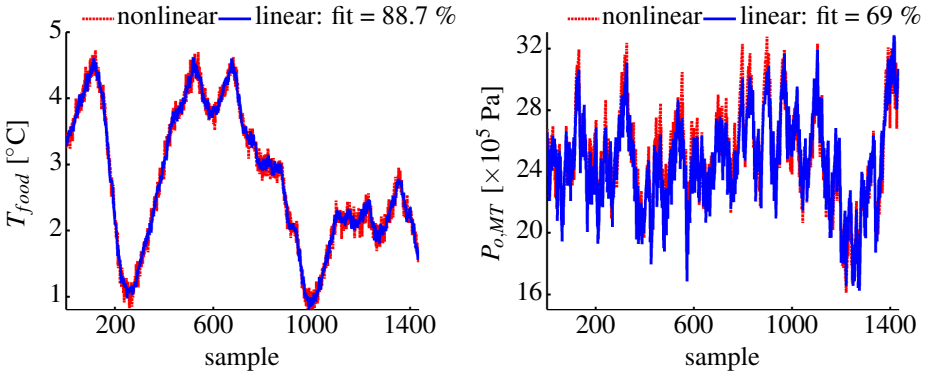

Figure 2.19: Model validation: (a) Food temperature in the 5th MT cold reservoir; (b) Suction pressure of the MT section.

where Q_k and R_k are weighting matrices, r is the reference signal, N_f and N_c are prediction and control horizon, respectively, and $\hat{y}_{k+n}$, with $n = 1,\ldots,N_f$, is the n-step-ahead predicted output at time instant k. Defining $\hat{y}_f = (\hat{y}_{k+1},\ \hat{y}_{k+2},\ \cdots,\ \hat{y}_{k+N_f})$ and $u_f = (u_{k+1},\ u_{k+2},\ \cdots,\ u_{k+N_c})$, the above objective can be rewritten in the matrix form as:

$$J = (r_f - \hat{y}_f)^T Q (r_f - \hat{y}_f) + \Delta u_f^T R \Delta u_f, \tag{2.46}$$

where r_f is defined in the same way as $\hat{y}_f$, and $Q \in \mathbb{R}^{N_f l \times N_f l}$ and $R \in \mathbb{R}^{N_c m \times N_c m}$ are block diagonal matrices constructed from Q_k, for $k = 1,\ldots,N_f$, and R_k, for $k = 1,\ldots,N_c$, respectively.
The predicted output is obtained from (2.38) as:

$$\hat{y}_f = l_w w_p + l_u u_f, \tag{2.47}$$

where $w_p = (y_{k-N_p+1},\ \cdots,\ y_k,\ u_{k-N_p+1},\ \cdots,\ u_k)$ is the vector of past input and output data with the past horizon N_p, and subspace matrices are

$$l_w = L_w(p,q), \quad p = 1,\ldots,mN_f, \text{ and } q = 1,\ldots,(l+m)N_p, \text{ and} \tag{2.48}$$
$$l_u = L_u(p,k), \quad p = 1,\ldots,mN_f, \text{ and } k = 1,\ldots,lN_c. \tag{2.49}$$

Incorporating the input and output constraints, SPC algorithm can be implemented by solving the following quadratic programming (QP) problem in a receding horizon manner. The derivation of the subspace dynamics in terms of the incremental input Δu_f is presented in Paper F [Shafiei et al., 2015].

$$\begin{aligned} \min_{\Delta u_f} \quad & (r_f - \hat{y}_{f,c})^T Q (r_f - \hat{y}_{f,c}) + \Delta u_f^T R \Delta u_f \\ \text{subject to} \quad & \hat{y}_f = \mathbf{y}_k + \Lambda l_w \Delta w_p + \Lambda l_u \Delta u_f \\ & (\mathbf{u}_{min} - \mathbf{u}_k) \le \Lambda \Delta u_f \le (\mathbf{u}_{max} - \mathbf{u}_k) \\ & \mathbf{y}_{min} \le \hat{y}_f \le \mathbf{y}_{max} \end{aligned} \tag{2.50}$$

where $\hat{y}_{f,c}$ is the vector of controlled outputs included in $\hat{y}_f$, $(\mathbf{u}_{min} - \mathbf{u}_k)$ and $(\mathbf{u}_{max} - \mathbf{u}_k)$ are expanded column vectors of $(u_{min} - u_k)$ and $(u_{max} - u_k)$ with u_{min} and u_{max} being the input magnitude constraints, and finally $\mathbf{y}_{min}$ and $\mathbf{y}_{max}$ are expanded column vectors of the measured output constraints. The reference signal r_f consists of power and pressure set-point which tries to keep the pressure close the maximum possible level. Λ is a coefficient matrix including zero and identity block matrices given by

$$\Lambda = \begin{bmatrix} I & 0 & \cdots & 0 \\ I & I & \cdots & 0 \\ \vdots & \vdots & \ddots & \vdots \\ I & I & \cdots & I \end{bmatrix}. \tag{2.51}$$

2.3.5 Direct Load Control and SPC

A realistic balancing service scenario is intended to investigate the ability of the proposed advanced control strategy for direct load control of the large scale refrigeration system. The two other methods presented in Paper D [Shafiei et al., 2013a] and Paper E [Shafiei et al., 2014] are also simulated for the sake comparison with the results achieved in this work. In each case, the control method is applied to the nonlinear simulation model tool in [SRSim, 2013].

Fig. 2.20 shows a period of 1300 min operation including the normal operation, a downward regulation service, and an upward regulation service. The default is the normal operation, where the food temperatures are kept at the middle of the range that provides a symmetric flexibility in terms of preparation for the regulation in both directions. At time 300 min, the imbalance contingency takes place which demands a downward regulation by raising the power to 6 kW in 5 minutes; keeping it regulated for 60 minutes; and then moving it back to the baseline in 5 minutes.

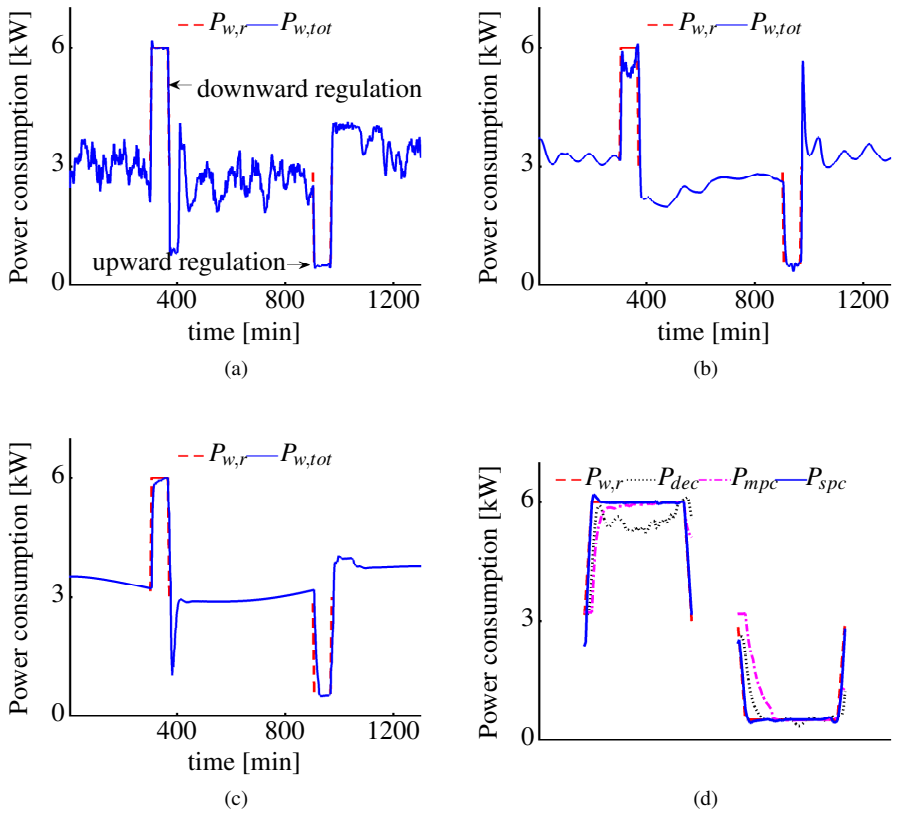

Figure 2.20: Total electrical power consumption of the compressor racks. The period includes two DR events: downward regulation service from 300 to 370 minutes, and upward regulation service from 900 to 970 minutes. (a) Simulation results after applying the data-driven SPC method proposed in Paper F [Shafiei et al., 2015]; (b) simulation using the decentralized supervisory control method presented in Paper D [Shafiei et al., 2013a]; (a) simulation using the MPC method presented in in Paper E [Shafiei et al., 2014]; (d) comparing the three methods in terms of the load following performance where P_{dec}, P_{mpc} and P_{spc} denote the power consumptions after applying the decentralized control, the MPC and the SPC, respectively. The two DR event periods are zoomed for a better visibility. The decentralized method cannot keep the power regulated during the downward regulation service. The proposed SPC method shows a superior tracking performance comparing to the other two methods.

2.4 Control of Hybrid Thermal Systems

So far we have presented different control methods for demand-side management of supermarket refrigeration systems under the two indirect and direct load control schemes. Here in the last contribution we present the energy management of hybrid refrigeration

systems for transport applications.

In Paper G [Shafiei and Alleyne, 2015], we have assumed two basic states of the vehicle: (a) driving at some nominal speed, similar to a highway or major road, and (b) driving at a very low, or zero, speed akin to being in traffic or stopped to deliver goods. The TES unit is utilized depending on which driving state the vehicle is in. An optimal charge scheduling is proposed to distribute the charging demand across the drive cycle using load predictions achieved by predicting both the anticipated driving profile and the thermal load from the ambient temperature. The driving profile can be easily obtained nowadays from GPS references and cloud-based traffic predictions. Similarly, ambient temperatures are accessible at any location along a route via cellular communication. Fig. 2.21 shows the external information utilized in the thermal load prediction.

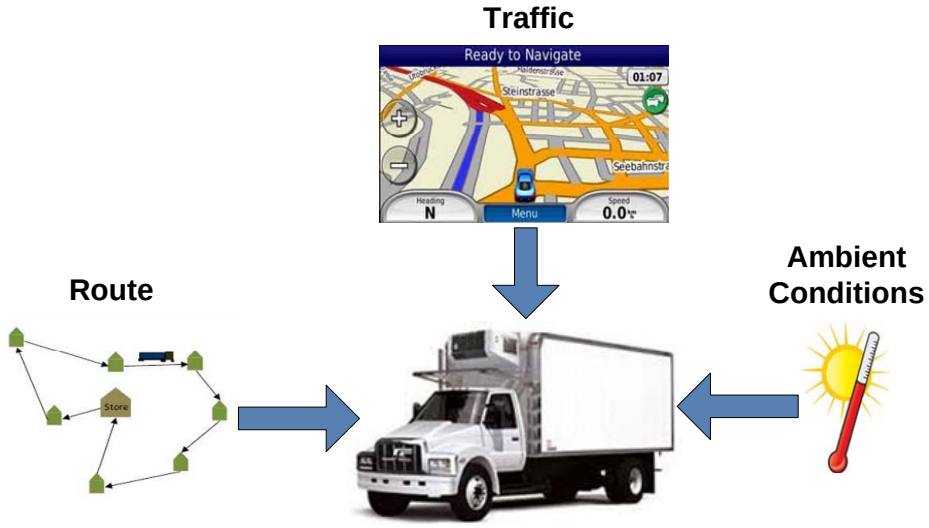

Figure 2.21: Driving profile and environmental conditions are used for thermal load predictions during the heavy traffic periods. Delivery paths and GPS traffic data are used for prediction of the driving profile.

From control point of view there are similarities between the method presented in this contribution and those presented in previous sections for demand-side management. The similarities might be recognized as using MPC and lumped parameter gray-box model for control design and taking advantage of the disturbance preview for energy management. The specific transport refrigeration problem considered in this study is differentiated from the building energy management challenge in two aspects: (i) the disturbance profile contains more rapid transients due to the nature of the delivery process; and (ii) building control systems typically focus on economic cost plus performance optimization while the focus here is on an energy plus performance optimization. Economic cost is less relevant than buildings because there is no dynamic pricing of the energy asset (vehicle fuel) as there is for grid electricity for buildings.

2.4.1 Parallel Hybrid VCC System

Fig. 2.22 shows a VCC system that includes a TES unit operating in a parallel configuration. The VCC operation has been already explained in Section 1.1.2, here we describe the TES operation in the system.

The TES unit is in parallel with the evaporation unit. In our configuration, heat will be taken from the PCM by the refrigerant. This will lead to a solidification of the PCM in the TES and is considered the charging mode. The TES charging operation is controlled by the expansion valve (EV_2). Similar to the evaporator, the TES unit is also equipped with a fan to circulate air from the container across the unit. As the solid fraction of PCM is reduced, the amount of latent heat capacity remaining is being reduced. Consequently, when the TES fan is running, the unit is discharging. The parallel VCS system in Fig. 2.22 has 4 modes of active operation as detailed in [Fasl, 2013]: (i) using the refrigeration system only, (ii) charging of the TES either with or without active refrigeration, (iii) using the TES only, and (iv) both the refrigeration and TES systems active, termed boost. In the current work, we consider a subset of the first three modes to limit complexity and demonstrate potential benefits.

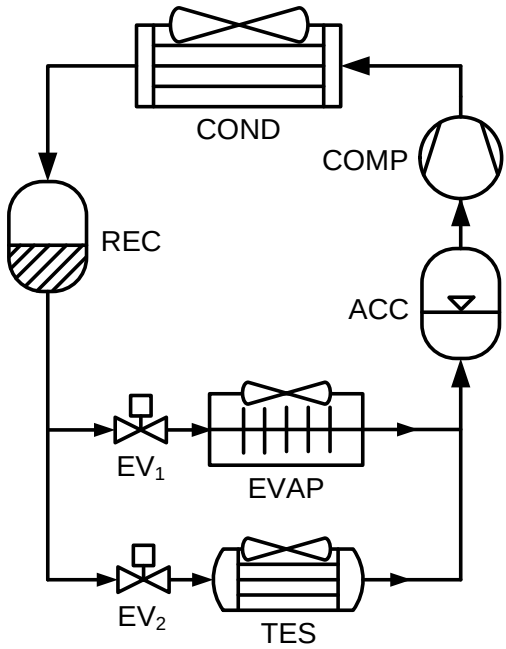

Figure 2.22: A typical parallel hybrid configuration for a VCC system.

2.4.2 Problem Statement and Control Strategy

Given the flexibility of the hybrid transport VCC system, how best is to use this capability? We seek to maintain a given temperature within the container and do so as efficiently

as possible. However, there are now multiple modes in which to achieve this objective and choosing the mode of operation is the first part of the overall problem.

Once the mode of operation is chosen, the system focus becomes operational efficiency. The controller objectives include both maintaining container temperature as well as providing sufficient cooling to charge the TES if that is the current mode. Assuming the primary energy consumer is the compressor, the goals can be expressed as achieving temperature setpoints, providing charging if necessary, and doing so at the maximum efficiency of the compressor.

This two-tiered control problem of mode selection followed by operational efficiency is best met by a two-tiered controller design. First, a logic based algorithm must decide what mode of operation is best. Second, a continuously operating algorithm must achieve specific setpoints while minimizing energy consumption. For this purpose a two stage controller is developed to match the dual stage objectives.

The three modes of operation under consideration are defined, based on TES activity, as: *normal*, *charging* and *discharging*. Table 2.1 presents the control actions for each mode. In the normal operation, the container temperature is regulated by controlling the compressor speed in a standard refrigeration cycle while the evaporator fan is set to its maximum value. In the charging mode, the compressor regulates the charging demand while the evaporator fan regulates the container temperature. In the discharging mode, the container temperature is regulated by controlling the TES fan.

Table 2.1: Three different modes of operation considered.

Mode	Evap. valve	TES valve	Evap. fan	TES fan	compressor
normal	PI	closed	on	off	PI
charging	PI	PI	P	off	MPC
discharging	closed	closed	off	P	off

In order to deal with the two-tiered controller approach outlined in Section 2.2, a cascade control loop is proposed in Fig. 2.23. An outer optimization loop is responsible for selecting the desired charge to hold in the TES, and whether or not the TES is active, based on the current and predicted thermal loads. An inner control loop includes an MPC to control the compressor for maximizing efficiency as well as proportional (P) and proportional-integral (PI) controllers for the other components. The PI controllers of expansion valves regulate the required superheat temperatures, and the P controllers of the evaporator and TES fans regulate the container temperature in the charging and discharging mode. In the normal mode, compressor speed is controlled by a simple PI controller to regulate the container temperature while the evaporator fan is turned on.

2.4.3 Gray-Box Modeling

The highly nonlinear and high order model obtained in [Fasl, 2013, Fasl et al., 2014] using a first principles method makes the optimization problem — to be formulated for implementation of the control strategy in Fig. 2.23 — nonlinear and non-convex. As such, while it is suitable for system simulation and controller evaluation, it is not suitable for on-line decision making. In Paper G [Shafiei and Alleyne, 2015] a simpler gray-box model is presented that captures only the essential dynamics of the refrigeration and TES system thereby allowing a convex optimization formulation for MPC to be implemented.

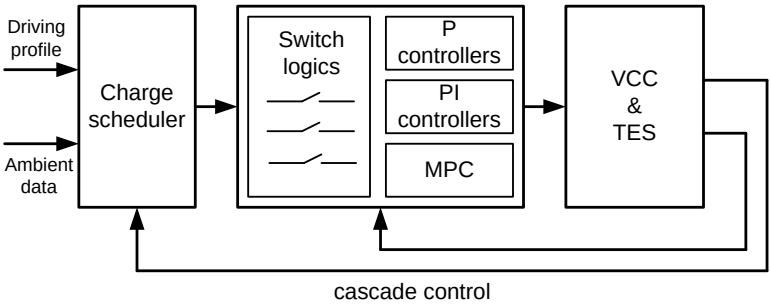

Figure 2.23: Control strategy for handling operating modes and decentralized local control loops, and inclusion of optimal control scheme.

Here we describe the general relevance and skip the details of the mathematical formulas. Some of the results are also presented in this section.

Parameters of the gray-box model are estimated and the model is validated against a more complicated nonlinear MATLAB/Simulink model presented in [Fasl, 2013, Fasl et al., 2014].

Container Model

The dynamics of the container being cooled by the hybrid VCS/TES are described using the energy balance principle and lumped parameter modeling similar to the approach taken in Paper A [Shafiei et al., 2013c]. A linear approximation method is proposed to estimate the UA_e value needed for calculation of the cooling capacity in (6.5).

To identify the parameters associated with container dynamics, a simulation experiment is performed based on the relay-based thermostatic control of the container temperature with compressor speed as an input. The result is shown in Fig. 2.24.

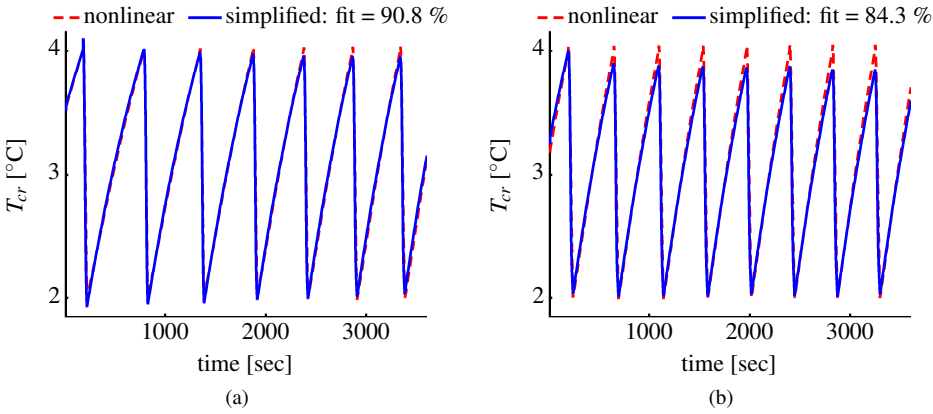

Figure 2.24: Estimation of the container temperature governed by only VCC ($\dot{Q}_s = 0$): (a) identification; (b) model validation.

2.4.4 TES Model

The full TES model presented in [Fasl, 2013] uses the fixed grid method [Dincer and Rosen, 2010] to solve the heat transfer and phase change problem where the enthalpy is used for the thermodynamic state variable. The following assumptions have been made to avoid a very high order model while capturing the relevant dynamics within the PCM.

Assumption 1*: Heat is transferred in the radial direction through the fins and in the azimuthal direction between the PCM and the fin in each node.*

Assumption 2*: The PCM has lumped thermodynamic properties in single phase regions.*

Assumption 3*: The pressure in the PCM is constant over time, space and phase.*

Assumption 4*: The density in the PCM is constant over time and space but can vary through phase change.*

Assumption 5*: The fin nodes are assumed to have no heat storage capacity.*

It is shown in paper G [Shafiei and Alleyne, 2015] that the PCM solid fraction within the TES can be estimated in two ways: (a) in terms of the cooling power applied by the VCC system when the TES is charging, and (b) in terms of the cooling capacity applied by the TES when it is discharging. When charging, it is assumed that the solid fraction is linearly correlated with the cooling energy received from the VCC, *i.e.,*

$$\frac{ds_f}{dt} = K_s \dot{Q}_{rs}, \tag{2.52}$$

where s_f is the PCM solid fraction, K_s is a constant, and $\dot{Q}_{rs}$ is the heat transfered from refrigerant to the storage. Similar to the charging mode, when the storage is discharging, the dynamic behavior of the PCM solid fraction is given by a simple integrator

$$\frac{ds_f}{dt} = -K_s \dot{Q}_s \tag{2.53}$$

where $\dot{Q}_s$ is the cooling capacity applied by the thermal storage unit when activated. Fig. 2.25b presents the variation of K_s across discharging time. It shows that K_s can be considered constant in the simplified model. Estimation of the solid fraction is illustrated in Fig. 2.26. Even though the TES is modeled as a simple linear integrator, the estimation results are sufficiently satisfactory for incorporation into a model-based predictive controller.

Compressor Model

The compressor drives the mass flow throughout the entire VCC system and can be used to control the suction pressure (or equivalently the saturation temperature). Without a direct mass flow measurement, the relation between the compressor speed and the saturated refrigerant temperature can be reasonably modeled as a black-box transfer function

$$T_{st}(s) = G(s)\omega_c(s), \tag{2.54}$$

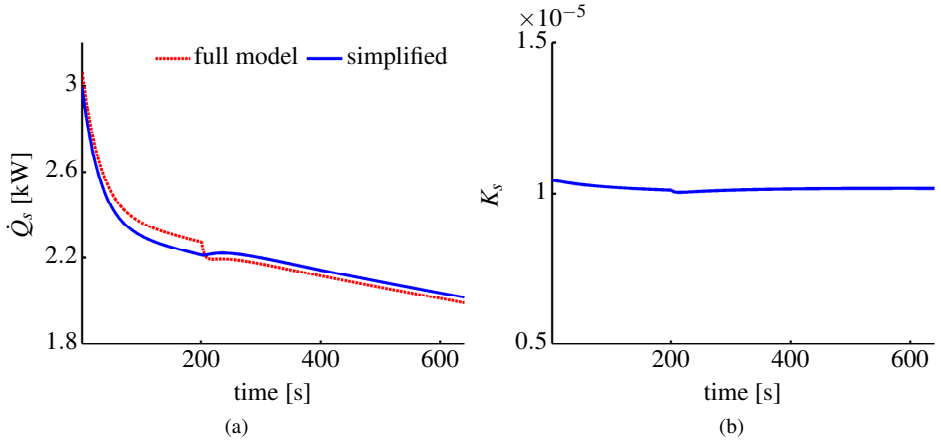

Figure 2.25: Simplification of the TES model: (a) cooling power applied to the container when discharging the TES; (b) justification of assuming K_s to be constant.

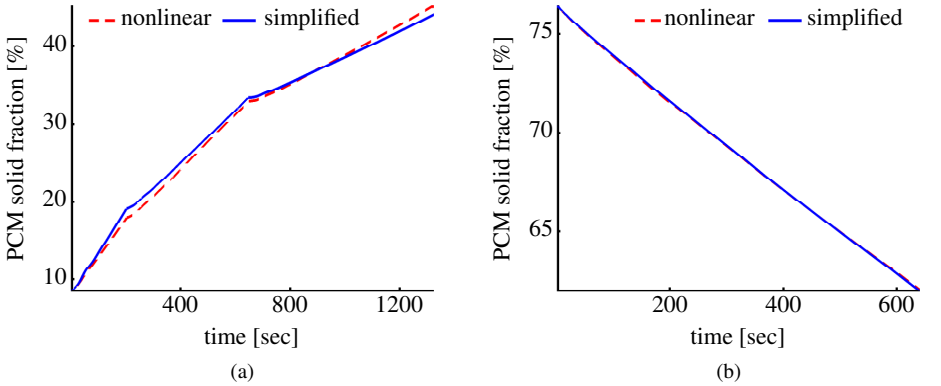

Figure 2.26: Estimation of the TES solid fraction when: (a) charging; (b) discharging.

where ω_c is the compressor speed used here as a control input variable. Fig. 2.27 shows the results of the compressor model in predicting the saturation temperature.

2.4.5 Control System Design

The design of the two cascaded loops proposed in Fig. **??** is provided in this section. In order to simulate the hybrid VCC system, we have used a nonlinear modeling tool, the Thermosys Toolbox, [Rasmussen, 2002], for MATLAB/SIMULINK, which has been previously validated on a variety of thermal systems. The Thermosys blocks are configured as shown in Fig. 2.22.Fig. 2.28 illustrates the simulation environment where the full nonlinear model is included in the rightmost block to simulate the hybrid VCC system and the developed simplified model is included in the middle block and is employed by the control system.

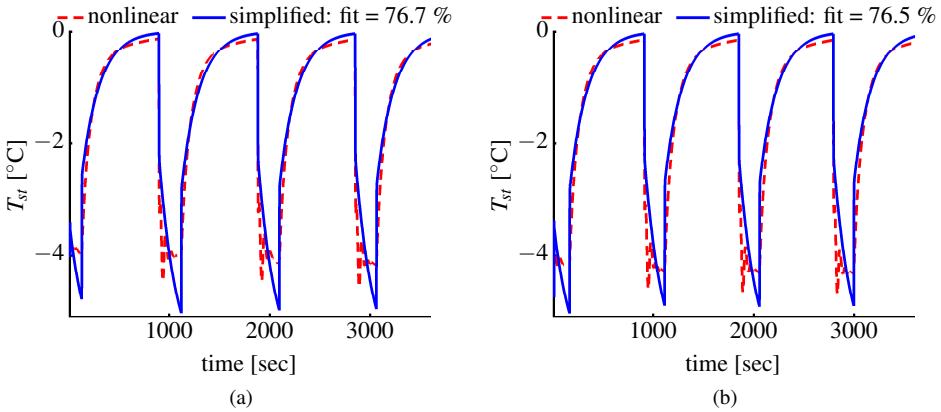

Figure 2.27: Estimation of the evaporation temperature using compressor model: (a) identification; (b) model validation.

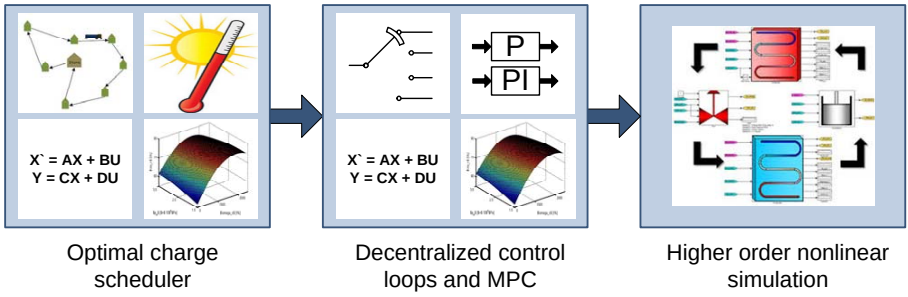

Figure 2.28: Simulation environment for testing the proposed approach. The three blocks correspond to that of Fig. 10.3 with the same placement order. A detailed nonlinear simulation model is employed to simulate the hybrid VCC/TES dynamical behavior.

Performance Objective

The control objectives is to minimize the power/energy consumption of the overall VC-C/TES system by focusing on the compressor consumption. In general a detailed derivation of the compressor power in terms of the relevant variables such as compressor speed or suction/discharge pressure leads to a nonlinear and non-convex formulation which is not appropriate for MPC implementations. Empirical evidence indicates that the volumetric efficiency of the compressor can be estimated as a 2nd order convex function of the compressor speed and the pressure ratio across the compressor [Rasmussen and Alleyne, 2006] as

$$\eta_v = c_1\omega_c + c_2\omega_c^2 + c_3\omega_c p_{oi} + c_4 p_{oi} + c_5 p_{oi}^2 \tag{2.55}$$

where c_i are constants and p_{oi} is the ratio of the outlet pressure over the inlet pressure of the compressor. The relationship in (2.55) will be used for the MPC formulation. The parameters c_i are estimated using the lab experimentation data obtained by [Rasmussen and Alleyne, 2006]. The estimation results are shown in Fig. 2.29.

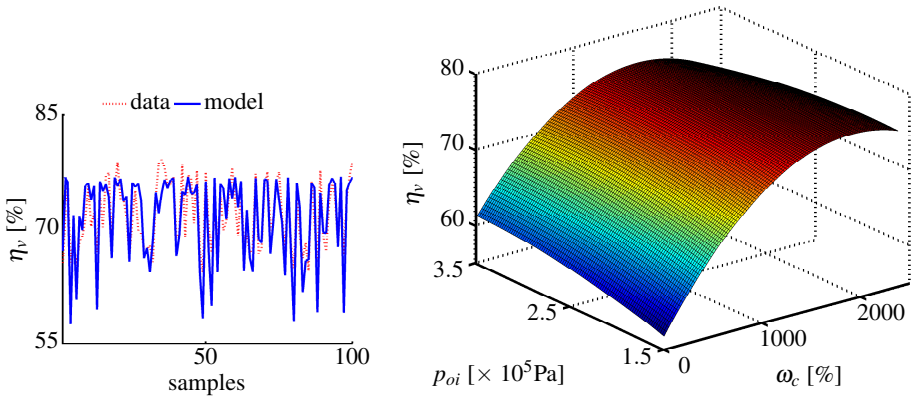

Figure 2.29: Volumetric efficiency: (a) parameter estimation; (b) objective function to be used in convex optimization.

Charge Scheduler

The outer loop in Fig. 2.23 schedules the charging demands for a specific period of time using a given driving profile and thermal load predictions. Here, for simplicity, we classify traffic data patterns into either light or heavy traffic with the primary difference being average vehicle speed. In the light traffic case, the vehicle travels with an average nominal speed V_N and in the heavy traffic case, it operated with average speed V_0. The specifics of traffic data analysis and identification of average speed levels are outside the scope of the current study but readers may refer to [Walkowicz et al., 2014] for details of how this would be accomplished.

For a time horizon T_p, using the on-line traffic and GPS data and the average vehicle speed, a driving profile may be obtained. An example of such profile is shown in Fig. 2.30. Maximizing the COP associated with the air flow over the condenser, the intuition would be that the storage unit should be charged during the light traffic (high average velocity) periods and discharged during the heavy traffic (low average velocity) intervals.

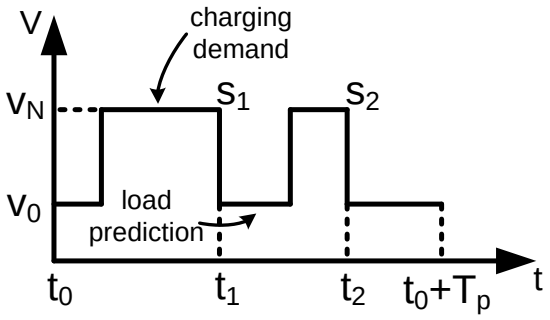

Figure 2.30: An example of a predicted driving profile.

The gray-box model is employed to calculate the thermal load in the discharging periods and the corresponding charging demand. The charge scheduling problem is solved by optimal distribution of charging demand among the available charging periods for which the following optimization problem is proposed:

$$\begin{aligned}
\min_{\omega_c,\, s_f} \quad & -\sum_{i=1}^{N_o} \eta_v + W_o \sum_{i=1}^{N_o} \|\Delta\omega_c\|_2^2 \\
\text{subject to} \quad & \\
& \begin{cases} X_{st}[k+1] = \mathbf{A}_{st} X_{st}[k] + \mathbf{B}_{st}\,\omega_c \\ T_{st}[k] = \mathbf{C}_{st} X_{st}[k] \end{cases} \quad k \in \mathbb{I}^{ch} \\
& s_f[k+1] = s_f[k] + t_{so} K_{rs}\,(T_s - T_{st}[k]) \quad k \in \mathbb{I}^{ch} \\
& \dot{Q}_s = UA_a(T_a - T_w) \\
& s_f[k+1] = s_f[k] - t_{so} K_s \dot{Q}_s \quad k \in \mathbb{I}^{dis} \\
& 0 \le s_f \le 100 \\
& 0 \le \omega_c \le \omega_{max} \\
& S_I \ge L \\
& X_{st}[N_o+1] \le S_T
\end{aligned} \quad , \tag{2.56}$$

where N_o is the prediction horizon, t_{so} is the sampling time, $\Delta\omega_c$ is the rate of change of the compressor speed which is penalized in the cost function by the weighting factor W_o, ω_{max} is the maximum speed of the compressor, and S_I and L are vectors including s_i and l_i as their elements, respectively. The output of the optimization problem (10.31) is the next time instant during the driving profile where charging would be initiated, *i.e.,* $s_1^* = s_f^*[t_1]$ where s_f^* is the argument resulting from solving the above problem. Note that t_1 is updated at each sampling instant where optimization problem should be solved again. Further details regarding the discretized dynamics and constraints used in (2.58) is given in Paper G [Shafiei and Alleyne, 2015].

Model Predictive Control

The objective of maximizing the efficiency factor η_v clearly falls within the scope of a well-designed MPC. The second objective is to regulate the TES charge to the solid fraction set-point s_i at time t_i as given by the outer loop controller. Consider the nominal desired solid fraction trajectory provided in Fig. 2.31 where the goal is to transition from s_0^* at time t_0 to s_1^* at time t_1. At any time instant, an optimization problem is solved to maximize η_v. The following constraint on the rate of solidification is imposed to guarantee s_i regulation:

$$\Delta s_f \ge \delta s_{min} \tag{2.57}$$

where $\Delta s_f = s_f[k] - s_f[k-1]$, and $\delta s_{min} = (s_1 - s_f(t))/(t_1 - t)$. Satisfying the constraint in (2.57) means that the s_f trajectory would always lie above the dashed line shown in Fig. 2.31. This guarantees reaching the s_1^* level before time t_1.

If the value of the s_1^* level is reached at time t_r as shown in Fig. 2.31, then the TES should deactivate and the refrigeration system works in the normal mode to regulate the container temperature and MPC is stopped until the next charging period. To summarize, the following optimization problem is proposed for the MPC implementation:

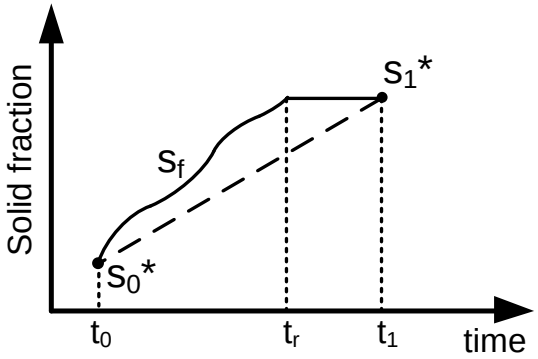

Figure 2.31: An example of a solid fraction trajectory.

$$
\begin{aligned}
\max_{\omega_c,\, s_f} \quad & -\sum_{j=1}^{N_i} \eta_v + W_i \sum_{j=1}^{N_i} \|\Delta\omega_c\|_2^2 \\
\text{subject to} \quad & \\
& \begin{cases} X_{st}[k+1] = \mathbf{A}_{st} X_{st}[k] + \mathbf{B}_{st}\,\omega_c \\ T_{st}[k] = \mathbf{C}_{st} X_{st}[k] \end{cases} , \\
& s_f[k+1] = s_f[k] + t_{si} K_{rs}\,(T_s - T_{st}[k]) \\
& 0 \le s_f \le 100 \\
& 0 \le \omega_c \le \omega_{max} \\
& \Delta s_f \ge \delta s_{min}
\end{aligned}
\tag{2.58}
$$

where N_i is the prediction horizon, t_{si} is the sampling time, and W_i is the weighting factor. The output of the above problem is the optimum compressor speed ω_c^* applied as a control signal.

The driving profile used in the following simulations is shown in Fig. 2.32. Intentionally, it is designed to include long periods of heavy traffic (e.g. a delivery stop) such that the overall cooling required for load compensation is larger than the capacity of the TES. Doing so, the capability and effectiveness of the optimal charging scheme for distribution of charge demand across the heavy traffic periods are tested.

The TES solid fraction resulting from the optimal control is shown in Fig. **??**. As can be seen, the whole charging demand is shifted to the first and third charging modes and no charging takes place during the second cycle. Examining Fig. **??**, the compressor speed during the charging mode is approximately 1,200 rpm which is approximately the optimal efficiency point as given in Fig. 10.15b. Therefore, the proposed optimal control scheme ensures that the compressor will charge TES unit with maximum efficiency while guaranteeing the cooling requirements will be met during the heavy traffic period.

In Paper G [Shafiei and Alleyne, 2015] three different simulation scenarios are performed. The first simulation illustrates the importance of taking the current traffic mode (light vs. heavy) into account for performing the TES charging. The second simulation shows that further energy saving can be achieved by scheduling the charging demand according to the predicted load using the predicted traffic mode. Finally, the third simulation illustrates the effectiveness of the proposed optimal control to maximize the compressor

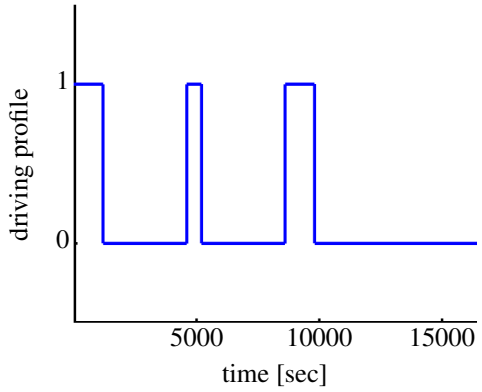

Figure 2.32: The driving profile considered for simulation experiments.

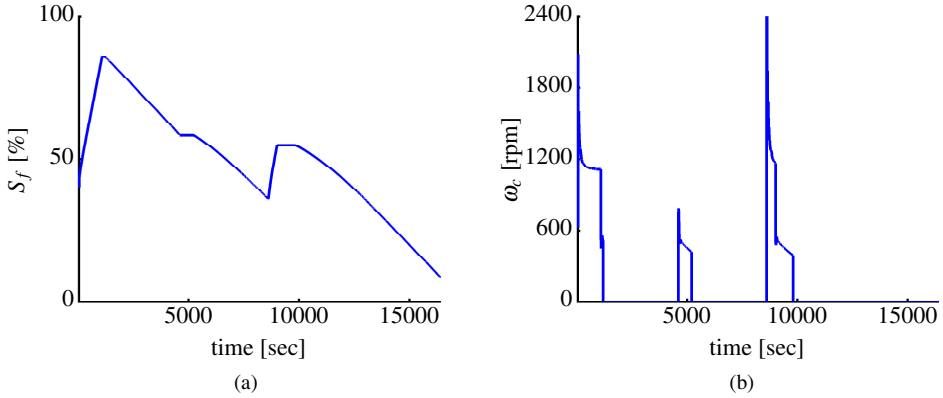

Figure 2.33: Optimal charge scheduling and model predictive control: (a) PCM solid fraction (state of charge); (b) compressor speed.

volumetric efficiency factor. To compare the results an integrated coefficient of performance IC is defined as the ratio of the total cooling energy over the total electrical power consumption for the entire drive cycle

$$IC = \frac{Q_{rs} + Q_e}{E_f + E_c}, \tag{2.59}$$

where E_f and E_c are the energy consumption of the evaporator fans and the compressor. The corresponding power consumptions of the two latter components are illustrated in Fig. 10.24. The results of integrated COP calculations are

$$IC_n = \frac{550 + 4179}{993 + 2280} = 1.44, \quad IC_{opt} = \frac{840 + 4065}{713 + 2070} = 1.76 \tag{2.60}$$

where IC_n is the performance resulting from the simple logic based control and load prediction, and IC_{opt} is the performance in the case of the proposed optimal control. The results show that a 22% performance improvement is achieved by the optimal control over the logic-based hybrid VCC/TES system operation, even accounting for load preview.

3 | Concluding Remarks

3.1 Conclusions

Throughout this research, we have addressed an smart grid challenge in terms of maintaining the balance between the consumption and supply in case of large integration of renewable resources by means of energy management at the consumption side. Supermarket refrigeration systems have been considered as the consumers with significant potential for demand-side management. Then the research was extended to which we have investigated the energy management of an state-of-the-art hybrid thermal energy system in transport refrigeration. Different research objectives have been established and we have shown that advanced control methods play a significant role in achievement of those objectives. Allocated control strategies have been proposed for enabling demand-side management for supermarket refrigeration systems under realistic smart grid balancing scenarios. It has been accomplished based on the idea that the thermal mass of refrigerated goods inside the supermarket display cases and freezing rooms can be employed for storing energy in form of coldness, which can be used later on when it is needed to reduce the power consumption.

We have developed a nonlinear gray-box model by which we can estimate the thermodynamic states such as the cooling unit temperatures and suction line pressures as well as estimation of the electrical power consumption of the compressors. It justifies the first hypothesis that the electricity usage of the compressors in supermarket refrigeration systems can be estimated using the thermodynamic states. Based on the obtained model, a simulation benchmark has been built for developing and examining the demand-side management methods in smart grid. The model has been validated against real data collected from a supermarket in Denmark.

Two different demand-side management schemes has been investigated: Indirect and direct load control schemes. The problem of energy cost minimization for supermarket refrigeration systems is considered under the indirect load control scheme and assuming that the forecast of disturbances like electricity price and weather temperature are available. An intuitive method for controlling the suction pressure has been proposed that can separate it from the temperature set-point control loops thereby facilitating formulation of the MPC. Two different supervisory controllers using MPC have been designed such that for each a convex optimization problem has been formulated. In the first one, the dynamics of the local linear controllers are embedded inside the system dynamics. In the second design, thermostatic local controllers are used that impose discrete dynamics into the system due to the hysteresis behavior. For this case we have proposed an MPC

algorithm that can still allow for convex programming. In both cases an electricity cost reduction of around 30% has been achieved that justifies our second hypothesis on cost reduction using MPC. All input and output constraints are also respected in the presented model predictive controllers.

We have presented three different control strategies for direct load control of refrigeration systems which are verifications for hypothesis H3. In the first strategy, a decentralized set-point control structure including P and PI controllers has been proposed that can enable balancing services of supermarket refrigeration systems in the smart grid. The heuristic algorithm proposed in the earlier methods for the pressure set-point control is replaced by a proportional controller. An adaptive saturation filter has been designed to maintain the food temperatures within the safety limits and at the same time to provide more flexibility on variation of the air temperatures inside the cooling units. No model information is required in this method and the local controllers are remained unchanged in the system. In the second control strategy, we have formulated an MPC by using the cooling capacity as fictitious manipulated variable. The MPC method outperforms the simple decentralized control in terms of the power tracking performance. We have also shown that by means of a novel incorporation of the evaporation temperature into the optimization problem a COP improvement of around 22% can be achieved. In the third direct load control strategy, we have applied a data-driven subspace predictive control scheme substantiating hypothesis H4. It improves the load following performance comparing to the first control strategy and, at the same time, overcomes the disadvantages associated with the model based predictive control design such as significant performance degradation in case of model mismatches and the fact that it is not generally applicable to different supermarket systems. Moreover, a method for input signal design for subspace identification of refrigeration systems has been proposed.

Exploration of TES control for energy management of refrigeration systems has been addressed at the final round of this research. We have investigated the optimal utilization of TES devices for transport refrigeration. A particular parallel-hybrid vapor compression system has been considered where the TES unit can preserve the container temperature when discharging. A simplified model has been introduced for the purpose of controller design and implementation and a more detailed nonlinear simulation model has been employed for simplified model validation and controller simulations. Initially, results show that active TES charging and discharging corresponding to the traffic status was beneficial. For TES charging, a 17% energy saving can be achieved by performing the energy storage activity during light traffic vs heavy traffic. It verifies the hypothesis H5. We have proposed a cascade optimal control approach which uses preview of disturbances and road profile using traffic data for charge scheduling of TES and performance optimization of the VCC. The results indicate that a 22% performance improvement can achieved by the proposed approach over the type of logic based switching approach which confirms our last hypothesis.

3.2 Perspectives

There are several recommendations for future research based on the findings of the present study. If we contemplate the research in control system society as an spectrum having fundamental research of control theories in one side, developing control methods in be-

tween, and investigating applications of the methods in the other side, then the present study belongs mostly to the application side. Nonetheless, in the following we will give some recommendations that may include the other side of the spectrum that has not been investigated here.

In large chain supermarkets there exist other thermal subsystems such as HVAC and heat recoveries that may interact dynamically with the refrigeration systems. Investigation of those dynamical interactions and their inclusion in a complete model of a supermarket system might reveal the full potential of supermarkets as smart buildings which can contribute to demand-response programs.

In order for flexible energy consumers to take part in an energy balancing market, their flexible consumption should be aggregated to provide a significant potential. An abstract level mathematical formulation can be devised to characterize the consumer flexibilities by giving exact definitions. The level and rate of energy storage can be described by sets of trajectories. Then partial ordering can be utilized to compare the different consumer flexibilities as such be of use for aggregator design.

We have proposed a supervisory MPC algorithm for thermostatic control systems. This MPC scheme can be generalized to include a class of system with ON/OFF logic local controllers. Different analysis can be given on the constraint sets and reachability of the set-points in case of applying the full gain controllers. This approach can avoid mixed integer programming when a convex programming is preferred.

The identification part in the subspace predictive control relies on a simple QR decomposition for which there exist fast and robust numerical computation algorithms. This provides an opportunity for adaptation of the method by online updating the subspace matrices [Lovera et al., 2000]. The online adaptation can improve the control performance in case of variation of the system parameters, which is likely to happen in the large-scale thermal systems. The use of such adaptive algorithm can be investigated in the future works.

To the knowledge of the author, this work reports some of the earliest results on optimal hybridization and management of transport refrigeration systems. The reader should note that the numbers given here will obviously change depending on the particular operating conditions and they should be interpreted as such. Additionally, the approach could be extended to include other types of modes (e.g boost) or operating characteristics (constraints of fixed speed compressors). However, from this investigation, the potential should be clear. There is significant value to be explored in (i) the hybridization of transport refrigeration systems, (ii) model-based optimization of these systems, and (iii) the use of preview information that is currently available in most vehicle systems.

References

[Agüero and Goodwin, 2007] Agüero, J. C. and Goodwin, G. C. (2007). Choosing between open- and closed-loop experiments in linear system identification. *IEEE Transactions on Automatic Control*, 52(8):1475–1480.

[Albadi and El-Saadany, 2007] Albadi, M. H. and El-Saadany, E. F. (2007). Demand response in electricity markets: An overview. In *IEEE Power Engineering Society General Meeting*, pages 1–5, Tampa, FL, USA.

[Aprea and Renno, 2004] Aprea, C. and Renno, C. (2004). An experimental analysis of a thermodynamic model of a vapor compression refrigeration plant on varying the compressor speed. *International Journal of Energy Research*, 28:537–549.

[Arteconi et al., 2012] Arteconi, A., Hewitt, N. J., and Polonara, F. (2012). State of the art of thermal storage for demand-side management. *Applied Energy*, 93:371–389.

[Åström and Hägglund, 2006] Åström, K. J. and Hägglund, T. (2006). *Advanced Pid Control*. ISA-The Instrumentation, Systems, and Automation Society.

[Aswani et al., 2013] Aswani, A., Gonzalez, H., Sastry, S. S., and Tomlin, C. (2013). Provably safe and robust learning-based model predictive control. *Automatica*, 49(5):1216–1226.

[Aswani et al., 2012] Aswani, A., Master, N., Taneja, J., Culler, D., and Tomlin, C. (2012). Reducing transient and steady state electricity consumption in hvac using learning-based model-predictive control. *Proceedings of the IEEE*, 100(1):240–253.

[babar et al., 2013] babar, M., Ahamed, T. P. I., Al-Ammar, E. A., and Shah, A. (2013). A novel algorithm for demand reduction bid based incentive program in direct load control. *Energy Procedia*, 42:607–613.

[Balbis et al., 2006] Balbis, L., Katebi, R., and Ordys, A. (2006). Modeling predictive control design for industrial applications. In *International Control Conference (ICC2006)*, Glasgow, Scotland.

[Balijepalli et al., 2011] Balijepalli, V. S. K. M., Pradhan, V., Khaparde, S. A., and Shereef, R. M. (2011). Review of demand response under smart grid paradigm. In *Proceedings of the 2011 IEEE PES Innovative Smart Grid Technologies*, pages 236–243, Kollam, Kerala, India.

[Battegay et al., 2015] Battegay, A., Hadj-Said, N., Roupioz, G., Lhote, F., Chambris, E., Boeda, D., and Charge, L. (2015). Impacts of direct load control on reinforcement costs in distribution networks. *Electric Power Systems Research*, 120:70–79.

[Bristow et al., 2006] Bristow, D. A., Tharayil, M., and Alleyne, A. G. (2006). A survey of iterative learning control. *IEEE Control Systems Magazine*, 26(3):96–114.

[Callaway and Hiskens, 2011] Callaway, D. S. and Hiskens, I. A. (2011). Achieving controllability of electric loads. *Proceedings of the IEEE*, 99(1):184–199.

[Campi and Savaresi, 2006] Campi, M. and Savaresi, S. M. (2006). Direct nonlinear control design: The virtual reference feedback tuning (VRFT) approach. *IEEE Transactions on Automatic Control*, 51(1):14–27.

[Candanedo et al., 2013] Candanedo, J. A., Dehkordi, V. R., and Stylianou, M. (2013). Model-based predictive control of an ice storage device in a building cooling system. *Applied Energy*, 111:1032–1045.

[Castilla et al., 2015] Castilla, M., Álvarez, J. D., Normey-Rico, J. E., and Rodríguez, F. (2015). Thermal comfort control using a non-linear MPC strategy: A real case of study in a bioclimatic building. *Journal of Process Control*, 24:703–713.

[Chen et al., 2013] Chen, C., Wang, J., Heo, Y., and Kishore, S. (2013). MPC-based appliance scheduling for residential building energy management controller. *IEEE Transactions on Smart Grid*, 4(3):1401–1410.

[Chu and Jong, 2008] Chu, C. M. and Jong, T. L. (2008). A novel direct air-conditioning load control method. *IEEE Transactions on Power Systems*, 23(3):1356–1363.

[Chu et al., 2005] Chu, C. M., Jong, T. L., and H, Y. W. (2005). A direct load control of air-conditioning loads with thermal comfort control. In *Proceedings of the IEEE PES General Meeting*, San Francisco, CA, USA.

[Cigler and Privara, 2010] Cigler, J. and Privara, S. (2010). Subspace identification and model predictive control for buildings. In *Proceedings of the 11th International Conference on Control, Automation, Robotics and Vision*, Singapore.

[Clarke et al., 1987] Clarke, D. W., Mohtadi, C., and Tuffs, P. S. (1987). Generalized predictive control – part ii extensions and interpretations. *Automatica*, 23(2):149–160.

[Cleland, 1985] Cleland, A. (1985). Experimental verification of a mathematical model for simulation of industrial refrigeration plants. *International Journal of Refrigeration*, 8(5):275–282.

[Cole et al., 2012] Cole, W. J., Edgar, T. F., and Novoselac, A. (2012). Use of model predictive control to enhance the flexibility of thermal energy storage cooling systems. In *Proceedings of the American Control Conference*, Montréal, Canada.

[Conner and Seborg, 2004] Conner, J. S. and Seborg, D. E. (2004). An evaluation of mimo input designs for process identification. *Industrial & Engineering Chemistry Research*, 43:3847–3854.

[Corradi et al., 2006] Corradi, M., Cecchinato, L., and Schiochet, G. (2006). Modeling fin-and-tube gas-cooler for transcritical carbon dioxide cycles. In *International Refrigeration and Air Conditioning Conference*, Lafayette, Indiana, USA. Purdue University.

[CU Aerospace, 2013] CU Aerospace (2013). THERMOSYS toolbox for Matlab/Simulink. `http://thermosys.us`.

[Darby and Nikolaou, 2014] Darby, M. L. and Nikolaou, M. (2014). Identification test design for multivariable model-based control: An industrial perspective. *Control Engineering Practice*, 22:165–180.

[Dincer and Rosen, 2010] Dincer, I. and Rosen, M. A. (2010). *Thermal Energy Storage Systems and Applications*. John Wiley & Sons, New York.

[EIA, 2014] EIA (2014). Annual energy outlook 2014, with projections to 2040. Technical report, U.S. Energy Information Administration. `http://www.eia.gov/forecasts/aeo/pdf/0383(2014).pdf`.

[Elliott and Rasmussen, 2008] Elliott, M. and Rasmussen, B. (2008). Model-based predictive control of a multi-evaporator vapor compression cooling cycle. In *proceeding of the 2008 American Control Conference*, Seattle, Washington, USA.

[EUREL, 2013] EUREL (2013). Electrical power vision 2040 for europe. Technical report, EUREL General Secretariat. `http://www.eurel.org/home/taskforces/documents/eurel-pv2040-short\_version\_web.pdf`.

[Fallahsohi et al., 2010] Fallahsohi, H., Changenet, C., and Placé, S. (2010). Predictive functional control of an expansion valve for minimizing the superheat of an evaporator. *International journal of Refrigeration*, 33:409–418.

[Fasl, 2013] Fasl, J. (2013). Modeling and control of hybrid vapor compression cycles. Master's thesis, University of Illinois at Urbana-Champaign, Department of Mechanical Engineering.

[Fasl et al., 2014] Fasl, J. M., Briscoe, C. R., Mohs, W. F., and Alleyne, A. G. (2014). Dynamic model of a refrigeration system with active thermal energy storage. *ASHRAE Transactions*, 120(1):1–8.

[Favoreel et al., 1998] Favoreel, W., Moor, B. D., Gevers, M., and Overschee, P. V. (1998). Subspace predictive control. Technical Report ESAT-SISTA/TR 1998-49, Katholieke Universiteit Leuven, Leuven, Belgium.

[Finn and Fitzpatrick, 2014] Finn, P. and Fitzpatrick, C. (2014). Demand side management of industrial electricity consumption: Promoting the use of renewable energy through real-time pricing. *Applied Energy*, 113:11–21.

[Fischer et al., 2014] Fischer, D., Toral, T. R., Lindberg, K. B., Wille-Haussmann, B., and Madani, H. (2014). Investigation of thermal storage operation strategies with heat pumps in German multi family houses. *Energy Procedia*, 58:137–144.

[Gambier and Unbehauen, 1999] Gambier, A. and Unbehauen, H. (1999). Multivariable generalized state-space receding horizon control in a real-time environment. *Automatica*, 35:1787–1797.

[Ge and Tassou, 2011a] Ge, Y. and Tassou, S. (2011a). Performance evaluation and optimal design of supermarket refrigeration systems with supermarket model "supersim", part i: Model description and validation. *International Journal of Refrigeration*, 34:527–539.

[Ge and Tassou, 2011b] Ge, Y. T. and Tassou, S. A. (2011b). Thermodynamic analysis of transcritical CO_2 booster refrigeration systems in supermarket. *Energy Conversion and Management*, 52:1868–1875.

[Gehrke and Isleifsson, 2010] Gehrke, O. and Isleifsson, F. (2010). A aggregation friendly information model for demand side resources. In *1st IEEE Workshop on Smart Grid Networking Infrastructure*, pages 1019–1023, Denver, CO, USA.

[Gelazanskas and Gamage, 2014] Gelazanskas, L. and Gamage, K. A. A. (2014). Demand side management in smart grid: A review and proposals for future direction. *Sustainable Cities and Society*, 11:22–30.

[Goli et al., 2011] Goli, S., McKane, A., and Olsen, D. (2011). Demand response opportunities in industrial refrigerated warehouses in california. In *2011 ACEEE Summer Study on Energy Efficiency in Industry*, Niagara Falls, NY, USA.

[Han and Piette, 2008] Han, J. and Piette, M. (2008). Solutions for summer electric power shortages: Demand response and its applications in air conditioning and refrigerating systems. *Refrigeration, Air Conditioning, and Electric Power Machinery*, 29(1):1–4.

[Harish and Kumar, 2014] Harish, V. S. K. V. and Kumar, A. (2014). Demand side management in India: Action plan, policies and regulations. *Renewable and Sustainable Energy Reviews*, 33:613–624.

[Hayes et al., 2014] Hayes, B., Hernando-Gil, I., Collin, A., Harrison, G., and Djokić, S. (2014). Optimal power flow for maximizing network benefits from demand-side management. *IEEE Transactions on Power Systems*, 29(4):1739–1747.

[Heffner et al., 2007] Heffner, G., Goldman, C., Kirby, B., and Kintner-Meyer, M. (2007). Loads providing ancillary services: Review of international experience. Technical report, U.S. Department of Energy, Ernesto Orlando Lawrence Berkeley National Laboratory.

[Hermanus et al., 2014] Hermanus, H. M., Shafiei, S. E., Stoustrup, J., and Izadi-Zamanabadi, R. (2014). Model-based predictive control scheme for cost optimization and balancing services for supermarket refrigeration systems. In *Proceedings of the 19th IFAC World Congress*, pages 975–980, Cape Town, South Africa.

[Heussen et al., 2012] Heussen, K., you, S., Biegel, B., Hansen, L. H., and Andersen, K. B. (2012). Indirect control for demand side management – a conceptual introduction. In *Proceedings of the 3rd IEEE PES Innovative Smart Grid Technologies Europe (ISGT Europe)*, pages 1–8, Berlin, Germany.

[Hjalmarsson et al., 1998] Hjalmarsson, H., Gevers, M., Gunnarsson, S., and Lequin, O. (1998). Iterative feedback tuning: Theory and applications. *IEEE Control Systems*, 18(4):26–41.

[Hou and Jin, 2011] Hou, Z. and Jin, S. (2011). A novel data-driven control approach for a class of discrete-time nonlinear systems. *IEEE Transactions on Control Systems Technology*, 19(6):1549–1558.

[Hou and Wang, 2013] Hou, Z. and Wang, Z. (2013). From model-based control to data-driven control; survey, classification and perspective. *Information Sciences*, 235:3–35.

[Hovgaard et al., 2013] Hovgaard, T. G., Boyd, S., Larsen, L. F. S., and Jøregensen, J. B. (2013). Nonconvex model predictive control for commercial refrigeration. *International Journal of Control*, 86(8):1349–1366.

[Hovgaard et al., 2012] Hovgaard, T. G., Larsen, L. F. S., Edlund, K., and Jrgensen, J. B. (2012). Model predictive control technologies for efficient and flexible power consumption in refrigeration systems. *Energy*, 44:105–116.

[Hovgaard et al., 2011] Hovgaard, T. G., Larsen, L. F. S., Skovrup, M. J., and Jrgensen, J. (2011). Power consumption in refrigeration systems - modeling for optimization. In *Proceedings of the 2001 4th International Symposium on Advanced Control of Industrial Processes*, Hangzhou, China.

[Hu and Karava, 2014] Hu, J. and Karava, P. (2014). Model predictive control strategies for buildings with mixed-mode cooling. *Building and Environment*, 71:233–244.

[Huang and Kadali, 2008] Huang, B. and Kadali, R. (2008). *Dynamic Modeling, Predictive Control and Performance Monitoring: A Data-Driven Subspace Approach*. Lecture Notes in Control and Information Sciences. Springer, London.

[Javani et al., 2014] Javani, N., Dincer, I., Naterer, G. F., and Yilbas, B. S. (2014). Exergy analysis and optimization of a thermal management system with phase change material for hybrid electric vehicles. *Applied Thermal Engineering*, 64:471–482.

[Juelsgaard et al., 2013] Juelsgaard, M., Totu, L. C., Shafiei, S. E., Wisnewski, R., and Stoustrup, J. (2013). Control structures for smart grid balancing. In *Proceedings of the 4th IEEE PES Innovative Smart Grid Technologies Europe (ISGT Europe)*, pages 1–5, Lyng by, Denmark.

[Kadali et al., 2003] Kadali, R., Huang, B., and Rossiter, A. (2003). A data driven subspace approach to predictive controller design. *Control Engineering Practice*, 11:261–278.

[Karimi et al., 2004] Karimi, A., Mišković, L., and Bonvin, D. (2004). Iterative correlation-based controller tuning. *International Journal of Adaptive Control and Signal Processing*, 18:645–664.

[Kim, 2013] Kim, S. H. (2013). Building demand-side control using thermal energy storage under uncertainty: An adaptive multiple model-based predictive control (mmpc) approach. *Building and Environment*, 67:111–128.

[Knudsen, 2001] Knudsen, T. (2001). Consistency analysis of subspace identification methods based on a linear regression approach. *Automatica*, 37:81–89.

[Kosek et al., 2013] Kosek, A. M., Costanzo, G. T., Binder, H. W., and Gehrke, O. (2013). An overview of demand side management control schemes for buildings in smart grids. In *2013 IEEE International Conference on Smart Energy Grid Engineering (SEGE)*, pages 1–9, Oshawa, ON, Canada.

[Larimore, 1996] Larimore, W. (1996). statistical optimality and canonical variate analysis system identification. *Signal Processing*, 52:131–144.

[Larsen, 2005] Larsen, L. F. S. (2005). *Model Based Control of Refrigeration Systems*. PhD thesis, Section for Automation and Control, Aalborg University, Denmark.

[Leducq et al., 2006] Leducq, D., Guilpart, J., and Trystram, G. (2006). Non-linear predictive control of a vapor compression cycle. *International journal of Refrigeration*, 29:761–772.

[Lee and Lee, 2005] Lee, J. M. and Lee, J. H. (2005). Approximate dynamic programming-based approaches for input-output data-driven control of nonlinear processes. *Automatica*, 41:1281–1288.

[Li et al., 2008] Li, H., Jeong, S., Yoon, J., and You, S. (2008). An empirical model for independent control of variable speed refrigeration system. *Applied Thermal Engineering*, 28:1918–1924.

[Ljung, 1987] Ljung, L. (1987). *System Identification: Theory for the User*. Prentice-Hall information and system sciences series. Prentice-Hall.

[Lovera et al., 2000] Lovera, M., Gustafsson, T., and Verhaegen, M. (2000). Recursive subspace identification of linear and nonlinear wiener state-space models. *Automatica*, 36:1639–1650.

[Ma et al., 2014] Ma, J., Qin, S. J., and Salsbury, T. (2014). Application of economic MPC to the energy and demand minimization of a commercial building. *Journal of Process Control*, 24:1282–1291.

[Ma et al., 2012a] Ma, J., Qin, S. J., Salsbury, T., and Xu, P. (2012a). Demand reduction in building energy systems based on economic model predictive control. *Chemical Engineering Science*, 67(1):92–100.

[Ma et al., 2012b] Ma, Y., Borrelli, F., Hencey, B., Coffey, B., Bengea, S., and Haves, P. (2012b). Model predictive control for the operation of building cooling systems. *IEEE Transactions on Control Systems Technology*, 20(3):796–803.

[Macedo et al., 2015] Macedo, M. N. Q., Galo, J. J. M., Almeida, L. L., and Lima, A. C. C. (2015). Typification of load curves for DSM in Brazil for a smart grid environment. *Electrical Power and Energy Systems*, 67:216–221.

[Maciejowski, 2002] Maciejowski, J. (2002). *Predictive Control with Constraints*. Pearson Education. Prentice Hall, England.

[Mahmood et al., 2014] Mahmood, A., m. N. Ullah, Razzaq, S., Basit, A., Mustafa, U., m. Naeem, and Javaid, N. (2014). A new scheme for demand side management in future smart grid networks. *Procedia Computer Science*, 32:477–484.

[Mathieu and Callaway, 2012] Mathieu, J. L. and Callaway, D. S. (2012). State estimation and control of heterogeneous thermostatically controlled loads for load following. In *Proceedings of the 45th Hawaii International Conference on System Sciences*, Maui, HI, USA.

[Mendoza-Serrano and Chmielewski, 2014] Mendoza-Serrano, D. I. and Chmielewski, D. J. (2014). Smart grid coordination in building HVAC systems: EMPC and the impact of forecasting. *Journal of Process Control*, 24:1301–1310.

[Molina et al., 2000] Molina, A., Gabaldon, A., Fuentes, J. A., and Canovas, F. J. (2000). Approach to multivariable predictive control applications in residential HVAC direct load control. In *Proceedings of the IEEE Power Engineering Society Summer Meeting*, Seattle, WA, USA.

[Moonen et al., 1989] Moonen, M., Moor, B. D., Vandenberghe, L., and Vandewalle, J. (1989). On- and off-line identification of linear state-space models. *International Journal of Control*, 49(1):219–232.

[Navalkar et al., 2014] Navalkar, S. T., van Wingerden, J. W., van Solingen, E., Oomen, T., Pasterkamp, E., and van Kuik, G. A. M. (2014). Subspace predictive repetitive control to mitigate periodic loads on large scale wind turbines. *Mechatronics*, 24:916–925.

[Newsham and Bowker, 2010] Newsham, G. R. and Bowker, B. G. (2010). The effect of utility time-varying pricing and load control strategies on residential summer peak electricity use: A review. *Energy Policy*, 38:3289–3296.

[Ng and Sheblé, 1998] Ng, K. and Sheblé, G. B. (1998). Direct load control - a profit-based load management using linear programming. *IEEE Transactions on Power Systems*, 13(2):688–694.

[Ommen and Elmegaard, 2012] Ommen, T. and Elmegaard (2012). Numerical model for thermoeconomic diagnosis in commercial transcritical/subcritical booster refrigeration systems. *Energy Conversion and Management*, 60:161–169.

[Overschee and Moor, 1994] Overschee, P. V. and Moor, B. D. (1994). N4SID: Subspace algorithms for the identification of combined deterministic-stochastic systems. *Automatica*, 30(1):75–93.

[Overschee and Moor, 1996] Overschee, P. V. and Moor, B. D. (1996). *Subspace Identification for Linear Systems: Theory, Implementation, Applications*. Pearson Education. Kluwer Academic Publishers.

[Pérez-Segarra et al., 2005] Pérez-Segarra, C., Rigola, J., Sòria, M., and Oliva, A. (2005). Detailed thermodynamic characterization of hermetic reciprocating compressors. *International Journal of Refrigeration*, 28:579–593.

[Palensky and Dietrich, 2011] Palensky, P. and Dietrich, D. (2011). Demand side management: Demand response, intelligent energy systems, and smart loads. *IEEE Transactions on Industrial Informatics*, 7(3):381–388.

[Pedersen et al., 2014] Pedersen, R., Schwensen, J., Biegel, B., Stoustrup, J., and Green, T. (2014). Aggregation and control of supermarket refrigeration systems in a smart grid. In *Proceedings of the 19th IFAC World Congress*, pages 9942–9949, Cape Town, South Africa.

[Pedersen et al., 2013] Pedersen, R., Schwensen, J., Sivabalan, S., Corazzol, C., Shafiei, S. E., Vinther, K., and Stoustrup, J. (2013). Direct control implementation of a refrigeration system in smart grid. In *Proceedings of the American Control Conference*, pages 3954–3959, Washington DC, USA.

[Petersen et al., 2012] Petersen, L. N., Madsen, H., and Heerup, C. (2012). ESO2 optimization of supermarket refrigeration systems: Mixed integer MPC and system performance. Technical report, Department of Informatics and Mathematical Modeling, Technical University of Denmark.

[Petersen et al., 2013] Petersen, M. K., Edlund, K., Hansen, L. H., Bendtsen, J. D., and Stoustrup, J. (2013). A taxonomy for flexibility modeling and a computationally efficient algorithm for dispatch in smart grids. In *Proceedings of the 2013 American Control Conference*, pages 1150–1156, Washington, DC, USA.

[Petre et al., 2009] Petre, C., m. Feidt, Costea, M., and Petrescu, S. (2009). A model for study and optimization of real-operating refrigeration machines. *International Journal of Energy Research*, 33:173–179.

[Pfafferott and Schmitz, 2002] Pfafferott, T. and Schmitz, G. (2002). Modeling and simulation of refrigeration systems with the natural refrigerant CO2. In *International Refrigeration and Air Conditioning Conference*, Lafayette, Indiana, USA. Purdue University.

[Pfafferott and Schmitz, 2004] Pfafferott, T. and Schmitz, G. (2004). Modeling and transient simulation of co_2-refrigeration systems with modelica. *International Journal of Refrigeration*, 27:42–52.

[Prívara et al., 2011] Prívara, S., Širký, J., Ferkl, L., and Cigler, J. (2011). Model predictive control of a building heating system: The first experience. *Energy and Buildings*, 43:564–572.

[Rahnama et al., 2014] Rahnama, S., Shafiei, S. E., Stoustrup, J., Rasmussen, H., and Bendtsen, J. D. (2014). Evaluation of aggregators for integration of large-scale consumers in smart grid. In *Proceedings of the 19th IFAC Word Congress*, pages 1879–1885, Cape Town, South Africa.

[Rasmussen, 2002] Rasmussen, B. (2002). Control oriented modeling of transcritical vapor compression systems. Master's thesis, Department of Mechanical Engineering, University of Illinois at Urbana-Champaign, IL, USA.

[Rasmussen, 2012a] Rasmussen, B. P. (2012a). Dynamic modeling for vapor compression systems - part I: Literature review. *HVAC$R Research*, 18(5):934–955.

[Rasmussen, 2012b] Rasmussen, B. P. (2012b). Dynamic modeling for vapor compression systems - part II: Simulation tutorial. *HVAC$R Research*, 18(5):956–973.

[Rasmussen and Alleyne, 2006] Rasmussen, B. P. and Alleyne, A. G. (2006). Dynamic modeling and advanced control of air conditioning and refrigeration systems. Technical report, ACRC, University of Illinois at Urbana-Champaign.

[Ricker, 2010] Ricker, N. (2010). Predictive hybrid control of the supermarket process. *Control Engineering Practice*, 18:608–617.

[Safonov and Tsao, 1997] Safonov, M. G. and Tsao, T. (1997). The unfalsified control concept and learning. *IEEE Transactions on Automatic Control*, 42(6):843–847.

[Sarabia et al., 2009] Sarabia, D., Capraro, F., Larsen, L. F. S., and Prada, C. (2009). Hybrid NMPC of supermarket display cases. *Control Engineering Practice*, 17:428–441.

[Schurt et al., 2009] Schurt, L., Hermes, C., and Neto, A. (2009). A model-driven multivariable controller for vapor compression refrigeration systems. *International Journal of Refrigeration*, 32:1672–1682.

[Schurt et al., 2010] Schurt, L. C., Hermes, C., and Neto, A. T. (2010). Assessment of the controlling envelope of a model-based multivariable controller for vapor compression refrigeration systems. *Applied Thermal Engineering*, 30:1538–1546.

[Scott et al., 2012] Scott, D., Hoest, R., Yang, F., Goli, S., and Olsen, D. (2012). The impact of control technology on the demand response potential of california industrial refrigerated facilities. Technical Report, LBNL-5750E, Lawrence Berkeley National Laboratory, Berkeley, CA, USA.

[Shafiei and Alleyne, 2015] Shafiei, S. E. and Alleyne, A. (2015). Model predictive control of hybrid thermal energy systems in transport refrigeration. *Applied Thermal Engineering*, 82:264–280.

[Shafiei et al., 2013a] Shafiei, S. E., Izadi-Zamanabadi, R., Rasmussen, H., and Stoustrup, J. (2013a). A decentralized control method for direct smart grid control of refrigeration systems. In *Proceedings of the 52nd IEEE Conference on Decision and Control*, pages 6934–6939, Firenze, Italy.

[Shafiei et al., 2015] Shafiei, S. E., Knudsen, T., Wisniewski, R., and Andersen, P. (2015). Data-driven predictive direct load control of refrigeration systems. *IET Control Theory & Applications*. DOI: 10.1049/iet-cta.2014.0666, Online ISSN 1751-8652, Available online: 23 March 2015.

[Shafiei et al., 2013b] Shafiei, S. E., Rasmussen, H., and Stoustrup, J. (2013b). Model predictive control for a thermostatic controlled system. In *Proceedings of the European Control Conference*, pages 559–1564, Zürich, Switzerland.

[Shafiei et al., 2013c] Shafiei, S. E., Rasmussen, H., and Stoustrup, J. (2013c). Modeling supermarket refrigeration systems for demand-side management. *Energies*, 6(2):900–920.

[Shafiei et al., 2013d] Shafiei, S. E., Rasmussen, H., and Stoustrup, J. (2013d). Modeling supermarket refrigeration systems for supervisory control in smart grid. In *Proceedings of the American Control Conference*, pages 5660–5665, Washington DC, USA.

[Shafiei et al., 2013e] Shafiei, S. E., Stoustrup, J., and Rasmussen, H. (2013e). A supervisory control approach in economic MPC design for refrigeration systems. In *Proceedings of the European Control Conference*, pages 1565–1570, Zürich, Switzerland.

[Shafiei et al., 2014] Shafiei, S. E., Stoustrup, J., and Rasmussen, H. (2014). Model predictive control for flexible power consumption of large-scale refrigeration systems. In *Proceedings of the American Control Conference*, pages 412–417, Portland, OR, USA.

[Shao et al., 2008a] Shao, S., Shi, W., Li, X., and Yan, Q. (2008a). Simulation model for complex refrigeration systems based on two-phase fluid network – part i: Model development. *International Journal of Refrigeration*, 31:490–499.

[Shao et al., 2008b] Shao, S., Shi, W., Li, X., and Yan, Q. (2008b). Simulation model for complex refrigeration systems based on two-phase fluid network – part ii: Model application. *International Journal of Refrigeration*, 31:500–509.

[Shi et al., 2010] Shi, R., Fu, D., Feng, Y., Fan, J., and Mijanovic, S. (2010). Dynamic modeling of CO2 supermarket refrigeration system. In *International Refrigeration and Air Conditioning Conference*, Lafayette, Indiana, USA. Purdue University.

[Soderstrom and Stoica, 1989] Soderstrom, T. and Stoica, P. (1989). *System Identification*. Prentice Hall International Series in Systems and Control Engineering. Prentice Hall.

[Sonntag et al., 2007] Sonntag, C., Devanathan, A., Engell, S., and Stursberg, O. (2007). Hybrid nonlinear model-predictive control of a supermarket refrigeration system. In *Proceedings of the16th IEEE International Conference on Control Applications*, pages 1432–1437, Singapore.

[Spall, 2000] Spall, J. C. (2000). Adaptive stochastic approximation by the simultaneous perturbation method. *IEEE Transactions on Automatic Control*, 45(10):1839–1853.

[SRSim, 2013] SRSim (2013). A simulation benchmark for supermarket refrigeration systems using matlab. `http://www.es.aau.dk/projects/refrigeration/simulation-tools/`. Accessed: February 2015.

[Surles and Henze, 2012] Surles, W. and Henze, G. P. (2012). Evaluation of automatic priced based thermostat control for peak energy reduction under residential time-of-use utility tariffs. *Energy and buildings*, 49:99–108.

[Tahersima et al., 2011] Tahersima, F., Stoustrup, J., Meybodi, S. A., and Rasmussen, H. (2011). Contribution of domestic heating systems to smart grid control. In *Proceedings of the 50th IEEE Conference on Decision and Control and European Control Conference (CDC-ECC)*, pages 3677–3681, Orlando, FL, USA.

[Tascikaraoglu et al., 2014] Tascikaraoglu, A., Boynuegri, A. R., and Uzunoglu, M. (2014). A demand side management strategy based on forecasting of residential renewable sources: A smart home system inTurkey. *Energy and Buildings*, 80:309–320.

[Tassou et al., 2009] Tassou, S. A., De-Lille, G., and Ge, Y. T. (2009). Food transport refrigeration – approaches to reduce energy consumption and environmental impacts of road transport. *Applied Thermal Engineering*, 29:1467–1477.

[Touretzky and Baldea, 2014] Touretzky, C. R. and Baldea, M. (2014). Integrating scheduling and control for economic MPC for buildings with energy storage. *Journal of Process Control*, 24:1292–1300.

[Trangbaek et al., 2012] Trangbaek, K., M, P., Bendtsen, J., and Stoustrup, J. (2012). *Predictive Smart Grid Control with Exact Aggregated Power Constraints*, chapter 21, pages 649–668. Power Systems, ISSN: 1612-1287: Smart Power Grids, Eds: Ali Keyhani and Muhammad Marwali. Springer-Verlag Berlin Heidelberg.

[Trangbaek et al., 2011] Trangbaek, K., Petersen, M., Bendtsen, J., and Stoustrup, J. (2011). Exact power constraints in smart grid control. In *Proceedings of the 50th IEEE Conference on Decision and Control and European Control Conference*, Orlando, FL, USA.

[Verhaegen, 1994] Verhaegen, M. (1994). Identification of the deterministic part of MIMO state space models given in innovations from from input-output data. *Automatica*, 30(1):61–74.

[Vinther et al., 2013] Vinther, K., Rasmussen, H., Izadi-Zamanabadi, R., and Stoustrup, J. (2013). Single temperature sensor superheat control using a novel maximum slope-seeking method. *International Journal of Refrigeration*, 36(3):1118–1129.

[Walkowicz et al., 2014] Walkowicz, K., Kelly, K., Duran, A., and Burton, E. (2014). Fleet DNA project data. Technical report, National Renewable Energy Laboratory.

[Walsh et al., 2013] Walsh, B. P., Murray, S. N., and O'Sullivan, D. T. J. (2013). Free-cooling thermal energy storage using phase change materials in an evaporative cooling system. *Applied Thermal Engineering*, 59:618–626.

[Wang et al., 2007a] Wang, F., Maidment, G., Missenden, J., and Tozer, R. (2007a). The novel use of phase change materials in refrigeration plant. part 1: Experimental investigation. *Applied Thermal Engineering*, 27:2893–2901.

[Wang et al., 2007b] Wang, F., Maidment, G., Missenden, J., and Tozer, R. (2007b). The novel use of phase change materials in refrigeration plant. part 1: Experimental investigation. *Applied Thermal Engineering*, 27:2893–2901.

[Wang et al., 2007c] Wang, X., Huang, B., and Chen, T. (2007c). Data-driven predictive control for solid oxide fuel cells. *Journal of Process Control*, 17:103–114.

[Willatzen et al., 1998] Willatzen, M., Pettit, N. B., and Ploug-Srensen, L. (1998). A general dynamic simulation model for evaporators and condensers in refrigeration. part i: moving-boundary formulation of two-phase flows with heat exchange. *International Journal of Refrigeration*, 21(5):398–403.

[Wu et al., 2013] Wu, X., Shen, J., Li, Y., and Lee, K. Y. (2013). Data-driven modeling and predictive control for boiler-turbine unit. *IEEE Transactions on Energy Conversion*, 28(3):470–481.

[Zakula et al., 2015] Zakula, T., Armstrong, P. R., and Norford, L. (2015). Advanced cooling technology with thermally activated building surfaces and model predictive control. *Energy and Buildings*, 86:640–650.

[Zeng et al., 2010] Zeng, J., Gao, C., and Su, H. (2010). Data-driven predictive control for blast furnace ironmaking process. *Computers and Chemical Engineering*, 34:1854–1862.

[Zhang and Dear, 2015] Zhang, F. and Dear, R. (2015). Thermal environments and thermal comfort impacts of direct load control air-conditioning strategies in university lecture theatres. *Energy and Buildings*, 86:233–242.

[Zhao et al., 2015] Zhao, Y., Lu, Y., Yan, C., and Wang, S. (2015). MPC-based optimal scheduling of grid-connected low energy buildings with thermal energy storages. *Energy and Buildings*, 86:415–426.

[Zheng et al., 2014] Zheng, Y., Hu, Z., Wang, J., and Wen, Q. (2014). IRSP (integrated resource strategic planing) with interconnected smart grids in integrating renewable energy and implementing DSM (demand side management) in China. *Energy*, 76:863–874.

[Zhou et al., 2010] Zhou, R., Zhang, T., Catano, J., Wen, J. T., Michna, G. J., Peles, Y., and Jensen, M. K. (2010). The steady-state modeling and optimization of a refrigeration system for high heat flux removal. *Applied Thermal Engineering*, 30:2347–2356.

Contributions

Paper A: Modeling Supermarket Refrigeration Systems for Demand-Side Management **83**

Paper B: A Supervisory Control Approach in Economic MPC Design for Refrigeration Systems **109**

Paper C: Model Predictive Control for a Thermostatic Controlled System **125**

Paper D: A Decentralized Control Method for Direct Smart Grid Control of Refrigeration Systems **141**

Paper E: Model Predictive Control for Flexible Power Consumption of Large-Scale Refrigeration Systems **157**

Paper F: Data-Driven Predictive Direct Load Control of Refrigeration Systems **173**

Paper G: Model Predictive Control of Hybrid Thermal Energy Systems in Transport Refrigeration **197**

Paper A

Modeling Supermarket Refrigeration Systems for Demand-Side Management

Seyed Ehsan Shafiei, Henrik Rasmussen and Jakob Stoustrup

This paper was published in:
Energies, Special issue: Smart grid and the future electrical network, February 2013

Abstract

Modeling of supermarket refrigeration systems for supervisory control in the smart grid is presented in this paper. A modular modeling approach is proposed in which each module is modeled and identified separately. The focus of the work is on estimating the power consumption of the system while estimating the cold reservoir temperatures as well. The models developed for each module as well as for the overall integrated system are validated by real data collected from a supermarket in Denmark. The results show that the model is able to estimate the actual electrical power consumption with a high fidelity. Moreover a simulation benchmark is introduced based on the produced model for demand-side management in smart grid. Finally, a potential application of the proposed benchmark in direct control of the power/energy consumption is presented by a simple simulation example.

Nomenclature:

dc	display case	REC	receiver
e	evaporator	EV	expansion valve
o	outlet	MT	medium temperature
i	inlet	LT	low temperature
suc	suction manifold	EVAP	evaporator
comp	compressor	COMP_HI	high stage compressor rack
cnd	condenser	COMP_LO	low stage compressor rack
ref	refrigerant	BPV	bypass valve
		CV_HP	high pressure control valve

1 Introduction

The increase of renewable energy sources and distributed generation, like wind farms/PVs, creates new challenges for the power system. Power generations with intermittent and unpredictable characteristics create a significant balancing strain and are therefore difficult to integrate in large capacity in the electrical grid. To compensate, the power system will be required to manage actively not only the generation, but also the consumption.

The thermal mass existing in foodstuffs in supermarket refrigeration systems (SRS) makes it possible to store some amount of electrical energy as coldness by lowering the temperatures of the display cases and the freezing rooms down to permissible points. Considering the total number of supermarkets in a country (for example of around 4500 with a consumption of approximately 540 TWh/year in Denmark with 5.5 mio. inhabitants), this constitutes a significant potential for energy storage. In order to utilize this storage capability in either grid balancing or overall consumption cost (the economic cost of electricity consumption) reduction, a supervisory controller (in communication with the grid) should be responsible for doing so as demand-side management. Here, the supervisory controller is the control unit that provides the set-points (usually obtained as a result of an optimization algorithm) to the local/distributed controllers. The local controllers regulate the feedback signals to the assigned set-points. Producing a model that can fairly estimate the power consumption of the system as well as the cold reservoir temperatures can pave the way for developing such supervisory control methods.

Articles that present models for refrigeration systems can be divided into two main categories. The first category includes the modeling of individual components, like compressor [1], condenser [2], evaporator [3], etc. These models are usually too detailed and specific for the purpose at hand. They are suitable for doing performance and efficiency improvements at local control levels. The second category (e.g., [4–6]) presents the integrated refrigeration systems including several components but in various configurations and with different level of model complexities. Depending on the application in mind, there is a trade-off between model complexity and its accuracy. For smart grid applications, the modeling of refrigeration systems would be a challenging exercise. On one hand, we need a model that simplifies the behavior of the system while estimating the critical variables with desired degree of accuracy. On the other hand, developing a very detailed and highly accurate model, including all variables and factors, requires considerable amount of data, and also is not computationally efficient to simulate, for example, monthly operation of the system under demand-side management strategies.

This paper presents a model for the blocks included in the dashed box in Figure 5.2. It contains refrigeration system including different modules as well as distributed controllers that regulate the system states to the applied set-points. In order to develop supervisory control methods for demand-side management in smart grid as shown by dot-dashed box in the figure, the model should be able to predict the power consumptions of the compressors for the given set-points while estimating other required variables like cold room temperatures, suction pressure, etc.

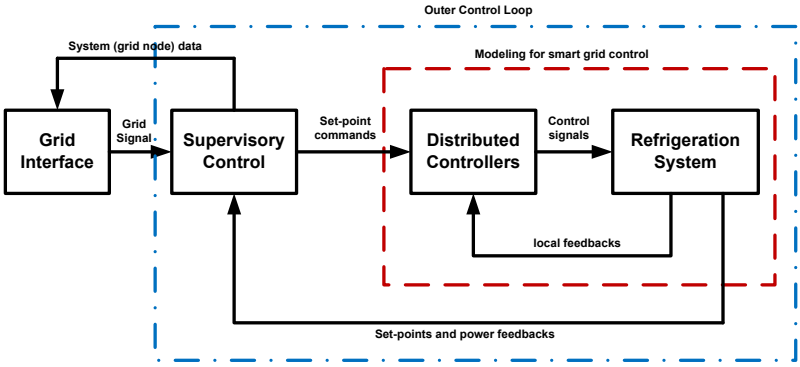

Figure 4.1: A typical control system structure for connecting supermarket refrigeration systems to the smart grid.

As mentioned above, numerous studies in the literature have been dedicated to modeling refrigeration systems with various levels of details and emphasis on different parts of the system behavior. In the sequel, we shall describe a few, which have inspired the present work in particular. A mathematical model for industrial refrigeration plants has been proposed by [7] for simulation of food refrigeration processes. Only the air temperature of the cold rooms is estimated by the model and there is discrepancy between predicted and measured air temperatures. The development of a Modelica library for CO_2 refrigeration systems have been presented by Pfafferott and Schmitz [8]. The heat exchanger model has been explained, and only the steady-state conditions have been

validated by experimental data. Subsequently, they extended their model for transient simulation and validation provided in [9]. The pressures are well estimated, but the air temperature of cold rooms is not reported, and estimation of the mass flow rate is not very accurate. The study of a thermodynamic model supported by experimental analysis has been accomplished in [4]. The method has been proposed to improve the coefficient of performance (COP) by matching the compressor capacity to the load, replacing the classical thermostatic control. A similar work has been performed by [10] to provide an excellent transient characteristics by using a decoupling model. Although the latter two methods can be applied to a single vapor compression cycle (VCR), they are not applicable to the multi-evaporator systems in supermarkets. Ref [5] presents a dynamic mathematical model for coupling the refrigeration system and phase change materials. But this model can only predict the refrigerant states and dynamic COP.

A more generalized model has been introduced by [11] based on a two-phase fluid network. The proposed model can simulate different kinds of complex refrigeration systems in different operating modes and conditions, but it can only estimate the steady-state values in different operating modes. Applications of the developed model to estimate the different operating points of the multi-unit inverter air conditioner, heat pump with domestic hot water and multi-unit heat pump dehumidifier have been demonstrated in [12]. It should be noted that the steady-state models without considering cold room dynamics cannot be employed for demand-side managements, in which playing with the cold room temperatures is required for energy solutions. Another such steady-state model is proposed in [6].

The model presented in [13] provides an analytical method for COP optimization. This model does not simulate the system operation and has applicability to the design of the refrigerating machines in terms of selection, design and optimization of the main parameters. With focus on local controls, Schurt *et al*. proposed a model-driven linear controller as well as its assessment for a single vapor compression cycle in [14, 15]. A dynamic model of a transcritical CO_2 SRS has been developed by [16] using the equation-based modeling language Modelica, which can be simulated e.g., in Dymola. Only gas cooler equations and model validation are provided in that paper. As a different perspective, a numerical model has been recently developed by [17] for the evaluation of the use of thermoeconomic diagnosis in transcritical refrigeration.

None of the integrated models in the above cited works can predict the power consumption of compressors that is necessary for demand-side management of supermarket refrigeration systems. There is however a model developed by [18] for simulating the energy consumption of supermarket refrigeration systems. In this work, however, the cold room dynamics have not been modeled and the map-based routing proposed for estimating the compressor power consumption is not very accurate. Considering power consumption in refrigeration systems, Ref [19] has proposed a modeling for optimization purposes. There is however no identification and model validation reported by that work, and the first order model presented for the cold room regarding its air temperature results in storing the energy in the air instead of foodstuffs.

By analyzing the thermodynamics of the system, we develop a model that simulates the electrical behavior. This enables us to control the electrical power consumption (needed for demand-side management) by controlling the cooling capacity (utilizing the existing thermal mass). The proposed model possesses most advantages of the preceding researches like (i) simplifying the behavior of supermarket refrigeration systems

as a simulation benchmark for supervisory control; (ii) being very accurate despite its simplicity; (iii) having modularity and reconfigurability; and (iv) being validated by real data. Our modeling is the first principle approach using the physical insight to define the model structure.

The modeling exercise is performed by a modular approach in which the system is separated into different subsystems (modules), each modeled and validated separately. This modularity leaves open the possibility of modeling refrigeration systems with different configurations that are adopted in various supermarkets. Finally, an illustrative example is provided to show how the developed model can be utilized as a simulation benchmark for implementing a simple demand-side management scenario.

2 System Description

In this work, the case study is a large-scale CO_2 refrigeration system including several display cases and freezing rooms as well as two compressor banks configured in a booster layout as shown in Figure 9.1. The corresponding pressure-enthalpy (P-H) diagram describing the thermodynamic cycle of the system is provided in Figure 4.2b. Due to low ambient temperature, the high pressure side operates below the critical value, which keeps the operating condition in the subcritical cycle, as shown in the figure.

Starting from the receiver (REC), two-phase refrigerant (mix of liquid and vapor) at point "8" is split out into saturated liquid ("1") and saturated gas ("1b"). The latter is bypassed by BPV, and the former flows into expansion valves where the refrigerant pressure drops to the medium ("2") and low ("$2'$") pressures. The expansion valves EV_MT and EV_LT are driven by hysteresis ON/OFF controllers to regulate the temperature of the fridge display cases and freezing rooms, respectively. Flowing through medium and low temperature evaporators (EVAP_MT and EVAP_LT), the refrigerant absorbs heat from the cold reservoir while a superheat controller is also operating on the valves. That is to make sure the refrigerant leaving the evaporators toward compressors is completely vaporized (only in gas phase). Both pressure and enthalpy of the refrigerant are increased by the low stage compressor rack (COMP_LO) from "$3'$" to "$4'$". All mass flows at the outlet of COMP_LO, EVAP_MT and BPV are collected by the suction manifold at point "5" where the pressure and enthalpy are increased again to the highest point, "6", by the high stage compressors (COMP_HI). Afterward, the gas phase refrigerant enters the condenser to deliver the absorbed heat from cold reservoirs to the surrounding where its enthalpy decreased significantly from "6" to "7" accompanied by a small pressure drop. At the outlet of the high pressure control valve (CV_HP), the pressure drops to an intermediate level and the refrigerant, which is now in two-phase, flows into the receiver and the cycle is completed.

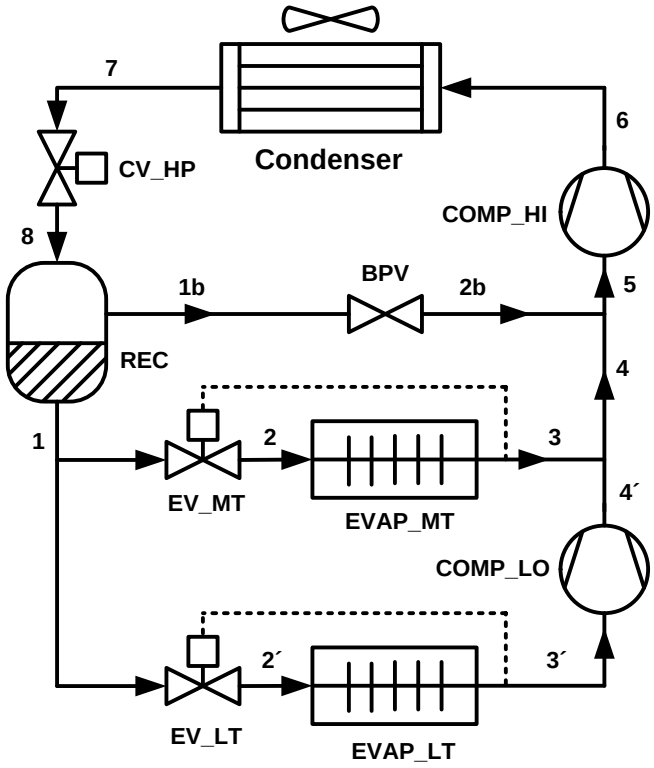

(a)

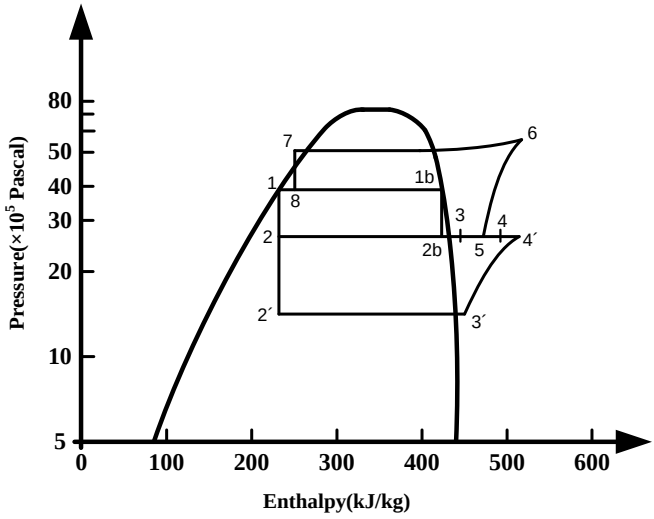

(b)

Figure 4.2: CO_2 refrigeration systems, (a): A typical booster configuration; (b): Corresponding P-H diagram of subcritical cycle in the booster system.

3 Modeling

There are three major subsystems to be modeled, including *display cases*, *suction manifold* together with high stage compressors, and *condenser*. The modeling of low temperature section is similar to the medium temperature and will be addressed at the end of the modeling section. The operation of the high pressure valve and the receiver are not modeled since the intermediate pressure at the outlet of the receiver is assumed constant.

Display Cases

In display cases, heat is transferred from foodstuffs to evaporator, $\dot{Q}_{foods/dc}$, and then from evaporator to circulated refrigerant, $\dot{Q}_e$, also known as the cooling capacity. There is however heat load from the environment, $\dot{Q}_{load}$, formulated as a variable disturbance. Here, we consider the measured air temperature at the evaporator outlet as the display case temperature, T_{dc}. Assuming a lumped temperature model, the following dynamical equations are derived based on energy balances for the foregoing heat transfers.

$$MCp_{foods}\frac{dT_{foods}}{dt} = -\dot{Q}_{foods/dc} \tag{4.1}$$

$$MCp_{dc}\frac{dT_{dc}}{dt} = \dot{Q}_{load} + \dot{Q}_{foods/dc} - \dot{Q}_e \tag{4.2}$$

where MCp denotes the corresponding mass multiplied by the heat capacity. The energy flows are

$$\dot{Q}_{foods/dc} = UA_{foods/dc}(T_{foods} - T_{dc}), \tag{4.3}$$

$$\dot{Q}_{load} = UA_{load}(T_{indoor} - T_{dc}) \tag{4.4}$$

and

$$\dot{Q}_e = UA_e(T_{dc} - T_e) \tag{4.5}$$

where UA is the overall heat transfer coefficient, h_{oe} and h_{ie} are enthalpies at the outlet and inlet of the evaporators and are nonlinear functions of the evaporation temperature, and T_{indoor} is the supermarket indoor temperature. The heat transfer coefficient between the refrigerant and the display case temperature, UA_e, is described as a linear function of the mass of the liquefied refrigerant in the evaporator [20],

$$UA_e = k_m M_r, \tag{4.6}$$

where k_m is a constant parameter. The refrigerant mass, $0 \le M_r \le M_{r,max}$, is subject to the following dynamic [21],

$$\frac{dM_r}{dt} = \dot{m}_{r,in} - \dot{m}_{r,out}, \tag{4.7}$$

where $\dot{m}_{r,in}$ and $\dot{m}_{r,out}$ are the mass flow rate of refrigerant into and out of the evaporator, respectively. The entering mass flow is determined by the opening degree of the expansion valve and is described by the following equation:

$$\dot{m}_{r,in} = OD\ KvA\sqrt{2\rho_{suc}(P_{rec} - P_{suc})} \tag{4.8}$$

where OD is the opening degree of the valve with a value between 0 (closed) to 1 (fully opened), P_{rec} and P_{suc} are receiver and suction manifold pressures, ρ_{suc} is the density of the circulating refrigerant, and KvA denotes a constant characterizing the valve. The leaving mass flow is given by

$$\dot{m}_{r,out} = \frac{\dot{Q}_e}{\Delta h_{lg}} \tag{4.9}$$

where Δh_{lg} is the specific latent heat of the refrigerant in the evaporator, which is a nonlinear function of the suction pressure. When the mass of refrigerant in the evaporator reaches its maximum value ($M_{r,max}$), the entering mass flow is equal to the leaving one.

Suction Manifold

The suction manifold is modeled by a dynamical equation by using the suction pressure as the state variable and employing the mass balance as [20],

$$\frac{dP_{suc}}{dt} = \frac{\dot{m}_{dc} + \dot{m}_{dist} - \dot{V}_{comp}\rho_{suc}}{V_{suc}\, d\rho_{suc}/dP_{suc}} \tag{4.10}$$

where the compressor bank is treated as a big *virtual compressor*, $\dot{m}_{dc}$ is the total mass flow of the display cases, $\dot{m}_{dist}$ is the disturbance mass flow including the mass flow from the freezing rooms and the bypass valve, and V_{suc} is the volume of the suction manifold. $\dot{V}_{comp}$ is the volume flow out of the suction manifold,

$$\dot{V}_{comp} = f_{comp}\eta_{vol}V_d \tag{4.11}$$

where f_{comp} is the virtual compressor frequency (total capacity) of the high stage compressor rack in percentage, V_d denotes the displacement volume, and η_{vol} is clearance volumetric efficiency approximated by

$$\eta_{vol} = 1 - c\left(\left(\frac{P_c}{Psuc}\right)^{1/\gamma} - 1\right) \tag{4.12}$$

with constant clearance ratio c, and constant adiabatic exponent γ [1]. P_c is the compressor outlet pressure.

Since the main purpose of this modeling is to produce a suitable model for demand-side management, we need to estimate the power consumption of the compressor bank. The following equation estimates the electrical power consumption,

$$\dot{W}_{comp} = \frac{1}{\eta_{me}}\dot{m}_{ref}\left(h_{o,comp} - h_{i,comp}\right) \tag{4.13}$$

where $\dot{m}_{ref}$ is the total mass flow into suction manifold, and $h_{o,comp}$ and $h_{i,comp}$ are the enthalpies at the outlet and inlet of the compressor bank. These enthalpies are nonlinear functions of the refrigerant pressure and temperature at the calculation point. The constant η_{me} indicates overall mechanical/electrical efficiency considering mechanical friction losses and electrical losses [1]. The enthalpy of refrigerant at the manifold inlet is bigger than that of the evaporator outlet ($h_{i,comp} > h_{oe}$) due to disturbance mass flows. The outlet enthalpy is computed by

$$h_{o,comp} = h_{i,comp} + \frac{1}{\eta_{is}}\left(h_{o,is} - h_{i,comp}\right) \tag{4.14}$$

in which $h_{o,is}$ is the outlet enthalpy when the compression process is isentropic, and η_{is} is the related isentropic efficiency given by [6] (neglecting the higher order terms),

$$\eta_{is} = c_0 + c_1(f_{comp}/100) + c_2(P_c/P_{suc}) \tag{4.15}$$

where c_i are constant coefficients.

Condenser

Most of the models developed for condensers need physical details like fin and tube dimensions [2, 22, 23] and thus are not directly applicable here since our modeling approach is mainly based on general knowledge about the system. So, neglecting the condenser dynamics, the steady-state multi-zone moving boundary model developed in [6] is utilized here with further considerations.

The condenser is supposed to operate in three zones (superheated, two-phase, and subcooled). A pressure drop is assumed to take place across the first zone (superheated) given by [6],

$$\Delta P_c \triangleq P_c - P_{cnd} = \left(\frac{\dot{m}_{ref}}{A_c}\right)^2 \left(\frac{1}{\rho_{cnd}} - \frac{1}{\rho_c}\right) + \Delta P_f \tag{4.16}$$

where A_c is the cross-sectional area of the condenser, and P_{cnd} and ρ_{cnd} are the pressure and density at the outlet of the superheated zone. The first term at the right hand side of Equation (4.16) indicates acceleration pressure drop and the last term stands for the frictional pressure drop (ΔP_f) assumed constant. The Rate of the heat rejection is described by Equation (4.17) for superheated (first) and subcooled (third) zones,

$$\dot{Q}_{c,k} = UA_{c,k} \frac{T_{i,k} - T_{o,k}}{\ln\left[\frac{T_{i,k} - T_{outdoor}}{T_{o,k} - T_{outdoor}}\right]}, \quad k = 1, 3 \tag{4.17}$$

and the following is for the two-phase (second) zone,

$$\dot{Q}_{c,2} = UA_{c,2}(T_{i,2} - T_{outdoor}) \tag{4.18}$$

where UA_c is the overall heat transfer coefficient of the corresponding condenser zone, T_i and T_o are the refrigerant temperature at the inlet and outlet of each zone, and $T_{outdoor}$ is the outdoor temperature. Note that the inlet and outlet temperatures of the two-phase zone are the same when pressure does not change across it.

The heat transferred by refrigerant flow across the kth zone is provided by the following energy balance equation:

$$\dot{Q}_{c,k} = \dot{m}_{ref}(h_{i,k} - h_{o,k}), \quad k = 1, 2, 3 \tag{4.19}$$

in which h_i and h_o are enthalpies at the inlet and outlet of the kth zone. Accordingly, the total rate of the heat rejected by the condenser is:

$$\dot{Q}_c = \sum_{k=1}^{3} \dot{Q}_{c,k} \tag{4.20}$$

4 Parameter Estimation

The system under study is a large-scale CO_2 refrigeration system operating in a supermarket in Denmark. The system consists of seven display cases, four freezing rooms and two stages of the compressor banks configured in the booster setup explained in Section 2. The system is not a test setup and needs to keep its normal operation. Thus, we identify the model from the data collected by every minute logging the measurements. An off-line identification is performed to estimate the constant parameters and coefficients introduced before. The modeling error, computed by dividing the maximum absolute error over the maximum amplitude of variation of the measured signal, is provided on each plot. We use two sets of data:

- *Training set*: This contains the measured input/output data required for the estimations. The data are selected from an interval during the day time when no defrost cycle takes place.

- *Validation set*: This contains the measured input/output data required for validating the model after estimation. The data are selected in the same hours of interval as the previous one but from a different working day.

After estimating the model using the training data, we plot the simulated response of the estimated model using the validation data for comparison.

Thus far we have used the first principle modeling approach to describe the system with mathematical equations. For system identification, we make a nonlinear model using the foregoing equations with unknown parameters. An iterative prediction-error minimization (PEM) method, implemented in *System Identification Toolbox* of MATLAB, is employed to estimate the model parameters [24]. A modular parameter estimation approach is introduced in which the parameters of each subsystem are identified by providing related input-output pairs from measurement data. An example of estimating nonlinear models using PEM is given by [25].

Nonlinear thermophysical properties of the refrigerant (e.g., enthalpies) are calculated by the software package "RefEqns" [26].

(1) Display cases estimations: In this subsystem, the model should be able to estimate mass flow and display case temperatures. The mass flows are controlled by thermostatic actions as well as superheat control. These two result in a specific opening degree for the each expansion valve. So the input and output vectors used for estimation are

$$U_{dc} = \begin{bmatrix} P_{suc} & T_{indoor} & OD_1 & \cdots & OD_7 \end{bmatrix}^T \tag{4.21}$$

and

$$Y_{dc} = \begin{bmatrix} \dot{m}_{dc} & T_{dc,1} & \cdots & T_{dc,7} \end{bmatrix}^T \tag{4.22}$$

Estimated parameters for the total seven display cases are collected in Table 4.1 assuming constant superheat $T_{sh} = 5$ [°C], and constant receiver pressure $P_{rec} = 38 \times 10^5$ [pascal]. A frame of five hours' data sampled every minute is used.

Table 4.1: estimated parameters of the display cases.

D.C. No.	UA_{load}	$UA_{foods/dc}$	$MCp_{dc} \times 10^5$	$MCp_{foods} \times 10^5$	k_m	$KvA \times 10^{-6}$
1	41.9	72.9	1.9	4.6	141.7	2.33
2	56.3	82.6	4.8	88.6	250.9	2.27
3	57.5	118.5	2.7	2.8	175.3	2.71
4	32.2	230.5	4.1	2.7	182.9	0.86
5	36.1	158.9	6.3	1.5	810.6	2.38
6	58.2	75.3	1.7	6.5	196.8	2.33
7	24.1	150.2	4.6	60	800	0.70

The inputs are presented in Figure 4.3. The suction pressure, P_{suc}, is regulated around 26×10^5 [pascal] by the high stage compressors, and the indoor temperature, T_{indoor} is regulated around 26 [°C] by an air-conditioning system. The ON/OFF behavior of the OD signals is caused by the simple hysteresis control actions. During the ON period of action, the superheat controllers operate on the valves to ensure the completed vaporization of the refrigerant at the evaporator outlets. Incorporating the superheat control into the display case models needs a more complicated (e.g., a moving boundary) model for the evaporators. This incorporation seems unnecessary for our control purposes in the supervisory level. Thus for simplicity, we assume a constant superheat temperature and identify the plant directly instead of the closed loop system.

Estimation results for the display case temperatures and the overall mass flow from the expansion valves are illustrated in Figure 4.4 and Figure 4.5, respectively. For a fair comparison, all temperature plots have the same scale. Also, the value of the modeling error provided on each plot shows the best and worst fit for the 5th and 7th display case, respectively. The high fluctuation in the overall mass flow is the result of ON/OFF (thermostatic) actions of the expansion valves.

Despite the use of a simple model and relatively large number of estimated parameters (42 parameters), the display case models show satisfactory results.

(2) Suction manifold estimations: Although one of the main goals of modeling in this section is to estimate power consumption of the compressor bank, we also need to estimate P_{suc} for this purpose as stated in the previous section.

Suction pressure is computed from Equation (4.10) by entering the following inputs and output into the identification process and assuming $V_{suc} = 2$ and knowing $V_d = (6.5 \times 70/50 + 12.0)/3600$ from compressor label.

$$U_{suc} = \begin{bmatrix} \dot{m}_{dc} & \dot{m}_{dist} & P_c & f_{comp} \end{bmatrix}^T, \quad Y_{suc} = P_{suc} \tag{4.23}$$

This results in estimating parameters required for volumetric efficiency in Equation (4.12) as $c = 0.65$ and $\gamma = 0.47$.

It is worth mentioning that the compressor speed is regulated by a local PI controller having a transient faster than the one minute used for data log. So the closed loop response of the compressor speed is considered in estimating the suction pressure and the compressor power consumption. The following inputs and output are chosen to estimate the power consumption of the compressor bank.

$$U_{comp} = \begin{bmatrix} P_{suc} & P_c & f_{comp} & \dot{m}_{ref} \end{bmatrix}^T, \quad Y_{comp} = \dot{W}_{comp} \tag{4.24}$$

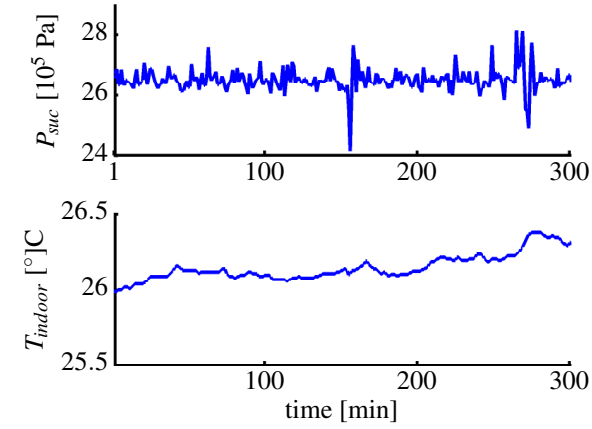

(a)

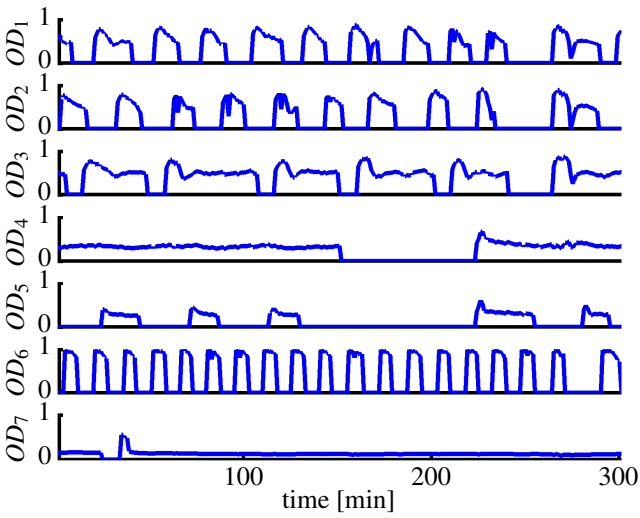

(b)

Figure 4.3: The input signals provided in the training set for the display case estimations.

The parameters needed for calculating isentropic efficiency are estimated as $c_0 = 1$, $c_1 = -0.52$ and $c_2 = 0.01$, and the mechanical/electrical efficiency is also obtained as $\eta_{me} = 0.65$. Figure 4.6 shows estimation results for the suction pressure and power consumption. Even though the simple first order model introduced for suction manifold cannot generate the high frequency parts of the pressure signal, it can fairly estimate a low pass filtered version of the suction pressure. The bottom plots show a very good estimation of the power consumption in so far as the validation result shows even a better estimation.

(3) Condenser estimations: In the condenser model, the corresponding parameters should be estimated such that the heat transfer generated by the steady-state model has to be equal to the heat transfer delivered by the refrigerant mass flow. The speed of the

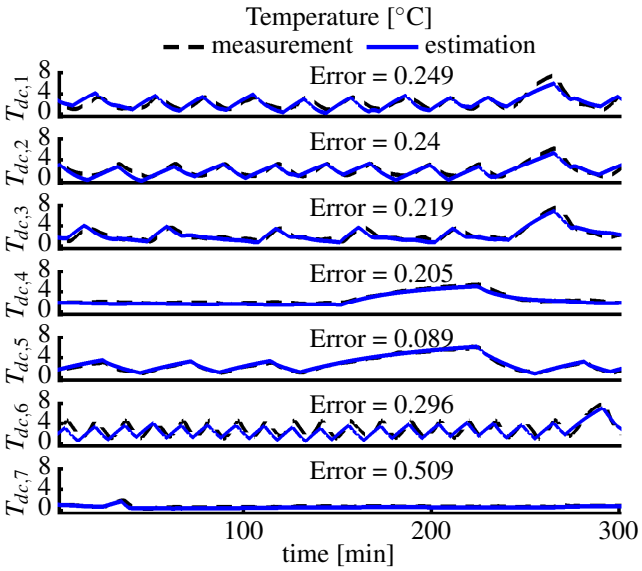

(a)

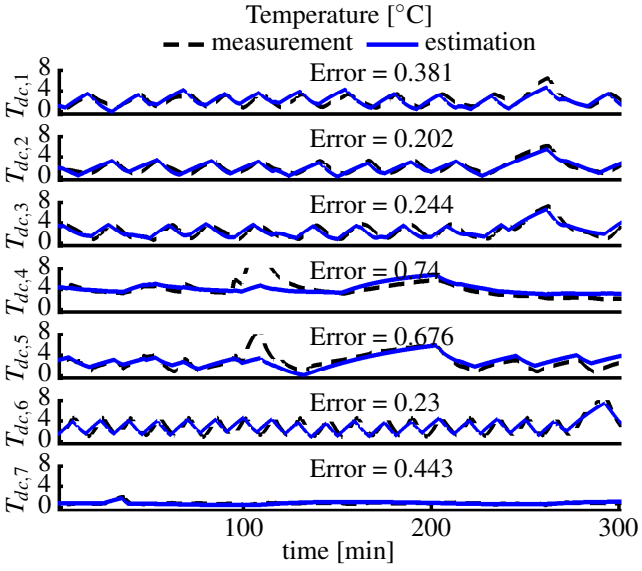

(b)

Figure 4.4: Estimation of display case temperatures. The 5th display case shows the best fit and the worst fit is related to 7th display case, which is still a good estimation. (a) Estimation using training data; (b) Estimation using validation data.

condenser fan has been fixed to the maximum value, so the developed static model can fairly describe its behavior without incorporating the fan speed. The input vector used for identification is

$$U_{cnd} = \begin{bmatrix} T_{i,cnd} & \dot{m}_{ref} & T_{outdoor} \end{bmatrix}^T \tag{4.25}$$

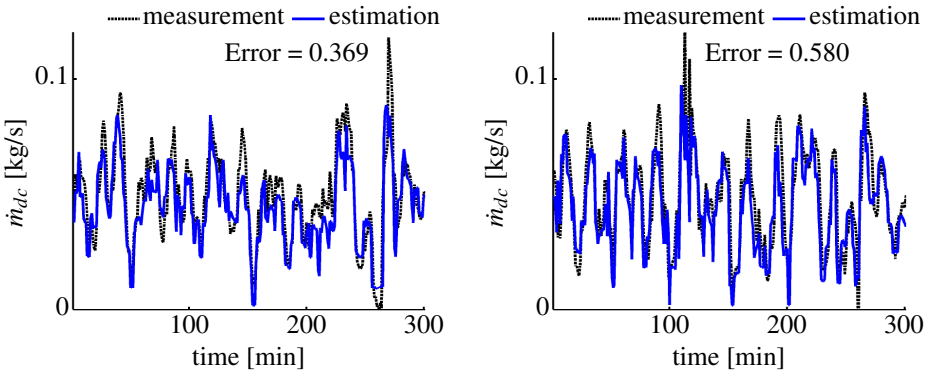

Figure 4.5: Estimation of the total mass flow from display cases. It is the sum of the mass flows through the expansion valves. (a) Estimation using training data; (b) Estimation using validation data.

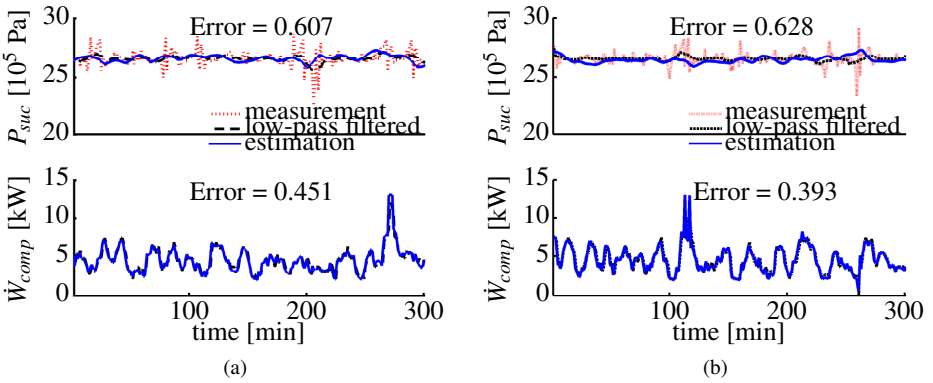

Figure 4.6: Suction pressure and power consumption estimations. Variation of consumption is mainly because of changing mass flow due to hysteresis and superheat control of expansion valves. Mechanical-electrical efficiency is obtained as $\eta_{me} = 0.65$. (a) Estimation using training data; (b) Estimation using validation data.

where $T_{i,cnd}$ is the refrigerant temperature at the condenser inlet, which is also the inlet of the first zone. Enthalpies $h_{o,1} = h_{i,2}$ and $h_{o,2} = h_{i,3}$ are the enthalpies of saturated vapor and saturated liquid at the pressure P_{cnd}, respectively. The output temperature is also calculated by assuming 2 °C constant subcooling. The desired output for estimation is

$$Y_{cnd} = P_c \tag{4.26}$$

Estimation results are shown in Figure 4.7 with the following parameters. The associate result for the pressure drop can justify the assumption that it mainly takes place in the first (superheated) condenser zone. Despite considering a simple steady-state model for

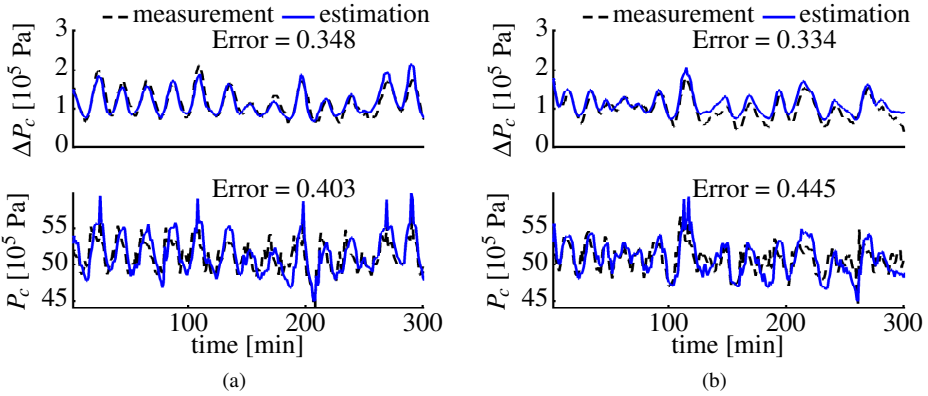

Figure 4.7: Estimation of the pressure drop and the pressure at the condenser inlet. (a) Estimation using training data; (b) Estimation using validation data.

condenser and also not using any of its physical details, the estimation is still acceptable and valid.

A_c	ΔP_f	$UA_{c,1}$	$UA_{c,2}$	$UA_{c,3}$
0.0073	0.52	332	3185	148

5 System Integration and Simulation Benchmark

Thus far, three separate models have been developed for different subsystems using the corresponding measured input and output pairs. In this section, we integrate all subsystems to build a complete model for supermarket refrigeration systems ready for use as a simulation benchmark.

The inputs used in the model are the opening degree of expansion valves (OD_i) and the running capacity of the compressor bank (f_{comp}).

$$U_{sys} = \begin{bmatrix} OD_1 & \cdots & OD_7 & f_{comp} \end{bmatrix} \tag{4.27}$$

The disturbance vector is

$$U_{dist} = \begin{bmatrix} \dot{m}_{dist} & T_{indoor} & T_{outdoor} \end{bmatrix} \tag{4.28}$$

In order to simulate the control strategy depicted in Figure 5.2, the SRS model should be able to estimate display case temperatures and compressor power consumptions with satisfactory degrees of accuracy. Figures 4.8 and 4.9 show the results of running the model by Equations (4.27) and (4.28) using the data set used for both identification and validation in the previous section. As can be seen from these results, estimation errors do not increase significantly and the results are still convincing and can satisfy our expectation to have a model as a simulation benchmark.

The modularity of the model makes it possible to simply add the freezing rooms and low stage compressors to the model. There is no need to do changes in the model

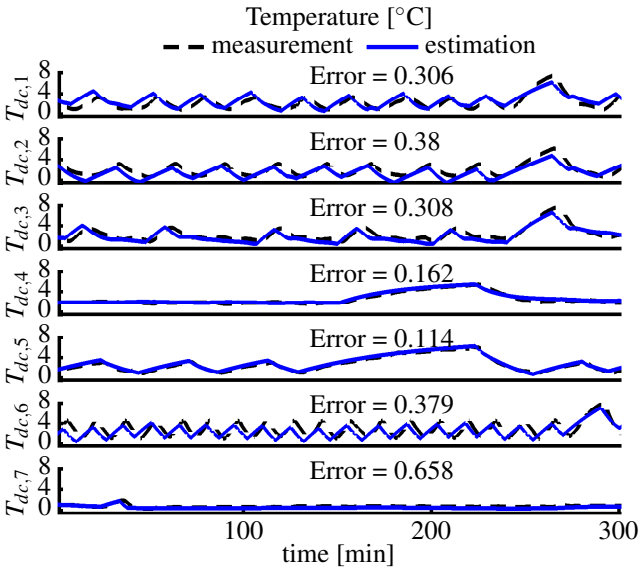

(a)

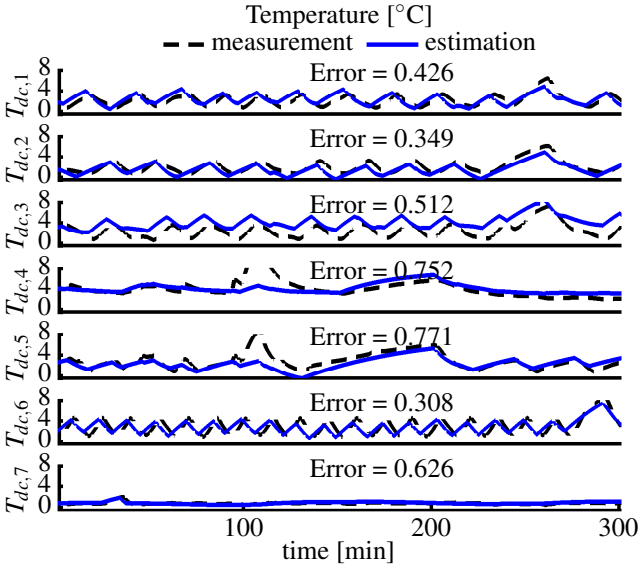

(b)

Figure 4.8: Estimation of display case temperatures after system integration. The estimation error increases slightly due to modeling error associated with each subsystem. (a) Estimation using training data; (b) Estimation using validation data.

since the mass flow of this section is already included in the disturbance mass flow in Equation (4.10). The estimated parameters for the total four freezing rooms are collected

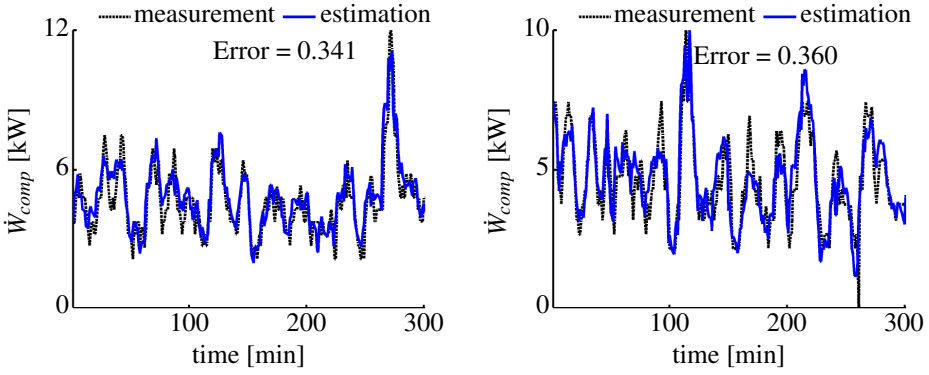

Figure 4.9: Power consumption estimation of the compressor bank after system integration. The estimation is still satisfactory in spite of existing estimation errors associated with each subsystem model. (a) Estimation using training data; (b) Estimation using validation data.

in Table 4.2.

Table 4.2: estimated parameters of the freezing rooms.

F.R. No.	UA_{load}	$UA_{foods/fr}$	$MCp_{fr} \times 10^5$	$MCp_{foods} \times 10^6$	k_m	$KvA \times 10^{-6}$
1	23	185	1.7	84.5	184.4	2.97
2	28	250	1.9	38	218.9	1.28
3	4	83	0.7	52	395.9	0.54
4	17	250	7.7	20.8	237.2	2.47

Figures 4.10 and 4.11 show the estimation results for the freezing room temperatures and the corresponding power consumption of the low stage compressor bank. The pulse shape of power consumption in the low stage compressor rack is due to the fact that it contains several ON/OFF controlled compressors, in contrast with the high stage rack that contains a continuous frequency control compressor as well as other ON/OFF control types.

So far we have applied the expansion valve control signals (OD) and the compressor capacity (f_{comp}) to the model from the values obtained from data to have a fair comparison with measured outputs. In order to complete the simulation benchmark, the model should contain these local controllers to be ready for demand-side management as will be explained in the next section. As realized from the measurements, condenser fans are working in their full speed and thus the high-side pressure is not regulated to a specific value in this system.

The expansion valve control is a hysteresis controller operating between hysteresis bounds defined based on the temperature limits. We can estimate the compressor capacity such that the suction pressure and low-side pressure are regulated to predefined set-points. For this purpose, the compressor capacity should provide a volume flow in

Equation (4.11) that keeps Equation (4.10) equal to zero at the desired pressure set-point. The result illustrated in Figure 4.12 justifies that the proposed estimation method is nearly the same as what is used in the real system.

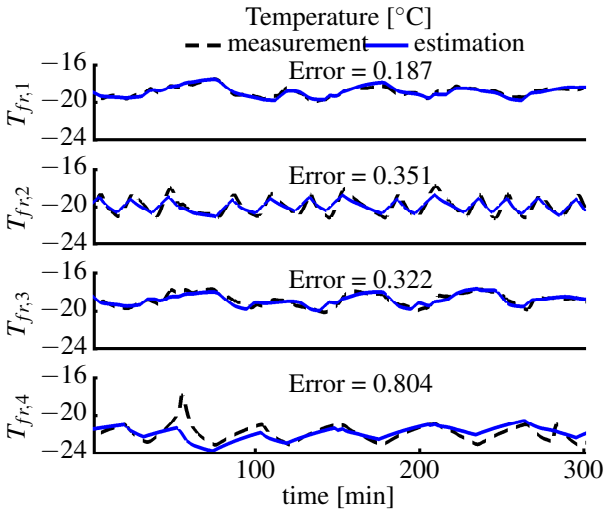

(a)

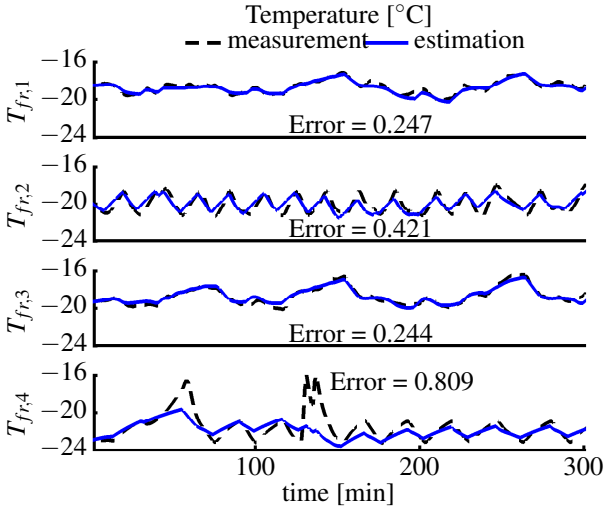

(b)

Figure 4.10: Estimation of freezing room temperatures. The temperature peaks at the 4th freezer may be caused by unmodeled disturbances like personnel activities. (a) Estimation using training data; (b) Estimation using validation data.

The disturbances can be modeled by sinusoidal signals with the amplitudes and frequencies equal to the average values for real disturbances. The simulation benchmark is now largely ready to be employed by a supervisory control in order to develop different demand-side management scenarios.

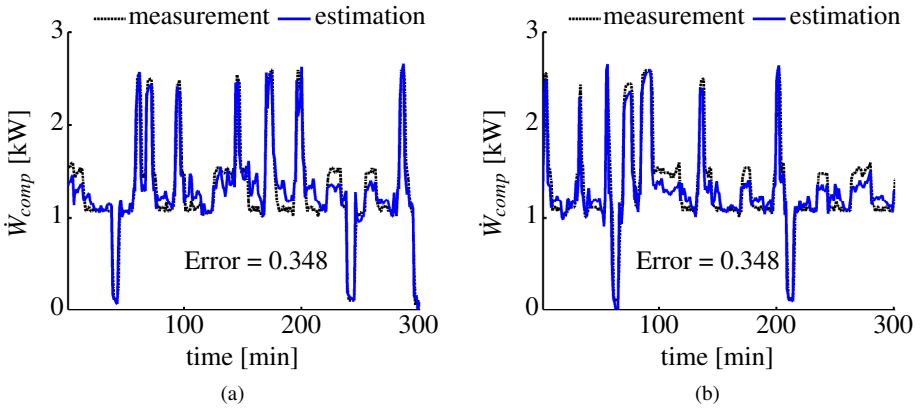

Figure 4.11: Power consumption estimations for low stage compressor bank of the freezing section. (a) Estimation using training data; (b) Estimation using validation data.

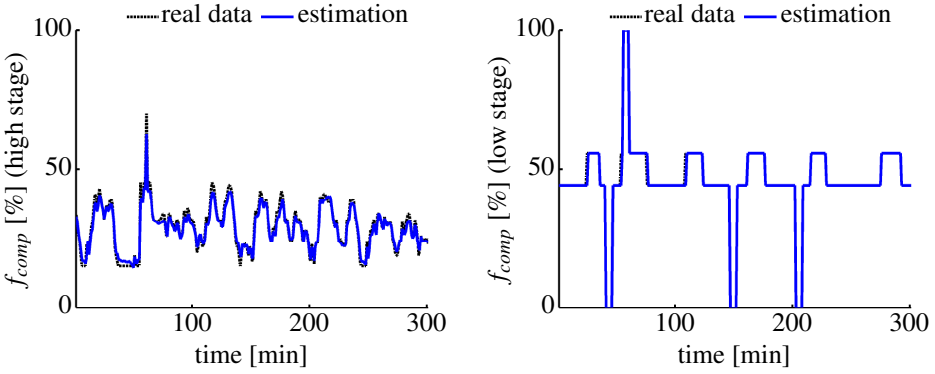

Figure 4.12: Estimation of compressor capacity such that the suction pressure and low-side pressure are regulated to 26×10^5 [pascal] and 14×10^5 [pascal], respectively.

6 Demand-Side Management

There are two major approaches for demand-side management in smart grid: *direct control* and *indirect control*. In the case of direct control, consumers in a smart grid should follow the power reference sent by the grid in accordance with their storage and consumption limitations [27]. On the other hand, in the indirect approach, consumers receive real-time price signal from the grid and manage their consumption such that the operating cost in a specific time interval is minimized [28].

Discussing the flexibilities, and the corresponding storage and consumption limits, and other details in this context is however out of the scope of this paper. In the following, we will show by a simple example how the produced model can be utilized in implementing direct control with the structure explained in Figure 5.2.

The supervisory controller (see Figure 4.13) includes a PI controller that regulates the power consumption (sum of low stage and high stage compressor powers) to the reference level received from the grid. The output of the PI controller is downscaled by

the gains G_i to provide the required differences ΔT_i for the set-points for each cold room. This difference values are added to predefined set-points T_i and the results are applied as new set-points to the refrigeration system model. The suction and low-side pressures are regulated to constant levels.

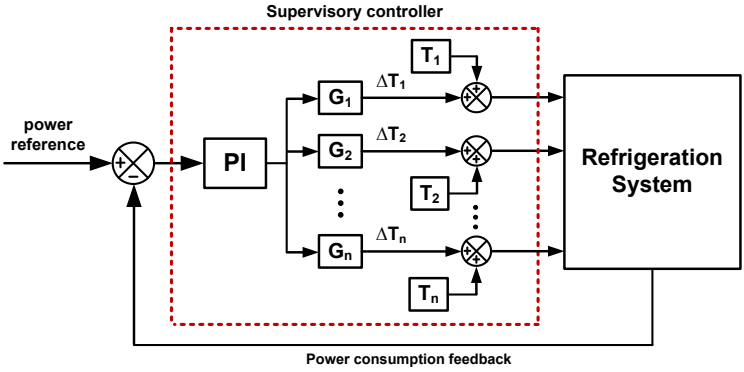

Figure 4.13: A simple direct control structure. T_i are temperature set-points for normal operation of the system, and ΔT_i are temperature changes applied for consumption regulation.

Figure 4.14 shows the power consumption in a normal operation when no supervisory control affects the system on the top, and the related direct control at the bottom. The system is simulated for one day. The 60-minute moving average of the power is shown in the plot. A sinusoidal shape of change in the average consumption in normal operation is because of the sinusoidal change assumed for the outdoor temperature.

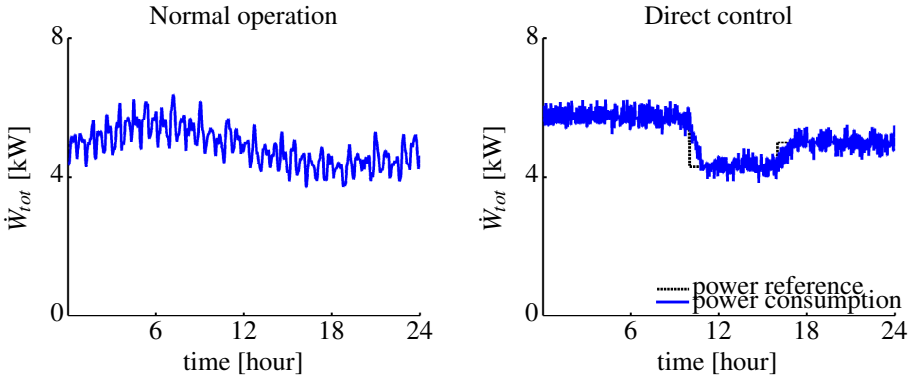

Figure 4.14: Power consumption for one day operation. High frequency fluctuations are mainly caused by hysteresis control of display cases. Direct control can successfully follow the reference.

The objective of the control is to have the average power consumption of refrigeration system follow the power reference while respecting the temperature limits in cold reser-

voirs. The corresponding cold reservoir temperatures are also depicted in Figure 4.15. The regulator gains G_i are defined such that each display case or freezing room temperature remains in the permissible range required for no food damage.

It is worthwhile to mention that this is only a simple example to show how the produced model can be employed for demand-side management in smart grid. The design of advanced controllers with predictive ability and conducting COP optimization is left for the future works. In order to respect the limitations on food temperatures, a predictive controller can be supported by a state estimator for estimating food temperatures.

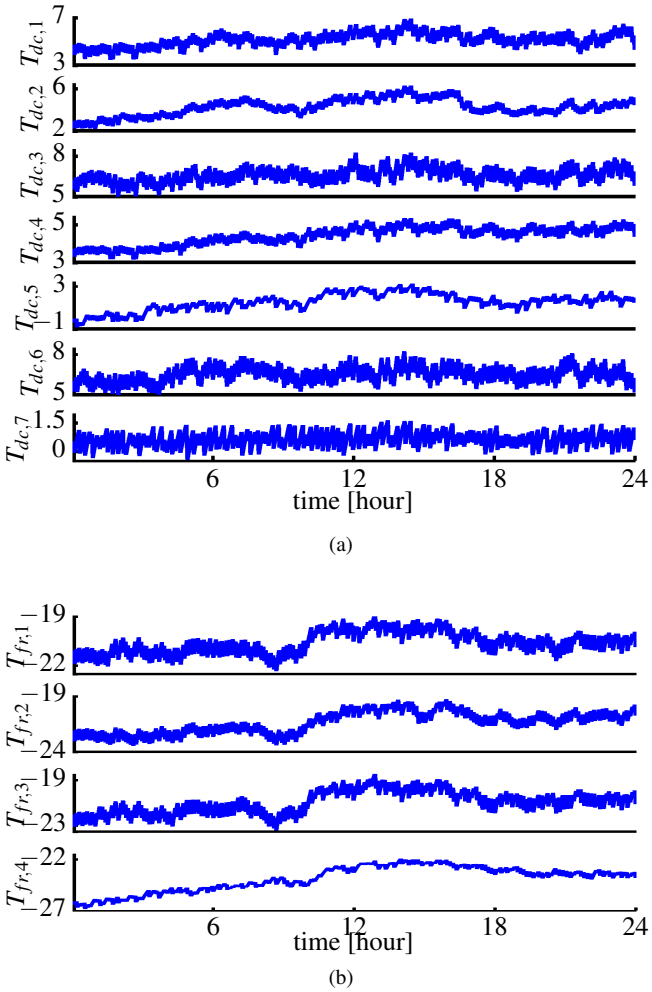

Figure 4.15: Cold reservoir temperatures are changed by supervisory controller to regulate the power/energy consumption. (a) Display case temperatures; (b) Freezing room temperatures.

7 Conclusions

A supermarket refrigeration system suitable for supervisory control in smart grid is modeled. The system was divided into three subsystems, each modeled and validated separately. The proposed modular modeling approach leaves open the possibility of modeling refrigeration systems with different configurations and operating conditions. A first principle approach was taken and supported by the PEM method for parameter estimation. The models give satisfactory results in which the electrical power consumption is estimated very accurately by the accurate estimation of the thermal states. These subsystem models were finally integrated to make a booster configuration and the corresponding results confirmed the effectiveness of the proposed modeling approach. It was also explained how a simulation benchmark including the integrated model and local controllers can be configured for the purpose of supervisory control implementations. Using the produced model, appropriate control algorithms can be developed to govern the electrical power consumption (required for demand-side management) by controlling the cooling capacity. At the end, a simple simulation example was provided to demonstrate the utilization of the developed benchmark in demand-side management in smart grid within a direct electrical power control scenario.

Acknowledgements

This work is supported by the Southern Denmark Growth Forum and the European Regional Development Fund under the Project Smart & Cool. The authors also wish to thank Danfoss Refrigeration & Air Conditioning for supporting this research by providing valuable data under the ESO2 research project.

References

[1] C. Pérez-Segarra, J. Rigola, M. Sòria, and A. Oliva, "Detailed thermodynamic characterization of hermetic reciprocating compressors," *International Journal of Refrigeration*, vol. 28, pp. 579–593, 2005.

[2] M. Corradi, L. Cecchinato, and G. Schiochet, "Modeling fin-and-tube gas-cooler for transcritical carbon dioxide cycles," in *International Refrigeration and Air Conditioning Conference*. Lafayette, Indiana, USA: Purdue University, 2006.

[3] M. Willatzen, N. B. Pettit, and L. Ploug-Srensen, "A general dynamic simulation model for evaporators and condensers in refrigeration. part i: moving-boundary formulation of two-phase flows with heat exchange," *International Journal of Refrigeration*, vol. 21, no. 5, pp. 398–403, 1998.

[4] C. Aprea and C. Renno, "An experimental analysis of a thermodynamic model of a vapor compression refrigeration plant on varying the compressor speed," *International Journal of Energy Research*, vol. 28, pp. 537–549, 2004.

[5] F. Wang, G. Maidment, J. Missenden, and R. Tozer, "The novel use of phase change materials in refrigeration plant. part 1: Experimental investigation," *Applied Thermal Engineering*, vol. 27, pp. 2893–2901, 2007.

[6] R. Zhou, T. Zhang, J. Catano, J. T. Wen, G. J. Michna, Y. Peles, and M. K. Jensen, "The steady-state modeling and optimization of a refrigeration system for high heat flux removal," *Applied Thermal Engineering*, vol. 30, pp. 2347–2356, 2010.

[7] A. Cleland, "Experimental verification of a mathematical model for simulation of industrial refrigeration plants," *International Journal of Refrigeration*, vol. 8, no. 5, pp. 275–282, 1985.

[8] T. Pfafferott and G. Schmitz, "Modeling and simulation of refrigeration systems with the natural refrigerant CO2," in *International Refrigeration and Air Conditioning Conference*. Lafayette, Indiana, USA: Purdue University, 2002.

[9] ——, "Modeling and transient simulation of co_2-refrigeration systems with modelica," *International Journal of Refrigeration*, vol. 27, pp. 42–52, 2004.

[10] H. Li, S. Jeong, J. Yoon, and S. You, "An empirical model for independent control of variable speed refrigeration system," *Applied Thermal Engineering*, vol. 28, pp. 1918–1924, 2008.

[11] S. Shao, W. Shi, X. Li, and Q. Yan, "Simulation model for complex refrigeration systems based on two-phase fluid network – part i: Model development," *International Journal of Refrigeration*, vol. 31, pp. 490–499, 2008.

[12] ——, "Simulation model for complex refrigeration systems based on two-phase fluid network – part ii: Model application," *International Journal of Refrigeration*, vol. 31, pp. 500–509, 2008.

[13] C. Petre, m. Feidt, M. Costea, and S. Petrescu, "A model for study and optimization of real-operating refrigeration machines," *International Journal of Energy Research*, vol. 33, pp. 173–179, 2009.

[14] L. Schurt, C. Hermes, and A. Neto, "A model-driven multivariable controller for vapor compression refrigeration systems," *International Journal of Refrigeration*, vol. 32, pp. 1672–1682, 2009.

[15] L. C. Schurt, C. Hermes, and A. T. Neto, "Assessment of the controlling envelope of a model-based multivariable controller for vapor compression refrigeration systems," *Applied Thermal Engineering*, vol. 30, pp. 1538–1546, 2010.

[16] R. Shi, D. Fu, Y. Feng, J. Fan, and S. Mijanovic, "Dynamic modeling of CO2 supermarket refrigeration system," in *International Refrigeration and Air Conditioning Conference*. Lafayette, Indiana, USA: Purdue University, 2010.

[17] T. Ommen and Elmegaard, "Numerical model for thermoeconomic diagnosis in commercial transcritical/subcritical booster refrigeration systems," *Energy Conversion and Management*, vol. 60, pp. 161–169, 2012.

[18] Y. Ge and S. Tassou, "Performance evaluation and optimal design of supermarket refrigeration systems with supermarket model "supersim", part i: Model description and validation," *International Journal of Refrigeration*, vol. 34, pp. 527–539, 2011.

[19] T. G. Hovgaard, L. F. S. Larsen, M. J. Skovrup, and J. Jrgensen, "Power consumption in refrigeration systems - modeling for optimization," in *Proceedings of the 2001 4th International Symposium on Advanced Control of Industrial Processes*, Hangzhou, China, May 2011.

[20] D. Sarabia, F. Capraro, L. F. S. Larsen, and C. Prada, "Hybrid NMPC of supermarket display cases," *Control Engineering Practice*, vol. 17, pp. 428–441, 2009.

[21] L. N. Petersen, H. Madsen, and C. Heerup, "ESO2 optimization of supermarket refrigeration systems: Mixed integer MPC and system performance," Department of Informatics and Mathematical Modeling, Technical University of Denmark, Tech. Rep., 2012.

[22] J. M. Yin, C. W. Bullard, and P. S. Hrnjak, "R744 gas cooler model development and validation," University of Illinois, Air Conditioning and Refrigeration Center, Tech. Rep., 2000.

[23] Y. Ge and R. Cropper, "Simulation and performance evaluation of finned-tube co_2 gas cooler for refrigeration systems," *Applied Thermal Engineering*, vol. 29, pp. 957–965, 2009.

[24] L. Ljung, "Prediction error estimation methods," *Circuits, Systems, and Signal Processing*, vol. 21, no. 1, pp. 11–21, 2002.

[25] "Estimating nonlinear grey-box models," http://www.mathworks.se/help/ident/ug/estimating-nonlinear-grey-box-models.html, accessed: 01/12/2012.

[26] M. J. Skovrup, *Thermodynamic and Thermophysical Properties of Refrigerants, Version 3.00*, Technical University of Denmark, 2000.

[27] K. Trangbaek, M. Petersen, J. Bendtsen, and J. Stoustrup, "Exact power constraints in smart grid control," in *Proceedings of the 50th IEEE Conference on Decision and Control and European Control Conference*, Orlando, FL, USA, 2011.

[28] A. Mohsenian-Rad and A. Leon-Garcia, "Optimal residential load control with price prediction in real-time electricity pricing environments," *IEEE Transactions on Smart Grid*, vol. 1, no. 2, pp. 120–133, 2010.

Paper B

A Supervisory Control Approach in Economic MPC Design for Refrigeration Systems

Seyed Ehsan Shafiei, Jakob Stoustrup and Henrik Rasmussen

This paper was published in:
The Proceedings of the European Control Conference, July 2013

The layout has been revised

Abstract

A model predictive control at supervisory level is proposed for refrigeration systems including distributed local controllers. Prediction of the electricity price and outdoor temperature are assumed available. The control objective is to minimize the overall energy cost within the prediction horizon. The method is mainly developed for demand-side management in the future smart grid, but a simpler version can be applied in the current electricity market. Due to the system nonlinearity, the minimization is in general a complicated nonconvex optimization problem. A new supervisory control structure as well as an algorithmic pressure control scheme is presented to rearrange the problem to facilitate convex programming. A nonlinear continuous time model validated by real data is employed to simulate the system operation. The results show a considerable economic saving as well as a trade-off between the saving level and the design complexity.

1 Introduction

The structure of power systems, especially in Europe, is changing from a centralized one to a decentralized one due to distributed generation with high penetration of renewable sources. This change leads to several new challenges that can be handled in a smart grid, where both production and consumption of electricity are managed efficiently. To achieve such efficient demand-side management, consumers should be equipped with control systems that can actively respond to grid requirements.

Supermarket refrigeration systems are one of the consumers that have significant potential to take part in demand-side management by shifting their energy consumption. The large potential for demand-side management can be illustrated by Denmark alone with 5 mio. inhabitants having approx. 4.500 supermarkets, using annually approx. 540.000 MWh for refrigeration. This can be achieved by storing energy as coldness in foodstuffs. The authors believe that this storage capability can be utilized effectively by developing appropriate control methods. However, existing nonlinearities and constraints in refrigeration systems challenges the control design.

One of the best control schemes that can take into account the required predictions and can handle such a multivariable system as well as respecting the state and input constraints is model predictive control (MPC), [1]. Various MPC formulations have successfully been applied for different improvements in refrigeration systems. With hybrid system formulation, MPC was employed in [2, 3] and [4] to solve the synchronization problem in display cases that causes wearing of the compressors. Fallahsohi, *et al* in [5] applied predictive functional control to minimize the superheat in an evaporator. For multi-evaporator systems, a decentralized MPC was proposed to control the cooling capacity of each evaporator [6]. A nonlinear predictive control scheme was designed in [7] to reduce the total power consumption of the compressor in a vapor compression cycle.

An optimal demand-side management can be realized in a real-time electricity pricing market by taking price predictions into account [8]. Optimizing economic objectives in MPC formulation for process systems was presented in [9]. A thorough study has been performed by Hovgaard, *et al*, [10], where an economic MPC was designed to reduce operating costs of refrigeration systems by utilizing the thermal storage capabilities. Predictions of the electricity price and the outdoor temperature were considered and a

nonlinear optimization tool was used to handle the nonconvex cost function. They also showed that their proposed method can successfully contribute with ancillary services to balance power markets in the smart grid.

In this paper, we propose a new supervisory control structure for commercial refrigeration systems. In order to minimize the energy consumption, the optimizing value for cooling capacity of each unit as well as the optimal set-point for suction pressure (common evaporation temperature) should be calculated. This will however lead to solve a nonlinear and nonconvex optimization problem. To avoid this nonconvexity, we propose a simple heuristic algorithm to regulate the suction pressure in the local control level. The energy consumption is reduced significantly as a result of this algorithmic pressure control. Finally, a model predictive control in the supervisory level is proposed that can further reduce the total energy costs using predictions of the price and the outdoor temperature. The supervisory MPC controls the cooling capacity of each unit by providing an optimal temperature set-point for each distributed PI controller.

2 Refrigeration System

A basic layout of a typical refrigeration system including several fridge and freezer display cases with two compressor banks in a booster configuration is shown in Fig. 9.1. Starting from the receiver (REC), two-phase refrigerant (mix of liquid and vapor) at point '8' is split out into saturated liquid ('1') and saturated gas ('1b'). The latter is bypassed by a bypass valve (BPV), and the former flows into expansion valves where the refrigerant pressure drops to medium ('2') and low ('2′') pressures. The expansion valves EV_MT and EV_LT are driven by thermostatic ON/OFF controllers to regulate the air temperature inside the fridge and freezer display cases, respectively. Flowing through medium and low temperature evaporators (EVAP_MT and EVAP_LT), the refrigerant absorbs heat from the cold reservoir. The pressure of low temperature units (LT) is increased by the low stage compressor rack (COMP_LO). All mass flows from COMP_LO, EVAP_MT and BPV outlets are collected by a suction manifold at point '5' where the pressure is increased again by high stage compressors (COMP_HI). Afterward, the gas phase refrigerant enters the condenser to deliver the absorbed heat from cold reservoirs to the surroundings. The detailed thermodynamic analysis of such systems is described in [11].

Dynamical Model

In the cold reservoirs (display cases and cold rooms), heat is transfered from the foodstuffs to the cooled air, $\dot{Q}_{foods/cr}$, and then from the cooled air to the circulated refrigerant, $\dot{Q}_e$, which the latter is also known as cooling capacity. There is however heat load from supermarket indoor, $\dot{Q}_{load}$, formulated as a variable disturbance. Here, we consider the measured air temperature at the evaporator outlet as the cold reservoir temperature, T_{cr}. Assuming a lumped temperature model, the following dynamical equations are derived based on energy balances for the mentioned heat transfers.

$$MCp_{foods}\frac{dT_{foods}}{dt} = -\dot{Q}_{foods/cr} \tag{5.1}$$

$$MCp_{cr}\frac{dT_{cr}}{dt} = \dot{Q}_{load} + \dot{Q}_{foods/cr} - \dot{Q}_e \tag{5.2}$$

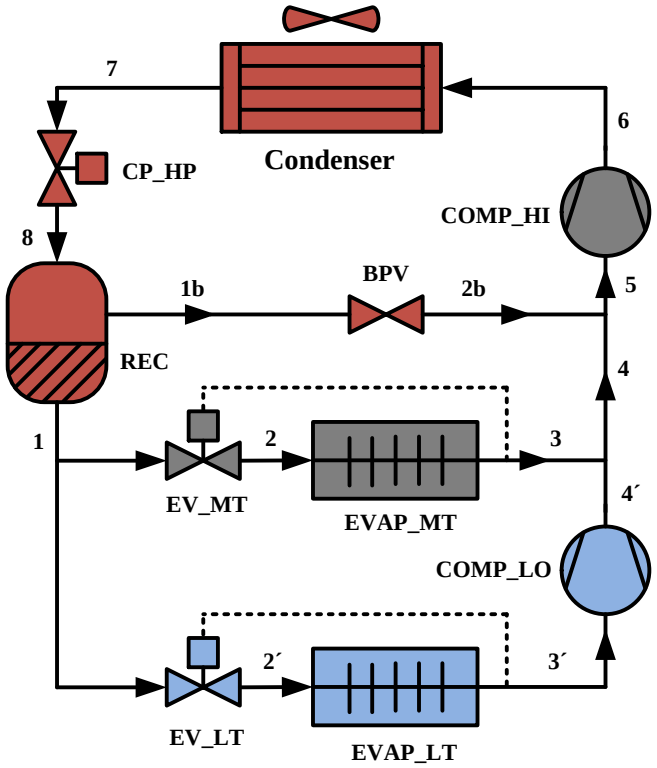

Figure 5.1: Basic layout of a typical supermarket refrigeration system with booster configuration.

where MCp denotes the corresponding mass multiplied by the heat capacity. The energy flows are

$$\dot{Q}_{foods/cr} = UA_{foods/cr}(T_{foods} - T_{cr}), \tag{5.3}$$

$$\dot{Q}_{load} = UA_{load}(T_{indoor} - T_{cr}), \tag{5.4}$$

and

$$\dot{Q}_e = \dot{m}_r \Delta h_{lg}, \tag{5.5}$$

where UA is the overall heat transfer coefficient, Δh_{lg} is the specific latent heat of the refrigerant in the evaporator, which is a nonlinear functions of the evaporation temperature (or equivalently the suction pressure), and T_{indoor} is the supermarket indoor temperature. The term $\dot{m}_r$ denotes the mass flow of refrigerant into the evaporator which is determined by the opening degree of the expansion valve and described by the following equation:

$$\dot{m}_r = OD\ KvA\sqrt{2\rho_{suc}(P_{rec} - P_{suc})10^5} \tag{5.6}$$

in which OD stands for the opening degree of the valve with a value ranging from 0 (closed) to 1 (fully opened), P_{rec} and P_{suc} are the receiver and the suction pressures in [bar], ρ_{suc} is density of the circulating refrigerant, and KvA denotes a constant characterizing the valve [12].

Compressor Power and System COP

The electrical power consumption of each compressor bank is calculated by

$$\dot{W}_c = \frac{1}{\eta_{me}} \dot{m}_{ref} (h_{o,c} - h_{i,c}), \tag{5.7}$$

where $\dot{m}_{ref}$ is the total mass flows into the compressors, and $h_{o,c}$ and $h_{i,c}$ are the enthalpies at the outlet and inlet of the compressor bank and are nonlinear functions of the refrigerant pressure and temperature at the calculation points. The constant η_{me} indicates overall mechanical/electrical efficiency considering mechanical friction losses and electrical motor inefficiencies [13]. The outlet enthalpy is computed by

$$h_{o,c} = h_{i,c} + \frac{1}{\eta_{is}} (h_{is} - h_{i,c}), \tag{5.8}$$

in which h_{is} is the outlet enthalpy when the compression process is isentropic, and η_{is} is the related isentropic efficiency given by [14] (neglecting higher order terms).

$$\eta_{is} = c_0 + c_1 (f_c/100) + c_2 (P_{c,o}/P_{suc}) \tag{5.9}$$

Where f_c is the virtual compressor frequency (total capacity) of the compressor rack in percentage, $P_{c,o}$ is pressure at the compressor outlet, and c_i are constant coefficients.

The total coefficient of performance (COP) is defined as ratio of the total cooling capacity over the total power consumption of the compressors.

$$COP = \frac{\dot{Q}_{e,tot}}{\dot{W}_{c,tot}} \tag{5.10}$$

The COP is calculated by

$$COP = \frac{x_{MT} \Delta h_{lg,MT} + x_{LT} \Delta h_{lg,LT}}{\frac{1}{\eta_{MT}} (h_{oc,MT} - h_{ic,MT}) + \frac{x_{LT}}{\eta_{LT}} (h_{oc,LT} - h_{ic,LT})}, \tag{5.11}$$

where indices MT and LT relate the calculated values to the medium and low temperature sections, respectively. Parameters x_{MT} and x_{LT} are ratio of the refrigerant mass flow of MT and LT evaporators to the total flow rate, and $\eta_{MT} = \eta_{me,MT} \eta_{is,MT}$ and $\eta_{LT} = \eta_{me,LT} \eta_{is,LT}$.

3 Supervisory Control

Fig. 5.2 shows the control system structure including local inner loop control and supervisory outer loop one. The local controllers are responsible for regulating the pressures and the temperatures to the required set-points, and the supervisory control, here, has to send the temperature set-points to the cold reservoirs such that the total energy cost is minimized.

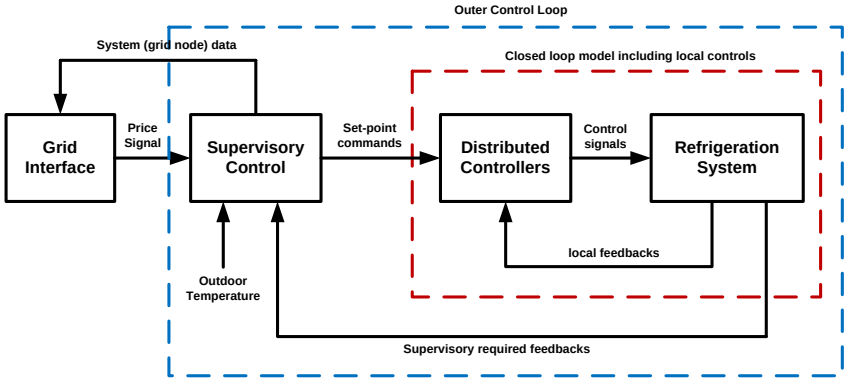

Figure 5.2: A supervisory control structure for refrigeration systems.

Distributed/local Controllers

In the most available set-ups of refrigeration systems, air temperature inside a display case is governed by a thermostatic expansion valve between an upper and a lower temperature limit. The new technologies of the expansion valves allows the pulse with modulation techniques in the control signals. Consequently, air temperature inside the displace cases can be regulated by local PI controllers instead of the thermostatic ON/OFF operations.

The compressors are responsible for regulating the suction pressure to a usually fixed set-point. Due to the different timescales between the dynamics of the compressors and the display case, a static model for the compressors are considered [15].

We propose the following algorithm that keeps the suction pressure as high as possible while ensuring the system functionality in presence of varying loads. A sampling time equal to one minute ensures that the compressor speed is regulated to its steady-state value. Moreover, an upper limit $P_{suc,max}$ is put to keep a safety margin for pressure difference required for circulating the refrigerant. The lower limit $P_{suc,min}$ is due to the limitations of compressor total capacities, and also the safety issues regarding the high pressure difference.

Algorithm 4 Calculate set-point value for the suction pressure

if $P_{suc} < P_{suc,max}$ and $\max(OD_i) < \delta_{max}$ **then**
    Increase the pressure set-point
else if $P_{suc} > P_{suc,min}$ and $\max(OD_i) > \delta_{min}$ **then**
    Decrease the pressure set-point
else
    Keep the previous set-point

The above algorithm is based on an optimality hypothesis, where the pressure should be increased until one of the expansion valves is kept almost fully open. It increases and decreases the pressure set-point with a constant ramp and within the pressure limits.

Now, we have a system with higher energy efficiency. Still, there exists a potential to further reduce the energy cost by shifting the power consumption using a predictive

control algorithm.

Economic MPC

The control objective of economic MPC is to minimize the operating cost while respecting the operation and imposed constraints. The economic objective function is simply formulated by the instantaneous energy cost as multiplication of the real-time electricity price $e_p(t)$ by the power consumption at given time t. So, the energy cost, J_{ec} is computed over the specified time interval $[T_0 \;\; T_N]$ as

$$J_{ec} = \int_{T_0}^{T_N} e_p \dot{W}_{c,tot} dt. \tag{5.12}$$

Linear Model and Constraints

Considering $\dot{Q}_e$ in (6.2) as an input manipulated variable, we will have a linear system with the standard form. But we cannot directly apply $\dot{Q}_e$ as an input signal to the system. Considering (8.5) and (6.6), $\dot{Q}_e$ is a function of OD, P_{rec}, and P_{suc}. P_{rec} is regulated to a fixed set-point and is taken constant. At each time step we can measure P_{suc} and assumed it constant all over the horizon. Bearing in mind that Algorithm 5 tries to keep the pressure at its maximum possible level, it would not be a highly restrictive assumption for our predictive model. So at time step k we will have

$$\dot{Q}_e = \beta_k OD \tag{5.13}$$

where

$$\beta_k = \Delta h_{lg} K v A \sqrt{2\rho_{suc}(P_{rec} - P_{suc})10^5} \tag{5.14}$$

is assumed constant for the next N samples of prediction (*i.e.,* $\beta_{k|k} = \beta_{k|k+i}$ for $i = 1 \cdots N$).

Now the following linear model is derived for each cooling unit.

$$\begin{cases} \dot{x}_p = A_p x_p + B_{1,p} u + B_{2,p} d \\ y_p = C_p x_p \end{cases} \tag{5.15}$$

with the states $x_p = \begin{bmatrix} T_{foods} & T_{cr} \end{bmatrix}^T$, the input $u = OD$, and the disturbance $d = T_{indoor}$. The parameters are

$$A_p = \begin{bmatrix} -\frac{UA_{foods/cr}}{MCp_{foods}} & \frac{UA_{foods/cr}}{MCp_{foods}} \\ \frac{UA_{foods/cr}}{MCp_{cr}} & -\frac{UA_{foods/cr}+UA_{load}}{MCp_{cr}} \end{bmatrix}, \tag{5.16}$$

$$B_{1,p} = \beta_k \begin{bmatrix} 0 \\ \frac{-1}{MCp_{cr}} \end{bmatrix}, \;\; B_{2,p} = \begin{bmatrix} 0 \\ \frac{UA_{load}}{MCp_{cr}} \end{bmatrix}, \tag{5.17}$$

and

$$C = \begin{bmatrix} 1 & 1 \end{bmatrix}. \tag{5.18}$$

The output $y_{p_1} = x_{p_1}$ is the measured variable and subjected to constraint, and $y_{p_2} = x_{p_2}$ is the output to be controlled.

System (6.13) is subjected to the constraints

$$T_{foods,min} \leq y_{p_1} \leq T_{foods,max}, \tag{5.19}$$

and

$$0 \leq u \leq 1, \tag{5.20}$$

where $T_{foods,min}$ and $T_{foods,max}$ are defined based on the types of foods are placed in the display cases.

MPC Formulation

We use a discrete-time receding horizon approach, in which at each time step, an optimization problem is solved over a prediction N step horizon. The result consists of the N moves of manipulated variables where the first one is applied as the MPC control law. So, for the MPC formulation we should discretize the plant model (6.13) with sampling time T_s which results in

$$\begin{cases} x_p[k+1] = A_d x_p[k] + B_{d,1} u[k] + B_{d,2} d[k] \\ y_p[k] = C_d x_p[k] \end{cases} \tag{5.21}$$

with the discrete-time system matrices A_d, $B_{d,1}$, $B_{d,2}$ and C_d. To keep the optimization problem feasible in case of uncertain loads, the state constraint (5.19) is changed to the set of soft constraints

$$\begin{gathered} T_{foods,min} - \varepsilon \Delta T_{foods} \leq y_{p_1} \leq T_{foods,max} + \varepsilon \Delta T_{foods} \\ \varepsilon \geq 0 \end{gathered} \tag{5.22}$$

where the violations from temperature limits are penalized by adding the term $\rho_\varepsilon \varepsilon$ to the objective function. ΔT_{foods} and ρ_ε should be defined such that the violation occurence is very rare and its amount is also negligible.

In order to implement the MPC scheme in a cascade configuration shown in Fig. 9.1, the predictive model should also include the local controller dynamics [16],

$$\begin{cases} x_c[k+1] = A_c x_p[k] + B_c e[k] \\ u[k] = C_c x_c[k] + D_c e[k] \end{cases} \tag{5.23}$$

The error signal is defined as $e[k] = r[k] - y_{p_2}[k]$, where $r[k]$ is the temperature set-point. The combined predictive model for the cascade structure is derived as follow:

$$\begin{cases} X[k+1] = AX[k] + B_1 r[k] + B_2 d[k] \\ Y[k] = CX[k] + Dr[k] \end{cases} \tag{5.24}$$

where $X = \begin{bmatrix} x_p & x_c \end{bmatrix}^T$, and $Y = \begin{bmatrix} y_p & u \end{bmatrix}^T$. The corresponding state space matrices for this formulation can be found in [16]. Using the state-space model (5.24) the control signal applying to the system will be the temperature reference r.

The cost function (6.12) is rewritten using (8.13) as

$$J_{ec} = \sum_{k=0}^{N-1} \left\| e_p \frac{\dot{Q}_{e,tot}}{COP} \right\|_2^2, \tag{5.25}$$

where COP is given by (9.1), and $\dot{Q}_{e,tot} = \sum_{i=1}^{m} \dot{Q}_e^i$ with m indicating the number of cooling units. In the next section we will show how we can predict the COP by estimating it as a linear function depending on the outdoor temperature. Now, the optimization problem is defined as

$$\begin{aligned} \underset{r,\varepsilon}{minimize} \quad & J_{ec} + J_{\Delta u} + \rho_\varepsilon \varepsilon \\ subject\ to \quad & \text{system dynamics } (5.24) \\ & \text{state constraints } (5.22) \\ & \text{input constraints } (5.20) \end{aligned} , \tag{5.26}$$

with

$$J_{\Delta u} = \sum_{k=1}^{N-1} \| R_{\Delta u} \left(r[k] - r[k-1] \right) \|_2^2 . \tag{5.27}$$

where $R_{\Delta u}$ is a diagonal matrix of tuning weights. The above objective function penalizes the rate of change of the set-point to avoid the oscillatory behavior in control commands. The tuning parameters are defined by considering two opposing objectives: cost and stability. From the cost point of view, the units (e.g. display cases) with larger costs of storing energy should be more penalized, and from the stability point of view, the units with faster dynamics should be assigned larger values for their corresponding weights in $R_{\Delta u}$.

4 Simulation Results

In this section, the proposed methods are applied to a high-fidelity simulation benchmark developed based on the model explained in [15]. The model is validated against real data obtained from a supermarket including 7 MT and 4 LT fridge and freezer display cases and a cold room, and the two-stage compressor racks. A two-step simulation is provided to show the gradually improvement from a simple PI replacements together with Algorithm 1 to the complicated supervisory MPC. For each case, the simulation results for a 24-hour operation are presented.

The outdoor temperature is obtained from an hourly measurement with linear interpolation between the hours. The temperature prediction can for example be provided by the national meteorological institute, sometimes on a commercial basis. One week period of hourly el-spot price was downloaded from NordPool spot market [17]. Fig. 5.3 shows the $T_{outdoor}$ and e_p for 24 hours related to the next results. In the simulations, we used a normalized version of the electricity prices and compare the methods based on the percentage in reduction of the operating cost.

Distributed PI Temperature Control together with Algorithmic Pressure Control

At this step, the thermostatic controllers are replaced by PI ones and the Algorithm 1 is applied for the pressure set-point control. The temperature set-points for each PI is set to the middle of the range of the display case temperature the same as the thermostatic control case. The power consumption for 24 hours with thermostatic control is shown in Fig. 6.4. Fluctuations in power consumption is mainly because of the mass flow

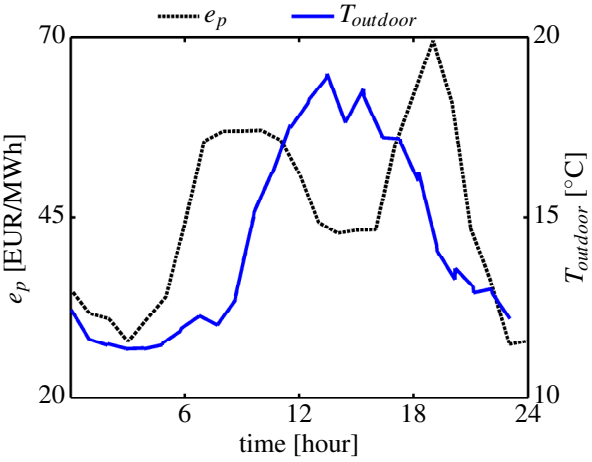

Figure 5.3: Outdoor temperature and electricity price.

change due to thermostat actions. The total energy consumption and electricity cost are E_{tot} = 95.1 [kWh] and e_c = 47.6.

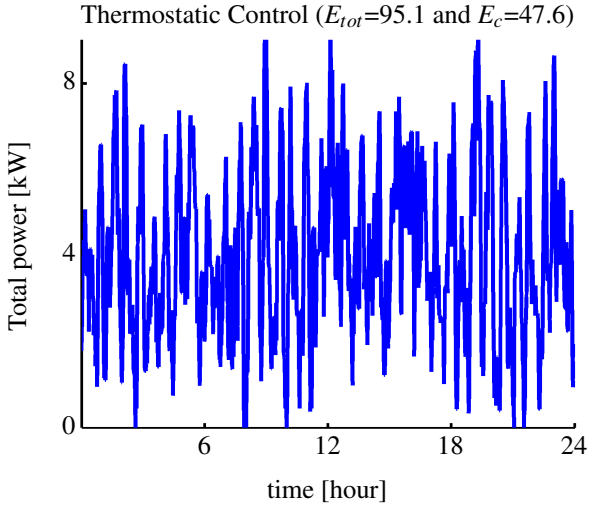

Figure 5.4: Power consumption in case of the thermostatic control valves. The total energy consumption and the corresponding electricity cost are E_{tot} = 95.1 [kWh] and e_c = 47.6.

The energy consumption and the corresponding electricity cost in case of using the PI control valves as well as applying the Algorithm 1 are reduced to E_{tot} = 76 [kWh] (20% reduction) and e_c = 38.4 (19% reduction). The suction pressures of two LT and MT sections are illustrated in Fig. 7.6b. The design parameters are $\delta_{max,MT}$ = 0.95, $\delta_{min,MT}$ = 0.9, $\delta_{max,LT}$ = 0.95,$\delta_{min,LT}$ = 0.85, $P_{max,MT}$ = 34 and $P_{max,LT}$ = 15. The suction pressures vary between δ_{min} and δ_{max} with a constant ramp.

Further improvement can be achieved by running the system in an energy-efficient scenario, where the temperature set-points are fixed to highest levels (only 0.5 °C below the maximum limits). The result is shown in the same plot with the MPC case in Fig. 6.6. Using this simple scenario E_{tot} and e_c are reduced to $E_{tot} = 67.8$ [kWh] (29% reduction) and $e_c = 34.3$ (28% reduction) which is a considerable reduction.

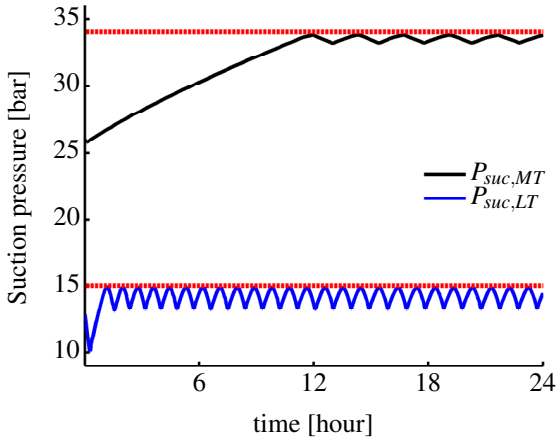

Figure 5.5: Suction pressures of two LT and MT sections after applying Algorithm 5.

Economic MPC

Considering the slow dynamics of the display cases, and different time constant for the food temperatures ranging from 1 hour to more than 10 hours, a 15 minute sampling period and a 24 h prediction horizon ($N = 96$) is chosen for implementation. The tuning parameters are $\rho_{\varepsilon,MT} = 10^6$, $\rho_{\varepsilon,LT} = 100$, and $R_{\Delta u} = 0.01 I_{m\times m}$, where $m = 7$ for MT and $m = 4$ for LT units. To solve the optimization problem (8.23) we have used CVX, a package for specifying and solving convex programs [18, 19].

Considering (9.1), the COP is a nonlinear function of the both suction and the condensation pressures. So its relation cannot be placed directly in the convex programming. Since we have already assumed the pressure set-point unchanged for the prediction horizon (note that it is updated at each sample), the COP would mainly depend on the condensation pressure which is highly correlated with the outdoor temperature. So it is rational to calculate it from (9.1) based on the measurements and then use it as the historical data for prediction. As shown in Fig. 5.6a, the COP is linearly estimated from the outdoor temperature. Fig. 5.6b shows the COP prediction for the next horizon based on the linear fit estimation obtained from the previous 24 hours of the historical data, and the prediction of the outdoor temperature for the next 24 hours. Since the pressure may change during the operation and also the outdoor temperature varies during the day, the linear fit is updated in each time step to avoid the significant bias in predictions.

The power consumption resulted from applying the economic MPC scheme in the supervisory level is depicted in Fig. 5.7. The food temperatures of the fridge display cases are represented in Fig. 5.8. The trends for the freezer units are almost similar.

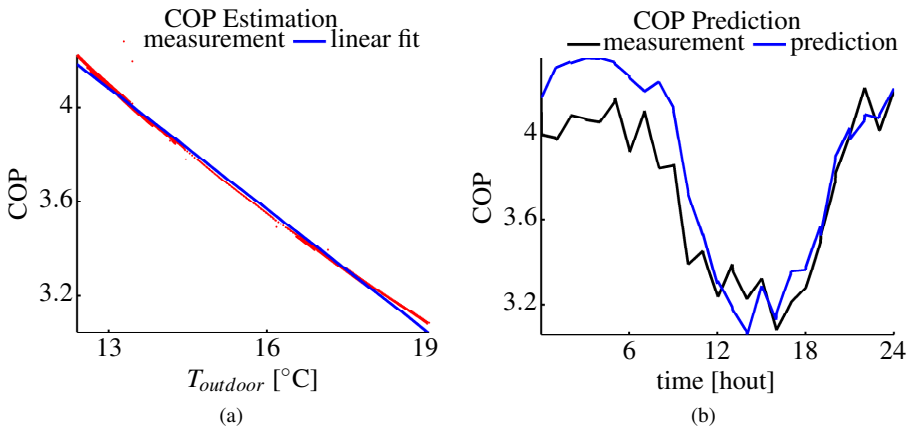

Figure 5.6: COP estimation and prediction. (a): Estimation of the system COP as a linear function of the outdoor temperature. (b): Prediction of the system COP using the obtained linear estimation and prediction of the outdoor temperature.

Using the economic MPC, the energy consumption is reduced to E_{tot} = 64.6 [kWh] (32% reduction) that justifies the COP prediction method. The electricity cost become e_c = 30.3 (36% reduction) which indicates the effectiveness of the proposed scheme. As can be seen from Fig. 5.3, around 3 h both e_p and $T_{outdoor}$ are low (the COP is high), so the supervisory control starts storing energy by lowering the temperatures while respecting the imposed constraints. Around 15 h, e_p is low but $T_{outdoor}$ is high (the COP is low), but the proposed control can handle this trade-off very well by storing some amount of energy in an optimal way.

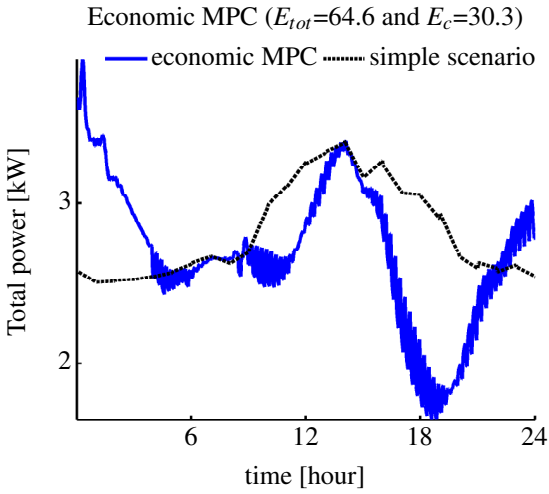

Figure 5.7: Power consumption after applying economic MPC (solid) and the energy-efficient scenario (dash).

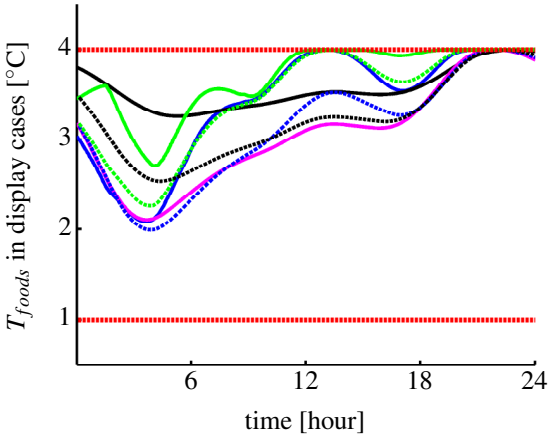

Figure 5.8: Food temperatures in the fridge display cases. The temperature limits are [1, 4].

5 Discussions

From the results provided in the previous section, one can recognize a big gap between a very simple traditional thermostatic control in a commercial refrigeration system and a complicated economic MPC regarding the operating cost (36% reduction was reported). In order to avoid jumping from a primary design to an advanced one, we explained how we can increase the efficiency of the system, regarding its energy consumption, by simple practically applicable methods. For this purpose, we proposed a predictive control in a supervisory level to minimize the cost of operation. The following steps were investigated concerning the economic saving they can offer with respect to the simple non-efficient thermostatic control.

1. Using PI control together with Algorithm 5, (19%)
2. Using the energy-efficient scenario, (28%)
3. Using the economic MPC scheme, (36%)

The largest saving is realized by using the economic MPC, but the method is complicated and needs advanced numerical methods to solve an optimization problem. On the other hand, the proposed energy-efficient scenario can be easily applied, but the operating cost is not minimized by this method. So, there is a visible trade-off between the performance and the design complexity.

6 Conclusions

In general, the economic cost function in refrigeration systems including the cooling capacity of each cold reservoir as well as the suction pressure as manipulated variables

is a nonconvex function which makes the optimization problem more troublesome. To avoid this nonconvexity, we have proposed a supervisory control structure with a simple algorithm for set-point control of the suction pressure that facilitates a reformulation of the problem to a more numerically efficient convex programing. Incorporating the PI controller dynamic into the predictive model enables the MPC to apply the tempreture set-point as the manipulated variable. The results showed the superiority of the proposed economic MPC with 36% reduction of the operating cost over an energy-efficient scenario offering 28% reduction.

References

[1] J. Maciejowski, *Predictive Control with Constraints*, ser. Pearson Education. England: Prentice Hall, 2002.

[2] N. Ricker, "Predictive hybrid control of the supermarket process," *Control Engineering Practice*, vol. 18, pp. 608–617, 2010.

[3] D. Sarabia, F. Capraro, L. F. S. Larsen, and C. Prada, "Hybrid NMPC of supermarket display cases," *Control Engineering Practice*, vol. 17, pp. 428–441, 2009.

[4] C. Sonntag, A. Devanathan, S. Engell, and O. Stursberg, "Hybrid nonlinear model-predictive control of a supermarket refrigeration system," in *Proceedings of the16th IEEE International Conference on Control Applications*, Singapore, Oct. 2007, pp. 1432–1437.

[5] H. Fallahsohi, C. Changenet, and S. Placé, "Predictive functional control of an expansion valve for minimizing the superheat of an evaporator," *International journal of Refrigeration*, vol. 33, pp. 409–418, 2010.

[6] M. Elliott and B. Rasmussen, "Model-based predictive control of a multi-evaporator vapor compression cooling cycle," in *proceeding of the 2008 American Control Conference*, Seattle, Washington, USA, Jun. 2008.

[7] D. Leducq, J. Guilpart, and G. Trystram, "Non-linear predictive control of a vapor compression cycle," *International journal of Refrigeration*, vol. 29, pp. 761–772, 2006.

[8] A. Mohsenian-Rad and A. Leon-Garcia, "Optimal residential load control with price prediction in real-time electricity pricing environments," *IEEE Transactions on Smart Grid*, vol. 1, no. 2, pp. 120–133, 2010.

[9] J. Rawlings and R. Amrit, *Optimizing Process Economic Performance using Model Predictive Control*, ser. Nonlinear Model Predictive Control: Towards New Challenging Applications, ISBN: 978-1-4614-1832-0. Springer, 2009, pp. 119–138.

[10] T. G. Hovgaard, L. F. S. Larsen, K. Edlund, and J. B. Jrgensen, "Model predictive control technologies for efficient and flexible power consumption in refrigeration systems," *Energy*, vol. 44, pp. 105–116, 2012.

[11] Y. T. Ge and S. A. Tassou, "Thermodynamic analysis of transcritical CO_2 booster refrigeration systems in supermarket," *Energy Conversion and Management*, vol. 52, pp. 1868–1875, 2011.

[12] L. N. Petersen, H. Madsen, and C. Heerup, "ESO2 optimization of supermarket refrigeration systems: Mixed integer MPC and system performance," Department of Informatics and Mathematical Modeling, Technical University of Denmark, Tech. Rep., 2012.

[13] C. Pérez-Segarra, J. Rigola, M. Sòria, and A. Oliva, "Detailed thermodynamic characterization of hermetic reciprocating compressors," *International Journal of Refrigeration*, vol. 28, pp. 579–593, 2005.

[14] R. Zhou, T. Zhang, J. Catano, J. T. Wen, G. J. Michna, Y. Peles, and M. K. Jensen, "The steady-state modeling and optimization of a refrigeration system for high heat flux removal," *Applied Thermal Engineering*, vol. 30, pp. 2347–2356, 2010.

[15] S. E. Shafiei, H. Rasmussen, and J. Stoustrup, "Modeling supermarket refrigeration systems for supervisory control in smart grid," in *Proceedings of the American Control Conference*, Washington DC, USA, Jun. 2013, pp. 5660–5665.

[16] L. Balbis, R. Katebi, and A. Ordys, "Modeling predictive control design for industrial applications," in *International Control Conference (ICC2006)*, Glasgow, Scotland, Aug. 2006.

[17] "Nord pool spot," http://www.nordpoolspot.com.

[18] I. CVX Research, "CVX: Matlab software for disciplined convex programming, version 2.0 beta," http://cvxr.com/cvx, Sep. 2012.

[19] M. Grant and S. Boyd, "Graph implementations for nonsmooth convex programs," in *Recent Advances in Learning and Control*, ser. Lecture Notes in Control and Information Sciences, V. Blondel, S. Boyd, and H. Kimura, Eds. Springer-Verlag Limited, 2008, pp. 95–110, http://stanford.edu/~boyd/graph_dcp.html.

Paper C

Model Predictive Control for a Thermostatic Controlled System

Seyed Ehsan Shafiei, Henrik Rasmussen and Jakob Stoustrup

This paper was published in:
The Proceedings of the European Control Conference, July 2013

The layout has been revised

Abstract

This paper proposes a model predictive control scheme to provide temperature set-points to thermostatic controlled cooling units in refrigeration systems. The control problem is formulated as a convex programming problem to minimize the overall operating cost of the system. The foodstuff temperatures are estimated by reduced order observers and evaporation temperature is regulated by an algorithmic suction pressure control scheme. The method is applied to a validated simulation benchmark. The results show that even with the thermostatic control valves, there exists significant potential to reduce the operating cost.

1 Introduction

Increasing the energy demand, on one hand, and penetration of the intermittent renewable recourses into the electricity grid, on the other hand, enforce a lot of researches to cope with the current and the future challenges. Control theory has been proven to be able to offer strong solutions for various problems regarding from the production units to the end-point consumers.

To be able to implement advanced cost efficient control algorithms, some systems need significant redesigns like hardware replacements, system reconfiguration, software changes, etc. Hysteresis controllers that regulate the controllable variables within hysteresis bounds can be found in various process systems like a thermostatic controller that regulate the temperature in a cooling unit. So, it would be more cost effective if we can implement the advanced control methods without replacing these simple local controllers by more expensive ones. This paper proposes a solution for such a control problem in refrigeration systems.

Model predictive control (MPC) has successfully been applied to refrigeration systems for intending different kinds of improvements. With hybrid system formulation, MPC was employed in [1,2] and [3] to solve the synchronization problem in display cases that causes wearing of the compressors. Fallahsohi, *et al* in [4] applied predictive functional control to minimize the superheat in an evaporator. For multi-evaporator systems, a decentralized MPC was proposed to control the cooling capacity of each evaporator [5].

There are also valuable researches that use MPC to reduce the energy consumption and/or electricity cost. A nonlinear predictive control scheme was designed in [6] to reduce the total power consumption of the compressor in a vapor compression cycle. The cooling capacity is regulated by a variable speed compressor. But this method cannot be applied directly to the refrigeration systems with different cooling units in which the cooling capacity is regulated by expansion valves as well. As a thorough study that proposes a MPC to reduce the operating cost of such systems, we can point to [7]. But it replaced the hysteresis control valves with the floating point control ones for implementation. Moreover, the nonlinear optimization tool employed to handle a nonconvex cost function imposes a heavy computation burden into the control system.

This paper proposes a MPC for thermostatic controlled cooling units in commercial refrigeration systems. To deal with nonlinear dynamics of the cooling units, the cooling capacity is treated as a fictitious manipulated variable by which we can formulate the standard linear system dynamics for each cooling unit. A simple efficient algorithm, proposed by the authors in [8], is slightly modified and employed for set-point control of the

suction pressures. The predictions of the electricity price and the outdoor temperature are used in the MPC formulation. In order to preserve food temperatures within the permissible range, a reduced order observer is designed to estimate those temperatures for each cooling unit. Finally, the formulated MPC is implemented using a convex programming on a validated simulation benchmark including several fridge and freezer display cases.

2 Refrigeration System

Fig. 9.1 shows a typical refrigeration system with a booster configuration. The cooling section consists of a low temperature (LT) section including display cases and low stage compressor racks (COMP_LO), and a medium temperature section including freezing rooms and high stage compressor racks (COMP_HI). The air temperatures at the evaporator outlets are considered as controllable variables regulated by ON/OFF thermostatic control valves (EV_MT and EV_LT). A detailed thermodynamic analysis of such a booster configuration is explained in [9].

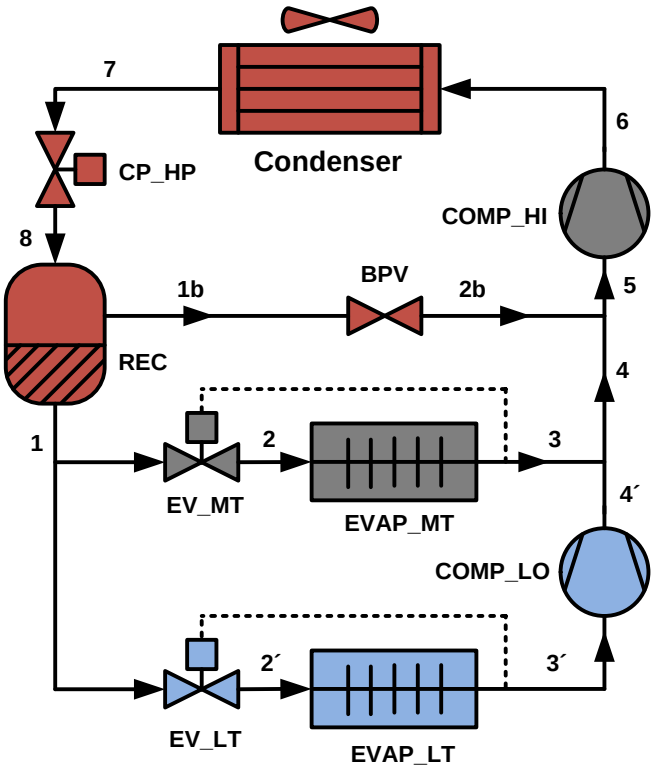

Figure 6.1: Basic layout of a typical supermarket refrigeration system with booster configuration.

Display Case Dynamics

Considering energy balances, the heat transfers in display cases are described by the following equations based on a lumped temperature model.

$$MCp_{foods}\frac{dT_{foods}}{dt} = -\dot{Q}_{foods/cr} \tag{6.1}$$

$$MCp_{cr}\frac{dT_{cr}}{dt} = \dot{Q}_{load} + \dot{Q}_{foods/cr} - \dot{Q}_{e} \tag{6.2}$$

Where MCp denotes the corresponding mass multiplied by the heat capacity, and T_{cr} is the controllable air temperature inside the cooling unit. $\dot{Q}_{foods/cr}$ is the heat transfer from food to cooled air,

$$\dot{Q}_{foods/cr} = UA_{foods/cr}(T_{foods} - T_{cr}), \tag{6.3}$$

$\dot{Q}_{load}$ is the heat load due to indoor temperature, T_{indoor},

$$\dot{Q}_{load} = UA_{load}(T_{indoor} - T_{cr}), \tag{6.4}$$

and $\dot{Q}_{e}$ is the heat transfer from cooled air to the circulated refrigerant,

$$\dot{Q}_{e} = \dot{m}_{r}(h_{oe} - h_{ie}), \tag{6.5}$$

where UA is the overall heat transfer coefficient, h_{oe} and h_{ie} are enthalpies at the outlet and the inlet of the evaporators which are nonlinear functions of the evaporation temperature (or equivalently suction pressure). The term $\dot{m}_{r}$ denotes the mass flow of refrigerant into the evaporator described by the following equation:

$$\dot{m}_{r} = OD\ KvA\sqrt{2\rho_{suc}(P_{rec} - P_{suc})10^{5}} \tag{6.6}$$

where OD stands for the opening degree of the valve with value between 0 (closed) to 1 (fully opened), P_{rec} and P_{suc} are receiver and suction pressures in [bar], ρ_{suc} is the density of the circulating refrigerant, and KvA denotes a constant characterizing the valve [10]. However, in case of thermostatic control, OD is only 0 or 1.

There is also a superheat controller operating on the valve when the valve state is ON (OD = 1). From the energy consumption point of view, and also regarding the control design in a supervisory level, the superheat control dynamics are negligible. So, here we have assumed a constant superheat degree for the model as explained by the authors in [11].

Power Consumption and COP

The electrical power consumption of each compressor bank is calculated by

$$\dot{W}_{c} = \frac{1}{\eta_{me}}\dot{m}_{ref}(h_{o,c} - h_{i,c}), \tag{6.7}$$

where $\dot{m}_{ref}$ is the total mass flows into the compressor, and $h_{o,c}$ and $h_{i,c}$ are the enthalpies at the outlet and inlet of the compressor bank. These enthalpies are nonlinear functions of the refrigerant pressure and temperature at the calculation point. The constant η_{me}

indicates overall mechanical/electrical efficiency considering mechanical friction losses and electrical losses [12]. The outlet enthalpy is computed by

$$h_{o,c} = h_{i,c} + \frac{1}{\eta_{is}}(h_{is} - h_{i,c}), \tag{6.8}$$

in which h_{is} is the outlet enthalpy when the compression process is isentropic, and η_{is} is the related isentropic efficiency given by [13] (neglecting higher order terms),

$$\eta_{is} = c_0 + c_1(f_c/100) + c_2(P_{c,o}/P_{suc}), \tag{6.9}$$

where f_c is the virtual compressor frequency (total capacity) of the compressor rack in percentage, $P_{c,o}$ is the pressure at compressor outlet, and c_i are constant coefficients.

The total coefficient of performance (COP) is defined as the ratio of total cooling capacity over the total power consumption of the compressors.

$$COP = \frac{\dot{Q}_{e,tot}}{\dot{W}_{c,tot}} \tag{6.10}$$

The COP is calculated by

$$COP = \frac{x_{MT}(h_{oe,MT} - h_{ie,MT}) + x_{LT}(h_{oe,LT} - h_{ie,LT})}{\frac{1}{\eta_{MT}}(h_{is,MT} - h_{i,c,MT}) + \frac{x_{LT}}{\eta_{LT}}(h_{is,LT} - h_{i,c,LT})}, \tag{6.11}$$

where indices MT and LT relate the calculated values to the medium and low temperature sections, respectively. Parameters x_{MT} and x_{LT} are the ratio of refrigerant mass flow of MT and LT evaporators to the total flow rate, and $\eta_{MT} = \eta_{me,MT}\eta_{is,MT}$ and $\eta_{LT} = \eta_{me,LT}\eta_{is,LT}$.

3 Set-Point Control

In the control structure illustrated in Fig. 6.2, the distributed controllers are responsible for regulating controllable variables to the values provided by the set-point control unit. Distributed controllers consist of thermostatic and PI controllers regulating the temperatures and compressors speeds, respectively. So, the desired set-points are the air temperatures of display cases and the suction pressures of LT and MT sections.

In general, providing optimal set-points for both the suction pressure and the display cases temperatures leads to solve a nonconvex optimization problem which imposes a heavy computational burden. To avoid this nonconvexity, we use a simple algorithm presented in [8] for the pressure set-points, and a new MPC scheme using convex programing for the temperature set-points. This leads to a nearly optimal solution.

Algorithmic Pressure Control

The authors proposed a heuristic algorithm for the pressure set-point control using the fact that the near optimal pressure value will be achieved by increasing the suction pressure until one of the expansion valves is kept almost fully open [8]. Because of the ON and OFF states of the valves, we slightly modified the algorithm by taking the moving average of the opening degree for calculation of the maximum state between the valves.

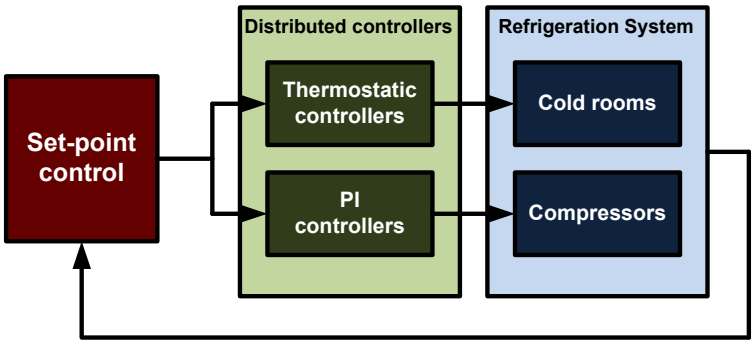

Figure 6.2: Set-point control structure for refrigeration systems.

A sampling time equal to one minute (for implementing this static control algorithm) ensures that the compressor speed is regulated to its steady-state value. Thus, the static model for the compressors are considered for the simulations [11]. The upper limit $P_{suc,max}$ gives a safety margin for the pressure difference required for circulating the refrigerant. The lower limit $P_{suc,min}$ is due to the limitations of the compressor total capacities, and also the safety issues regarding the high pressure difference.

Algorithm 5 Calculate the set-point value for each suction pressure

if $P_{suc} < P_{suc,max}$ and $\max(\mathbf{OD}_{avr}) < \delta_{max}$ **then**
  Increase the pressure set-point
else if $P_{suc} > P_{suc,min}$ and $\max(\mathbf{OD}_{avr}) > \delta_{min}$ **then**
  Decrease the pressure set-point
else
  Keep the previous set-point
end

In the above algorithm, $\mathbf{OD}_{avr}$ is the moving average vector of opening degree of the expansion valves, and δ_{max} and δmin are design parameter.

Model Predictive Control

Here, the control objective is to minimize the operating cost while respecting the imposed constraints. The economic objective function is simply formulated by the instantaneous energy cost as multiplication of the real-time electricity price $e_p(t)$ by the power consumption $\dot{W}_{c,tot}$ at given time t. So, the energy cost, J_{ec} is computed over the specified time interval $[T_0 \;\; T_N]$ as

$$J_{ec} = \int_{T_0}^{T_N} e_p \dot{W}_{c,tot} dt. \tag{6.12}$$

Linear Model and Constraints

Considering $\dot{Q}_e$ in (6.2) as a fictitious input manipulated variable, we will have a linear system with the standard form,

$$\dot{x} = Ax + B_1 u + B_2 d \tag{6.13}$$

with the states $x = \begin{bmatrix} T_{foods} & T_{cr} \end{bmatrix}^T$, the input $u = \dot{Q}_e$, and the disturbance $d = T_{indoor}$. The parameters are

$$A = \begin{bmatrix} -\frac{UA_{foods/cr}}{MCp_{foods}} & \frac{UA_{foods/cr}}{MCp_{foods}} \\ \frac{UA_{foods/cr}}{MCp_{cr}} & -\frac{UA_{foods/cr}+UA_{load}}{MCp_{cr}} \end{bmatrix}, \tag{6.14}$$

and

$$B_1 = \begin{bmatrix} 0 \\ \frac{-1}{MCp_{cr}} \end{bmatrix}, \quad B_2 = \begin{bmatrix} 0 \\ \frac{UA_{load}}{MCp_{cr}} \end{bmatrix}. \tag{6.15}$$

System (6.13) is subjected to the constraints

$$T_{foods,min} \leq T_{foods} \leq T_{foods,max}, \tag{6.16}$$

and

$$0 \leq \dot{Q}_e \leq \dot{Q}_{e,max}, \tag{6.17}$$

where $T_{foods,min}$ and $T_{foods,max}$ are defined based on the type of foods in the display cases, and $\dot{Q}_{e,max}$ is calculated from (6.5) and (6.6) by putting $OD = 1$.

Note that the $\dot{Q}_e$ in (6.17) is not directly applicable to the system. In [8], a supervisory MPC was formulated by incorporating the local controllers dynamics in the predictive model. Here, due the nonlinearity of the thermostatic action, we cannot formulate the same supervisory MPC. Instead, we propose a new MPC scheme for this purpose, where the fictitious input is used to one step prediction of the next temperature value, and then it is applied as the temperature set-point to the cooling unit. This practical point will be addressed in section 3.

Estimator Design

In order to estimate the food temperature in each cooling unit, we design a reduced order observer [14, Ch. 8]. We rewrite (6.13) as

$$\begin{bmatrix} \dot{x}_1 \\ \dot{x}_2 \end{bmatrix} = \begin{bmatrix} a_{11} & a_{12} \\ a_{21} & a_{22} \end{bmatrix} \begin{bmatrix} x_1 \\ x_2 \end{bmatrix} + \begin{bmatrix} b_{11} & b_{12} \\ b_{21} & b_{22} \end{bmatrix} \begin{bmatrix} u \\ d \end{bmatrix}. \tag{6.18}$$

The reduced order observer is designed to estimate $x_1 = T_{foods}$ with the following estimator equation,

$$\dot{\hat{x}}_1 = A_o \hat{x}_1 + B_{o,1} u_o + B_{o,2} d + L(y_o - C_o \hat{x}_1), \tag{6.19}$$

where $A_o = a_{11}$, $B_{o,1} = \begin{bmatrix} a_{12} & b_{11} \end{bmatrix}$, $u_o = \begin{bmatrix} x_2 & u \end{bmatrix}^T$, $B_{o,2} = b_{12}$, $C_o = a_{21}$, and

$$y_o = \dot{x}_2 - a_{22} x_2 - b_{21} u - b_{22} d. \tag{6.20}$$

The observer gain L is defined based on the classical pole placement method. Implementation of the above estimator needs further considerations explained in [14, Ch. 8].

MPC Design

We use a discrete-time receding horizon approach, in which at each time step, an optimization problem is solved over a N-step prediction horizon. The result consists of the N moves of manipulated variables where the first one is applied as the MPC control law. So, for this MPC formulation, we should discretize the multivariable extension of system (6.13) with sampling time T_s which results in

$$x[k+1] = A_d x[k] + B_{d,1} u[k] + B_{d,2} d[k]. \tag{6.21}$$

with the discrete-time system matrices A_d, $B_{d,1}$ and $B_{d,2}$. The states are $x = \begin{bmatrix} \hat{x}_1^T & x_2^T \end{bmatrix}^T$ where $\hat{x}_1$ is the vector of estimated food temperatures and x_2 is the vector of air temperature.

To keep the optimization problem feasible in case of uncertain loads, the state constraint (6.22) is changed to the set of soft constraints

$$\begin{gathered} T_{min} - \varepsilon \Delta T_{foods} \leq \hat{x}_1 \leq T_{max} + \varepsilon \Delta T_{foods} \\ \varepsilon \geq 0 \end{gathered} \tag{6.22}$$

where the violations from temperature limits are penalized by adding the term $\rho_\varepsilon \varepsilon$ to the objective function. ΔT_{foods} and ρ_ε should be defined such that the violation occurs rarely. To avoid the temperature violation caused by state estimation error, a safety margin is imposed by defining $T_{min} = T_{foods,min} + T_{safe}$ and $T_{max} = T_{foods,max} - T_{safe}$.

The cost function (6.12) is rewritten using (8.13) as

$$J_{ec} = \sum_{k=0}^{N-1} \left\| e_p \frac{\dot{Q}_{e,tot}}{COP} \right\|_2^2, \tag{6.23}$$

where COP is given by (9.1), and $\dot{Q}_{e,tot} = \sum_{i=1}^{m} \dot{Q}_e^i$ with m indicating the number of display cases. In the next section, we will show how we can predict the COP by estimating it as a linear function depending on outdoor temperature. Now, the optimization problem is defined as

$$\begin{array}{ll} \underset{\dot{Q}_e, \varepsilon}{\text{minimize}} & J_{ec} + J_{\Delta u} + \rho_\varepsilon \varepsilon \\ \text{subject to} & \text{system dynamics } (6.21) \\ & \text{state constraints } (6.22) \\ & \text{input constraints } (6.17) \end{array}, \tag{6.24}$$

with

$$J_{\Delta u} = \sum_{k=1}^{N-1} \left\| R_{\Delta u} \left(\dot{Q}_e[k] - \dot{Q}_e[k-1] \right) \right\|_2^2, \tag{6.25}$$

where $R_{\Delta u}$ is a diagonal matrix of tuning weights. The above objective function penalizes the rate of change of cooling capacity to avoid the oscillatory behavior in set-point commands. The tuning parameters are defined by considering two opposing objectives: cost and stability. From the cost point of view, the units (e.g. display cases) with larger costs of storing energy should be more penalized, and from the stability point of view, the units with faster dynamics should be assigned larger values for their corresponding weights in $R_{\Delta u}$.

At each time step a new set of control commands $\dot{Q}_e$ are given by the above MPC. But as mention in section 3, these commands are not directly applicable to the cooling units. So we use the predicted states ($T_{ref,cr} = x_2[k+1]$) by updating (6.21) using the obtained $\dot{Q}_e$, and then apply them as temperature set-points to the corresponding cold rooms. The ON/OFF limits of thermostatic controllers are also set to the small values around the set-point. The proposed supervisory MPC is summed up in Algorithm 7.

Algorithm 6 Supervisory MPC including the economic cost in its objective function

Prediction

Load

COP and $T_{outdoor}$ from previous horizon

e_p and $T_{outdoor}$ predictions

Compute

COP prediction based on its previous horizon values and $T_{outdoor}$

Solve

$$\begin{aligned} \underset{u,\varepsilon}{\text{minimize}} \quad & J_{ec} + J_{\Delta u} + \rho_\varepsilon \varepsilon \quad \text{(over the horizon)} \\ \text{subject to} \quad & x[k+1] = A_d x[k] + B_{d,1} u[k] + B_{d,2} d[k] \\ & \hat{x}_1 \geq T_{min} - \varepsilon \Delta T_{foods} \\ & \hat{x}_1 \leq T_{max} + \varepsilon \Delta T_{foods} \\ & \varepsilon \geq 0 \\ & 0 \leq u \leq \dot{Q}_{e,max} \end{aligned}$$

Update

$u[k]$ = first move in obtained u

$x[k+1] = A_d x[k] + B_{d,1} u[k] + B_{d,2} d[k]$

$T_{ref,cr} = x_2[k+1]$ where $x = \begin{bmatrix} \hat{x}_1 & x_2 \end{bmatrix}^T$

4 Simulation Study

In this section, the proposed method is applied to a high-fidelity simulation benchmark including 7 fridge display cases, 4 freezer display cases and cold room, and the two-stage compressor racks. The details of the model validation against real data are found in [11]. At first, we apply a traditional scenario in which the thermostat action occurs between the upper and the lower temperature limits. For a fair comparison, the pressure set-points are fixed to the maximum values. The designed MPC together with algorithmic pressure control are applied to the system.

Simulation Set-up

The outdoor temperature is obtained from an hourly measurement with linear interpolation between hours. The temperature prediction can for example be provided by the national meteorological institute, sometimes on a commercial basis. One week period of hourly el-spot price was downloaded from NordPool spot market [15]. Fig. 6.3 shows

the $T_{outdoor}$ and e_p for 24 hours related to the upcoming results. In the simulations, we used a normalized version of the electricity prices and evaluate the results based on the percentage in reduction of the operating cost.

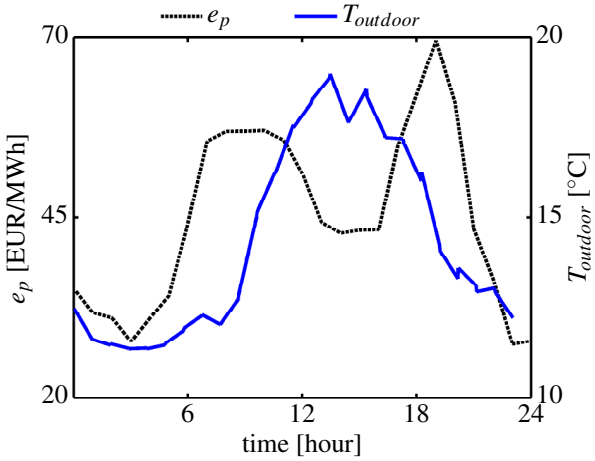

Figure 6.3: Outdoor temperature (top) and electricity price (bottom).

The estimator is designed as a digital observer with sampling time of 1 min where the observer poles are selected as follows.

$$P_o = [0.99,\ 0.995,\ 0.99,\ 0.99,\ 0.99,\ 0.99,\ 0.9,\ \ldots \\ 0.999,\ 0.5,\ 0.999,\ 0.1]$$

Because of the slow dynamics of the cooling parts, the MPC sampling time is set to 15 min. A 24 h prediction horizon is considered which needs $N = 96$ samples for implementation. The tuning parameters are $\rho_\varepsilon = 5$ and

$$R_{\Delta u} = diag(0.1,\ 0.1,\ 0.1,\ 0.1,\ 0.1,\ 0.05,\ 0.1,\ \ldots \\ 0.0025,\ 0.01,\ 0.0025,\ 0.01),$$

with the first 7 elements for the fridge and the last 4 for the freezer units. The safety temperatures are chosen as $T_{safe} = 0.5$ °C for display cases and $T_{safe} = 1$ °C for freezing rooms. A 5 min moving average as well as $\gamma_{OD} = 0.9$ are used for the implementation of Algorithm 5. To solve the optimization problem (8.23) we used CVX, a package for specifying and solving convex programs [16, 17].

Simulation Results

Power consumption of the compressors, resulted from applying the traditional scenario explained before, is depicted in Fig. 6.4. The total energy consumption and corresponding electricity cost are $E_{tot} = 64$ [kWh] and $e_c = 32.5$.The air and food temperatures of the first and third fridge display cases are provided in Fig. 6.5 for a 6 h period. The trends are similar for the other units.

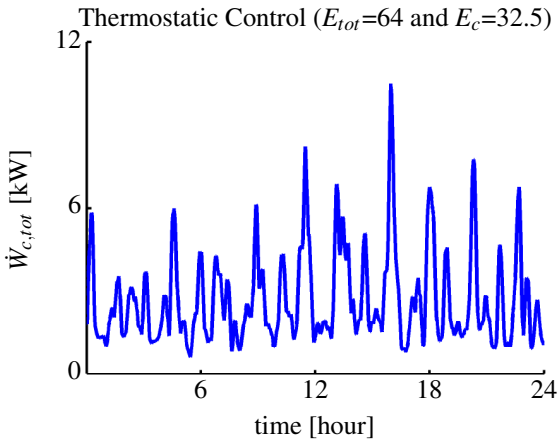

Figure 6.4: Power consumption in case of traditional fixed set-point control.

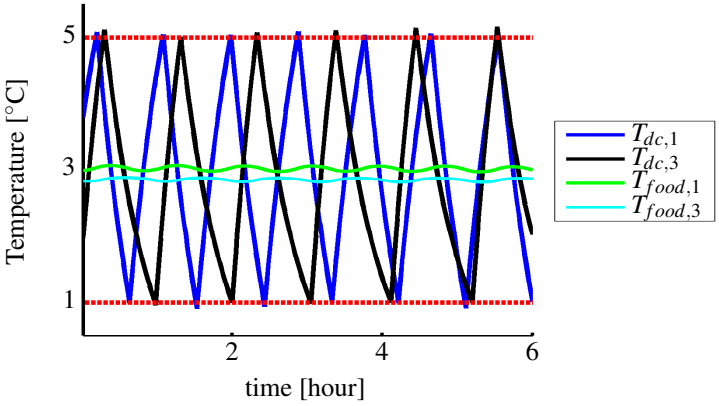

Figure 6.5: Air temperatures of the first and third fridge display cases, T_{dc}, and the corresponding food temperatures. Dashed red lines indicate the temperature limits.

Fig. 6.6 shows the power consumption after applying the designed MPC together with Algorithm 5. The energy consumption and operating cost are E_{tot} = 50 [kWh] and e_c = 21.4 (34% reduction) which are considerable reductions.

The actual food temperatures for fridge units are illustrated in Fig. 6.7. The details of the COP prediction with correlation to the outdoor temperature are explained in [8]. As can be seen from Fig. 6.3, around 3 h both e_p and $T_{outdoor}$ are low (the COP is high), so the supervisory control starts storing energy by lowering the temperatures while respecting the imposed constraints. Around 15 h, e_p is low but $T_{outdoor}$ is high (the COP is low), but the proposed control can handle this trade-off very well by storing some amount of energy in an optimal fashion.

The suction pressures for both low and medium temperature sections regulated by low and high stage compressor banks are shown in Fig. 7.6b. The pressure related to MT units is kept at the maximum level. It is because there is not a quick change in display case

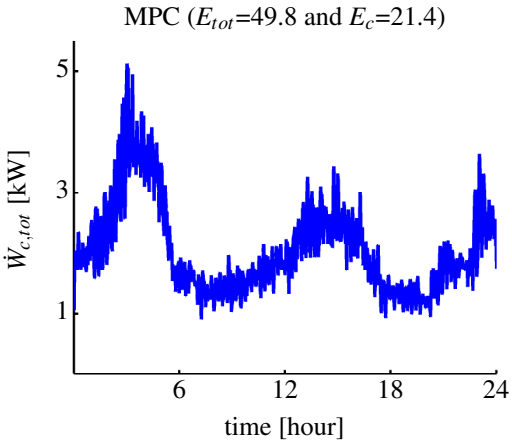

Figure 6.6: Power consumption after applying MPC (Algorithm 7) together with algorithmic suction pressure control (Algorithm 5).

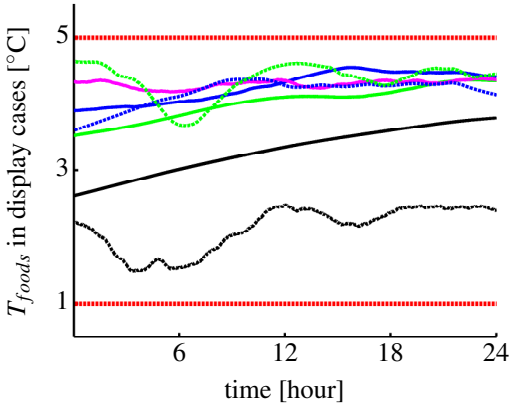

Figure 6.7: Actual food temperatures in fridge display cases. The temperature limits for are [1, 5] except the lower one which is [1, 3].

set-points that causes a quick variation in cooling capacity. Thus, the moving average of opening degree of the related valves do not exceed the decision value (γ_{OD} = 0.9). On the other hand, the pressure related to LT units is decreased by quickly increasing the request for cooling capacity due to quickly lowering the freezing room temperatures by MPC.

The state estimation results given by the reduced order observer are provided in Fig. 6.9 for display cases 1, 3 and 7, and freezing rooms 1, 2 and 4. Some temperature plots show perfect estimations and a small (0.5 °C) estimation error is seen in the second freezing room. The imposed safety margin in MPC state constraints can very well prevent the constraint violation in the presence of such estimation errors.

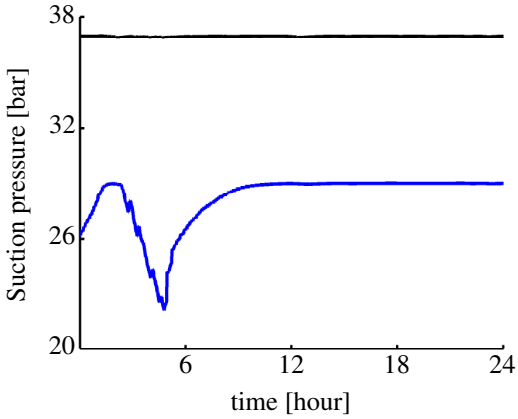

Figure 6.8: Suction pressures of two LT and MT sections resulted from applying Algorithm 5.

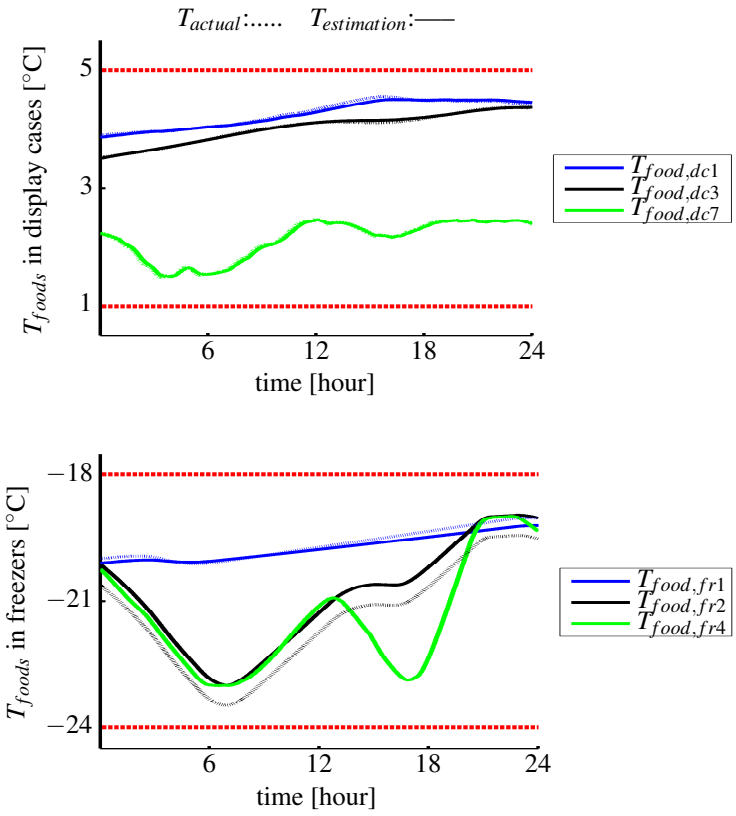

Figure 6.9: Estimation of the food temperatures by reduced order observer. The imposed safety margin prevent the violation of temperature constraints due to the estimation error.

5 Conclusions

This paper presented a set-point control method for reducing the overall operating cost of a refrigeration system. A model predictive control algorithm was proposed to set-point control of the thermostatic controlled cooling units. In order to preserve food temperatures within the permissible range, a reduced order estimator was designed to estimate those temperatures. The formulated MPC was implemented by convex programming. Moreover, a simple and efficient algorithm was used for set-point control of the suction pressures. A considerable 34% cost reduction was obtained by applying the designed algorithms to a large scale refrigeration system including several display cases and freezing rooms.

References

[1] N. Ricker, "Predictive hybrid control of the supermarket process," *Control Engineering Practice*, vol. 18, pp. 608–617, 2010.

[2] D. Sarabia, F. Capraro, L. F. S. Larsen, and C. Prada, "Hybrid NMPC of supermarket display cases," *Control Engineering Practice*, vol. 17, pp. 428–441, 2009.

[3] C. Sonntag, A. Devanathan, S. Engell, and O. Stursberg, "Hybrid nonlinear model-predictive control of a supermarket refrigeration system," in *Proceedings of the16th IEEE International Conference on Control Applications*, Singapore, Oct. 2007, pp. 1432–1437.

[4] H. Fallahsohi, C. Changenet, and S. Placé, "Predictive functional control of an expansion valve for minimizing the superheat of an evaporator," *International journal of Refrigeration*, vol. 33, pp. 409–418, 2010.

[5] M. Elliott and B. Rasmussen, "Model-based predictive control of a multi-evaporator vapor compression cooling cycle," in *proceeding of the 2008 American Control Conference*, Seattle, Washington, USA, Jun. 2008.

[6] D. Leducq, J. Guilpart, and G. Trystram, "Non-linear predictive control of a vapor compression cycle," *International journal of Refrigeration*, vol. 29, pp. 761–772, 2006.

[7] T. G. Hovgaard, L. F. S. Larsen, K. Edlund, and J. B. Jrgensen, "Model predictive control technologies for efficient and flexible power consumption in refrigeration systems," *Energy*, vol. 44, pp. 105–116, 2012.

[8] S. E. Shafiei, J. Stoustrup, and H. Rasmussen, "A supervisory control approach in economic MPC design for refrigeration systems," in *Proceedings of the European Control Conference*, Zürich, Switzerland, Jul. 2013, pp. 1565–1570.

[9] Y. T. Ge and S. A. Tassou, "Thermodynamic analysis of transcritical CO_2 booster refrigeration systems in supermarket," *Energy Conversion and Management*, vol. 52, pp. 1868–1875, 2011.

[10] L. N. Petersen, H. Madsen, and C. Heerup, "ESO2 optimization of supermarket refrigeration systems: Mixed integer MPC and system performance," Department of Informatics and Mathematical Modeling, Technical University of Denmark, Tech. Rep., 2012.

[11] S. E. Shafiei, H. Rasmussen, and J. Stoustrup, "Modeling supermarket refrigeration systems for supervisory control in smart grid," in *Proceedings of the American Control Conference*, Washington DC, USA, Jun. 2013, pp. 5660–5665.

[12] C. Pérez-Segarra, J. Rigola, M. Sòria, and A. Oliva, "Detailed thermodynamic characterization of hermetic reciprocating compressors," *International Journal of Refrigeration*, vol. 28, pp. 579–593, 2005.

[13] R. Zhou, T. Zhang, J. Catano, J. T. Wen, G. J. Michna, Y. Peles, and M. K. Jensen, "The steady-state modeling and optimization of a refrigeration system for high heat flux removal," *Applied Thermal Engineering*, vol. 30, pp. 2347–2356, 2010.

[14] G. Franklin, J. Powell, and M. Workman, *Digital Control of Dynamic Systems*. Ellis-Kagle Press, 1998.

[15] "Nord pool spot," http://www.nordpoolspot.com.

[16] I. CVX Research, "CVX: Matlab software for disciplined convex programming, version 2.0 beta," http://cvxr.com/cvx, Sep. 2012.

[17] M. Grant and S. Boyd, "Graph implementations for nonsmooth convex programs," in *Recent Advances in Learning and Control*, ser. Lecture Notes in Control and Information Sciences, V. Blondel, S. Boyd, and H. Kimura, Eds. Springer-Verlag Limited, 2008, pp. 95–110, http://stanford.edu/~boyd/graph_dcp.html.

Paper D

A Decentralized Control Method for Direct Smart Grid Control of Refrigeration Systems

Seyed Ehsan Shafiei, Roozbeh Izadi-Zamanabadi, Henrik Rasmussen and Jakob Stoustrup

This paper was published in:
The Proceedings of the 52nd IEEE Conference in Decision and Control,
December 2013

Abstract

A decentralized control method is proposed to govern the electrical power consumption of supermarket refrigeration systems (SRS) for demand-side management in the smart grid. The control structure is designed in a supervisory level to provide desired set-points for distributed level controllers. No model information is required in this method. The temperature limits/constraints are respected. A novel adaptive saturation filter is also proposed to increase the system flexibility in storing and delivering the energy. The proposed control strategy is applied to a simulation benchmark that fairly simulates the CO_2 booster system of a supermarket refrigeration.

1 Introduction

The growing demand for electrical energy and the increasing utilization of renewable energy sources create significant challenges for the power grid to provide a stable and sustainable supply of electricity. As part of the smart grid solutions, the consumption of electricity should be actively managed as well as the generation.

Demand response (DR) is a component of smart energy demand for managing costumer consumption of electricity. One strategy for DR implementation is real-time pricing [1] in which the load level of a consumer is optimized in response to electricity prices. Another strategy (considered for this study) is to directly manage the energy consumption of consumers. Implementation of such strategy requires at least two levels of design [2]: a higher level to dispatch the energy/power demand to consumers, and a lower level control design specific for each autonomous consumer providing balancing services. The latter is the focus of this paper.

Industrial refrigeration systems have been proven to be highly potential consumers for DR implementations [3]. Utilizing full DR potential of such consumers requires development of advanced control methods like model predictive control (MPC) [4]. Different MPC schemes have been proposed to minimize the cost of operation of refrigeration systems in smart grid. An economic-optimizing MPC scheme has been proposed by [5], where the objective function is formulated for cost minimization as well as peak load reduction. A complex nonlinear solver is employed and the local display case controllers are replaced by a centralized MPC. In [6] a MPC scheme has been designed in a supervisory control level. Two sets of set-point (*i.e.,* pressure for suction manifold and temperatures for display cases) are separately calculated in different control loops and assigned to the distributed local controllers. A direct control implementation for multiple units of single vapor-compression cycle systems has been presented in [7]. An energy storage model is proposed and utilized by a predictive controller for implementation. The main reasons that MPC is widely used in such application are its mightiness at controlling multi-variable systems subject to constraints, and at incorporation of the model prediction in an optimal control problem.

Implementation of model-based controllers like MPC for supermarket refrigeration systems requires developing a high fidelity model which is itself a nontrivial and expensive procedure; especially considering the fact that the system dimension and configuration vary from one supermarket to another. Moreover, utilization of an optimizing controller for large-scale systems highly increases the complexity regarding the practical

implementations. Nevertheless, the model-based controls are still valuable methods for investigating the full potential of demand response implementations.

In this paper, we propose a simple but efficient supervisory control structure including P and PI controllers that can enable balancing services of SRSs in smart grid. The heuristic algorithm proposed in [6] for the pressure set-point control is replaced by a proportional controller, and an *agility factor* is also introduced. Like [6], the supervisory controller (which is now simply a PI) assigns set-points to the air temperatures inside the cooling sites. No model information is required for the control implementation. The food temperatures should be constrained within the permissible limits. So we put a saturation filter at the control output that restricts the air temperature and consequently the food temperature. To handle windup problem due to the saturation filter, a decentralized structure equipped with anti-windup features is designed. In contrast to the MPC schemes, the model free controller cannot predict the future temperatures of the air and of the foodstuffs. So, to ensure the food safety, the same limits for the food temperatures should be considered for saturation limits applying to the air temperature. This however limits the range of control effort, and consequently decreases the control system flexibility in governing the power consumption. We have proposed an *adaptive saturation filter* that can effectively remove this restriction, yet respecting the food temperatures.

2 System Description and Problem Statement

In this section, we briefly explain a CO_2 booster configuration of a typical supermarket refrigeration system. Subsequently, the thermodynamics involving the cooling sites are introduced, and finally, the control problem is stated.

CO_2 Booster Refrigeration System

A basic layout of a typical refrigeration system including several display cases and freezing rooms with two compressor banks in a booster configuration is shown in Fig. 9.1. Starting from the receiver (REC), two-phase refrigerant (mix of liquid and vapor) at point '8' is split out into saturated liquid ('1') and saturated gas ('1b'). The latter is bypassed by a bypass valve (BPV), and the former flows into expansion valves where the refrigerant pressure drops to medium ('2') and low ('2′') pressures. The expansion valves EV_MT and EV_LT are responsible for regulating the air temperature inside the medium temperature (MT) and the low temperature (LT) cooling sites, respectively, by controlling the entering mass flow into the evaporators. Flowing through medium and low temperature evaporators (EVAP_MT and EVAP_LT), the refrigerant absorbs heat from the cold reservoir. The pressure of low temperature units (LT) is increased by the low stage compressor rack (COMP_LO). All mass flows from COMP_LO, EVAP_MT and BPV outlets are collected by a suction manifold at point '5' where the pressure is increased again by high stage compressors (COMP_HI). Afterward, the gas phase refrigerant enters the condenser to deliver the absorbed heat from cold reservoirs to the surrounding. The detailed thermodynamic analysis of such systems is described in [8].

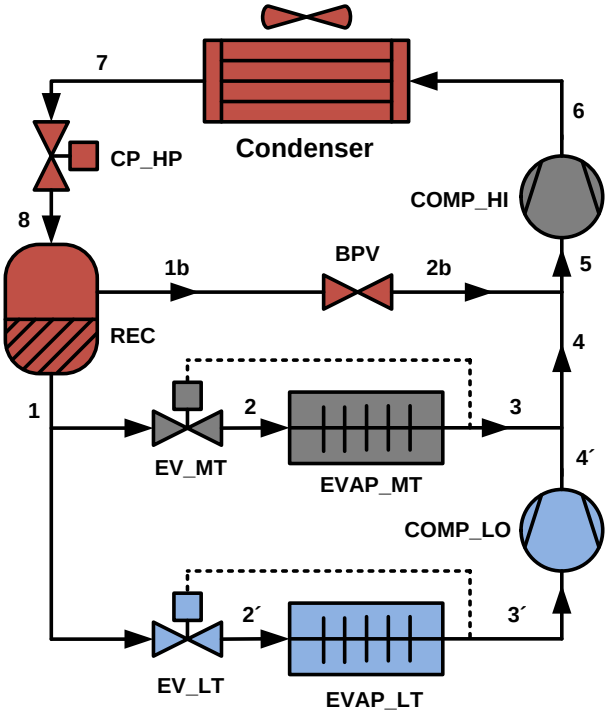

Figure 7.1: Basic layout of a typical supermarket refrigeration system with booster configuration.

Cooling Unit Dynamics

The purpose of this subsection is to introduce the dynamical equations describing the thermodynamic processes involve the system. However, the model information are not used for the control design. The detailed modeling for such control applications have been explained in [9].

In the cold units (display cases and freezing rooms), heat is transfered from foodstuffs to cooled air, $\dot{Q}_{foods/air}$, and then from cooled air to circulated refrigerant, $\dot{Q}_e$, which the latter is also known as cooling capacity. There is however heat load from supermarket indoor, $\dot{Q}_{load}$, formulated as a variable disturbance. Here, we consider the measured air temperature entering the evaporator area as the cold unit temperature, T_{air}. Assuming a lumped temperature model, the following dynamical equations are derived based on energy balances for the mentioned heat transfers.

$$MCp_{foods}\frac{dT_{foods}}{dt} = -\dot{Q}_{foods/air} \tag{7.1}$$

$$MCp_{air}\frac{dT_{air}}{dt} = \dot{Q}_{load} + \dot{Q}_{foods/air} - \dot{Q}_e \tag{7.2}$$

where MCp denotes the corresponding mass multiplied by the heat capacity. The energy

flows are

$$\dot{Q}_{foods/air} = UA_{foods/air}(T_{foods} - T_{air}), \tag{7.3}$$

$$\dot{Q}_{load} = UA_{load}(T_{indoor} - T_{air}), \tag{7.4}$$

and

$$\dot{Q}_e = UA_e(T_{air} - T_e) \tag{7.5}$$

where UA is the overall heat transfer coefficient, T_e is the evaporation temperature, and T_{indoor} is the supermarket indoor temperature. The heat transfer coefficient between the refrigerant and the display case temperature, UA_e, is described as a linear function of the mass of the liquefied refrigerant in the evaporator [10],

$$UA_e = k_m M_r, \tag{7.6}$$

where k_m is a constant parameter. The refrigerant mass, $0 \leq M_r \leq M_{r,max}$, is subject to the following dynamic [11],

$$\frac{dM_r}{dt} = \dot{m}_{r,in} - \dot{m}_{r,out}, \tag{7.7}$$

where $\dot{m}_{r,in}$ and $\dot{m}_{r,out}$ are the mass flow rate of refrigerant into and out of the evaporator, respectively. The entering mass flow is determined by the opening degree of the expansion valve and is described by the following equation:

$$\dot{m}_{r,in} = OD\ KvA\sqrt{2\rho_{suc}(P_{rec} - P_e)} \tag{7.8}$$

where OD is the opening degree of the valve with a value between 0 (closed) to 1 (fully opened), P_{rec} and P_e are receiver and suction manifold (evaporating) pressures, ρ_{suc} is the density of the circulating refrigerant, and KvA denotes a constant characterizing the valve. The leaving mass flow is given by

$$\dot{m}_{r,out} = \frac{\dot{Q}_e}{\Delta h_{lg}} \tag{7.9}$$

where Δh_{lg} is the specific latent heat of the refrigerant in the evaporator, which is a non-linear function of the suction pressure. When the mass of refrigerant in the evaporator reaches its maximum value ($M_{r,max}$), the entering mass flow is equal to the leaving one.

Problem Statement

In framework of the direct smart grid control, the SRS is supposed to follow a power reference assigned by the aggregator. Here the problem is to design a control structure enabling the SRS to regulate its electrical power consumption by storing and delivering energy into and out from the existing thermal masses in cooling sites.

The practical issues are, first, we do not use any model information in our control practice, and second, we do not replace the existing local distributed controllers in the system.

3 Design of Control Structure

In order to keep the local distributed controllers at their places, the smart grid control scheme should be implemented in a supervisory level with an outer control loop including the closed-loop system. There are two sets of control variables to which the supervisory controllers can assign set-points: the suction pressure, and the air temperatures circulating inside the cooling sites.

Pressure Set-Point Control

The coupling variable between the cooling units is the suction pressure. If it was possible to assign the pressure set-points disregarding the cooling air temperatures, then we could apply the temperature set-point to each unit decoupled from the other ones. A simple minded method is to assign a constant pressure set-point that is low enough to support the cooling capacity required for low temperatures. But this will increase the power consumption in a normal operation.

A near optimal algorithm was designed in [6] by which the pressure set-point is changed such that always one of the expansion valve is kept fully opened. Here we apply such optimality by designing a simple proportional controller with saturation limits (to respect the pressure constraints). In order to prevent a large proportional gain and consequently a large variation of the set-point, the control command is considered as the change of set-point,

$$\Delta P_{ref} = K_p\left(r_{OD} - \overline{OD}_{max}\right) \tag{7.10}$$

where K_p is the proportional gain, $\overline{OD}$ is the vector of opening degree of the valves, and $\overline{OD}_{max}$ corresponds to the maximum element of it. $r_{OD} = 1 - \varepsilon$ is the maximum value that the fully open valve should follow. It should be a little bit smaller than 1, because the optimality hypothesis is to keep only one valve fully opened.

Remark 1*: The larger* ε*, the larger gain is applied while decreasing the pressure. This can increase the flexibility considering the rate of change of the temperatures. So that* ε *is called* agility factor*. It means when the system is demanded to store energy by decreasing the cooling site temperatures, it can respond more agile with a larger* ε*. On the other hand, the optimal condition corresponds to* $\varepsilon = 0$*. So there is a* trade-off *between the flexibility and the optimality.*

The control command (7.10) is then added to the pressure feedback to form the applied set-point,

$$P_{ref} = \Delta P_{ref} + P_e. \tag{7.11}$$

In order to respect the pressure limits, this set-point is passed through a saturation filter before applying to the system. The saturation filter is given by the following relation.

$$\mathrm{sat}(u) = \begin{cases} u_{max} & u \geq u_{max} \\ u & u_{min} < u < u_{max} \\ u_{min} & u \leq u_{min} \end{cases} \tag{7.12}$$

Fig. 7.2 shows the designed structure for set-point control of the suction pressure.

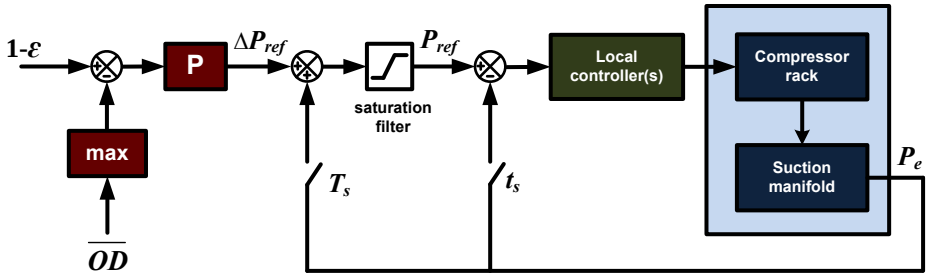

Figure 7.2: Control structure for set-point control of the suction pressure. The local controllers use a very shorter sampling period (t_s) than of the supervisory P controller (T_s).

Remark 2: *The local controller in Fig. 7.2 regulates the suction pressure to the assigned reference within the operating range. There are also superheat controllers governing the valve opening degrees to ensure the refrigerants exiting the evaporators are completely vaporized. The saturation filter is imposed to guarantee that the pressure set-point does not exceed the range of operations of the local pressure controller as well as the distributed superheat controllers. Therefor, the transfer function from P_{ref} to P_e describes a stable close loop system. In practice, the settling time of the inner closed loop system is less than one minute. So, by considering the sampling time larger than one minute for the outer supervisory loop, and assuming a perfect regulation, the transfer function of the inner closed loop system would be a unit delay which means $P_e[k] = P_{ref}[k-1]$.*

Temperature Set-Point Control

This section proposes a supervisory control structure for set-point control of the air temperatures of the cooling sites. The main idea is to regulate the electrical power consumption of the compressors by changing these temperature set-points. So that in case of increasing the power above the base-line — decided by the aggregator — the control system starts storing energy in cooling sites, and vice versa.

Fig. 7.3 illustrates the designed control structure. Because of the food safety, there are strict limits on variation range of the food temperatures. The local controllers operating on the valves control the air temperature inside the cold storages (see (7.1)). Since the food temperature (due to a higher heat capacity) cannot vary larger than the air temperature, applying the same limits on the air temperatures can guarantee the limits on the food temperatures as well (see (7.2)). The constraints are applied by putting the saturation filters with the following saturation bounds at the output of the ith PI controller.

$$\overline{U}_i = (\overline{T}_i - T_{0,i}), \tag{7.13}$$

and

$$\underline{U}_i = (\underline{T}_i - T_{0,i}), \tag{7.14}$$

where $\overline{T}$ and $\underline{T}$ are respectively the upper and lower limits of the food temperature, and T_0 is the fixed set-point for normal operation (that is when the system is not under the direct control feedback loop).

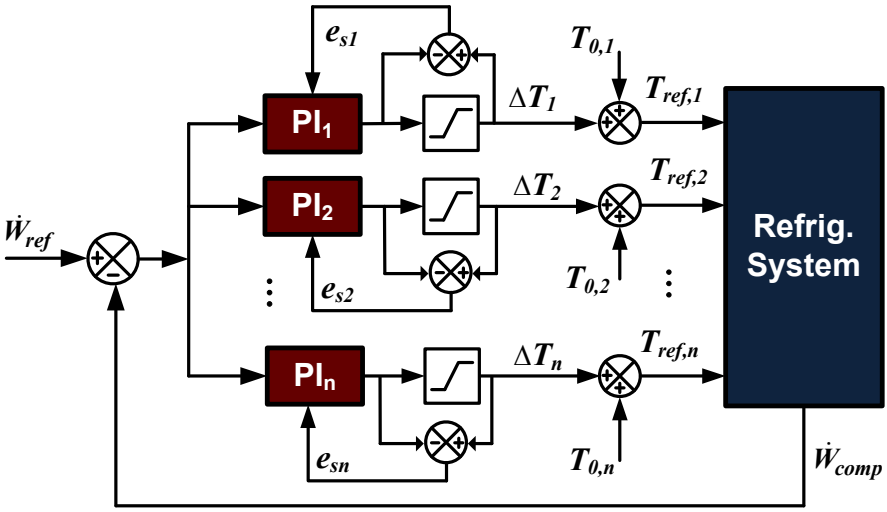

Figure 7.3: Control structure for set-point control of the air temperatures in cooling sites.

The supervisory controllers apply the set-point change ΔT_i to each unit. Then this control command is added to a fixed set-points $T_{0,i}$ to form the temperature reference ($T_{ref,i}$) for the *i*th unit.

$$T_{ref,i} = \Delta T_i + T_{0,i} \tag{7.15}$$

The advantages of designing decentralized structure for supervisory PIs instead of designing a single PI with distributed weighting factors (gains) are explained as follows. The first reason is that this structure leaves two degrees of freedom in designing the controller for each cooling site. This can however facilitate the future investigations to find the optimum controller parameters. The second and the most important reason is that because of the saturation filters, the integral term will windup once the control effort reaches the limits. The anti-windup feature can be easily supported by this decentralization.

The error feedbacks $e_{s,i}$ go to the PI controllers in Fig. 7.3 are required for the anti-windup design as explained in [12]. A sample PI unit including the anti-windup feature is shown in Fig. 7.4.

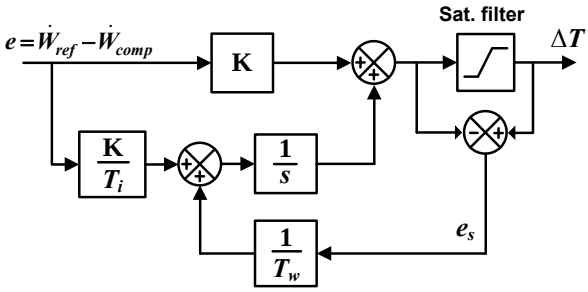

Figure 7.4: PI controller with anti-windup.

Putting as the same constraints on the air temperatures as the food temperatures cuts down the demand response ability of the system from the speed of response point of view. In model-based designs like MPC, this can be easily handled by just putting the constraints on the food temperatures that is honored by the prediction of the future states/outputs. In case of lack of the model, there is no specific solution for such problems. The next section proposes a novel method that can deal with the problem by replacing the fixed saturation filters by adaptive ones.

Adaptive Saturation Filter

In the proposed adaptive saturation filter, the saturation limits are adaptively updated based on the current value of the food temperature. Each PI unit in the control structure of Fig. 7.3 should be updated to the one shown in Fig. 7.5.

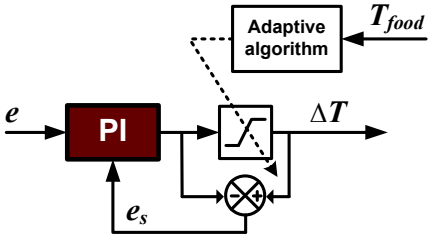

Figure 7.5: PI controller with anti-windup and adaptive saturation filter.

The adaptive algorithm for updating the saturation limits is described by

$$u_{max,i}(t) = \overline{U}_i + K_{u,i}(\overline{T}_i - T_{foods,i}(t)), \tag{7.16}$$

and

$$u_{min,i}(t) = \underline{U}_i + K_{l,i}(\underline{T}_i - T_{foods,i}(t)), \tag{7.17}$$

where $K_{u,i}$ and $K_{l,i}$ are constant parameters defined as *saturation limit gains*. The right-hand side of the above equations are the adaptive terms added to (7.13) and (7.14). For the rest of this section we discuss some features of the designed filter considering (7.16); the similar discussion can be also made for the case of (7.17). For example consider the case that the food temperature is below of its maximum limit ($T_{foods,i} < \overline{T}_i$) and we want to increase it to deliver the storage. At this time, depending on the saturation limit gains, a higher saturation limit is applied by the filter that lets the air temperature goes to a higher level. The higher air temperature ($T_{air} > T_{foods}$), the higher absolute value of $\dot{Q}_{foods/air}$ is applied to (7.2) that can govern the food temperature more effectively. While T_{foods} approaching its limit, the saturation limit decreases until once the food temperature touches the limit, the adaptive term in (7.16) will disappear.

Remark 3: The adaptive saturation filter can compensate the disturbance effect more efficient than the fixed parameter filter. In case of violation of the upper temperature limit due to a large disturbance, the adaptive term in (7.16) becomes negative that makes the saturation limit tighter than of (7.13). It means that a larger input gain is applied to the food temperature dynamics in the opposite direction of the disturbance effect.

Remark 4: The value of the saturation limit gains (K_u or K_l) can be specified by considering the rate of change of the food temperature. Taking the first derivative of (7.16) gives

$$\frac{du_{max,i}}{dt} = -K_{u,i}\frac{dT_{foods,i}}{dt}. \tag{7.18}$$

So, for instance if $K_u = 1$, the saturation limit changes with the same rate of the food temperature.

4 Simulation Results

In this section, the proposed method is applied to a supermarket refrigeration system including 7 MT display cases and 4 LT freezing storages [9, 13]. Each cooling unit is equipped with a local PI controller regulating the air temperature inside the unit to the assigned set-point.

Normal Operation

In normal operation the system is not in the closed-loop smart grid control. The temperature limits for food safeties are $\overline{T} = 3.5$ °C and $\underline{T} = 0.5$ °C for the MT sites, and $\overline{T} = -19$ °C and $\underline{T} = -25$ °C for the LT sites. The temperature set-points are set fixed to the upper limits to minimize the energy consumption.

Fixed pressure set-point

The suction pressure set-point is set to $P_{ref} = 24$ bar that can provide the pressure low enough to cool the air temperature down to the lower limit in case of necessity. Total electrical power consumption of the compressor racks with this set-up are shown in Fig. 7.6a with dotted line.

Pressure set-point control

At this step we apply the pressure set-point control using (7.10) and (7.11). The pressure limits are $\underline{P}_e = 20$ bar and $\overline{P}_e = 31$ bar. The proportional gain and the agility factor are set to $K_p = 5$ and $\varepsilon = 0.1$, respectively. As can be seen from Fig. 7.6a, the base-line of the power consumption in normal operation is decreased by applying the pressure control method. The suction pressure is also shown in Fig. 7.6b.

In a period of 24 hours, the power reference scenario is such that the aggregator demands the base-line power consumption until 5:00 AM. Following that, it demands an increase up to 20% over the base-line for 5:00-15:00, and a reduction down to 20% below the base-line for 15:00-20:00. Finally the reference gets back to the base-line for 20:00-24:00 to be ready for demand response for the next day. In the sequel, different responses by different controls are compared and the results are shown in a single plot.

Centralized Control

The centralized control has the same feedback structure as Fig. 7.3 but includes only one centralized PI controller. The controller gain and integration time are $K = 0.1$ and $T_i = 30$ for both MT and LT units. The result is shown in Fig. 7.7 where the response to this control is depicted by dotted line. During the the increase period, saturation limits are not

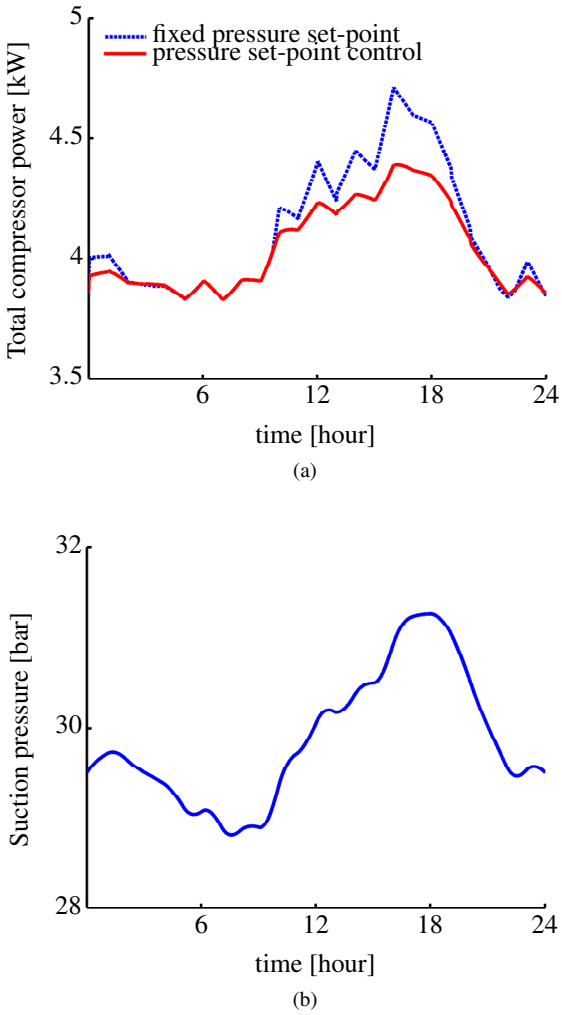

Figure 7.6: Simulation results for normal operation. (a) The base-line of the electrical power consumptions of the compressor racks gets lower by applying the proposed pressure set-point control method. (b) The suction pressure after applying the control method.

reached, so the controller can fairly increase the power. But it cannot decrease the power enough during the reduction demand because of activation of the saturation limits. After the reduction period, because of the integrator windup the centralized controller is also not able to regulate the power back to the base-line.

Decentralized Control

In order to have a fair comparison, the same gain and integration time as the centralized control are considered for each decentralized PI controller. The anti-windup gain [12]

is $T_w = 0.5T_i$. Now the controller can regulate the power back to the base-line after the reduction period where the saturation limits were activated.

Adaptive Saturation Filter

Fig. 7.8 shows the air and food temperatures of one of the LT display cases after applying the adaptive saturation filter. The trends are similar for the other cooling sites. The adaptive saturation filter lets the air temperature goes above the limit and while the food temperature is getting close to it, the air temperature is decreased adaptively. So the food temperature limits are not violated using this method. As a result, the power consumption can be decreased effectively during the reduction period as illustrated in Fig. 7.7. This result shows the superiority of the proposed method in delivering the stored energy. The same argument is also valid in case of storing energy when a higher increase of power is demanded that can lead to activation of the lower saturation limits for the temperature set-points.

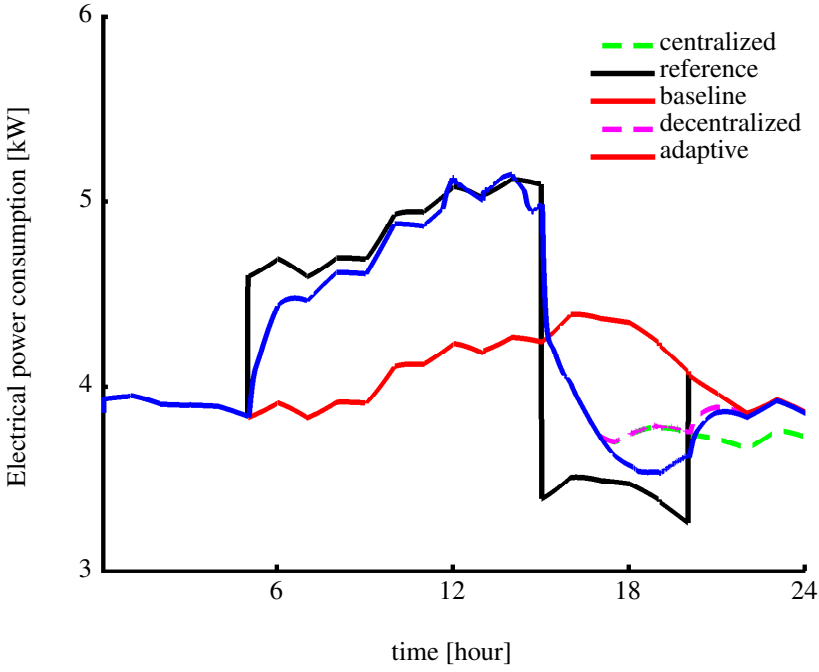

Figure 7.7: Electrical power consumption of the compressor racks in case of centralized control (dotted), decentralized control (dashed), and decentralized control with adaptive saturation filter (solid).

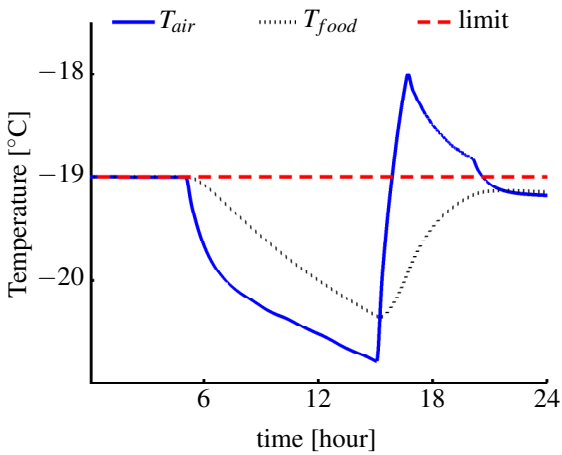

Figure 7.8: The air and food temperatures for one of the LT display cases. The trends are similar for the other display cases.

5 Discussions

It should be noted that our purpose here is not a perfect power following control. The perfect power reference tracking can be obtained by directly controlling the compressor speeds. But it does not necessarily mean that we are storing energy in display cases during the increase period. On the other hand, just turning off the compressors during the reduction period can make problems in the high pressure CO_2 systems. By applying the mentioned power reference we could analyze the control response in case of a likely upward and downward power demands.

The LT cooling sites due to better isolations and consequently less disturbance loads are better candidate to be employed in the balancing services than the MT sites. Because of the booster configuration (Fig. 9.1) the low stage compressors corresponding to LT units have a lower capacity than the higher stage compressors. By applying the same control gain to both LT and MT units (as we did here) the low stage compressors are more excited than of the higher stage that means the LT units will be more involved in the balancing services that is a desired objective.

The optimal gains for the proposed controllers can be obtained using an accurate model, or by designing some data-driven experiments to tune the gains. Addressing this issue is however out of the scope of the current paper. Heuristically, the display cases with larger existing thermal masses and better isolations should be assigned more gains for their decentralized controllers.

6 Conclusion

A new control structure including P and PI controllers for direct control of refrigeration systems in smart grid was proposed. No model information is required for the control implementation. The control was designed in a supervisory level to provide desired set-

points to the local distributed controllers. Two different control loops were designed for decoupling the pressure set-point control from the temperature set-point control. In order to respect the temperature constraints, and at the same time avoiding windup problem, a decentralized control method was proposed. A new adaptive scheme for the saturation filter was designed to utilize the most potential of energy storages in the cooling sites. This is a new control structure for this specific application that leaves the possibility of further improvements and developments for the future works.

References

[1] A. J. Conejo, J. M. Morales, and L. Barino, "Real-time demand response model," *IEEE Transactions on Smart Grid*, vol. 1, no. 3, pp. 236–242, 2010.

[2] K. Trangbaek, J. D. Bendtsen, and J. Stoustrup, "Hierarchical control for smart grids," in *Proceedings of the 18th IFAC World Congress*. Milan, Italy: IFAC, Aug. 2011.

[3] S. Goli, A. McKane, and D. Olsen, "Demand response opportunities in industrial refrigerated warehouses in california," in *2011 ACEEE Summer Study on Energy Efficiency in Industry*, Niagara Falls, NY, USA, Jul. 2011.

[4] T. G. Hovgaard, L. F. S. Larsen, K. Edlund, and J. B. Jrgensen, "Model predictive control technologies for efficient and flexible power consumption in refrigeration systems," *Energy*, vol. 44, pp. 105–116, 2012.

[5] T. G. Hovgaard, L. F. S. Larsen, and J. B. Jrgensen, "Flexible and cost efficient power consumption using economic mpc: A supermarket refrigeration benchmark," in *50th IEEE Conference on Decision and Control and European Control Conference*, Orlando, Florida, USA, Dec. 2011.

[6] S. E. Shafiei, J. Stoustrup, and H. Rasmussen, "A supervisory control approach in economic MPC design for refrigeration systems," in *Proceedings of the European Control Conference*, Zürich, Switzerland, Jul. 2013, pp. 1565–1570.

[7] R. Pedersen, J. Schwensen, S. Sivabalan, C. Corazzol, S. E. Shafiei, K. Vinther, and J. Stoustrup, "Direct control implementation of a refrigeration system in smart grid," in *Proceedings of the American Control Conference*, Washington DC, USA, Jun. 2013, pp. 3954–3959.

[8] Y. T. Ge and S. A. Tassou, "Thermodynamic analysis of transcritical CO_2 booster refrigeration systems in supermarket," *Energy Conversion and Management*, vol. 52, pp. 1868–1875, 2011.

[9] S. E. Shafiei, H. Rasmussen, and J. Stoustrup, "Modeling supermarket refrigeration systems for demand-side management," *Energies*, vol. 6, no. 2, pp. 900–920, 2013.

[10] D. Sarabia, F. Capraro, L. F. S. Larsen, and C. Prada, "Hybrid NMPC of supermarket display cases," *Control Engineering Practice*, vol. 17, pp. 428–441, 2009.

[11] L. N. Petersen, H. Madsen, and C. Heerup, "ESO2 optimization of supermarket refrigeration systems: Mixed integer MPC and system performance," Department of Informatics and Mathematical Modeling, Technical University of Denmark, Tech. Rep., 2012.

[12] K. J. Åström and T. Hägglund, *Advanced Pid Control*. ISA-The Instrumentation, Systems, and Automation Society, 2006.

[13] SRSim, "A simulation benchmark for supermarket refrigeration systems using matlab," http://www.es.aau.dk/projects/refrigeration/simulation-tools/, Feb. 2013, accessed: February 2015.

Paper E

Model Predictive Control for Flexible Power Consumption of Large-Scale Refrigeration Systems

Seyed Ehsan Shafiei, Jakob Stoustrup and Henrik Rasmussen

This paper was published in:
The Proceedings of the American Control Conference, June 2014

The layout has been revised

Abstract

A model predictive control (MPC) scheme is introduced to directly control the electrical power consumption of large-scale refrigeration systems. Deviation from the baseline of the consumption is corresponded to the storing and delivering of thermal energy. By virtue of such correspondence, the control method can be employed for regulating power services in the smart grid. The proposed scheme contains the control of cooling capacity as well as optimizing the efficiency factor of the system, which is in general a nonconvex optimization problem. By introducing a fictitious manipulated variable, and novel incorporation of the evaporation temperature set-point into optimization problem, the convex optimization problem is formulated within the MPC scheme. The method is applied to a simulation benchmark of large-scale refrigeration systems including several medium and low temperature cold reservoirs.

1 Introduction

The structure of power systems, especially in Europe, is changing from a centralized one to a decentralized one due to distributed generation with high penetration of renewable sources. This change leads to several new challenges that can be handled in a smart grid, where both production and consumption of electricity are managed efficiently. To achieve such efficient demand-side management, consumers should be equipped with control systems that can actively respond to the grid requirements.

Demand response (DR) is a component of smart energy demand for managing costumer consumption of electricity. One strategy for DR implementation is real-time pricing [1] in which the load level of a consumer is optimized in response to electricity prices. Another strategy (considered for this study) is to directly manage the energy consumption of consumers. Implementation of such strategy requires at least two levels of design [2]: a higher level to dispatch the energy/power demand to consumers, and a lower level control design specific for each autonomous consumer providing balancing services. The latter is the focus of this paper.

A typology of ancillary services was identified by [3], where different services like continuous regulation, energy imbalance management, instantaneous contingency reserves, replacement reserves, voltage control and black start were investigated. Based on this typology, the present method facilitates the energy imbalance management services for large-scale refrigeration systems. Regarding the power grid balancing services, the potential of corresponding demand response activities was investigated by [4] for heating, ventilation and refrigeration systems. Considering the refrigeration systems, the associated demand response opportunities were reported in [5].

By means of flexible power consumption, the refrigeration system is supposed to consume at the baseline of its power consumption profile during the normal operation, increase the consumption for downward regulation, and decrease it for upward regulation services in favor of the power grid. The thermal capacity of refrigerated goods are employed for storing and delivering of thermal energy. In the present work, it is assumed that a power reference signal is provided by an aggregator to be followed.

One important challenge of control design for multiple evaporator refrigeration systems is coming from the fact that different cooling units have the same evaporation temperature while providing different cooling capacities. The power/energy management

is performed by controlling the individual cooling capacities each depends on the same evaporation temperature as others. Finding optimal cooling capacities as well as optimal evaporation temperature is in general a nonconvex optimization problem. This problem is addressed in [6] using nonconvex model predictive control in a real-time pricing market. In [7], the evaporation temperature is controlled in a separated loop while a supervisory MPC is proposed for energy cost optimization.

Another difficulty arises from the existence of nonlinear dynamics — caused by the fluid dynamics inside the evaporator — between the expansion valve and the actual cooling capacity. In the relevant works presented in [6] and [8], the cooling capacity is taken as control variable that simplifies the dynamic model, but the problem is that it cannot be applied as a control signal to the system.

It is shown in the present paper that by virtue of the faster dynamics of the flow change inside the evaporator comparing to the thermal dynamics, it is possible to describe the cooling capacity by static nonlinearity in terms of the valve opening degree and the evaporation temperature. It is simply achieved by choosing an appropriate sampling time for the MPC. At this point, the model would look like a Hammerstein model. Then, by taking the cooling capacity as fictitious manipulated variable, a model predictive control is formulated using a novel incorporation of the evaporation temperature into the optimization problem. It leads to a higher system coefficient of performance (COP). The proposed method is applied to a simulation benchmark of large-scale refrigeration systems including several medium and low temperature cold reservoirs with a booster configuration of two racks of compressors.

2 System Description and Problem Statement

In this section, configuration and model of a typical supermarket refrigeration system is described.

CO_2 Booster Refrigeration System

A basic layout of a typical refrigeration system including several cooling units with two racks of compressors in a booster configuration is shown in Fig. 9.1. Starting from the receiver (REC), two-phase refrigerant (mix of liquid and vapor) at point ‘8’ is split out into saturated liquid (‘1’) and saturated gas (‘1b’). The latter is bypassed by a bypass valve (BPV), and the former flows into expansion valves where the refrigerant pressure drops to medium (‘2’) and low (‘2′’) pressures. The electronic expansion valves EV_MT and EV_LT are responsible for regulating the air temperature inside the medium temperature (MT) and the low temperature (LT) cooling units, respectively, by controlling the entering mass flows into the evaporators. Flowing through medium and low temperature evaporators (EVAP_MT and EVAP_LT), the refrigerant absorbs heat from the cold reservoir. The pressure of low temperature units (LT) is increased by the low stage compressor rack (COMP_LO). All mass flows from COMP_LO, EVAP_MT and BPV outlets are collected by a suction manifold at point ‘5’ where the pressure is increased again by high stage compressors (COMP_HI). Afterward, the gas phase refrigerant enters the condenser to deliver the absorbed heat from cold reservoirs to the surrounding. The receiver pressure is regulated by the high pressure valve CP_HP. The detailed thermodynamic analysis of such systems is described in [9].

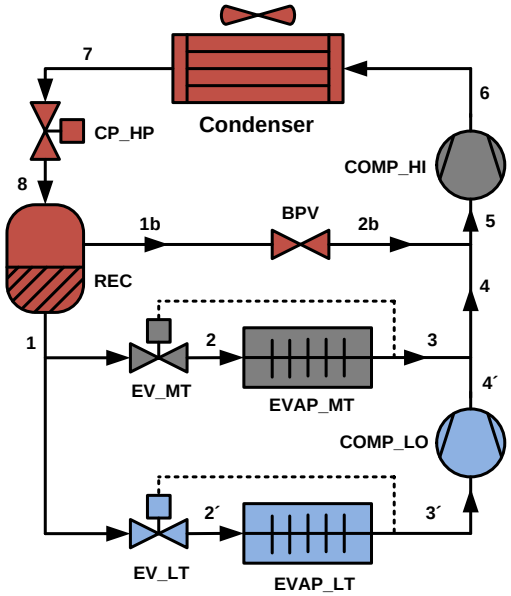

Figure 8.1: Basic layout of a typical supermarket refrigeration system with booster configuration.

Cooling Unit Dynamics

In the cooling units, heat is transfered from foodstuffs to cooled air, $\dot{Q}_{foods/air}$, and then from cooled air to circulated refrigerant, $\dot{Q}_e$, which the latter is also known as cooling capacity. There is however heat load from supermarket indoor, $\dot{Q}_{load}$, formulated as a variable disturbance. Here, we consider the measured air temperature entering the evaporator area as the cold unit temperature, T_{air}. Using lumped modeling approach [10], the following dynamical equations are derived based on energy balances for the mentioned heat transfers.

$$MCp_{foods}\frac{dT_{foods}}{dt} = -\dot{Q}_{foods/air} \tag{8.1}$$

$$MCp_{air}\frac{dT_{air}}{dt} = \dot{Q}_{load} + \dot{Q}_{foods/air} - \dot{Q}_e \tag{8.2}$$

where MCp denotes the corresponding mass multiplied by the heat capacity. The energy flows are

$$\dot{Q}_{foods/air} = UA_{foods/air}(T_{foods} - T_{air}), \tag{8.3}$$

$$\dot{Q}_{load} = UA_{load}(T_{indoor} - T_{air}), \tag{8.4}$$

and

$$\dot{Q}_e = UA_e(T_{air} - T_e) \tag{8.5}$$

where UA is the overall heat transfer coefficient, T_e is the evaporation temperature, and T_{indoor} is the supermarket indoor temperature. The heat transfer coefficient between the

refrigerant and the display case temperature, UA_e, is described as a linear function of the mass of the liquefied refrigerant in the evaporator [11],

$$UA_e = k_m M_r, \tag{8.6}$$

where k_m is a constant parameter. The refrigerant mass, $0 \le M_r \le M_{r,max}$, is subject to the following dynamic [12],

$$\frac{dM_r}{dt} = \dot{m}_{r,in} - \dot{m}_{r,out}, \tag{8.7}$$

where $\dot{m}_{r,in}$ and $\dot{m}_{r,out}$ are the mass flow rate of refrigerant into and out of the evaporator, respectively. The entering mass flow is determined by the opening degree of the expansion valve and is described by the following equation:

$$\dot{m}_{r,in} = OD\ KvA\sqrt{\rho_{suc}(P_{rec} - P_e)} \tag{8.8}$$

where OD is the opening degree of the valve with a value between 0 (closed) to 1 (fully opened), P_{rec} and P_e are receiver and suction manifold (evaporating) pressures, ρ_{suc} is the density of the circulating refrigerant, and KvA denotes a constant characterizing the valve. The leaving mass flow is given by

$$\dot{m}_{r,out} = \frac{\dot{Q}_e}{\Delta h_{lg}} \tag{8.9}$$

where Δh_{lg} is the specific latent heat of the refrigerant in the evaporator, which is a nonlinear function of the suction pressure (or equivalently evaporation temperature). When the mass of refrigerant in the evaporator reaches its maximum value ($M_{r,max}$), the entering mass flow is equal to the leaving one.

Compressor Power and System COP

The electrical power consumption of each compressor bank is calculated by

$$Pow_c = \frac{1}{\eta_{me}} \dot{m}_{ref}(h_{o,c} - h_{i,c}), \tag{8.10}$$

where $\dot{m}_{ref}$ is the total mass flows into the compressors, and $h_{o,c}$ and $h_{i,c}$ are the enthalpies at the outlet and inlet of the compressor bank and are nonlinear functions of the refrigerant pressure and temperature at the calculation points. The constant η_{me} indicates overall mechanical/electrical efficiency considering mechanical friction losses and electrical motor inefficiencies [13]. The outlet enthalpy is computed by

$$h_{o,c} = h_{i,c} + \frac{1}{\eta_{is}}(h_{is} - h_{i,c}), \tag{8.11}$$

in which h_{is} is the outlet enthalpy when the compression process is isentropic, and η_{is} is the related isentropic efficiency given by [14] (neglecting higher order terms).

$$\eta_{is} = c_0 + c_1(f_c/100) + c_2(P_{c,o}/P_{suc}) \tag{8.12}$$

Where f_c is the virtual compressor frequency (total capacity) of the compressor rack in percentage, $P_{c,o}$ is pressure at the compressor outlet, and c_i are constant coefficients.

The total coefficient of performance is defined as ratio of the total cooling capacity over the total power consumption of the compressors.

$$COP = \frac{\dot{Q}_{e,tot}}{Pow_{c,tot}} \tag{8.13}$$

The COP is calculated by

$$COP = \frac{x_{MT}\Delta h_{lg,MT} + x_{LT}\Delta h_{lg,LT}}{\frac{1}{\eta_{MT}}(h_{oc,MT} - h_{ic,MT}) + \frac{x_{LT}}{\eta_{LT}}(h_{oc,LT} - h_{ic,LT})}, \tag{8.14}$$

where indices MT and LT relate the calculated values to the medium and low temperature sections, respectively. Parameters x_{MT} and x_{LT} are ratio of the refrigerant mass flow of MT and LT evaporators to the total flow rate, and $\eta_{MT} = \eta_{me,MT}\eta_{is,MT}$ and $\eta_{LT} = \eta_{me,LT}\eta_{is,LT}$. The enthalpy terms are nonlinear function of the evaporation temperature (T_e) and/or the condensation pressure (P_c) as $\Delta h_{lg}(T_e)$, $h_{oc}(P_c)$, and $h_{ic}(T_e)$ as well as the corresponding refrigerant temperatures.

Problem Statement

Here the problem is to designing a control algorithm enabling large-scale refrigeration systems to follow the assigned power reference by an aggregator while optimizing the coefficient of performance.

It can be seen from (8.14) and the corresponding dependences of enthalpies that the COP is a function of mass flows coming from evaporators, condensation pressure, and evaporation temperature. The mass flows are dictated by operating conditions of the display cases and controlled by the corresponding expansion devices. We assumed the condenser fan speed is at the maximum level, so the condensation pressure is changed by changing the outdoor temperature. The only remained manipulated variable to change the COP is the evaporation temperature. Therefore, the maximum COP can be achieved by maximizing the evaporation temperature.

3 MPC Formulation

A model predictive control scheme that can address the above problem is formulated in this section. The objective function for power following is defined as:

$$J_{Pow} = \sum_{k=1}^{N} \|Pow_c[k] - Pow_{ref}[k]\|_2^2 \tag{8.15}$$

where Pow_{ref} is the power reference, k denotes the current time instant, and N is the prediction horizon in terms of number of time steps (samples). Manipulated variables are the opening degrees of the expansion valves (OD) and the evaporation temperature set-point ($\hat{T}$).

Looking into system dynamics, it turns out that the power consumption (Pow_c) is the nonlinear function of the evaporation temperature (T_e); and the cooling capacity ($\dot{Q}_e$) is also a nonlinear function of both the evaporation temperature and opening degree of expansion valves (OD). In the following it is shown that how a convex optimization

problem can be formulated by (i) introducing a fictitious manipulated variable; (ii) novel incorporation of T_e into the MPC scheme; and (iii) choosing appropriate sampling time and prediction horizon.

Problem Convexification using Synthetic Input

Considering $\dot{Q}_e$ as fictitious manipulated variable, the indoor temperature (T_{indoor}) as measurable disturbance and the cold reservoir temperatures (T_{air}, T_{food}) as state variables, we can formulate the discrete-time linear dynamics for each cooling unit as follows.

$$x[k+1] = Ax[k] + Bu[k] + B_d d[k] \tag{8.16}$$

where $x = \begin{bmatrix} T_{foods} & T_{air} \end{bmatrix}^T$, $u = \dot{Q}_e$, and $d = T_{indoor}$. The parameters are

$$A = \begin{bmatrix} -\frac{UA_{foods/air}}{MCp_{foods}} & \frac{UA_{foods/air}}{MCp_{foods}} \\ \frac{UA_{foods/air}}{MCp_{air}} & -\frac{UA_{foods/air}+UA_{load}}{MCp_{air}} \end{bmatrix}, \tag{8.17}$$

and

$$B_1 = \begin{bmatrix} 0 \\ \frac{-1}{MCp_{air}} \end{bmatrix}, \quad B_2 = \begin{bmatrix} 0 \\ \frac{UA_{load}}{MCp_{air}} \end{bmatrix}. \tag{8.18}$$

The first state variable is subject to the following constraint due to food safety promise:

$$x_{1,min} \le x_1 \le x_{1,max} \tag{8.19}$$

where $x_{1,min} = T_{foods,min}$ and $x_{1,max} = T_{foods,max}$ are the limitations on the food temperature. The input constraint is given by

$$0 \le u \le u_{max} \tag{8.20}$$

with $u_{max} = UA_{e,max}(T_{air} - T_e)$ where $UA_{e,max} = k_m M_{r,max}$.

Substituting (8.13) into (8.15) and treating $\dot{Q}_{e,tot}$ as the sum of fictitious control inputs give

$$J_{Pow} = \sum_{k=1}^{N} \left\| \frac{\sum_{i=1}^{m} u_i[k]}{COP} - Pow_{ref}[k] \right\|_2^2, \tag{8.21}$$

where COP is calculated using (8.14) at time instant k and kept constant all over the horizon. In order to avoid the oscillation of the control signal, the following cost function is introduced that is a standard approach in MPC formulations.

$$J_{\Delta u} = \sum_{k=1}^{N} \|u[k] - u[k-1]\|_2^2 \tag{8.22}$$

For now, the optimization problem ca be defined as:

$$\begin{aligned} \min_{\mathbf{u}} \quad & J_{pow} + W_{\mathbf{u}} J_{\Delta \mathbf{u}} \\ \text{subject to} \quad & \mathbf{x}[k+1] = \mathbf{A}x[k] + \mathbf{B}u[k] + \mathbf{B}_d d[k] \\ & \mathbf{x}_{1,min} \le \mathbf{x}_1[k] \le \mathbf{x}_{1,max} \\ & 0 \le \mathbf{u}[k] \le \mathbf{u}_{max} \end{aligned} \tag{8.23}$$

where the vector and matrix notations are used to show all cooling dynamics as a large-scale multivariable system, and $W_{\mathbf{u}}$ is a weighting factor.

Note that the solution of the above optimization problem, $\mathbf{u}$, cannot directly be applied as a control input to the system. This is more elaborated in the sequel.

Novel Incorporation of T_e into MPC Scheme

Note that the $\hat{T}_e$ of MT section is different from of LT section, and remind the fact that several cooling units at each section have the same corresponding evaporation temperature. The COP can be kept at the highest point by keeping T_e as high as possible up to the point that enough cooling capacity is provided to cold reservoirs to preserve the required temperatures. This can be achieved by adding the following cost to the objective function.

$$J_{T_e} = \sum_{k=1}^{N} \|\hat{T}_e[k] - T_{e,max}\|_2^2 \tag{8.24}$$

where $T_{e,max}$ is the maximum value that T_e is allowed to reach. Thus the MPC pushes the evaporation temperature up to the highest value. It should also be constrained as $\hat{T}_e \leq T_{e,max}$. Moreover, in order to make sure that the resulted cooling capacity from the optimization problem is coincide with the evaporation temperature, the upper limit of the input constraint (8.20) is modified as

$$u_{max} = UA_{e,max}(x_2 - \hat{T}_e) \tag{8.25}$$

with $x_2 = T_{air}$. Now, the MPC algorithm can be formulated using the following optimization problem with novel incorporation of $\hat{T}_e$.

$$\begin{aligned} \min_{\mathbf{u},\hat{T}_e} \quad & J_{pow} + W_{\mathbf{u}} J_{\Delta\mathbf{u}} + W_e J_{T_e} \\ \text{subject to} \quad & \mathbf{x}[k+1] = \mathbf{A}x[k] + \mathbf{B}u[k] + \mathbf{B}_d d[k] \\ & \mathbf{x}_{1,min} \leq \mathbf{x}_1[k] \leq \mathbf{x}_{1,max} \\ & 0 \leq \mathbf{u}[k] \leq \mathbf{U}A_{e,max}(\mathbf{x}_2 - \hat{T}_e) \\ & \hat{T}_e \leq T_{e,max} \end{aligned} \tag{8.26}$$

where W_e is the weighting factor for compromising between the evaporation temperature and the other terms in the objective function.

Remark 5: Choosing a small value for W_e may result in a lower T_e (larger distance to $T_{e,max}$) which is equivalent to a smaller COP value. Choosing a large value for W_e, on the other hand, leads to a higher $\hat{T}_e$ and consequently a better COP, but a smaller constraint set for the decision variable (cooling capacity). So it curtails the flexibility in controlling the power consumption. Thus, depending on the DR services that the refrigeration system would provide, W_e compromises between the flexibility of power consumption control and optimality of COP.

Remark 6: The direct physical relationship between $\dot{Q}_e$ and T_e is not included in the optimization problem. In lieu, to make sure that the resulted $\dot{Q}_e$ is feasible to achieve at the concluded T_e, its constraint set is manipulated by $\hat{T}_e$ as another decision variable in (8.26).

Control Inputs

As pointed out in Section 3, the cooling capacity ($u = \dot{Q}_e$) resulted from the optimization problem is not an actual control signal. It is however function of the manipulated variables, *i.e.,* the evaporation temperature and the opening degree of expansion valve. The former is directly given by the MPC algorithm, but the latter needs more elaboration.

After applying a new OD, the latent mass dynamic (8.7) reaches the steady-state after around 4 minutes which results:

$$\text{steady-state} \;\Rightarrow\; \dot{M}_r \simeq 0 \;\Rightarrow\; \dot{m}_{r,in} \simeq \dot{m}_{r,out}. \tag{8.27}$$

Using (8.27), (8.8), and (8.9), the opening degree is calculated as

$$OD \simeq \frac{\dot{Q}_e}{\Delta h_{lg} K v A \sqrt{\rho_{suc}(P_{rec} - P_e)}}, \tag{8.28}$$

where P_{rec} is assumed constant [10], and Δh_{lg}, ρ_{suc} and P_e all are functions of T_e which is regulated to $\hat{T}_e$. All in all, for MPC implementation, at each sampling time, u and $\hat{T}_e$ are the solutions for (8.26) based upon which the opening degree is calculated as

$$OD = K_e(\hat{T}_e)u, \tag{8.29}$$

where $K_e(\hat{T}_e) = \left[\Delta h_{lg} K v A \sqrt{\rho_{suc}(P_{rec} - P_e)}\right]^{-1}$ is updated at each sample time k. The proposed MPC scheme is summarized in Algorithm 7.

Algorithm 7 MPC implementation

Prediction

Load

Pow_{ref} from higher level aggregator

Compute

COP and keep it fixed all over the horizon

Solve

$$\begin{aligned} \min_{\mathbf{u},\hat{T}_e,\varepsilon} \quad & J_{pow} + W_{\mathbf{u}} J_{\Delta\mathbf{u}} + W_e J_{T_e} + W_r \|\varepsilon\|_2^2 \\ \text{subject to} \quad & \mathbf{x}[k+1] = \mathbf{A}x[k] + \mathbf{B}u[k] + \mathbf{B}_d d[k] \\ & \mathbf{x}_{1,min} - \varepsilon \le \mathbf{x}_1[k] \le \mathbf{x}_{1,max} + \varepsilon \\ & \varepsilon \ge 0 \\ & 0 \le \mathbf{u}[k] \le \mathbf{U}A_{e,max}(\mathbf{x}_2 - \hat{T}_e) \\ & \hat{T}_e \le T_{e,max} \end{aligned}$$

Update

$\mathbf{u}[k]$ = first move in obtained $\mathbf{u}$

$\hat{T}_e[k]$ = first move in obtained $\hat{T}_e$

$\mathbf{O}D[k] = \mathbf{K}_e(\hat{T}_e)\mathbf{u}[k]$

Control inputs

$\mathbf{O}D[k],\ \hat{T}_e[k]$

Remark 7: There are local stable superheat controllers operating on the expansion valves to make sure the refrigerant is completely vaporized (superheated) at the outlet of the valves. This is for compressors safety. The superheat control loop is much faster than the MPC and is in the steady-state at each MPC step. In this work, we impose a certain value of superheat degree in our simulation model to take its effect into account.

Sampling Time and Prediction Horizon

In order to choose an appropriate sampling time, T_s, and prediction horizon, N, the limits of each should be investigated. For energy balancing services, the consumer should respond in around 10 minutes [3], and for the proposed power following approach even a faster sampling period, $T_s < 10$ min, would be more favorable. In accordance with the discussion made in Section 3, the sampling time should also be $T_s > 4$ min.

A very short prediction horizon may jeopardize stability of the control system [15]. It is too difficult — if not impossible — to determine the lowest possible prediction horizon analytically. In the objective function (8.21), COP is kept constant all over the horizon. The longer the horizon, the more bias in COP variations due to the variation of the outdoor temperature — the latter affect the condensation pressure and accordingly the COP. Therefor, the prediction horizon should be long enough to ensure the stability, and, on the other hand, not be so long to fulfill the prediction performance in terms of the COP assumption.

4 Simulation Results

In this section, the proposed MPC scheme is applied to a high-fidelity simulation benchmark developed based on the model explained in [10]. The model is validated against real data obtained from a supermarket refrigeration system including 7 MT and 4 LT fridge and freezer display cases and a cold room, and two stages of compressor racks.

Based upon the discussion made in Section 3, the sampling time and prediction horizon are chosen as $T_s = 5$ min and $N = 12$, respectively. In order to have a feasible solution for the optimization problem, slack variables, ε, are employed to soften the state constraints as explained in [16] and also shown in Algorithm 7.

COP Optimization

A simple power reference contains the baseline of the power consumption profile during a day is applied to investigate the COP improvement made by the novel $\hat{T}_e$ control method. For this purpose, the proposed method is compared to the case where a fixed $\hat{T}_e$ in the middle of its possible range is applied. The MPC design of the latter is the same as of Algorithm 7, but using a fixed set-point for evaporation temperature.

Fig. 8.2 shows that how the MPC using the $\hat{T}_e$ control can track a very low baseline while the fixed $\hat{T}_e$ failed to follow, because, otherwise, it would violate the temperature constraints. The reason of rising the baseline after around 9 AM is that the load increases due to increase of the outdoor temperature. The COPs are compared in Fig. 8.3 where an improvement with the average of 22% is achieved by the COP optimization. The lower baseline the consumer can follow, the lower energy cost it should pay.

Energy Balancing Service

The purpose of the following simulation experiment is to show the ability of the proposed control algorithm in case of significant change in the power reference for upward and downward regulation services. The power reference is increased 75% at 12 PM up to 13 PM for downward regulation services. For upward regulation, the refrigeration system

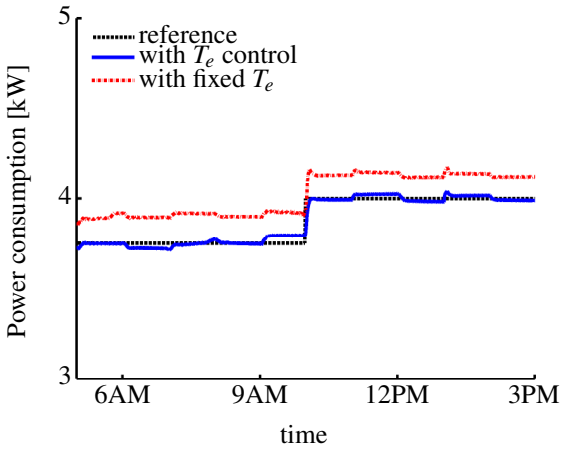

Figure 8.2: Following a low baseline profile of a power reference. The MPC scheme with $\hat{T}_e$ optimization shows a satisfactory performance while it fails with the constant $\hat{T}_e$.

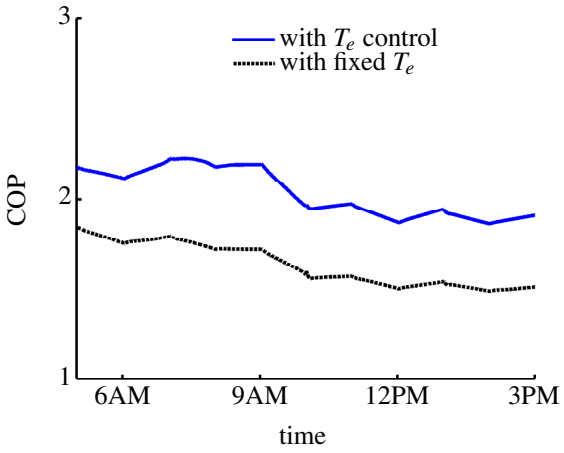

Figure 8.3: A higher COP is achieved by the $\hat{T}_e$ control method.

needs to store thermal energy sometime ahead of the service start time. Consequently, at 15 PM the power reference is increased 12.5% for energy storage, and then is dropped significantly (87.5%) at 18 PM up to 19 PM.

The tracking result is represented in Fig. 8.4. A high performance for the power regulation is obtained by the MPC algorithm. The first step in the power reference after 9 AM is due to the baseline profile. The evaporation temperatures of MT and LT units are shown in Fig. 8.5. The two big caves in the figures come about when the MPC needs to decrease the evaporation temperature to be able to apply the required large cooling capacity during the significant increase of the power reference.

Fig. 8.6 shows the opening degrees of the expansion valves. There is a visible cor-

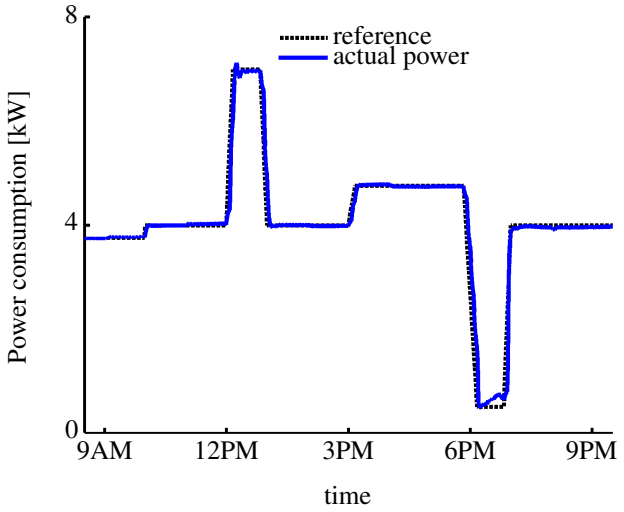

Figure 8.4: Power reference following for energy balancing services.

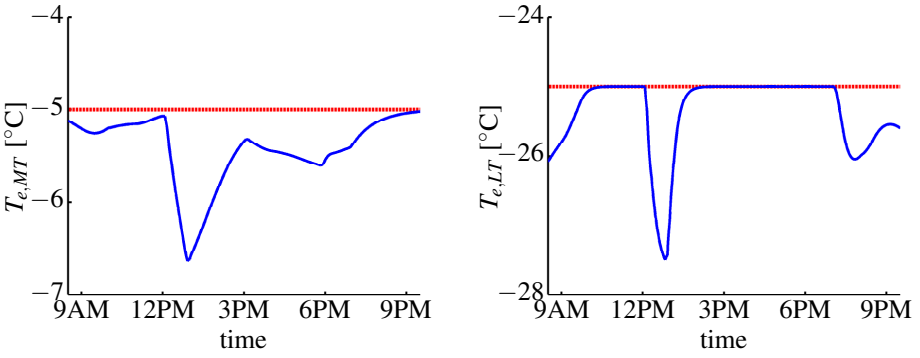

Figure 8.5: Evaporation temperatures for both the MT and LT sections.

relation between the *OD* variations and variations of the power consumption. The food temperatures and constraints are provided in Fig. 8.7. The food temperatures increase/decrease by decreasing/increasing the power consumption which shows the correspondence of the electrical power regulations with storing and delivering of the thermal energy.

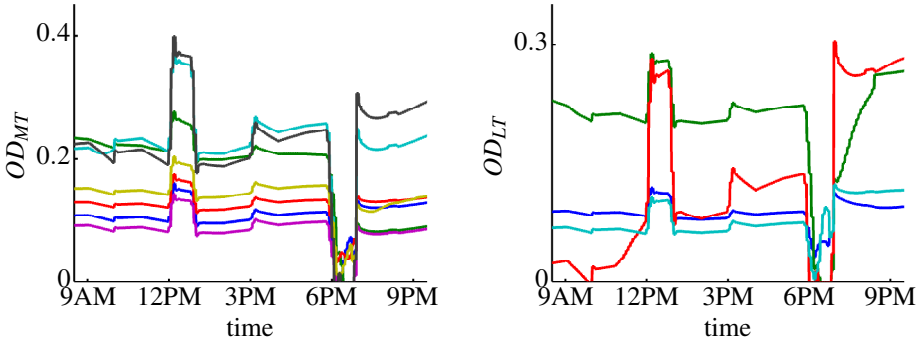

Figure 8.6: Opening degree of the electronic expansion valves.

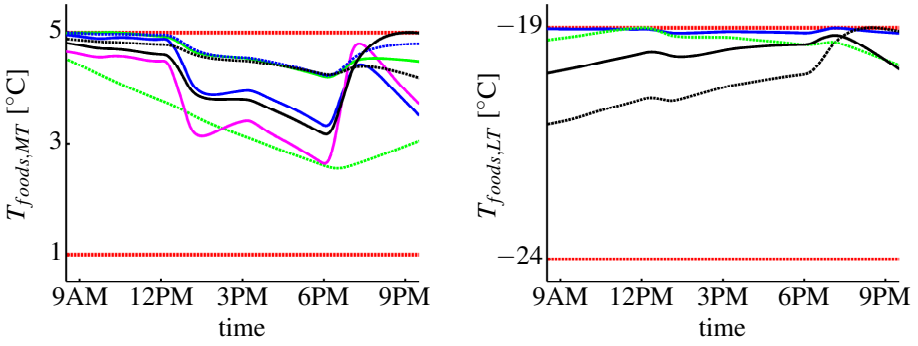

Figure 8.7: Food temperatures of the different cooling sites belong to the MT and LT sections. All the temperature constraints are respected.

5 Conclusions

A model predictive control scheme was proposed for flexible power consumption of refrigeration systems. The proposed control strategy facilitates the demand response required for energy imbalance management services. By introducing a fictitious manipulated variable, a convex optimization problem was formulated within the MPC scheme. A novel incorporation of the evaporation temperature set-point into MPC formulation was presented for COP optimization. The COP improvement with the average of 22% and, consequently, the lower baseline of the power consumption were achieved by the COP optimization method. Simulation experiments showed that the proposed MPC algorithm is able to regulate the power references with significant magnitude changes of at least 75% from the baseline.

References

[1] A. J. Conejo, J. M. Morales, and L. Barino, "Real-time demand response model," *IEEE Transactions on Smart Grid*, vol. 1, no. 3, pp. 236–242, 2010.

[2] K. Trangbaek, J. D. Bendtsen, and J. Stoustrup, "Hierarchical control for smart grids," in *Proceedings of the 18th IFAC World Congress*. Milan, Italy: IFAC, Aug. 2011.

[3] G. Heffner, C. Goldman, B. Kirby, and M. Kintner-Meyer, "Loads providing ancillary services: Review of international experience," U.S. Department of Energy, Ernesto Orlando Lawrence Berkeley National Laboratory, Tech. Rep., May 2007.

[4] I. Stadler, "Power grid balancing of energy systems with high renewable energy penetration by demand response," *Utilities Policy*, vol. 16, pp. 90–98, 2008.

[5] S. Goli, A. McKane, and D. Olsen, "Demand response opportunities in industrial refrigerated warehouses in california," in *2011 ACEEE Summer Study on Energy Efficiency in Industry*, Niagara Falls, NY, USA, Jul. 2011.

[6] T. G. Hovgaard, S. Boyd, L. F. S. Larsen, and J. B. Jøregensen, "Nonconvex model predictive control for commercial refrigeration," *International Journal of Control*, vol. 86, no. 8, pp. 1349–1366, 2013.

[7] S. E. Shafiei, J. Stoustrup, and H. Rasmussen, "A supervisory control approach in economic MPC design for refrigeration systems," in *Proceedings of the European Control Conference*, Zürich, Switzerland, Jul. 2013, pp. 1565–1570.

[8] T. G. Hovgaard, L. F. S. Larsen, K. Edlund, and J. B. Jrgensen, "Model predictive control technologies for efficient and flexible power consumption in refrigeration systems," *Energy*, vol. 44, pp. 105–116, 2012.

[9] Y. T. Ge and S. A. Tassou, "Thermodynamic analysis of transcritical CO_2 booster refrigeration systems in supermarket," *Energy Conversion and Management*, vol. 52, pp. 1868–1875, 2011.

[10] S. E. Shafiei, H. Rasmussen, and J. Stoustrup, "Modeling supermarket refrigeration systems for demand-side management," *Energies*, vol. 6, no. 2, pp. 900–920, 2013.

[11] D. Sarabia, F. Capraro, L. F. S. Larsen, and C. Prada, "Hybrid NMPC of supermarket display cases," *Control Engineering Practice*, vol. 17, pp. 428–441, 2009.

[12] L. N. Petersen, H. Madsen, and C. Heerup, "ESO2 optimization of supermarket refrigeration systems: Mixed integer MPC and system performance," Department of Informatics and Mathematical Modeling, Technical University of Denmark, Tech. Rep., 2012.

[13] C. Pérez-Segarra, J. Rigola, M. Sòria, and A. Oliva, "Detailed thermodynamic characterization of hermetic reciprocating compressors," *International Journal of Refrigeration*, vol. 28, pp. 579–593, 2005.

[14] R. Zhou, T. Zhang, J. Catano, J. T. Wen, G. J. Michna, Y. Peles, and M. K. Jensen, "The steady-state modeling and optimization of a refrigeration system for high heat flux removal," *Applied Thermal Engineering*, vol. 30, pp. 2347–2356, 2010.

[15] D. Q. Mayne, J. B. Rawlings, C. V. Rao, and P. O. M. Scokaert, "Constrained model predictive control: Stability and optimality," *Automatica*, vol. 36, pp. 789–814, 2000.

[16] S. E. Shafiei, H. Rasmussen, and J. Stoustrup, "Model predictive control for a thermostatic controlled system," in *Proceedings of the European Control Conference*, Zürich, Switzerland, Jul. 2013, pp. 559–1564.

Paper F

Data-Driven Predictive Direct Load Control of Refrigeration Systems

Seyed Ehsan Shafiei, Torben Knudsen, Rafael Wisniewski and Palle Andersen

This paper was published in:
IET Control Theory & Applications, Special issue: Data-based control and process monitoring with industrial applications, 2015

The layout has been revised

Abstract

A predictive control using subspace identification is applied for the smart grid integration of refrigeration systems under a direct load control scheme. A realistic demand response scenario based on regulation of the electrical power consumption is considered. A receding horizon optimal control is proposed to fulfill two important objectives: To secure high coefficient of performance, and to participate in power consumption management. Moreover, a new method for design of input signals for system identification is put forward. The control method is fully data-driven without an explicit use of model in the control implementation. As an important practical consideration, the control design relies on a cheap solution with available measurements than using the expensive mass flow meters. The results show successful implementation of the method on a large-scale nonlinear simulation tool which is validated against real data. The performance improvement results in a 22% reduction in the energy consumption. A comparative simulation is accomplished showing the superiority of the method over the existing approaches in terms of the load following performance.

1 Introduction

The future smart grid requires smart consumers who are able to manage their energy consumption profile in a flexible manner. The flexible consumption can be incorporated either into an incentive on electricity price market, or into a direct load control (DLC) frameworks provisioned by the power market independent service operator.

The dominant approaches in DLC developments have been load-shedding and load shifting approaches. In the former, part of the load is curtailed during the demand response (DR) event [1, 2], and in the latter, the electricity consumption is moved from high-pick to off-pick hours [3, 4]. The need for power grid services has been increased by more integration of variable generation which emphasizes the significance of DLC in which the electricity consumption should follow a reference load profile (power consumption) during the DR event [5].

Consumers with thermal storage capabilities, such as supermarket refrigeration systems, are envisioned to contribute to grid balancing services [6]. This valuable potential can be released under a direct load control framework by provision of advanced control strategies [7–9].

A direct load control for supermarket refrigeration systems is proposed in [9] where a convex optimization problem is formulated within an MPC scheme. This proposed MPC scheme, in particular, and other suggested model based designs [8, 10] in general, may lead to significant performance degradation in case of model mismatches. Another issue is that such model based methods are not easily generalizable to include different supermarket systems and, consequently, a comprehensive modeling effort should be accomplished for each specific refrigeration system before control system design. As a different approach, a supervisory control method, based on decentralized proportional-integral (PI) control loops, is presented in [11]. No model information is required in that method and it is easily applicable to different supermarket refrigeration systems. The price that should be paid for this simplification in the method is the performance decay in terms of the load following, especially during the downward regulation services.

The problem of load tracking during the DR event is considered in this paper. The data-driven control method proposed here improves the load following performance comparing to [11] and, at the same time, overcomes the mentioned disadvantages associated with the model based design proposed in [9].

Subspace identification (SSID) methods are outstanding candidates for multivariable large-scale process systems to develop state-space model directly from input-output data [12]. These methods are noniterative and robust, and based on convex optimization that can avoid the convergence problems existing in conventional prediction-error methods [13]. Recent surveys on data-driven control and monitoring methods for different industrial applications can be found for example in [14] and [15].

In this paper, the estimated subspaces matrices are directly employed for predictive control design indicating which is referred as data-driven predictive control. In this case, only a single matrix algebraic calculation like a QR-decomposition would be required for obtaining the prediction matrices. Predictive control using subspace matrices is also called subspace predictive control (SPC) [16]. No model order assumption nor estimation needs to be done considering the fact that the state-space matrices are not retrieved here. The main contribution of this work is a new application of the subspace predictive control for facilitating the smart grid balancing services by direct load control of supermarket refrigeration systems. For balancing services, the power consumption is controlled directly to undertake the upward and downward regulation services [17]. In order to ensure a high coefficient of performance (COP), a novel objective function is formulated by incorporating the suction pressures into the optimization problem.

Moreover, an open-loop experiment based on uncorrelated random input sequences is presented. A new method based on tuning the average duty cycle of the input signals is proposed. The tuning is performed using the data available from the normal thermostatic operation of the system. This is seen as a substantial advantage as it can avoid the difficulties may arise in formulating and solving the problem of rotated input design [18]. Furthermore, the proposed method does not produce the linearly dependent inputs as opposed to the case when using the rotated input approach [19].

As a practical consideration, the control design does not rely on the mass flow measurements which is of great interest because these costly measurements are usually not available in commercial refrigeration applications. But, on the other hand, a flow measurement could enhance the performance of the suction pressure estimation. As an alternative, a feedforward inclusion of the condensation pressure into the SPC formulation is suggested in oder to regain similar performance with a cheaper measurement.

All in all, the contributions of the present paper are summarized as: (1) demand response implementation for refrigeration systems using subspace predictive control; (2) maximization of the coefficient of performance by incorporating the suction pressure into the optimal control formulation; (3) a new design of experiment for refrigeration systems; (4) elimination of mass flow measurements from control implementation.

There were no real supermarket refrigeration system available for test and experiment during this research. Instead, a nonlinear simulation tool for dynamical simulation of large-scale refrigeration systems, “SRSim”, is employed for test of the methods for the design of experiment, identification and control, [20]. It has been produced based on a high fidelity model created using first principle modeling and validated by real data obtained from a supermarket in Denmark under another research project [21]. SRSim development has been supported by Danfoss, the industrial partner involved in this research.

Throughout the paper, the specific notation of $(x_1, \cdots, x_n) = \begin{bmatrix} x_1^T & \cdots & x_n^T \end{bmatrix}^T$ is used.

2 System Description and Problem Statement

This section briefly explains a CO_2 booster configuration of a typical supermarket refrigeration system. Subsequently, the control problem is stated.

CO_2 Booster Refrigeration System

A basic layout of a typical refrigeration system including several cold reservoirs (display cases and cold rooms) with two compressor banks in a booster configuration is shown in Fig. 9.1. The cycle can be explained by starting from the receiver (REC) where two-phase refrigerant (mix of liquid and vapor) at point '8' is split into saturated liquid ('1') and saturated gas ('1b'). The latter is bypassed through a bypass valve (BPV), and the former flows into expansion valves where the refrigerant pressure drops to medium ('2') and low ('2′') pressures. The expansion valves EV_MT and EV_LT are responsible for regulating the air temperature inside the medium temperature (MT) and the low temperature (LT) cold reservoirs by controlling the entering mass flow into the evaporators. Flowing through evaporators in medium and low temperature units (EVAP_MT and EVAP_LT), the refrigerant absorbs the heating load from the cold reservoirs. The suction pressure of low temperature section is increased by working performed by the low stage compressor rack (COMP_LT). All mass flows from COMP_LT, EVAP_MT and BPV outlets are collected by a suction manifold at point '5' where the pressure is increased again by the higher stage compressor rack (COMP_MT). Afterwards, the gas phase refrigerant enters the condenser to deliver the absorbed heat load from the cold reservoirs to the surroundings. The detailed thermodynamic analysis of such systems is described in [22].

Problem Statement

Large inclusion of decentralized electric power generation from intermittent renewable energy recourses challenges the grid stability and sustainability. In order to keep demand and supply balanced at all times, the consumption is seen as an extra degree of freedom in addition to the electricity production of power plants. Various solutions for different kinds of (consumption) loads are underlined in the framework of demand response. Inert thermal processes like refrigeration systems are good candidates for such a demand response accomplishment where the load is directly controlled.

In the present study, the refrigeration system undertakes both upward and downward power consumption management under the direct load control framework for a specific period of time in response to an activation signal. An independent service operator aggregates a large number of loads for this purpose and sends the activation signals in accordance with the contingency conditions [23]. During the activation period, refrigeration systems should follow the power reference assigned by the aggregator which operates within a hierarchical structure shown in Fig. 9.2.

This set-up enables the aggregator to offer flexibility, in terms of the energy management, to the higher level operators like TSO (Transmission System Operator), DSO (Distribution System Operator) or BRP (Balance Responsible Party). The problem of

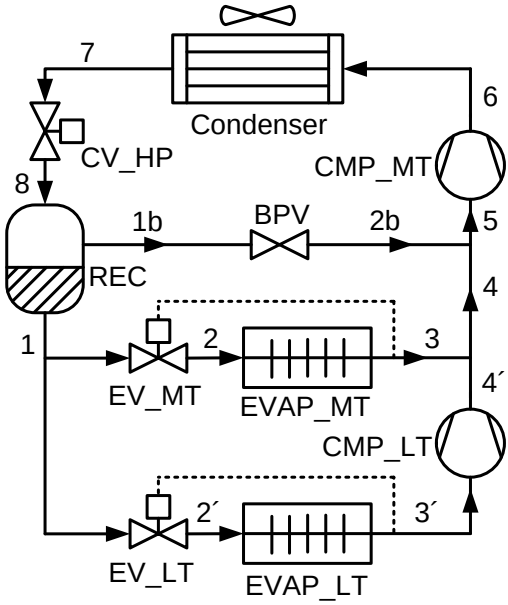

Figure 9.1: Basic layout of a typical supermarket refrigeration system with booster configuration.

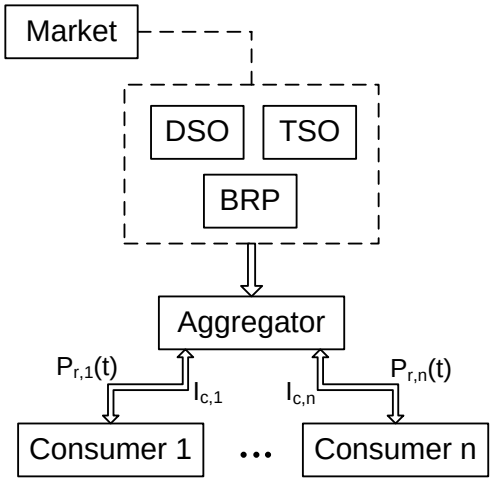

Figure 9.2: Hierarchical direct smart grid control layout. The higher level parties trade the flexibility, in terms of the energy management, with the aggregators according to the market conditions. The aggregators, on other hand, are in the two-way communication with the energy consumers. They receive the consumer information I_c and send the power reference signal P_r during the DR event.

aggregator design, information flow and grid side strategies is outside the scope of this work, but the general and specific relevances can for example be found in [24] and [25].

3 Control Strategy

Three modes of operations can be envisioned according to the regulation services: (1) normal operation; (2) downward regulation; and (3) upward regulation. In order to keep the system at the highest performance in all modes of operations, the COP should be maximized. It is defined as the ratio of cooling capacity ($\dot{Q}_e$) to the electrical power consumption of the compressors (P_w) as

$$\mathrm{COP} = \frac{\dot{Q}_e(\dot{m}_r, P_o)}{P_w}, \tag{9.1}$$

where the cooling capacity is a nonlinear function of the refrigerant mass flow $\dot{m}_r$, and the suction pressure P_o. The former is controlled by the expansion device and the latter is regulated by the compressors. The COP is maximized by letting the suction pressures increase up to the point that still enough cooling capacity can be provided to maintain the food temperatures within the safety bounds, [11].

Due to intermittency of the renewable energy resources, the exact time when the grid imbalance occurs is almost unpredictable, or at best can be predicted with a high degree of uncertainty. Thus, the control system should react to the activation signal quickly. In order for the refrigeration system to be able to react to both the upward and downward regulation signals, the food temperatures should be kept at the middle of the constraint limits in the normal operation. The total electrical power consumption of the compressor racks in this mode is called "baseline consumption".

The dynamical equations describing the cold reservoir temperatures in terms of cooling capacity are presented in the following. The equations are derived by assuming a lumped temperature model and based on energy balances for heat transfers, [26].

$$MC_{food}\frac{dT_{food}}{dt} = UA_{food/air}(T_{air} - T_{food}) \tag{9.2}$$

$$MC_{air}\frac{dT_{air}}{dt} = UA_{amb}(T_{amb} - T_{air}) + UA_{food/air}(T_{food} - T_{air}) - \dot{Q}_e, \tag{9.3}$$

where T_{air} and T_{food} are the air and food temperatures inside the cold reservoirs, respectively, MC denotes the corresponding mass multiplied by the heat capacity, $UA_{food/air}$ is the overall heat transfer coefficient between the food and the air, T_{amb} is the ambient temperature, and UA_{amb} is the associated heat transfer coefficient. It can be seen from (9.3) that the cooling capacity applied by the refrigeration cycle can cool down the air temperature by compensating for the ambient load. Then, the cooled air can regulate the food temperature according to (9.2).

In both normal operation and regulation services, it is also important to maintain a high COP to keep the energy losses — due to the thermal loads — as low as possible. The pressure control scheme which will be proposed in Section 5 is for this purpose.

4 Subspace Identification Method

In order to make the presentation self-contained, the subspace identification method is briefly explained in this section. A discrete-time state-space description of a linear time-invariant process in innovation form is given by

$$x_{k+1} = Ax_k + Bu_k + Ke_k \tag{9.4}$$

$$y_k = Cx_k + Du_k + e_k, \tag{9.5}$$

where $u_k \in \mathbb{R}^l$, $y_k \in \mathbb{R}^m$, and $x_k \in \mathbb{R}^n$ are the process inputs, outputs and states, respectively; $e_k \in \mathbb{R}^m$ is a white noise (innovation) sequence with zero mean and covariance $E[e_k e_k^T] = S$. The parameters A, B, C, and D are state-space matrices with appropriate dimensions, and K is the Kalman filter gain.

The following subspace matrix input-output equations are derived by recursive substitution of (9.4) and (9.5), [13],

$$Y_f = \Gamma X_f + H^d U_f + H^s E_f \tag{9.6}$$

$$Y_p = \Gamma X_p + H^d U_p + H^s E_p \tag{9.7}$$

where Y_p and Y_f are data block Hankel matrices for y_k with i-block rows and j-block columns defined as

$$Y_p = \begin{bmatrix} y_1 & y_2 & \cdots & y_j \\ y_2 & y_3 & \cdots & y_{j+1} \\ \vdots & \vdots & \ddots & \vdots \\ y_i & y_{i+1} & \cdots & y_{i+j-1} \end{bmatrix}, \tag{9.8}$$

$$Y_f = \begin{bmatrix} y_{i+1} & y_{i+2} & \cdots & y_{i+j} \\ y_{i+2} & y_{i+3} & \cdots & y_{i+j+1} \\ \vdots & \vdots & \ddots & \vdots \\ y_{2i} & y_{2i+1} & \cdots & y_{2i+j-1} \end{bmatrix}. \tag{9.9}$$

The similar formations are used for generation of data block Hankel matrices for the input (U) and noise (E) terms. The measured inputs and outputs, u_k, y_k for $k \in \{1, 2, \ldots, 2i + j - 1\}$, are partitioned into the past and the future blocks denoted by the subscripts p and f, respectively. The number of columns in these data matrices j should be much larger than the number of rows i, [16]. However, the number of row blocks, i, in the past blocks can be different from that of the future blocks, but for the sake of simplicity of the presentation, they are considered the same here. In Section 5, they are differentiated from each other by N_p for the number of past row blocks, and N_f for the number of future row blocks. The past and future state sequences are defined as

$$X_p = \begin{bmatrix} x_1 & x_2 & \cdots & x_j \end{bmatrix}, \tag{9.10}$$

$$X_f = \begin{bmatrix} x_{i+1} & x_{i+2} & \cdots & x_{i+j} \end{bmatrix}. \tag{9.11}$$

The extended observability matrix $\Gamma \in \mathbb{R}^{im \times n}$, and lower triangular Toeplitz matrices $H^d \in \mathbb{R}^{im \times il}$ and $H^s \in \mathbb{R}^{im \times im}$ are given by

$$\Gamma = (C, CA, \cdots, CA^{i-1}) \tag{9.12}$$

$$H^d = \begin{bmatrix} D & 0 & \cdots & 0 \\ CB & D & \cdots & 0 \\ \vdots & \vdots & \ddots & \vdots \\ CA^{i-2}B & CA^{i-3}B & \cdots & D \end{bmatrix}, \tag{9.13}$$

$$H^s = \begin{bmatrix} I_m & 0 & \cdots & 0 \\ CK & I_m & \cdots & 0 \\ \vdots & \vdots & \ddots & \vdots \\ CA^{i-2}K & CA^{i-3}K & \cdots & I_m \end{bmatrix}, \tag{9.14}$$

where superscripts d and s of H correspond to deterministic and stochastic inputs u_k and e_k.

It is shown in Appendix A in [27] that the future states, X_f can be expressed in terms of the past states, inputs and disturbances, and for sufficiently large data, (9.6) can be reformulated as:

$$Y_f = L_w W_p + L_u U_f + L_e E_f, \tag{9.15}$$

where $W_p = (Y_p,\ U_p)$, and L_w, L_u, and L_e are subspace matrices corresponding to the past inputs and outputs (states), the deterministic future inputs, and the stochastic future inputs, respectively. The deterministic part of (9.15) can be estimated by the following linear predictor:

$$\hat{Y}_f = L_w W_p + L_u U_f. \tag{9.16}$$

Under the conditions that: (i) the input u_k is uncorrelated with the noise e_k (open loop condition); (ii) u_k is persistently exciting of order $2i$; and (iii) the number of measurements is sufficiently large, *i.e.,* $j \to \infty$, the subspaces matrices can be consistently identified as the arguments of the following least squares problem, [28]:

$$\min_{L_w, L_u} \left\| Y_f - \begin{pmatrix} L_w & L_u \end{pmatrix} \begin{pmatrix} W_p \\ U_f \end{pmatrix} \right\|_F^2. \tag{9.17}$$

where $\|\cdot\|_F$ stands for the Frobenius norm. An efficient and robust method for numerical implementation of the above problem is QR-decomposition of $(W_p,\ U_f,\ Y_f)$ as:

$$\begin{bmatrix} W_p \\ U_f \\ Y_f \end{bmatrix} = \begin{bmatrix} R_{11} & 0 & 0 \\ R_{21} & R_{22} & 0 \\ R_{31} & R_{32} & R_{33} \end{bmatrix} \begin{bmatrix} Q_1^T \\ Q_2^T \\ Q_3^T \end{bmatrix}, \tag{9.18}$$

in which the subspace matrices $L = \begin{bmatrix} L_w & L_u \end{bmatrix}$ can be calculated as

$$L = \begin{bmatrix} R_{31} & R_{32} \end{bmatrix} \begin{bmatrix} R_{11} & 0 \\ R_{21} & R_{22} \end{bmatrix}^{\dagger} \tag{9.19}$$

where † represents the Moore-Penrose pseudo-inverse. The subspace matrices are identified as:

$$L_w = L(p,q), \quad p = 1,\ldots,im \ \text{ and } \ q = 1,\ldots,i(l+m) \tag{9.20}$$

$$L_u = L(p,k), \quad p = 1,\ldots,im \ \text{ and } \ k = i(l+m)+1,\ldots,i(2l+m). \tag{9.21}$$

The future outputs of the plant are predicted by (9.16) using the subspace matrices and future moves in the control signals. This predictor can conveniently be utilized for predictive control formulation without identifying a state-space model [16].

SSID for Refrigeration Systems

An open-loop identification problem is formulated to obtain the subspace matrices.

Input and Output Variables

The whole system is divided into two medium and low temperature sections for each a separated subspace data-driven model is developed. The only coupling between the two sections is the refrigerant mass flow from the LT compressors to the MT suction manifold. In the commercial refrigeration systems, there is no mass flow measurement available, so changes in the mass flow in the other sections are regarded as an unknown disturbances.

In the power regulation mode of operation, the controlled outputs are the electrical power consumption of the compressor rack, P_w, and the suction pressure, P_o. The measured outputs are the air and the food temperatures, T_{air} and T_{food}. The food temperatures are necessary to measure due to the safety constraints applied. In the normal operation, the food temperatures and the suction pressures are the only measured and controlled outputs. The MT and LT compressor capacities, ω_c, and the opening degree of the electronic expansion valves, v, are chosen as the vectors of manipulated input variables for the specific case considered in this work.

Constraints

The opening degree of expansion valves are constrained as $0 \leq v \leq 1$. Because a group of compressors are configured into a single rack, the compressor speed is specified as the capacity of the rack in terms of the volume flow that it can provide in percentage as $0 \leq \omega_c \leq 100$, [26]. The upper bound of the MT suction pressure should be less than a safety value, *i.e.,* $P_{o,MT} \leq P_{max}$. The food temperatures should also be within specified limits as $T_{min} \leq T_{food} \leq T_{max}$.

5 Data-Driven Predictive Control

In contrast to the classical MPC where an explicit model of the plant is used to predict its future behavior, in data-driven predictive control, the linear predictor constructed directly from the input-output data — obtained in a dedicated experiment — is used for the same purpose. In the following, predictive control combined with the subspace identification is presented. Subsequently, the subspace predictive control formulation for direct load control of refrigeration systems is introduced.

Subspace Predictive Control

In subspace predictive control, the following objective function should be minimized at each time instant for the receding horizon implementation:

$$J = \sum_{k=1}^{N_f} (r_{k+1} - \hat{y}_{k+1})^T Q_k (r_{k+1} - \hat{y}_{k+1}) + \sum_{k=1}^{N_c} \Delta u_k^T R_k \Delta u_k, \tag{9.22}$$

where Q_k and R_k are weighting matrices, r is the reference signal, N_f and N_c are prediction and control horizon, respectively, and $\hat{y}_{k+n}$, with $n = 1, \ldots, N_f$, is the n-step-ahead predicted output at time instant k. Defining $\hat{y}_f = (\hat{y}_{k+1},\ \hat{y}_{k+2},\ \cdots,\ \hat{y}_{k+N_f})$ and $u_f = (u_{k+1},\ u_{k+2},\ \cdots,\ u_{k+N_c})$, the above objective can be rewritten in the matrix form as:

$$J = (r_f - \hat{y}_f)^T Q (r_f - \hat{y}_f) + \Delta u_f^T R \Delta u_f, \tag{9.23}$$

where r_f is defined in the same way as $\hat{y}_f$, and $Q \in \mathbb{R}^{N_f l \times N_f l}$ and $R \in \mathbb{R}^{N_c m \times N_c m}$ are block diagonal matrices constructed from Q_k, for $k = 1, \ldots, N_f$, and R_k, for $k = 1, \ldots, N_c$, respectively.
The predicted output is obtained from (9.16) as:

$$\hat{y}_f = l_w w_p + l_u u_f, \tag{9.24}$$

where $w_p = (y_{k-N_p+1}, \cdots, y_k, u_{k-N_p+1}, \cdots, u_k)$ is the vector of past input and output data with the past horizon N_p, and subspace matrices are

$$l_w = L_w(p,q), \quad p = 1, \ldots, mN_f, \text{ and } q = 1, \ldots, (l+m)N_p, \text{ and} \tag{9.25}$$

$$l_u = L_u(p,k), \quad p = 1, \ldots, mN_f, \text{ and } k = 1, \ldots, lN_c. \tag{9.26}$$

In order to implement the objective function (9.23), the predictor (9.24) should include the incremental input Δu_f. In this way integral action can be included in the predictor design that will also lead to offset free tracking performance. A systematic approach to include the integral action is proposed by [27] considering the noise input e_k as an integrating noise, *i.e.,*

$$e_k = e_{k-1} + a_k \tag{9.27}$$

where a_k is a white noise signal. Substituting (9.27) in (9.4)–(9.5) and using a difference operator $\Delta = 1 - z^{-1}$ yields

$$\Delta x_{k+1} = A\Delta x_k + B\Delta u_k + Ka_k \tag{9.28}$$

$$\Delta y_k = C\Delta x_k + D\Delta u_k + a_k \tag{9.29}$$

Following the same procedure, the predictor (9.24) changes to

$$\Delta\hat{y}_f = l_w \Delta w_p + l_u \Delta u_f \tag{9.30}$$

that can be rearranged to

$$\hat{y}_f = \mathbf{y}_k + \Lambda l_w \Delta w_p + \Lambda l_u \Delta u_f \tag{9.31}$$

where $\mathbf{y}_k = (y_k, y_k, \cdots, y_k)$ and

$$\Lambda = \begin{bmatrix} I & 0 & \cdots & 0 \\ I & I & \cdots & 0 \\ \vdots & \vdots & \ddots & \vdots \\ I & I & \cdots & I \end{bmatrix}. \tag{9.32}$$

Incorporating the input and output constraints, SPC algorithm can be implemented by solving the following quadratic programming (QP) problem in a receding horizon manner.

$$\begin{aligned} \min_{\Delta u_f} \quad & (r_f - \hat{y}_{f,c})^T Q (r_f - \hat{y}_{f,c}) + \Delta u_f^T R \Delta u_f \\ \text{subject to} \quad & \hat{y}_f = \mathbf{y}_k + \Lambda l_w \Delta w_p + \Lambda l_u \Delta u_f \\ & (\mathbf{u}_{min} - \mathbf{u}_k) \le \Lambda \Delta u_f \le (\mathbf{u}_{max} - \mathbf{u}_k) \\ & \mathbf{y}_{min} \le \hat{y}_f \le \mathbf{y}_{max} \end{aligned} \tag{9.33}$$

where $\hat{y}_{f,c}$ is the vector of controlled outputs included in $\hat{y}_f$, $(\mathbf{u}_{min} - \mathbf{u}_k)$ and $(\mathbf{u}_{max} - \mathbf{u}_k)$ are expanded column vectors of $(u_{min} - u_k)$ and $(u_{max} - u_k)$ with u_{min} and u_{max} being the input magnitude constraints, and finally $\mathbf{y}_{min}$ and $\mathbf{y}_{max}$ are expanded column vectors of the measured output constraints.

SPC Formulation for Direct Load Control

Direct Load Control

As already discussed in Section 3, during the balancing service, the power consumption should track a reference signal while the suction pressures are kept at the highest possible points. The reference signals and controlled outputs in the QP problem (9.33) are

$$r_f = (P_{w,r},\ P_{o,r}) \tag{9.34}$$

and

$$\hat{y}_{f,c} = (P_{w,tot},\ P_o), \tag{9.35}$$

where $P_{w,r}$ is the power reference, $P_{o,r}$ contains the references for the MT and LT suction pressures to keep them close to the maximum limits. Only the MT suction pressure is constrained from above as $P_{o,MT} \leq P_{o,MT,max}$. Furthermore, $P_{w,tot}$ is sum of the power consumptions of both the MT and LT compressor racks

$$P_{w,tot} = P_{w,MT} + P_{w,LT}. \tag{9.36}$$

The prediction of the measured output variables, $\hat{y}_{f,m}$, are the food temperatures

$$\hat{y}_{f,m} = T_{food}, \tag{9.37}$$

with the constraints $T_{min} < T_{food} < T_{max}$. The input variables are

$$\Delta u_f = (\Delta v,\ \Delta \omega_c) \tag{9.38}$$

where the associated constraints are $u_{min} = (0,0)$ and $u_{max} = (1,100)$.

Remark 8: *The matrix weight Q comprises two separated parts,*

$$Q = \begin{bmatrix} Q_1 & 0 \\ 0 & Q_2 \end{bmatrix}, \tag{9.39}$$

where matrices Q_1 and Q_2 includes weighting factors corresponding to the power and the pressure regulations, respectively. Therefore, tuning of these weights is actually a trade-off between the tracking performance in terms of the power following and the efficiency performance in terms of the higher suction pressures.

Normal operation

For normal operation, the food temperatures should be kept close to the higher limits. This can be achieved by using the same subspace model employed by the balancing service operation. However, some small modifications are needed for the QP problem formulation. The power consumption part in the reference signal and in the controlled output are replaced by the food temperature.

$$r_f = (T_{food,r},\ P_{o,r,}) \tag{9.40}$$

$$\hat{y}_{f,c} = (T_{food},\ P_o) \tag{9.41}$$

The input variables and constraints are the same as of Section 5.

Inclusion of Feedforward Control

As already explained in Section 4, there is no mass flow measurement required for the proposed control method. The mass flows from the LT compressors and the bypass valve are regarded as unknown disturbances which affect the pressure of the MT suction manifold. On the other hand, the outlet pressure of the MT compressor rack, P_c is correlated with the total mass flow (including the disturbance flows) from the compressor rack. Therefore, this pressure is feedforwarded into the subspace model to improve the suction pressure (P_o) estimation and accordingly the predictive control performance.

Whereas the future information about the outlet pressure is not available, only the data Hankel matrix of its past measurements are included as an augmented external input, V_p, in the W_p term of the predictor equation.

$$\hat{Y}_f = L_w^+ W_p^+ + L_u U_f \tag{9.42}$$

where $W_p^+ = (Y_p,\ U_p,\ V_p)$. Identification of the subspace matrices and the predictive control algorithm are the same as before but with replacing U_p by $(U_p,\ V_p)$.

6 Simulation Results

A nonlinear dynamical simulation tool for a supermarket refrigeration system is utilized as a fully fledged application to examine the proposed data-driven control method. It is a high fidelity model identified based on the real data obtained from a supermarket in Denmark. The model description as well as the estimated parameters are presented in [26]. It includes 7 MT and 4 LT cold reservoirs and two racks of compressors with a booster configuration as well as the other subsystems shown in Fig. 9.1.

Design of Experiment

The input signal should be persistently exciting with an appropriate order. For this purpose, pseudo-random binary signals (PRBSs) are usually applied for identification of MIMO systems. There are two degrees of freedom for designing such input signals, *i.e.,* the bandwidth and the amplitude.

Thermostatic control is usually used for temperature control in refrigeration systems. The expansion valve is switched to the ON/OFF state once the air temperature reaches the upper/lower temperature limit. It ensures the food temperature be within the permissible range. It looks like a relay feedback experiment used in some self tuning systems. In the sequel, it is shown how the information contained in the relay feedback data can be used to tune the PRBS. Fig. 9.3 shows an example of variation of the air and the food temperatures due to applying the relay feedback test or thermostatic control effort. The food temperature is modeled as the low pass filtered version of the air temperature.

The sampling rate of applying the input sequences is chosen to be one minute. The input sequences applied to the expansion valves are designed as follows.

Bandwidth of the input sequences — In order for food temperatures to vary as much as possible within the constrained range, bandwidth of the input frequency should be limited. The low frequency signal is realized by changing the switching probability up to α_{bw} times of the normalized Nyquist frequency, where $0 < \alpha_{bw} < 1$. The details can be found in [29, Ch. 5, Example 5.11].

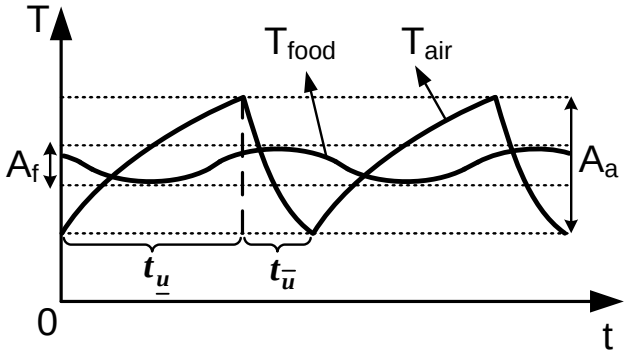

Figure 9.3: Periodic temperature change obtained from applying the relay feedback to the expansion valve. The time spans $t_{\bar{u}}$ and $t_{\underline{u}}$ correspond to the ON and OFF cycle of the expansion device, respectively.

In the relay feedback test, the frequency of the air temperature variation is the same as the input signal and its amplitude varies within the full range, but the food temperature amplitude is attenuated with the gain of $G_r = A_f/A_a$ at the frequency of $\omega_r = 2\pi/T_r$ with $T_r = t_{\underline{u}} + t_{\bar{u}}$ as depicted in Fig. 9.3. Having ω_r and G_r known, the following low pass filter transfer function from the air to the food temperature is computed

$$H_{af} = \frac{1}{\tau s + 1}. \tag{9.43}$$

The filtering effect from the air to the food temperature has a dominant pole comparing to the envisaged transfer function from the input signal to the air temperature. The attenuation gain below 5%, *i.e.,* $|H_{af}| < 0.05$, causes the variation of food temperature to be within the range of the measurement noise. Let the frequency corresponding to this gain be denoted by ω_{bw}. Thus, the bandwidth of the input sequences should be limited by

$$\alpha_{bw} = \omega_{bw}/\pi \tag{9.44}$$

Magnitude of the input sequences — For constrained and/or ill-conditioned systems, the dominant approach to respect the constraints is to limit the amplitude of the excitation signal by the so called rotated input method [19]. Yet larger input amplitudes are more favorable to have a better signal to noise ratio. Here, we suggest to tune the average duty cycle of the PRBS. It is much more intuitive and simpler than the rotated input approach, [30], as well as providing the largest possible amplitudes for input signals.

The difference between the time span values $t_{\underline{u}}$ and $t_{\bar{u}}$ in Fig. 9.3 is because of the difference in the gain directionality. In order to excite all directions with the same strength, the average duty cycle of the PRBS, $\overline{D}$, is proposed to be designed as

$$\overline{D} = \frac{t_{\bar{u}}}{t_{\underline{u}} + t_{\bar{u}}} \tag{9.45}$$

System Identification

The PRBSs are designed in accordance with the method presented in Section 6 and applied to the corresponding input channels such that for the expansion valves $\nu \in \{0,1\}$ and for the compressor racks $\omega_c \in \{0,100\}$. An example of the PRBS applied to the expansion valve is shown in Fig. 9.4a, where the first 1000 sequences of the signal used to excite the 6th MT cold reservoir dynamics are illustrated.

An example of the resulting food temperatures for the 6th MT cold reservoir is provided in Fig. 9.4b where the temperature constraints are shown by the dotted lines. Amplitudes of variation of the food temperature is almost as large as the constraint bounds which indicates a satisfactory signal to noise ratio. Fig. 9.4c and Fig. 9.4d show the power consumption and suction pressure of the MT section resulted from the identification experiment.

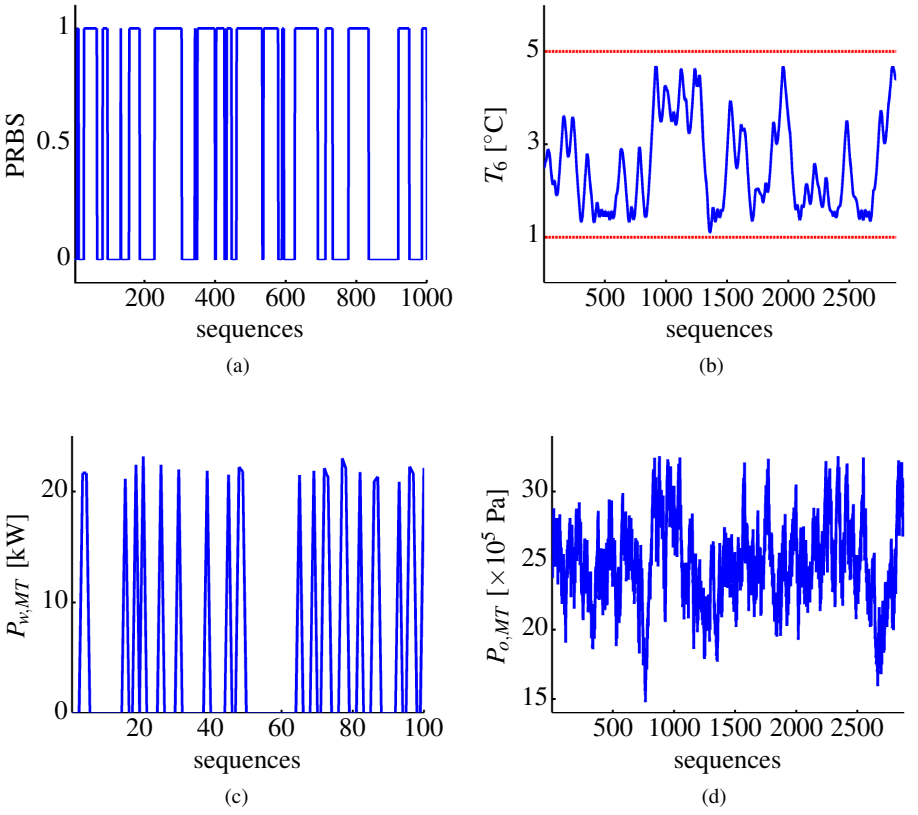

Figure 9.4: Identification experiment: (a) The firs 1000 sequences of the PRBS applied to the expansion valve of the 6th MT cold reservoir; (b) Corresponding food temperature; (c) Power consumption of the MT compressor rack (note that the first 100 minutes are illustrated); (d) Suction pressure of the MT section. The whole simulation data for the temperature and pressure are provided in the plots which show appropriate amplitude of variations due to the excitation signal applied.

Before applying the subspace identification, a normally distributed zero-mean measurement noise with a standard deviation of $\sigma = 0.1$ was added to each output signal. This amount of σ seems to be large enough considering the precision of the measurement sensors, even for the commercial applications. The data set is divided into two separate sets, one for subspace identification and another model validation.

Prediction residuals — The goodness of fit between the nonlinear simulation model and the linear data-driven subspace model is calculated by

$$\text{fit} = \left(1 - \frac{\|y - \hat{y}\|_2}{\|y - \bar{y}\|_2}\right) \times 100\% \tag{9.46}$$

where y is the measured output, $\hat{y}$ is the one-step-ahead predicted output, and $\bar{y}$ denotes the average of the measured output data [31].

The values for N_f and N_p should be chosen small enough to achieve a parsimonious model and such that the identification performance does not drop significantly. Choosing $N_p = 5$ and $N_f = 10$ shows an acceptable fit in both the identification and the model validation.

The identification results for the food temperatures of the 5th MT cold reservoir is shown in Fig. 9.5a. The other cold reservoirs show similar results. The results for the electrical power consumption and suction pressure of the MT section are illustrated in Fig. 9.5b and Fig. 9.5c, respectively. Fig. 9.5d shows the improvement in $P_{o,MT}$ estimation that can achieve up to 68% fit by feedforward inclusion of the outlet pressure of the MT compressor rack.

Direct Load Control and SPC

A simple scenario for power reference generation is considered here to examine the proposed control system ability to regulate the power consumption with a high coefficient of performance while respecting the food temperature limits. However, the optimal power reference generation or the best regulation service design for refrigeration systems is not within the scope of the present work.

Suction Pressure Control

The effectiveness of the proposed pressure control method is investigated by comparing two simulations, one with normal pressure control (fixed set-point) and another with the proposed optimal pressure control in the loop. There is no DR event happen in this simulation. Since in both cases the temperatures are regulated at the middle of the range and the load conditions are the same, the same cooling capacity is applied in each case.

The sampling time is $T_s = 1$ min that is fast enough for the intended imbalance management service. The past and the prediction horizons are chosen as $N_p = 5$ and $N_f = 10$. The control horizon is set to $N_c = 5$. The temperature constraints for all MT units are considered the same as $1 \leq T_{food,MT} \leq 5$, and for LT units as $-23 \leq T_{food,LT} \leq -18$. The references for the normal operation are chosen as $T_{r,MT} = 3$ [°C] and $T_{r,LT} = -20.5$ [°C] for the food temperatures, and $P_{max,MT} = 36$ [$\times 10^5$ Pa] and $P_{max,LT} = 20$ [$\times 10^5$ Pa] for the suction pressures. Note that the suction pressures should not necessarily be regulated to the assigned set-points. The set-points for the pressures is equivalent to the evaporation temperature that can provide enough cooling capacity in the absence of the thermal load.

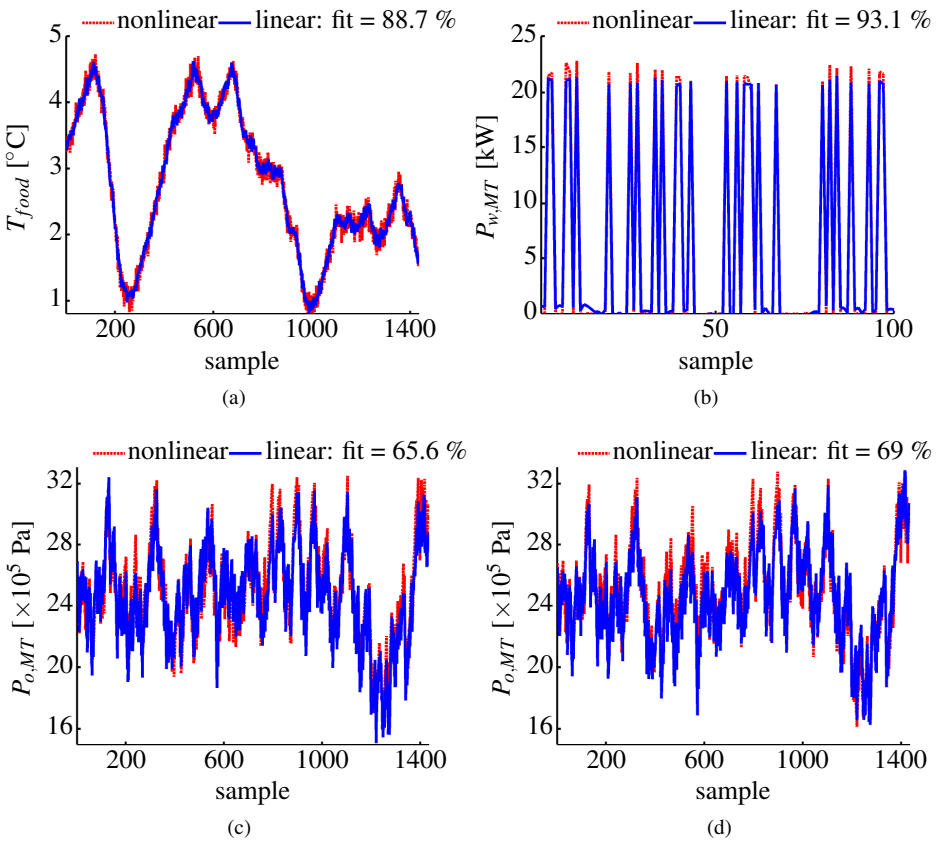

Figure 9.5: Model validation: (a) Food temperature in the 5th MT cold reservoir; (b) Power consumption of the MT compressor rack (note that the first 100 samples are illustrated); (c) Suction pressure of the MT section; (d) Model accuracy for the MT pressure is improved by feedforward inclusion of the outlet pressure of MT compressor rack.

Thus, the control effort keeps the pressure close to the upper constraint bound. The latter terms in the objective functions are assigned more weighting than the pressure term.

Regularization — During the power reference tracking, the food temperatures are constrained in the optimization problem. To avoid the likely infeasibility may occur by imposing such constraints, the following soft constraints are considered for the implementation. The food constraints are changed to

$$T_{food} < T_{max} + \varepsilon \tag{9.47}$$

$$T_{food} > T_{min} - \varepsilon \tag{9.48}$$

$$\varepsilon > 0 \tag{9.49}$$

where ε is a new optimization variable that should be close to zero. This method is also called softening the state constraints in the MPC literature. The following term should

also be minimized by adding it as a extra term into the objective function as

$$J_{reg} = w_{reg}\varepsilon^2. \tag{9.50}$$

where w_{reg} is the tuning weight.

In order to show the COP maximization achieved as one of the main contributions of the current work, the following simulation is performed. In conventional control of the refrigeration systems, cold reservoir temperatures are controlled by the thermostatic control of the valves around the temperature set-points, and the suction pressures are regulated to the nominal values that can provide enough low pressure and cooling capacity for the thermostatic action. Fig. 10.22a compares the power consumption of the conventional control to the case of the proposed optimal pressure control where a lower level of the consumption is achieved. Since the ambient loads are the same in both cases, and the temperatures are regulated to the same set-points, it can be concluded from (9.2) and (9.3) that the same cooling capacity is applied in each case. Therefore, the lower power consumption achieved by the control method implies that the higher COP is obtained according to (9.1). An energy saving of around 22% is achieved for the baseline operation. The suction pressure of the MT section is shown in Fig. 9.6b. As can be seen, the control algorithm tries to keep the pressure as high as possible.

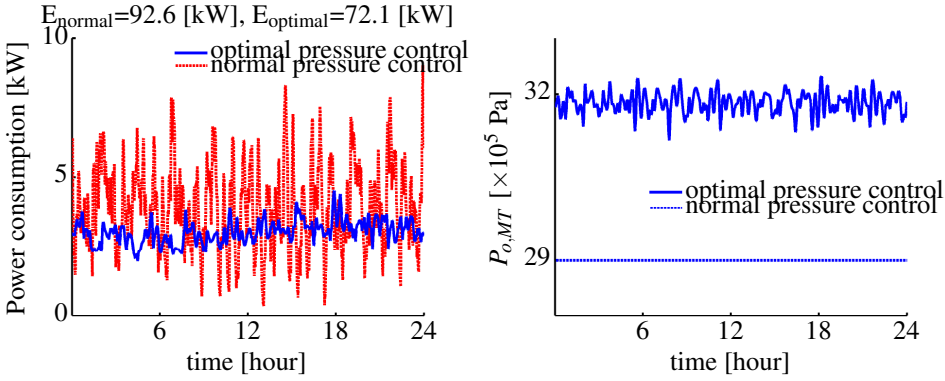

Figure 9.6: Baseline operation: (a) Total power consumption of both MT and LT compressor racks: Using conventional control the energy consumption is 92.6 [kWh] that is considerably decreased by using of the proposed optimal pressure control down to 72.1 [kWh]; (b) Suction pressure of the MT section (results for the LT section is similar).

Direct Load Control

A realistic balancing service scenario is intended to investigate the ability of the proposed advanced control strategy for direct load control of the large scale refrigeration system. The two other methods presented in [11] and [9] are also simulated for the sake comparison with the results achieved in this work. In each case, the control method is applied to the nonlinear simulation model derived in [26]. The total energy consumption of the compressor racks are compared for different simulations for the period when the DR events

are not activated (Off-DR period). It can compare the effectiveness of the different suction pressure controls to have a better energy efficiency. The tracking performance for the direct load control is compared for the DR periods.

Fig. 9.7 shows a period of 1300 min operation including the normal operation, a downward regulation service, and an upward regulation service. The default is the normal operation, where the food temperatures are kept at the middle of the range that provides a symmetric flexibility in terms of preparation for the regulation in both directions. At time 300 min, the imbalance contingency takes place which demands a downward regulation by raising the power to 6 kW in 5 minutes; keeping it regulated for 60 minutes; and then moving it back to the baseline in 5 minutes.

Subspace predictive control — The presented SPC scheme is utilized in the balancing service scenario mentioned earlier in this section. The linear data-driven subspace model is employed by SPC. Fig. 9.7a shows the simulation result. The control system is able to track the power reference during the DR event very well, even though it uses a linear data-driven subspace model (note that the method is applied to a nonlinear dynamical simulation tool [20]). The significant drop in the power consumption right after this service is due to the fact that the control system regulates the temperatures back to the middle points to (i) be ready for any likely upcoming balancing services; and (ii) release the stored energy as soon as possible to compensate for the extra power consumption during the regulation service. A similar imbalance contingency happens at time 900 min, but this time demands for an upward regulation service. The total energy consumption of the compressors for the Off-DR period is 57.5 [kWh] in this case.

Decentralized supervisory control — The decentralized control method presented in [11] is simulated here. The controller is designed at a supervisory level where the temperature references are manipulated to perform the direct load control. The supervisory control includes decentralized PI controllers equipped with anti-windup loops. The temperature limits are respected using an adaptive mechanism implemented as adaptive saturation filters [11]. The suction pressure is controlled by an heuristic algorithm. The simulation result is shown in Fig. 9.7b. The energy consumption in this case is 57 [kWh] which is very close to the SPC case.

Model predictive control — The model predictive control approach presented in [9] is simulated with the same scenario as the previous two cases. The MPC is based on a convex optimization and is designed for the direct load control. The suction pressure control is also included in the optimization scheme. The result of the MPC operation is shown in Fig. 10.24a where the energy consumption for the Off-DR period is 63.5 [kWh]. It is 9.4% higher than the energy consumption in the case of using SPC which shows that the proposed SPC approach can improve the coefficient of performance better than the MPC method presented in [9].

In a direct load control framework, the power tracking performance is important as the deviation from the reference signal might be penalized according to a contact with the aggregator. The tracking performance of the three simulated methods are compared in Fig. 9.7d where the DR periods are zoomed to have a better visibility. The decentralized control shows a good tracking performance during the upward regulation service but it cannot keep the power regulated during the downward regulation service. The MPC method, on the other hand, shows a good tracking performance in the both balancing services, but it has a slower response and there is also a delay in the response. The reason for the delay is that to be able to implement the MPC using a convex optimization, it is

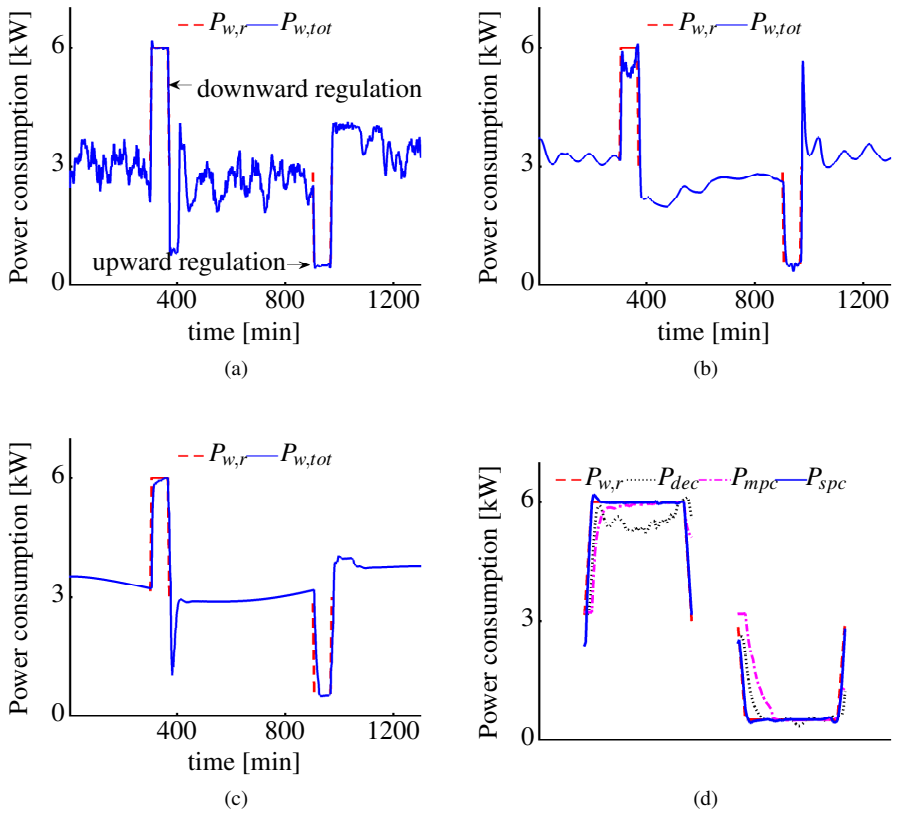

Figure 9.7: Total electrical power consumption of the compressor racks. The period includes two DR events: downward regulation service from 300 to 370 minutes, and upward regulation service from 900 to 970 minutes. (a) Simulation results after applying the proposed data-driven SPC method; (b) simulation using the decentralized supervisory control method [11]; (a) simulation using the MPC method [9]; (d) comparing the three methods in terms of the load following performance where P_{dec}, P_{mpc} and P_{spc} denote the power consumptions after applying the decentralized control, the MPC and the SPC, respectively. The two DR event periods are zoomed for a better visibility. The decentralized method cannot keep the power regulated during the downward regulation service. The proposed SPC method shows a superior tracking performance comparing to the other two methods.

suggested in [9] that the MPC sampling time should be higher than 4 minutes where a 5 minute sampling is chosen for the simulation. So the 5 minute delay in the response is due to the chosen sampling time for the control implementation. Finally, it can be seen that the proposed SPC outperforms both the other two methods in terms of the load following performance.

To provide more information about the SPC performance, the suction pressures are shown in Fig. 9.8a and Fig. 9.8b. They are pushed to the highest possible values while,

during the balancing services, are being changed accordingly. Fig. 9.8c and Fig. 9.8d show how the food temperatures in the 6th MT and the 4th LT cold reservoirs changes within the limits in accordance width the mode of operation. The other food temperatures also follow a similar pattern, so are omitted.

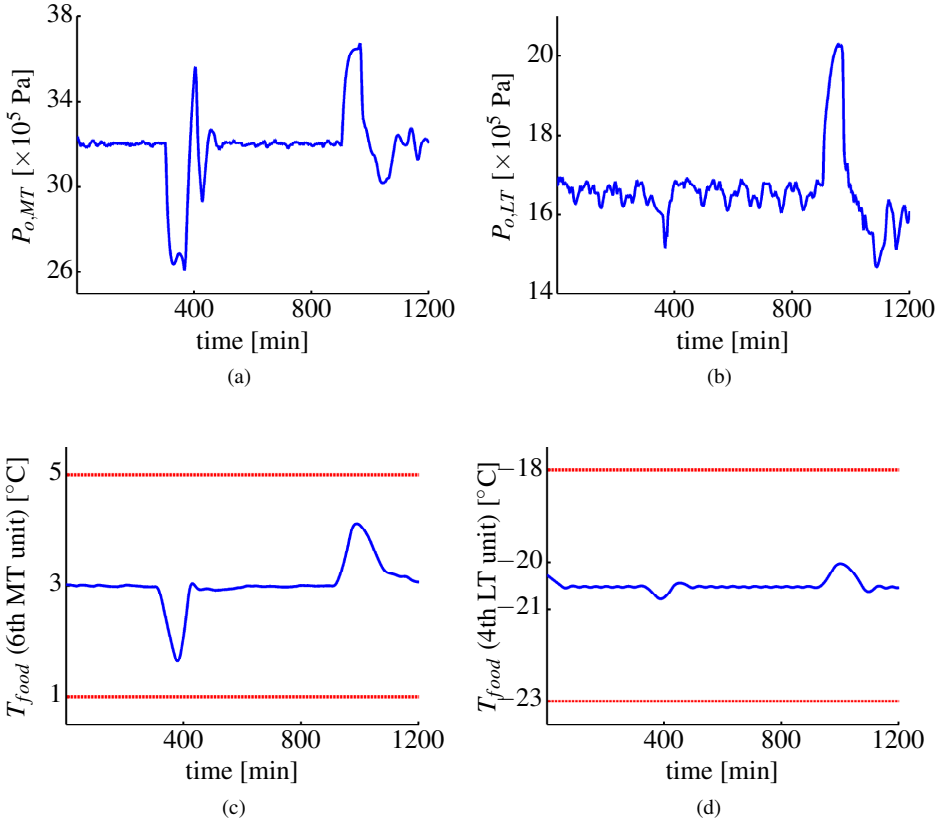

Figure 9.8: Direct load control: (a) MT suction pressure; (b) LT suction pressure; (c) Food temperature in the 6th MT cold reservoir; (d) Food temperature in the 4th LT cold reservoir. The proposed optimal suction pressure control keep the pressures to the highest possible point during the normal operation while being manipulated accordingly during the DR events. The constrained SPC algorithm can successfully keep the food temperatures within the constraint limits.

7 Conclusion

The problem of demand response implementation in the smart grid for large-scale refrigeration systems was addressed by directly controlling the electrical power consumption of the system. A data-driven predictive control based on the subspace identification method was shown as the key enabler of the envisioned DR services. The proposed control objective could compromise the two important factors: the system coefficient of performance

and the performance of the direct load control. Moreover, a method for input signal design for subspace identification of refrigeration systems was proposed. As an important practical consideration, the control design relies on a cheap solution with available measurements than using the expensive mass flow meters.

A thorough simulation study considering several practical matters such as food temperature constraints, actuator constraints, measurement noises and so on was carried out. The results showed 22% reduction in the energy consumption by the proposed COP improvement using the optimal pressure control. While keeping COP maximized, the control method was able to track a power reference accurately for the grid balancing service purposes. A comparative simulation study showed the superiority of the method in the load following performance comparing to the decentralized control method proposed in [11] and the MPC approach presented in [9].

The identification part in the subspace predictive control relies on a simple QR decomposition for which there exist fast and robust numerical computation algorithms. This provides an opportunity for adaptation of the method by online updating the subspace matrices [32]. The online adaptation can improve the control performance in case of variation of the system parameters, which is likely to happen in the large-scale thermal systems. The use of such adaptive algorithm will be investigated in a future work. Moreover, the future works should include the applications of the design in a whole supermarket system containing other systems like HVAC and heat recoveries as well as the refrigeration system.

References

[1] K. Y. Huang and Y. C. Huang, "Integrating direct load control with interruptible load management to provide instantaneous reserves for ancillary services," *IEEE Transactions on Power Systems*, vol. 19, no. 3, pp. 1626–1634, 2004.

[2] C. M. Chu and T. L. Jong, "A novel direct air-conditioning load control method," *IEEE Transactions on Power Systems*, vol. 23, no. 3, pp. 1356–1363, 2008.

[3] A. Arteconi, N. J. Hewitt, and F. Polonara, "Domestic demand-side management (DSM): Role of heat pumps and thermal energy storage (TES) systems," *Applied Thermal Engineering*, vol. 51, pp. 155–165, 2013.

[4] C. M. Chu, T. L. Jong, and Y. W. H, "A direct load control of air-conditioning loads with thermal comfort control," in *Proceedings of the IEEE PES General Meeting*, San Francisco, CA, USA, Jun. 2005.

[5] D. S. Callaway and I. A. Hiskens, "Achieving controllability of electric loads," *Proceedings of the IEEE*, vol. 99, no. 1, pp. 184–199, 2011.

[6] I. Stadler, "Power grid balancing of energy systems with high renewable energy penetration by demand response," *Utilities Policy*, vol. 16, pp. 90–98, 2008.

[7] J. L. Mathieu and D. S. Callaway, "State estimation and control of heterogeneous thermostatically controlled loads for load following," in *Proceedings of the 45th Hawaii International Conference on System Sciences*, Maui, HI, USA, Jan. 2012.

[8] A. Molina, A. Gabaldon, J. A. Fuentes, and F. J. Canovas, "Approach to multivariable predictive control applications in residential HVAC direct load control," in *Proceedings of the IEEE Power Engineering Society Summer Meeting*, Seattle, WA, USA, Jul. 2000.

[9] S. E. Shafiei, J. Stoustrup, and H. Rasmussen, "Model predictive control for flexible power consumption of large-scale refrigeration systems," in *Proceedings of the American Control Conference*, Portland, OR, USA, Jun. 2014, pp. 412–417.

[10] k. Kalsi, F. Chassin, and D. Chassin, "Aggregated modeling of thermostatic loads in demand response: A systems and control perspective," in *Proceedings of the 50 IEEE Conference on Decision and Control and European Control Conference (CDC-ECC)*, Orlando, FL, USA, Dec. 2011.

[11] S. E. Shafiei, R. Izadi-Zamanabadi, H. Rasmussen, and J. Stoustrup, "A decentralized control method for direct smart grid control of refrigeration systems," in *Proceedings of the 52nd IEEE Conference on Decision and Control*, Firenze, Italy, Dec. 2013, pp. 6934–6939.

[12] W. Favoreel, B. D. Moor, and P. V. Overschee, "Subspace sate space system identification for industrial processes," *Journal of Process Control*, vol. 10, pp. 149–155, 2000.

[13] P. V. Overschee and B. D. Moor, *Subspace Identification for Linear Systems: Theory, Implementation, Applications*, ser. Pearson Education. Kluwer Academic Publishers, 1996.

[14] S. Yin, X. Li, H. Gao, and O. Kaynak, "Data-based techniques focused on modern industry: An overview," *IEEE Transactions on Industrial Electronics*, vol. 62, no. 1, pp. 657–667, 2014.

[15] S. Yin, S. X. Ding, X. Xie, and H. Luo, "A review on basic data-driven approaches for industrial process monitoring," *IEEE Transactions on Industrial Electronics*, vol. 61, no. 11, pp. 6418–6428, 2014.

[16] W. Favoreel, B. D. Moor, M. Gevers, and P. V. Overschee, "Subspace predictive control," Katholieke Universiteit Leuven, Leuven, Belgium, Tech. Rep. ESAT-SISTA/ TR 1998-49, 1998.

[17] B. Zhang and J. Baillieul, "A two-level feedback system design to provide regulation reserve," in *Proceedings of the 52nd IEEE Conference on Decision and Control*, Firenze, Italy, Dec. 2013.

[18] A. Micchi and G. Pannocchia, "Comparison of input signals in subspace identification of multivariable ill-conditioned systems," *Journal of Process Control*, vol. 18, pp. 582–593, 2008.

[19] M. L. Darby and M. Nikolaou, "Identification test design for multivariable model-based control: An industrial perspective," *Control Engineering Practice*, vol. 22, pp. 165–180, 2014.

[20] SRSim, "A simulation benchmark for supermarket refrigeration systems using matlab," http://www.es.aau.dk/projects/refrigeration/simulation-tools/, Feb. 2013, accessed: February 2015.

[21] L. N. Petersen, H. Madsen, and C. Heerup, "ESO2 optimization of supermarket refrigeration systems: Mixed integer MPC and system performance," Department of Informatics and Mathematical Modeling, Technical University of Denmark, Tech. Rep., 2012.

[22] Y. T. Ge and S. A. Tassou, "Thermodynamic analysis of transcritical CO_2 booster refrigeration systems in supermarket," *Energy Conversion and Management*, vol. 52, pp. 1868–1875, 2011.

[23] G. Heffner, C. Goldman, B. Kirby, and M. Kintner-Meyer, "Loads providing ancillary services: Review of international experience," U.S. Department of Energy, Ernesto Orlando Lawrence Berkeley National Laboratory, Tech. Rep., May 2007.

[24] K. Trangbaek, M. Petersen, J. Bendtsen, and J. Stoustrup, "Exact power constraints in smart grid control," in *Proceedings of the 50th IEEE Conference on Decision and Control and European Control Conference*, Orlando, FL, USA, 2011.

[25] S. Rahnama, S. E. Shafiei, J. Stoustrup, H. Rasmussen, and J. D. Bendtsen, "Evaluation of aggregators for integration of large-scale consumers in smart grid," in *Proceedings of the 19th IFAC Word Congress*, Cape Town, South Africa, Aug. 2014, pp. 1879–1885.

[26] S. E. Shafiei, H. Rasmussen, and J. Stoustrup, "Modeling supermarket refrigeration systems for demand-side management," *Energies*, vol. 6, no. 2, pp. 900–920, 2013.

[27] R. Kadali, B. Huang, and A. Rossiter, "A data driven subspace approach to predictive controller design," *Control Engineering Practice*, vol. 11, pp. 261–278, 2003.

[28] T. Knudsen, "Consistency analysis of subspace identification methods based on a linear regression approach," *Automatica*, vol. 37, pp. 81–89, 2001.

[29] T. Soderstrom and P. Stoica, *System Identification*, ser. Prentice Hall International Series in Systems and Control Engineering. Prentice Hall, 1989.

[30] J. S. Conner and D. E. Seborg, "An evaluation of mimo input designs for process identification," *Industrial & Engineering Chemistry Research*, vol. 43, pp. 3847–3854, 2004.

[31] L. Ljung, *System Identification: Theory for the User*, ser. Prentice-Hall information and system sciences series. Prentice-Hall, 1987.

[32] M. Lovera, T. Gustafsson, and M. Verhaegen, "Recursive subspace identification of linear and nonlinear wiener state-space models," *Automatica*, vol. 36, pp. 1639–1650, 2000.

Paper G

Model Predictive Control of Hybrid Thermal Energy Systems in Transport Refrigeration

Seyed Ehsan Shafiei and Andrew Alleyne

This paper was published in:
Applied Thermal Engineering, 2015

Abstract

A predictive control scheme is designed to control a transport refrigeration system, such as a delivery truck, that includes a vapor compression cycle configured in parallel with a thermal energy storage (TES) unit. A novel approach to TES utilization is introduced and is based on the current and future estimate of the vehicle driving state and load prediction. This assumes vehicle communications are aware of the traffic state along the prescribed delivery route. For the test case under consideration, this paper first shows that a 17% savings in energy use is achieved for charging the TES by simply shifting the charging to the time when vehicle is moving above a threshold speed. Subsequently, a cascade control structure is proposed consisting of (i) an outer loop controller that schedules the TES charging profile using a receding horizon optimization, and (ii) an inner loop model predictive controller (MPC) which regulates the TES state of charge while maximizing a derived efficiency factor. For the test case under consideration, and utilizing a specifically derived performance metric, the cascaded control structure shows a 22% improvement over a baseline logic-based controller that focuses on state of charge regulation for the TES. A detailed nonlinear dynamical simulation tool for thermal system development is employed for control implementations.

Nomenclature:

Acronyms

TES	Thermal Energy Storage
MPC	Model Predictive Control
HVAC&R	Heating, Ventilation, Air-Conditioning and Refrigeration
PCM	Phase Change Material
VCC	Vapor Compression Cycle
COP	Coefficient of Performance
EV	Expansion Valve
EVAP	Evaporator
ACC	Accumulator
COMP	Compressor
COND	Condenser
REC	Receiver
P	Proportional
PI	Proportional-Integral

Greek Symbols

ω_c	compressor speed
η_v	volumetric efficiency
θ	azimuthal direction variable
ρ	density

Roman Symbols

MC	thermal mass capacity
T	temperature
$\dot{Q}$	heat transfer rate
UA	overall heat transfer coefficient

L_q	normalized zone fraction
s	solid fraction
p_{oi}	pressure ratio
P_w	power consumption
IC	integrated coefficient of performance
E	energy consumption
h	specific enthalpy
k	thermal conductivity
r	radial direction variable
c_p	specific heat capacity
A	area
V	volume

Subscripts

cr	container
e	evaporator
s	storage
w	wall
a	ambient
st	saturation
sh	superheat
eo	evaporator outlet
q	liquid
r	refrigerant
c	compressor
fus	fusion

1 Introduction

The energy usage of heating, ventilation, air-conditioning and refrigeration (HVAC&R) systems accounts for a significant amount of the total energy consumption in residential and commercial buildings. Consequently, improving the performance of these systems and minimizing their energy consumption have been the subject of many research efforts. An emerging technology for increasing the efficiency of HVAC&R systems in buildings is the active usage of thermal energy storage (TES) units. As an existing technology used in buildings, phase change materials (PCM) like ice storage tanks are employed by TES units which can provide a substantial heat storage capacity, [Dincer, 2002]. An exergy analysis in [Javani et al., 2014] shows that the overall exergy efficiency of cooling systems in hybrid electric vehicles can be increased when TES is used.

Often overlooked in the broader discussion is the energy consumption for various transport refrigeration applications which are also very important. The analysis provided by [Tassou et al., 2009] indicates that the refrigeration system commonly employed in food transportation can account for 40% of the total greenhouse gas emissions from the corresponding vehicle engines. The vapor compression cycle (VCC) system is the most common refrigeration system in use for transport refrigeration due to its high coefficient of performance (COP) compared with alternative solutions [Tassou et al., 2009]. In the thermal system literature, the integration of conventional refrigeration technology with

TES results in a hybrid refrigeration system. Optimization of these hybrid systems is the main focus of the present work since the optimization of the individual VCC process has been previously addressed in the literature.

The application of TES in transport refrigeration systems is not quite as mature as in the building HVAC case [Walsh et al., 2013]; primarily because the constraints (size, weight, etc.) are more stringent. Depending on the application, different configurations have been proposed. Three different placements of the TES, for passive use of PCM in contact with the suction and liquid lines, are investigated in [Wang et al., 2007]. The proposed layouts in [Wang et al., 2007] can all be framed as a series configuration as explained in [Fasl, 2013]. Series arrangements have benefits and drawbacks, as explained in [Fasl, 2013]. For transportation applications with highly transient loadings, a parallel configuration may provide more rapid response to load disturbances. In [Fasl et al., 2014], a detailed nonlinear thermal model of a refrigeration system is presented with a parallel configuration for an active TES unit. The TES is configured in parallel with the evaporator heat exchanger and a heuristic switching control logic is proposed to deal with the different modes of operations like charging, discharging, etc.

It is shown in [Fasl et al., 2014] that the system efficiency is improved by incorporating an active TES unit with simple switching logic. The question remains as to whether further energy efficiency can be achieved by advanced control design for this application. In particular, is it possible to take advantage of existing vehicle information such as GPS, traffic status, and traffic predictions? This work seeks to answer that question by utilizing on-line models and prediction in decision making; this naturally leads to model predictive control (MPC) algorithms. MPC has been widely used in HVAC&R applications as an advanced control technique for effectively accommodating input (e.g compressor) and output (temperature range) constraints. Several different studies have successfully applied MPC to building HVAC&R systems. In [Ma et al., 2012a] a simple switching nonlinear model of a storage tank is developed and weather prediction is integrated into an MPC scheme for optimization of a chiller's operation. A novel configuration of a TES in a water chiller system is presented in [Cole et al., 2012] where the MPC is proposed to optimize the charge and discharge of the TES for minimizing both the energy consumption and operation cost. A simplified linear thermal model is developed in [Candanedo et al., 2013] to predict the required cooling power which is utilized as the main manipulated variable for the MPC formulation in the control of a building. The problem of model uncertainty in different operating conditions is considered in [Kim, 2013] where multiple local models are used in the MPC formulation to make it responsive to the entire operation regime. The results show the superior performance comparing to the traditional logic based control. By comparison there are relatively few efforts to use MPC in the transport refrigeration domain even though it may benefit even more than building systems due to the tight regulations on food temperature and, as will be discussed, the ubiquity of real-time traffic information.

The specific transport refrigeration problem considered in this study is differentiated from the building energy management challenge [Ma et al., 2012b] in two aspects: (i) the disturbance profile contains more rapid transients due to the nature of the delivery process; and (ii) building control systems typically focus on economic cost plus performance optimization while the focus here is on an energy plus performance optimization. Economic cost is less relevant than buildings because there is no dynamic pricing of the energy asset (vehicle fuel) as there is for grid electricity for buildings.

In this paper, we assume two basic states of the vehicle: (a) driving at some nominal speed, similar to a highway or major road, and (b) driving at a very low, or zero, speed akin to being in traffic or stopped to deliver goods. The TES unit is utilized depending on which driving state the vehicle is in. An optimal charge scheduling is proposed to distribute the charging demand across the drive cycle using load predictions achieved by predicting both the anticipated driving profile and the thermal load from the ambient temperature. The driving profile can be easily obtained nowadays from GPS references and cloud-based traffic predictions. Similarly, ambient temperatures are accessible at any location along a route via cellular communication. Fig. 10.1 shows the external information utilized in the thermal load prediction.

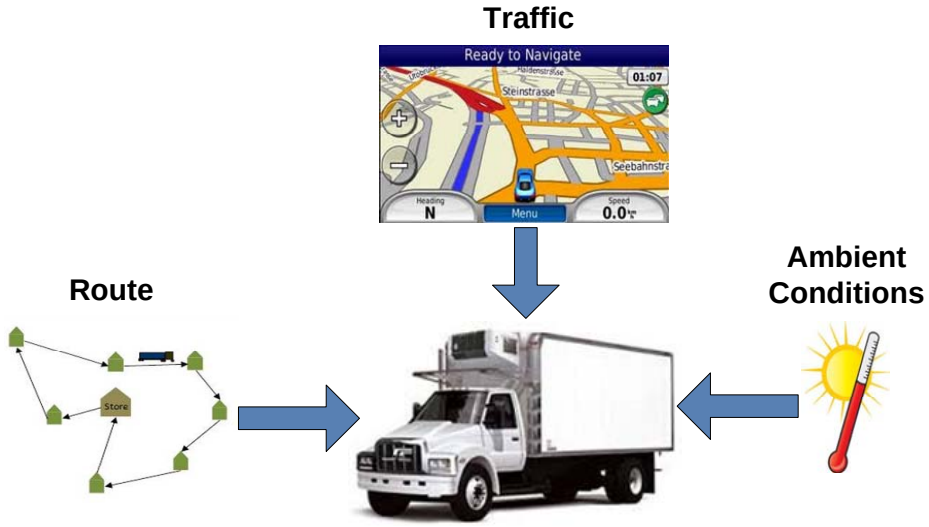

Figure 10.1: Driving profile and environmental conditions are used for thermal load predictions during the heavy traffic periods. Delivery paths and GPS traffic data are used for prediction of the driving profile.

2 System Description and Problem Statement

This section briefly details a parallel hybrid VCC system that was previously developed in, [Fasl et al., 2014]. Subsequently, the proposed control problem under study is described.

Parallel Hybrid VCC System

Fig. 10.2 shows a VCC system that includes a TES unit operating in a parallel configuration. A variety of hybrid configurations are thoroughly discussed and analyzed in [Fasl, 2013] along with the choice of a parallel system for transport refrigeration applications.

Starting at the low pressure side, the refrigerant in a nominal vapor compression cycle flows through the evaporator where the container temperature is cooled down. An expansion valve (EV_1) controls the refrigerant mass flow rate to ensure superheated refrigerant

exits the evaporator. The superheated refrigerant flows into the suction line where a liquid accumulator (ACC) is placed. The compressor (COMP) raises the pressure and enthalpy of the refrigerant by performing work on it. The high pressure refrigerant enters the condenser (COND) where heat is transferred from the hot refrigerant to the ambient air. Then the refrigerant flows into a liquid receiver (REC). From the receiver, it enters the expansion valve where the cycle starts again.

The TES unit is in parallel with the evaporation unit. If the refrigerant circulates into the TES, thermal energy is transferred between the refrigerant to the PCM contained in the TES. In our configuration, heat will be taken from the PCM by the refrigerant. This will lead to a solidification of the PCM in the TES and is considered the charging mode. The TES charging operation is controlled by the expansion valve (EV_2). The TES also has a discharging mode of operation. Similar to the evaporator, the TES unit is also equipped with a fan to circulate air from the container across the unit. The inlet air exchanges energy with the TES in a manner that cools the air returned to the container and heats the TES. As the solid fraction of PCM is reduced, the amount of latent heat capacity remaining is being reduced. Consequently, when the TES fan is running, the unit is discharging. Depending on the thermal load, the TES can run independently or in parallel with the evaporator to boost the cooling capacity. Therefore, the parallel VCS system in Fig. 10.2 has 4 modes of active operation as detailed in [Fasl, 2013]: (i) using the refrigeration system only, (ii) charging of the TES either with or without active refrigeration, (iii) using the TES only, and (iv) both the refrigeration and TES systems active, termed boost. In the current work, we consider a subset of the first three modes to limit complexity and demonstrate potential benefits.

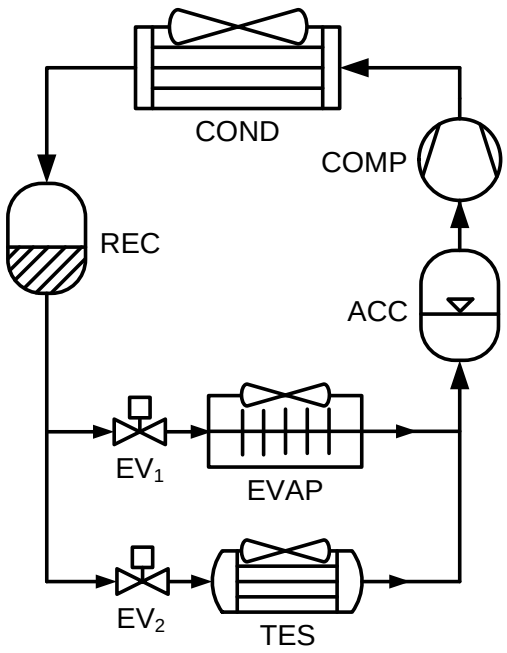

Figure 10.2: A typical parallel hybrid configuration for a VCC system.

Problem Statement

Given the flexibility of the hybrid transport VCC system, how best is to use this capability? The basic hybrid strategy problem is as follows. We seek to maintain a given temperature within the container and do so as efficiently as possible. However, there are now multiple modes in which to achieve this objective. Therefore, the first decision is which mode of operation to use at any given time. Here we propose to use the current and future times as source of information to choose the best mode of operation for a specified time horizon. Choosing the mode of operation is the first part of the overall problem.

Once the mode of operation is chosen, the system focus becomes operational efficiency. The controller must choose the optimal operating condition to meet the demands. The demands include both maintaining container temperature as well as providing sufficient cooling to charge the TES if that is the current mode. Assuming the primary energy consumer is the compressor, the goals can be expressed as achieving temperature setpoints, providing charging if necessary, and doing so at the maximum efficiency of the compressor.

This two-tiered control problem of mode selection followed by operational efficiency is best met by a two-tiered controller design. That is the focus of the next section.

3 Control Strategy

As mentioned there are two aspects to the controller design. First, a logic based algorithm must decide what mode of operation is best. Second, a continuously operating algorithm must achieve specific setpoints while minimizing energy consumption. For this purpose a two stage controller is developed to match the dual stage objectives.

The three modes of operation under consideration are defined, based on TES activity, as: *normal*, *charging* and *discharging*. Table 10.1 presents the control actions for each mode. In the normal operation, the container temperature is regulated by controlling the compressor speed in a standard refrigeration cycle while the evaporator fan is set to its maximum value. In the charging mode, the compressor regulates the charging demand while the evaporator fan regulates the container temperature. In the discharging mode, the container temperature is regulated by controlling the TES fan.

Table 10.1: Three different modes of operation considered.

Mode	Evap. valve	TES valve	Evap. fan	TES fan	compressor
normal	PI	closed	on	off	PI
charging	PI	PI	P	off	MPC
discharging	closed	closed	off	P	off

In order to deal with the two-tiered controller approach outlined in Section 2.2, a cascade control loop is proposed in Fig. 10.3. An outer optimization loop is responsible for selecting the desired charge to hold in the TES, and whether or not the TES is active, based on the current and predicted thermal loads. An inner control loop includes an MPC to control the compressor for maximizing efficiency as well as proportional (P) and proportional-integral (PI) controllers for the other components. The PI controllers of expansion valves regulate the required superheat temperatures, and the P controllers of the evaporator and TES fans regulate the container temperature in the charging and

discharging mode. In the normal mode, compressor speed is controlled by a simple PI controller to regulate the container temperature while the evaporator fan is turned on.

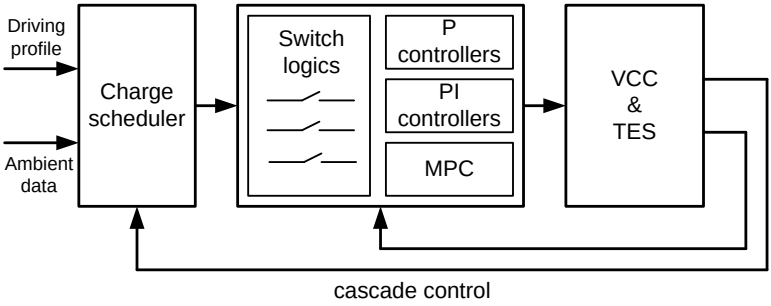

Figure 10.3: Control strategy for handling operating modes and decentralized local control loops, and inclusion of optimal control scheme.

Less common than PI control, model predictive control is a technique for digital implementation of optimal control formulations. Different constraints in the system such as input saturation limits and state or output constraints are handled using this method which also accommodates systems with multiple inputs and outputs. Fig. 10.4 shows the basic idea of the MPC implementation for set-point regulation problems. At time instant k, an optimization problem is solved for the next N_p samples — known as the prediction horizon — where the future output is predicted using a model. The future inputs can freely move within the next N_c samples — known as the control horizon — to minimize the output deviation from the set-point and the first move in the predicted inputs is applied as the control signal to the system. In the next time instant the optimization problem will be solved again by updating the output measurements and moving the prediction and control horizon one step forward.

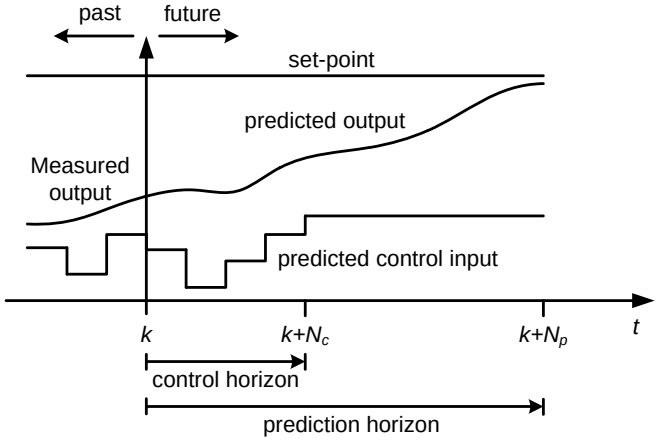

Figure 10.4: A typical MPC implementation for set-point regulation problems which is also known as receding horizon optimal control.

4 Gray-Box Modeling

The mode selection charge scheduler in the outer loop of Fig. 10.3, as well as the MPC in the inner loop, both rely on model-based optimization approaches. Therefore, a proper model that balances complexity and accuracy is important. The highly nonlinear and high order model obtained in [Fasl, 2013, Fasl et al., 2014] using a first principles method makes the optimization problem nonlinear and non-convex. As such, while it is suitable for system simulation and controller evaluation, it is not suitable for on-line decision making. This section describes a simpler gray-box model that captures only the essential dynamics of the refrigeration and TES system thereby allowing a convex optimization formulation for MPC to be implemented. In this section, we present the subsystem models; Section 6 demonstrates the validity of the assumptions.

Container Model

The dynamics of the container being cooled by the hybrid VCS/TES are described by the following equations based on the energy balance principle and lumped parameter modeling approach.

$$MC_{cr}\frac{dT_{cr}}{dt} = -\dot{Q}_e - \dot{Q}_s + \dot{Q}_w \tag{10.1}$$

$$MC_w\frac{dT_w}{dt} = -\dot{Q}_w + \dot{Q}_a \tag{10.2}$$

where MC_{cr} and MC_w are the thermal mass capacities of the container air and wall, T_{cr} and T_w are the temperatures of the container air and wall. Again, we are lumping the entire container air temperature into one variable and similarly with the container wall. The heat transfer equations are given by

$$\dot{Q}_e = UA_e(T_{cr} - T_{st}) \tag{10.3}$$

$$\dot{Q}_s = UA_s(T_{cr} - T_s) \tag{10.4}$$

$$\dot{Q}_w = UA_w(T_w - T_{cr}) \tag{10.5}$$

$$\dot{Q}_a = UA_a(T_a - T_w) \tag{10.6}$$

where $\dot{Q}_e$ is the cooling capacity applied by the evaporator, $\dot{Q}_s$ is the cooling capacity applied by the thermal storage unit when activated, $\dot{Q}_w$ is the heat transfer from the container wall to the container air, and $\dot{Q}_a$ is the heat load from the ambient temperature T_a. The container wall temperature is represented by T_w. The temperature of the container air is given by T_{cr}. The temperature of phase change material inside the TES unit is lumped in T_s which is simply referred to as the storage temperature. The corresponding lumped parameter heat transfer coefficients are denoted by UA with appropriate subscripts.

Due to the parallel configuration, both the TES and the evaporator are connected to the same suction line. Assuming the piping losses are negligible, the suction pressure, and therefore the saturation temperature, of the refrigerant in both units is the same. The common saturation temperature is represented by T_{st}.

The evaporator heat transfer is important in determining the simple gray box models desired. [Shafiei et al., 2013] showed that UA_e has an approximately linear relationship

with the latent mass inside the evaporator. However, this latent mass is not measurable and any type of estimation would require mass flow measurements that are usually not available in commercial applications. To deal with this problem, the following simple model is put forward. Section 6 will later examine the validity of the model.

Since the superheat, ΔT_{sh}, can be measured using temperature and pressure sensors, it can also be used to estimate UA_e.

$$\Delta T_{sh} = T_{eo} - T_{st}; \tag{10.7}$$

where T_{eo} is the refrigerant temperature at the outlet of the evaporator. Within the superheated zone, there is no liquid refrigerant only vapor. Fig. 10.5 illustrates the evaporator volume divided into two parts including the liquid refrigerant and the superheated zone. Hence if we had an idea of the fraction of the evaporator that was superheated, we could use it to estimate the amount of liquid contained in the rest of the evaporator.

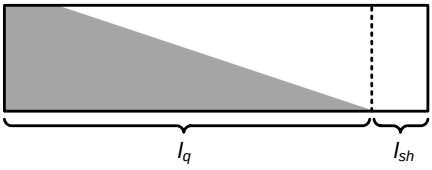

Figure 10.5: Illustration of the evaporator volume. l_q shows the length of the evaporator part including the liquid refrigerant and l_{sh} shows the length of the superheated zone.

We introduce a normalized zone fraction including the liquid mass, L_q, as follows:

$$L_q = 1 - \frac{\Delta T_{sh}}{\gamma_{sh}}, \tag{10.8}$$

where γ_{sh} is a positive constant used to project the superheat variations onto a smaller set. For example, it can be chosen as the norm of the superheat signal captured from a simple superheat regulation test. The overall heat transfer coefficient for the evaporator is then estimated by a linear assumption

$$UA_e = a_0 + a_1 L_q, \tag{10.9}$$

where a_i are constants. Note that the constant a_1 contains the conversion from the normalized zone fraction to actual refrigerant mass. This gives a linear approximation of the nonlinear system behavior.

TES Model

Because of the importance of the TES in hybridization of refrigeration systems and considering it as the focus of the control design in this work, this section first presents the TES dynamical model developed by [Fasl, 2013] in some detail. Subsequently, a simplified model will be proposed and justified. The geometry of the TES is a bank of coaxial cylinders. Fig. 10.6 shows a schematic of the interior and exterior view of the unit. It will be charged by flowing the refrigerant through the inner cylinder, where PCM is placed within the annulus, and will be discharged by flowing the air over the tubes.

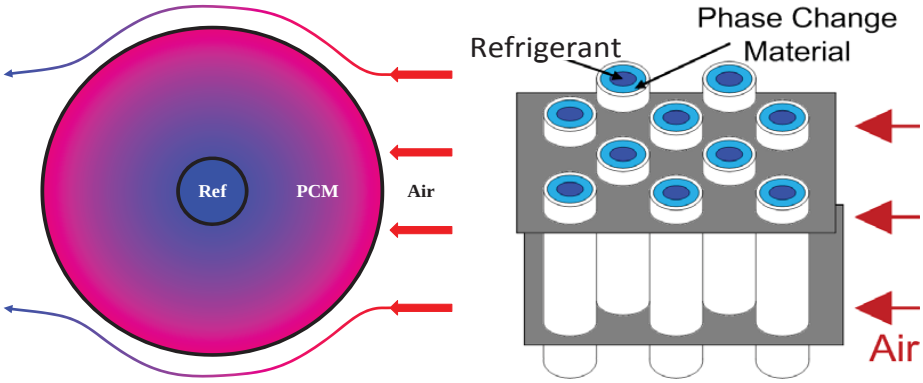

Figure 10.6: Geometry of a TES unit [Fasl, 2013]: (a) interior view of a cylinder; (b) exterior view of the unit.

Full Model

The fixed grid method [Dincer and Rosen, 2010] is employed to solve the heat transfer and phase change problem where the enthalpy is used for the thermodynamic state variable [Fasl, 2013]. Using this method, the PCM section is divided into several fixed volume nodes, and energy conservation equations are solved for each node. In order to facilitate the heat transfer through the PCM, metallic fins are added to the segments that span radial distance of the annulus. Fig. 10.7 shows a schematic view of the fixed grid method for N number of nodes with fin enhancements.

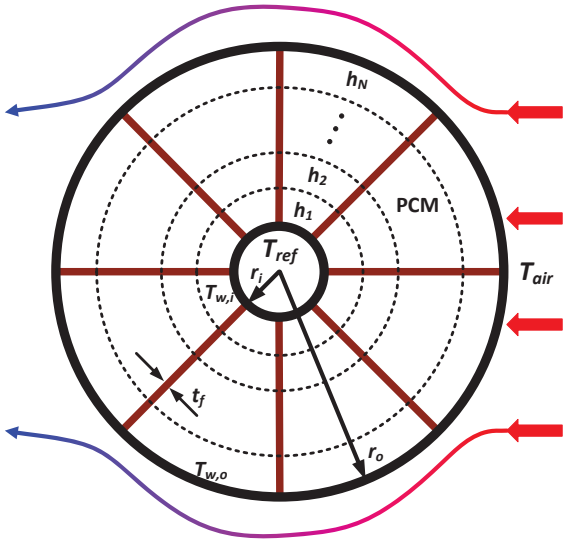

Figure 10.7: A schematic view of the fixed grid method where the PCM is separated into N number of nodes including fin enhancements [Fasl, 2013]. $T_{w,i}$ and $T_{w,o}$ are the temperatures of the inner and outer tube walls, and T_{ref} denotes the refrigerant temperature.

The following assumptions have been made to avoid a very high order model while capturing the relevant dynamics within the PCM.

Assumption 1*: Heat is transferred in the radial direction through the fins and in the azimuthal direction between the PCM and the fin in each node.*

Assumption 2*: The PCM has lumped thermodynamic properties in single phase regions.*

Assumption 3*: The pressure in the PCM is constant over time, space and phase.*

Assumption 4*: The density in the PCM is constant over time and space but can vary through phase change.*

Assumption 5*: The fin nodes are assumed to have no heat storage capacity.*

Assuming (4), there is no need for conservation of mass to be calculated. Each interior node in Fig. 10.7 is a closed system with no inlet and outlet mass flows and heat transfer only through conduction. So the conservation of energy is given by

$$\frac{\partial(\rho h - P)}{\partial t} = \nabla(k\nabla T), \tag{10.10}$$

where ρ is the density, h is the enthalpy, P is the pressure, k is the thermal conductivity and T is the temperature. (10.10) is applied for the PCM segments and fins to derive the dynamical equations. The derivation results are given in the following and the details of calculations are found in [Fasl, 2013]. The dynamics of the jth interior fin node is given by

$$\left(\frac{k_f t_f}{\Delta r} + \frac{k\Delta r}{r_j \Delta\theta}\right) T_{f,j} - \left(\frac{k_f t_f}{2\Delta r}\right)(T_{f,j-1} + T_{f,j+1}) = \left(\frac{k\Delta r}{r_j \Delta\theta}\right) T_j, \tag{10.11}$$

where t_f is the fin thickness, r is the node radius defined at the radial center of each node, θ is the azimuthal direction angle, and subscript "f" denotes the fin related variables. The grid model is designed such that there is an equal radial spacing (Δr) between node centers. For the innermost and the outermost nodes we have $T_{f,0} = T_{w,i}$ and $T_{f,N+1} = T_{w,o}$. The conservation of energy equation for the jth PCM node results in

$$\frac{dh_j}{dt} = \frac{\pi k}{\rho_j(2\pi r_j - N_f t_f)}\left[\frac{2r_j - \Delta r}{(\Delta r)^2}(T_{j-1} - T_j) + \frac{2r_j + \Delta r}{(\Delta r)^2}(T_{j+1} - T_j) + \frac{2}{\pi r_j \Delta\theta}(T_{f,j} - T_j)\right], \tag{10.12}$$

where N_f is the number of fins. Defining the enthalpy to be zero at the point where the solid PCM just begins to melt, the enthalpy of the liquid PCM at the point of beginning to freeze would be equal to the latent heat of fusion of the PCM (h_{fus}). The temperature of the jth PCM node is then defined as

$$T_j = \begin{cases} \frac{h_j}{c_{p,s}} + T_m & \text{if } h_j < 0 \\ T_m & \text{if } 0 \le h_j < h_{fus} \\ \frac{h_j - h_{fus}}{c_{p,l}} + T_m & \text{if } h_j \ge h_{fus}, \end{cases} \tag{10.13}$$

where T_m is the freezing point temperature of the PCM, and $c_{p,s}$ and $c_{p,l}$ are the specific heat capacity of the solid and liquid PCM.

In a latent heat TES, the state of charge is equivalent to the solid fraction of the PCM which can be algebraically calculated for an individual node as

$$s_j = \begin{cases} 1 & \text{if } h_j < 0 \\ \frac{h_j}{h_{fus}} & \text{if } 0 \le h_j < h_{fus} \\ 0 & \text{if } h_j \ge h_{fus}, \end{cases} \tag{10.14}$$

The total solid fraction of the TES (s_f) can then be calculated from the individual volumes and solid fractions of each node as

$$s_f = \frac{\sum_{j=1}^{N} V_j s_j}{\sum_{j=1}^{N} V_j}. \tag{10.15}$$

When discharging, the TES operates like an evaporator unit equipped with fans and cools down the container by applying the cooling power $\dot{Q}_s$. The complete evaporator model as well as the other units like the condenser, compressor, expansion valves, liquid accumulator, etc. are found in [Fasl, 2013]. Those models are employed for simulation of the hybrid transport refrigeration in this work.

Simplified Grey-Box Model

The detailed TES model presented in Section 4 includes a broad range of dynamics and is too detailed to be directly employed by an on-line optimization technique. In this section, it is shown that the PCM solid fraction within the TES can be estimated in two ways: (a) in terms of the cooling power applied by the VCC system when the TES is charging, and (b) in terms of the cooling capacity applied by the TES when it is discharging. When charging, it is assumed that the solid fraction is linearly correlated with the cooling energy received from the VCC, *i.e.,*

$$\frac{ds_f}{dt} = K_s \dot{Q}_{rs}, \tag{10.16}$$

where s_f is the PCM solid fraction, K_s is a constant, and $\dot{Q}_{rs}$ is the heat transfered from refrigerant to the storage given by

$$\dot{Q}_{rs} = UA_{rs}(T_s - T_{st}), \tag{10.17}$$

where UA_{rs} is the overall heat transfer coefficient between the refrigerant and the storage. It turns out that the UA_{rs} does not remain constant for different operating conditions at different suction pressures. Here it is assumed there exist a linear relationship between UA_{rs} and the suction pressure P_{suc} as $UA_{rs} = \alpha_s P_{suc}$ where α_s is a constant. This simple assumption for UA_{rs} would result in a better estimation of the solid fraction comparing to the case where it is assumed constant. The estimation result is shown in Fig. 10.13a. Combining (10.16) and (10.17) gives the first order relationship

$$\frac{ds_f}{dt} = K_{rs}(T_s - T_{st}), \tag{10.18}$$

with charging constant $K_{rs} = K_s UA_{rs}$. In a charging experiment, the values of K_s and α_s cannot be identified independently. Fortunately, the storage parameter K_s can be estimated independently in the discharging experiment as will be explained in the following.

Similar to the charging mode, when the storage is discharging, the dynamic behavior of the PCM solid fraction is given by a simple integrator

$$\frac{ds_f}{dt} = -K_s \dot{Q}_s \tag{10.19}$$

with $\dot{Q}_s$ given by (10.4) and the discharging constant K_s. By estimating K_s from (10.19), and K_{rs} from (10.18), the parameter UA_{rs} can be uniquely identified.

Fig. 10.8a shows the cooling power applied to the container by discharging the TES. The result of the simplified model is very close to that of the full model. Fig. 10.8b presents the variation of K_s across discharging time calculated from (10.19) where s_f and Q_s are obtained from the full model. It shows that K_s can be considered constant in the simplified model.

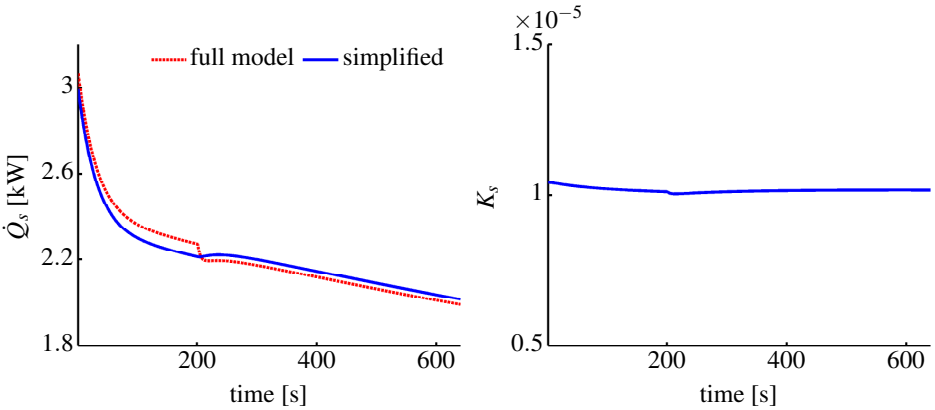

Figure 10.8: Simplification of the TES model: (a) cooling power applied to the container when discharging the TES; (b) justification of assuming K_s to be constant.

Compressor Model

The compressor drives the mass flow throughout the entire VCC system and can be used to control the suction pressure (or equivalently the saturation temperature). Without a direct mass flow measurement, the relation between the compressor speed and the saturated refrigerant temperature can be reasonably modeled as a black-box transfer function

$$T_{st}(s) = G(s)\omega_c(s), \tag{10.20}$$

where ω_c is the compressor speed used here as a control input variable.

Discretization

While the basic energy balances used to create the low dimensional models are all based on continuous time rate assumptions (d/dt), the implementation of the controller will

take place in the discrete-time digital environment of a micro-processor. Therefore a conversion is necessary with the continuous time t being replaced by the discrete time index k. The dynamical equations presented in the previous 3 sub-sections are discretized using the Euler method. The container dynamics (10.1)–(10.6) are discretized as

$$\begin{bmatrix} T_{cr}[k+1] \\ T_w[k+1] \end{bmatrix} = \mathbf{A}_d \begin{bmatrix} T_{cr}[k] \\ T_w[k] \end{bmatrix} + \mathbf{B}_d \begin{bmatrix} T_{st}[k] \\ T_a[k] \end{bmatrix}, \tag{10.21}$$

where $\mathbf{A}_d$ and $\mathbf{B}_d$ are state-space matrices with appropriate dimensions. The compressor dynamic is similarly described by

$$\begin{cases} X_{st}[k+1] = \mathbf{A}_{st} X_{st}[k] + \mathbf{B}_{st}\omega_c \\ T_{st}[k] = \mathbf{C}_{st} X_{st}[k] \end{cases}, \tag{10.22}$$

where $X_{st} \in \mathbb{R}^n$ is the state vector with the same dimension, n, as the order of the transfer function $G(s)$ in (10.20), and $\mathbf{A}_{st} \in \mathbb{R}^{n\times n}$, $\mathbf{B}_{st} \in \mathbb{R}^{n\times 1}$ and $\mathbf{C}_{st} \in \mathbb{R}^{1\times n}$ are state-space matrices. The TES dynamics (10.18) and (10.19) are discretized as

$$s_f[k+1] = s_f[k] + t_s K_{rs}\left(T_s - T_{st}\right), \quad k \in \mathbb{I}^{ch} \tag{10.23}$$

and

$$s_f[k+1] = s_f[k] - t_s K_s \dot{Q}_s, \quad k \in \mathbb{I}^{dis} \tag{10.24}$$

where t_s is sampling time, and $\mathbb{I}^{ch}$ and $\mathbb{I}^{dis}$ are the sets representing charging and discharging time periods.

Remark 9*: The sampling time of the outer loop charge scheduler in Fig. 10.3 is slower than that of the inner loop MPC. Therefore, when presenting or using the discrete-time equations for either the outer or inner loops, it is assumed that the corresponding sampling time is used for discretization.*

Remark 10*: The time varying parameters UA_e and UA_{rs} are updated at each sampling instant, but kept constant during the horizon of an inner-loop optimization calculation. This simplification is needed for convex formulation.*

5 Control System Design

The design of the two cascaded loops proposed in Section 3 is provided in this section.

Performance Objective

As stated in Section 2, one of the control objectives is to minimize the power/energy consumption of the overall VCC/TES system by focusing on the compressor consumption. In general a detailed derivation of the compressor power in terms of the relevant variables such as compressor speed or suction/discharge pressure leads to a nonlinear and non-convex formulation which is not appropriate for MPC implementations [Shafiei et al., 2014]. Empirical evidence indicates that the volumetric efficiency of the compressor can be estimated as a 2nd order convex function of the compressor speed and the pressure ratio across the compressor [Rasmussen and Alleyne, 2006] as

$$\eta_v = c_1\omega_c + c_2\omega_c^2 + c_3\omega_c p_{oi} + c_4 p_{oi} + c_5 p_{oi}^2 \tag{10.25}$$

where c_i are constants and p_{oi} is the ratio of the outlet pressure over the inlet pressure of the compressor. The relationship in (10.25) will be used for the MPC formulation.

Charge Scheduler

The outer loop in Fig. 10.3 schedules the charging demands for a specific period of time using a given driving profile and thermal load predictions. Here, for simplicity, we classify traffic data patterns into either light or heavy traffic with the primary difference being average vehicle speed. Only two states of vehicle velocity are used for simplicity and clarity of exposition. Clearly, more detailed gradations of traffic patterns can be utilized to extend the results presented here but the fundamental framework will apply. In the light traffic case, the vehicle travels with an average nominal speed V_N and in the heavy traffic case, it operated with average speed V_0. These two average speed levels can be identified by analyzing the historical vehicle speed and road data to determine appropriate classifications. The specifics of traffic data analysis and identification of average speed levels are outside the scope of the current study but readers may refer to [Walkowicz et al., 2014] for details of how this would be accomplished.

For a time horizon T_p, using the on-line traffic and GPS data and the average vehicle speed, a driving profile may be obtained. An example of such profile is shown in Fig. 10.9. Maximizing the COP associated with the air flow over the condenser, the intuition would be that the storage unit should be charged during the light traffic (high average velocity) periods and discharged during the heavy traffic (low average velocity) intervals. Section 6 will examine the extent to which this intuition would be correct.

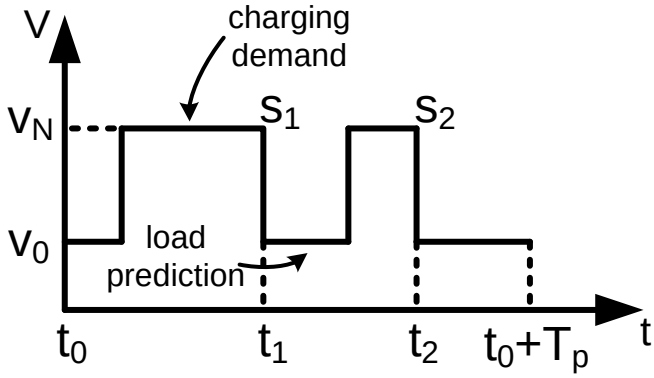

Figure 10.9: An example of a predicted driving profile.

In order to calculate the thermal load in the discharging periods, the steady-state conditions of (10.1) and (10.2) are used with the condition that $\dot{Q}_e = 0$. Thus, the required cooling capacity provided by the TES unit is given by

$$\dot{Q}_s = \dot{Q}_a = UA_a(T_a - T_w), \tag{10.26}$$

and the corresponding charging demand for the ith interval l_i is calculated using (10.19) and (10.26) as

$$l_i = K_s UA_a \int_0^{\Delta T_i} (T_a - T_w)dt, \quad i = 1, \ldots, n_p \tag{10.27}$$

where ΔT_i represents the length of the ith discharging interval, and n_p is the number of charging or discharging intervals during the prediction horizon.

The charge scheduling problem is solved by optimal distribution of charging demand among the available charging periods. In order to fulfill the charging demand required for the ith discharging period, the following constraint is introduced:

$$s_i \geq l_i \tag{10.28}$$

where s_i is the solid fraction at time t_i, *i.e.,* $s_i = s_f(t_i)$. The following constrained optimization problem is proposed for TES charge scheduling:

$$\begin{aligned}
\min_{\omega_c,\, s_f} \quad & -\sum_{i=1}^{N_o} \eta_v + W_o \sum_{i=1}^{N_o} \|\Delta\omega_c\|_2^2 \\
\text{subject to} \quad & \\
& \begin{cases} X_{st}[k+1] = \mathbf{A}_{st} X_{st}[k] + \mathbf{B}_{st}\,\omega_c & \\ T_{st}[k] = \mathbf{C}_{st} X_{st}[k] & \end{cases} \quad k \in \mathbb{I}^{ch} \\
& s_f[k+1] = s_f[k] + t_{so} K_{rs}\,(T_s - T_{st}[k]) \quad k \in \mathbb{I}^{ch} \\
& \dot{Q}_s = U A_a (T_a - T_w) \\
& s_f[k+1] = s_f[k] - t_{so} K_s \dot{Q}_s \quad k \in \mathbb{I}^{dis} \\
& 0 \leq s_f \leq 100 \\
& 0 \leq \omega_c \leq \omega_{max} \\
& S_I \geq L \\
& s_f[N_o+1] \leq S_T
\end{aligned} \tag{10.29}$$

where N_o is the prediction horizon, t_{so} is the sampling time, $\Delta\omega_c$ is the rate of change of the compressor speed which is penalized in the cost function by the weighting factor W_o, ω_{max} is the maximum speed of the compressor, and S_I and L are vectors including s_i and l_i as their elements, respectively. The output of the optimization problem (10.31) is the next time instant during the driving profile where charging would be initiated, *i.e.,* $s_1^* = s_f^*[t_1]$ where s_f^* is the argument resulting from solving the above problem. Note that t_1 is updated at each sampling instant where optimization problem should be solved again.

Model Predictive Control

The design of a model predictive control strategy for the inner loop in Fig. 10.3 is straightforward if the reduced order simplified linear models are utilized. For example, the objective of maximizing the efficiency factor η_v clearly falls within the scope of a well-designed MPC. However a challenge arises due to the potential length of the prediction horizon. The second objective is to regulate the TES charge to the solid fraction set-point s_i at time t_i as given by the outer loop controller. This means that the prediction horizon at time t should be chosen long enough to include t_i. The longer the prediction horizon, the larger the computational burden which could tax the type of embedded processors that would run on a transport refrigeration system.

To circumvent the potential computational challenge we invoke the assumption that the TES in this study is well insulated. Therefore, the thermal leakage from the TES to the environment is assumed negligible over the duration of interest. This assumption remains to be validated but it does proved some flexibility to develop the following MPC approach.

Prior to presenting the algorithm, we provide a simple illustration to explain it. Consider the nominal desired solid fraction trajectory provided in Fig. 10.10 where the goal is to transition from s_0^* at time t_0 to s_1^* at time t_1. At any time instant, an optimization problem is solved to maximize η_v. The following constraint on the rate of solidification is imposed to guarantee s_i regulation:

$$\Delta s_f \geq \delta s_{min} \tag{10.30}$$

where $\Delta s_f = s_f[k] - s_f[k-1]$, and $\delta s_{min} = (s_1 - s_f(t))/(t_1 - t)$. Satisfying the constraint in (10.30) means that the s_f trajectory would always lie above the dashed line shown in Fig. 10.10. This guarantees reaching the s_1^* level before time t_1.

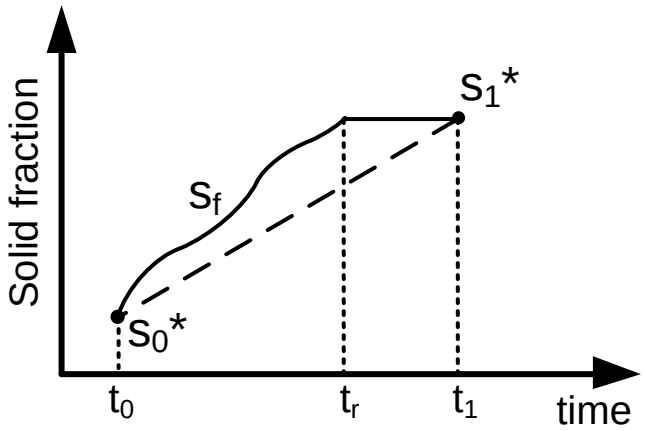

Figure 10.10: An example of a solid fraction trajectory.

If the value of the s_1^* level is reached at time t_r as shown in Fig. 10.10, then the TES should deactivate and the refrigeration system works in the normal mode to regulate the container temperature and MPC is stopped until the next charging period. To summarize, the following optimization problem is proposed for the MPC implementation:

$$\begin{aligned}
\max_{\omega_c,\, s_f} \quad & -\sum_{j=1}^{N_i} \eta_v + W_i \sum_{j=1}^{N_i} \|\Delta\omega_c\|_2^2 \\
\text{subject to} \quad & \\
& \begin{cases} X_{st}[k+1] = \mathbf{A}_{st} X_{st}[k] + \mathbf{B}_{st}\, \omega_c \\ T_{st}[k] = \mathbf{C}_{st} X_{st}[k] \end{cases} \\
& s_f[k+1] = s_f[k] + t_{si} K_{rs} \left(T_s - T_{st}[k]\right) \\
& 0 \leq s_f \leq 100 \\
& 0 \leq \omega_c \leq \omega_{max} \\
& \Delta s_f \geq \delta s_{min}
\end{aligned} \tag{10.31}$$

where N_i is the prediction horizon, t_{si} is the sampling time, and W_i is the weighting factor. The output of the above problem is the optimum compressor speed ω_c^* applied as a control signal.

6 Simulation Results

Validation Results of the gray-box model

Parameters of the gray-box model are estimated and the model is validated against a more complicated nonlinear MATLAB/Simulink model presented in [Fasl, 2013, Fasl et al., 2014]. Separate experiments are performed for the identification of independent parts of the model.

To identify the parameters associated with container dynamics (10.1)–(10.6), two tests are performed using a relay-based thermostatic control of the container temperature with compressor speed as an input. In either case, the collected data is divided into model identification and model validation data sets. In the first test, the container is cooled down by the VCC system without using the TES ($\dot{Q}_s = 0$). From Table 1, this would be considered the case when the system is in the charging mode. The result is shown in Fig. 10.11. In the second test, the storage is fully charged, and used to cool the container while the VCC system is turned off ($\dot{Q}_e = 0$). From Table 1, this is the case when the system is in the discharging mode. The result is shown in Fig. 10.12. The corresponding parameters are provided in Table 10.2.

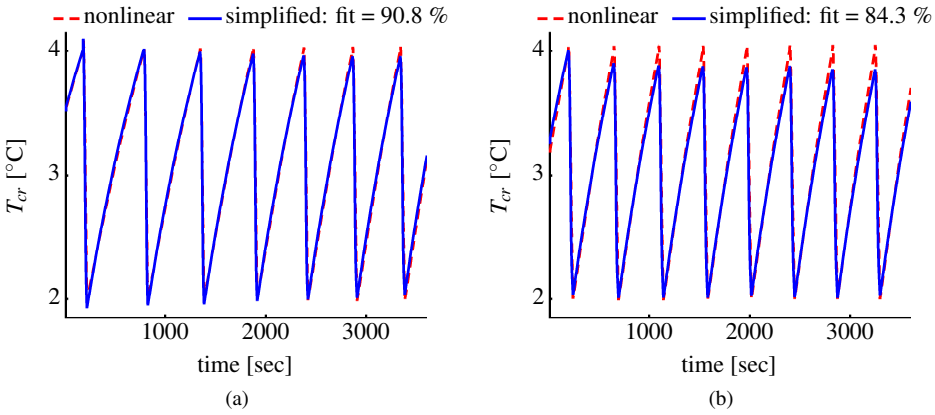

Figure 10.11: Estimation of the container temperature governed by only VCC ($\dot{Q}_s = 0$): (a) identification; (b) model validation.

The separate TES identification test is performed by charging the storage system using different magnitude steps in the compressor speed, which provides different saturated temperatures T_{st}. Subsequently we turn off the compressor and then discharge the TES to provide cooling $\dot{Q}_s$. The parameters are estimated as $K_s = 1 \times 10^{-5}$ and $\alpha_s = 0.27$. Estimation results are shown in Fig. 10.13. Even though the TES is modeled as a simple linear integrator, the estimation results are sufficiently satisfactory for incorporation into a model-based predictive controller.

The transfer function of the compressor model $G(s)$ is chosen to be of second order. The continuous time representation is shown here for consistency with the gray-box models of Section 4. For controller design, this gets converted to the discrete formulation

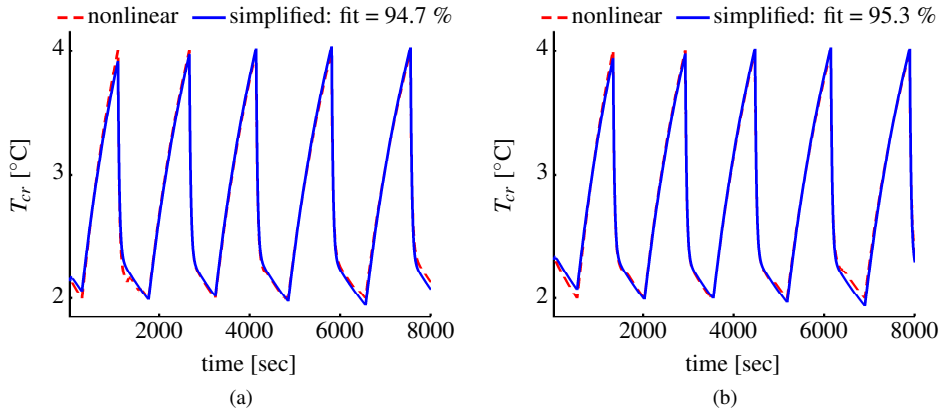

Figure 10.12: Estimation of the container temperature governed by only TES ($\dot{Q}_e = 0$): (a) identification; (b) model validation.

Table 10.2: Container parameters

MC_{cr} [kJ/K]	MC_w [kJ/K]	γ_{sh} [K]	a_0 [kW/(m^{2}K)]
1.07×10^5	9.5×10^5	20	0
a_1 [kW/(m^{2}K)]	UA_s [kW/(m^{2}K)]	UA_w [kW/(m^{2}K)]	UA_a [kW/(m^{2}K)]
628	1001	732	32

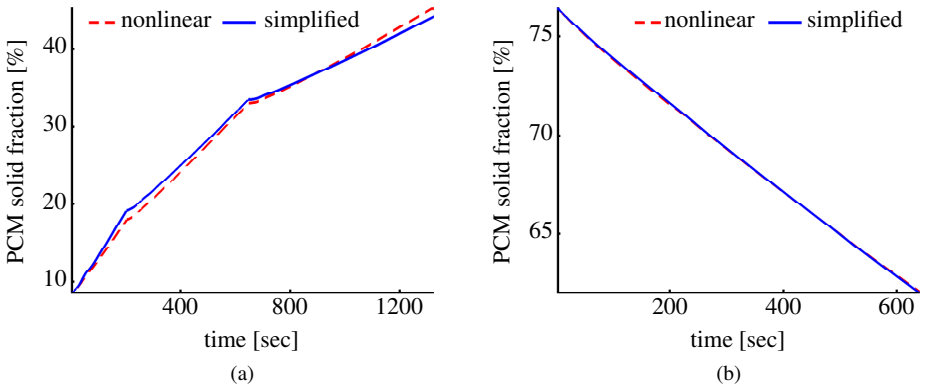

Figure 10.13: Estimation of the TES solid fraction when: (a) charging; (b) discharging.

illustrated in (10.22).

$$G(S) = \frac{-0.92 \times 10^{-5}(s - 1.6)}{S^2 + S + 0.006}. \tag{10.32}$$

Fig. 10.14 shows the results of the compressor model in predicting the saturation temperature.

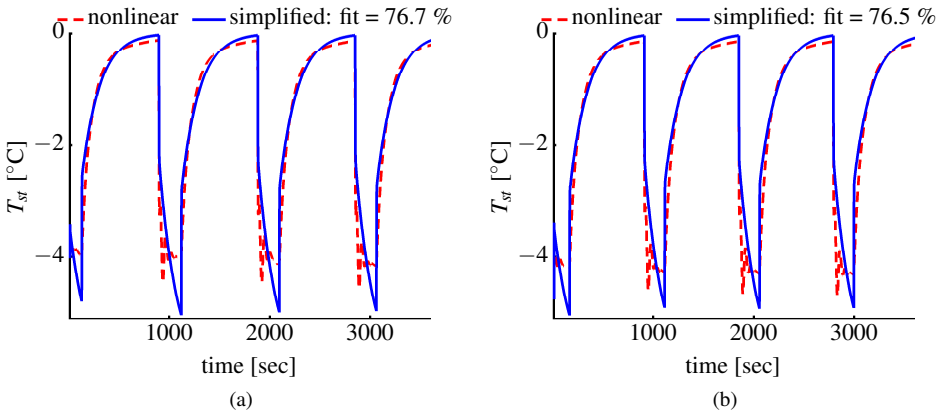

Figure 10.14: Estimation of the evaporation temperature using compressor model: (a) identification; (b) model validation.

The parameters c_i for volumetric efficiency in (10.25) are estimated using the lab experimentation data obtained by Rasmussen and Alleyne where similar results are reported in [Rasmussen and Alleyne, 2006]. They are provided in Table 10.3 and the estimation results are shown in Fig. 10.15.

Table 10.3: Parameters for estimation of the volumetric efficiency.

c_1 [RPM^{-1}]	c_2 [RPM^{-2}]	c_3 [RPM^{-1}]	c_4 [–]	c_5 [–]
7.4×10^{-3}	-7.9×10^{-7}	-2×10^{-3}	61.45	-9.86

Simulated Controller Results

Three different simulation scenarios are performed in this section. The first simulation illustrates the importance of taking the current traffic mode (light vs. heavy) into account for performing the TES charging. The second simulation shows that further energy saving can be achieved by scheduling the charging demand according to the predicted load using the predicted traffic mode. Finally, the effectiveness of the proposed optimal control to maximize the compressor volumetric efficiency factor will be illustrated.

In order to simulate the hybrid VCC system, we have used a nonlinear modeling tool, the Thermosys Toolbox, [Rasmussen, 2002], for MATLAB/SIMULINK, which has been previously validated on a variety of thermal systems. The Thermosys blocks are

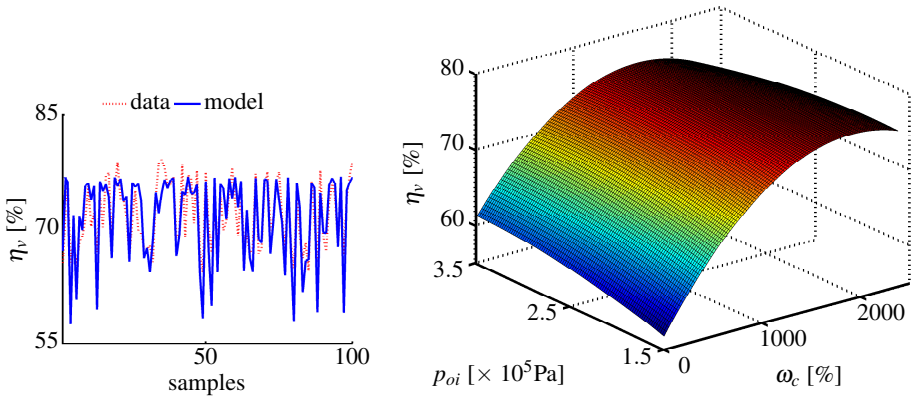

Figure 10.15: Volumetric efficiency: (a) parameter estimation; (b) objective function to be used in convex optimization.

configured as shown in Fig. 10.2 and details about the simulation parameters are provided in Appendix A. Fig. 10.16 illustrates the simulation environment where the full nonlinear model is included in the rightmost block to simulate the hybrid VCC system and the developed simplified model in this paper is included in the middle block and is employed by the control system. The chosen environmental parameters are provided in Table 10.4.

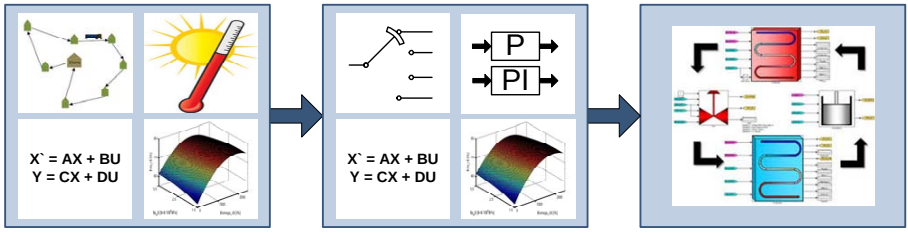

Figure 10.16: Simulation environment for testing the proposed approach. The three blocks correspond to that of Fig. 10.3 with the same placement order. A detailed nonlinear simulation model is employed to simulate the hybrid VCC/TES dynamical behavior.

Simulation I: Driving Profile

When the vehicle is running at a nominal speed (light traffic), the air flow across the condenser is several times higher than that of the low average speed (heavy traffic) case. This difference is included in the simulation model by scaling up the air flow of the condenser fan in light traffic mode by a factor of 10. The higher airflow across the condenser

Table 10.4: Environmental Parameters.

Parameter	Value
average ambient temperature [°C]	30
average wind speed [m/s]	8.8
solar radiation [W/m^2]	887

will decrease the condensation pressure and, consequently, reduce the pressure difference across the compressor thereby lessening the compressor work required to maintain the same suction pressure. The relevant equations describing the simulation model for the condenser unit is found in [Fasl, 2013, Section 2.3.1]. The coefficient of performance is defined as

$$\text{COP} = \frac{\dot{Q}_e}{P_w} \tag{10.33}$$

where P_w is the power consumption of the compressor. Hence, a higher coefficient of performance is achieved by the higher air flow. In the following it is shown that significant energy savings are obtained by charging the storage device when the vehicle is running with a nominal speed.

For this first simulation case, we do not yet introduce the optimal controller to demonstrate the benefits can accrue with any controller. A simple thermostatic control keeps the air temperature between the limits by turning on and off the refrigeration cycle while the TES is being charged when cooling is applied. The operation is performed for a full charge cycle. Fig. 10.17 shows the result when charging the TES during both the light and heavy traffic cases. Figure 12b indicates that the COP, when the compressor is on, is significantly higher for the case when the vehicle is moving at nominal speed thereby having a higher air flow across the condenser. The higher COP translates to a change in overall energy consumption to fully charge the TES. The energy consumption in the heavy traffic operation is 3,460 [kJ] that is reduced to 2,870 [kJ] in the light traffic case. The results show that for this particular system, and the environmental parameters chosen, a 17% energy saving is achieved by simply shifting the charging periods to the modes where vehicle is running with a nominal speed.

Simulation II: Charge Scheduling

It was shown in the previous example that shifting the charging operations to the periods when the vehicle is in light traffic can save considerable amount of energy. However, we cannot count on the traffic pattern being all of one type. The traffic pattern will vary throughout the duration of a delivery day for most transport refrigeration systems including when they are stopped completely to deliver products to customers. To accommodate the varying traffic patterns we use the idea of prediction. As stated before, with modern technology it is possible to obtain a fairly reliable estimate of traffic flow along a route and continuously update it in real time. This section shows that load prediction can be employed for improved charge management using a simple switching logic.

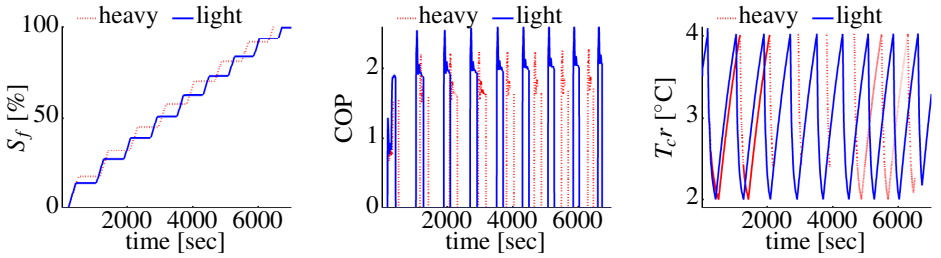

Figure 10.17: Comparison of thermal storage charging in heavy and light traffic conditions. (a) solid fraction: a full charge cycle is considered; (b) coefficient of performance. (c) container temperature: more cooling applied in case of higher COP.

The driving profile used in the following simulations is shown in Fig. 10.18. Intentionally, it is designed to include long periods of heavy traffic (e.g. a delivery stop) such that the overall cooling required for load compensation is larger than the capacity of the TES. Doing so, the capability and effectiveness of the optimal charging scheme for distribution of charge demand across the heavy traffic periods are tested.

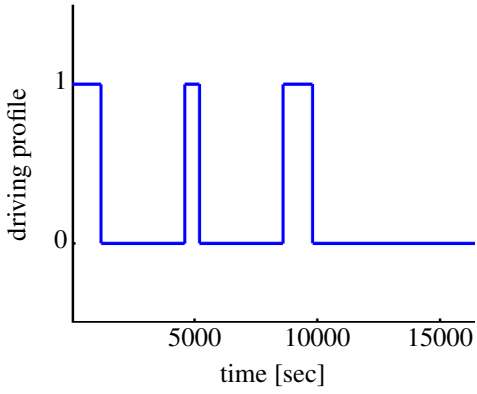

Figure 10.18: The driving profile considered for simulation experiments.

Fig. 10.19 shows the results for the case where maximum charging up to 100% is applied in the drive cycle. When the solid fraction becomes 100% (fully charged), the control switches to the normal mode until the heavy traffic period when it switches to discharging mode. At the end of the delivery mission, the remaining state of the charge for the TES is 51.5%. The total energy consumption of the compressor in this case is 2,828 [kJ].

As a simple option for inclusion of load prediction in the above logic-based control, the charging demand can be given by (10.27) at the end of each drive cycle t_i in Fig. 10.9. The load prediction takes this charge demand and adds 5% more charge demand as a

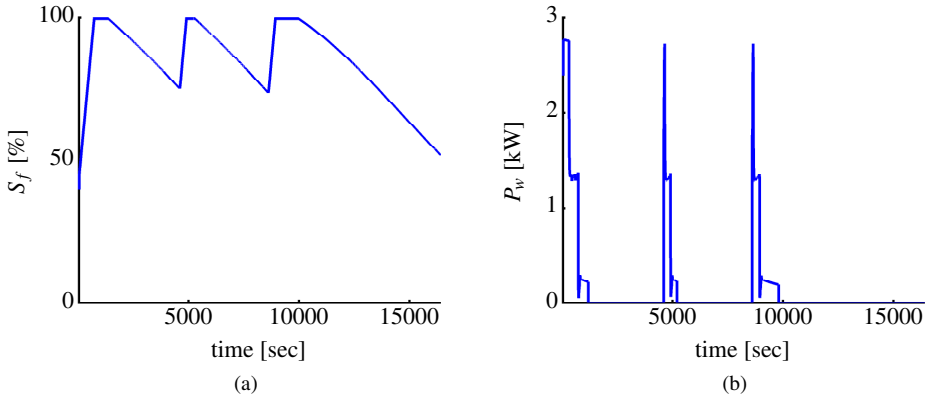

Figure 10.19: Maximum charging control scheme: (a) PCM solid fraction (state of charge); (b) compressor power consumption.

robustness factor to compensate for uncertainty in the load prediction. This charging demand is updated every 100 seconds and applied as a reference to the switching logic controller deciding whether to change from charging to normal mode. The control logic is defined such that if the current solid fraction is greater than or equal to the set-point the control would switch to the normal operation and the TES would not be activated. In order to avoid any frequent and unnecessary switching, a hysteresis function is used in the switching logic as shown in Fig. 10.20.

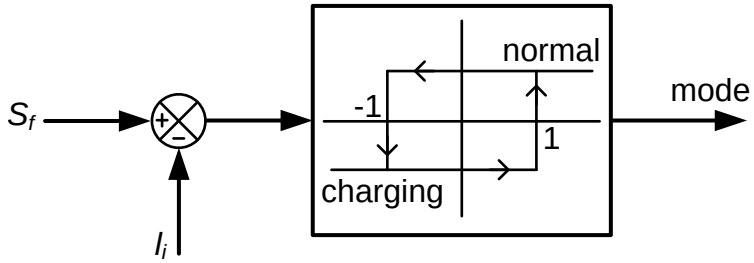

Figure 10.20: Hysteresis bound for switching decision from charging to normal mode.

Fig. 10.21 shows the simulation results after applying the simple charge scheduling. The state of the charge at the end of the mission is 5.5%, which is only slightly higher than the 5% safety factor. This shows the model effectiveness in load prediction for the given system. The total energy consumption of the compressor is 2,280 [kJ] which is significantly lower than the previous case which employed much higher charging control effort due to a lack of preview.

The simulation results of Fig. 10.21 are all based on a specific design taken from [Fasl et al., 2014]. If the last heavy traffic interval in the driving profile of Fig. 10.18 is the longest interval of that type which the vehicle can be expected to see, then the peak solid

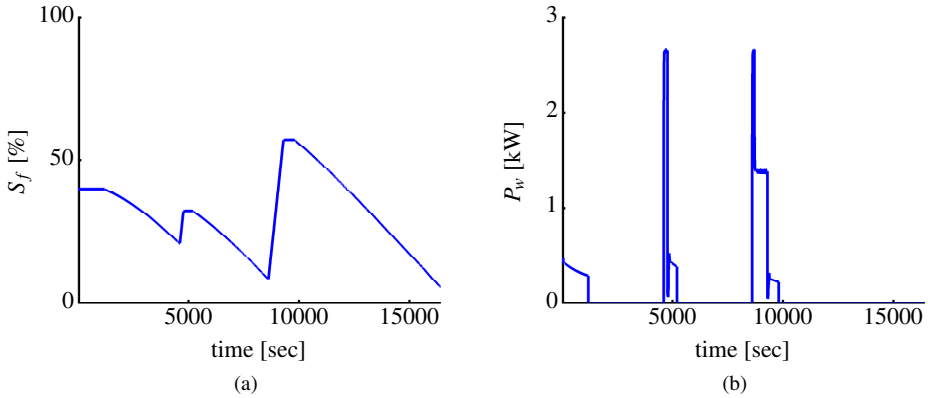

Figure 10.21: Simple charge scheduling and logic based control: (a) PCM solid fraction (state of charge); (b) compressor power consumption.

fraction in Fig. 10.21a shows that only 60% of the total capacity of the TES is actually required for compensating the associated load demand. Therefore, using historical data of delivery missions and the load prediction the results presented here can be used effectively in sizing studies to determine cost effective dimensioning of TES units for parallel hybrid transport refrigeration systems. The results state that the TES could be reduced in size by 40% with commensurate reductions in weight, size and vehicle fuel efficiency. The results would clearly vary depending on the operating conditions but the user would have a tool with which to evaluate her/his individual options. Reducing the TES size may also lead to improve the charging and discharging performance where numerical analysis and detailed investigation can be found in [Bellan et al., 2014].

Simulation III: Optimal Charge Scheduling and MPC

Operating the compressor at its maximum speed whilst charging the TES is far from the optimum approach as illustrated by the efficiency surface in Fig. 10.15b. Moreover, maximum compressor speed may also apply more strain on the compressor causing wear and tear of the device. Before simulating the optimal control scheme, a simple simulation is performed for the case where the system is running in the normal mode as presented in Table 10.1. This is the baseline operation when only the VCC system is in the loop. The compressor power consumption and the container temperature are shown in Fig. 10.22. The corresponding energy consumption of the compressor is 3,132 [kJ] which is higher than of any other cases where the TES is utilized in the hybrid VCC/TES system. It emphasizes the improvement of energy consumption by hybridization.

In the following, the proposed optimal charge scheduling of simulation 2 as well as the model predictive control of the compressor are applied to the nonlinear simulation model used in the previous results. Control tuning parameters are provided in Table 10.5. The maximum compressor speed is limited to ω_{max} = 2400 [rpm] and the terminal constraint S_T is chosen to be the same as the robustness factor of 5% in the previous simulation.

The TES solid fraction resulting from the optimal control is shown in Fig. 10.23a.

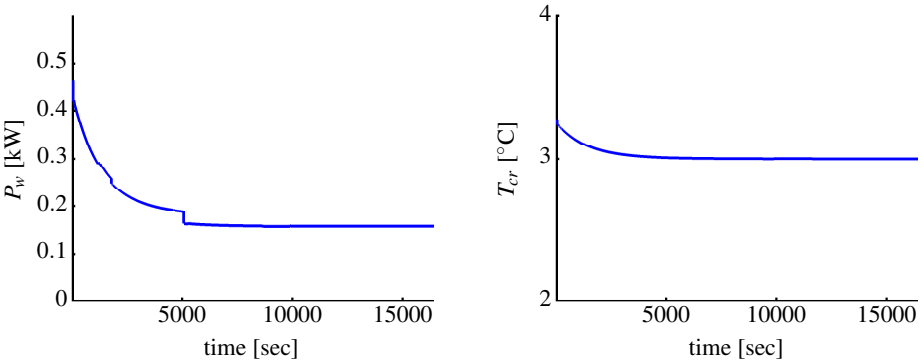

Figure 10.22: Baseline operation when only VCC system is in the loop with the normal mode of operation: (a) power consumption of the compressor; (b) container temperature.

Table 10.5: Control tuning parameters.

t_{so} [s]	N_o	W_o	S_T	t_{si} [s]	N_i	W_i
100	72	2×10^{-4}	5	10	30	1×10^{-4}

As can be seen, the whole charging demand is shifted to the first and third charging modes and no charging takes place during the second cycle. Examining Fig. 10.23b, the compressor speed during the charging mode is approximately 1,200 rpm which is approximately the optimal efficiency point as given in Fig. 10.15b. Therefore, the proposed optimal control scheme ensures that the compressor will charge TES unit with maximum efficiency while guaranteeing the cooling requirements will be met during the heavy traffic period. To compare the results of simulation cases 2 and 3, the following performance index is defined.

An integrated coefficient of performance IC is defined as the ratio of the total cooling energy over the total electrical power consumption for the entire drive cycle

$$IC = \frac{Q_{rs} + Q_e}{E_f + E_c} \tag{10.34}$$

where Q_{rs} is calculated by integration of (10.16) given the remaining TES charge which is 8.4% in simulation 3. Q_e is calculated by integration of the cooling capacity shown in Fig. 10.25a, and E_f and E_c are the energy consumption of the evaporator fans and the compressor. The corresponding power consumptions of the two latter components are illustrated in Fig. 10.24. The results of integrated COP calculations are

$$IC_n = \frac{550+4179}{993+2280} = 1.44, \quad IC_{opt} = \frac{840+4065}{713+2070} = 1.76 \tag{10.35}$$

where IC_n is the performance resulting from the simple logic based control and load prediction, and IC_{opt} is the performance in the case of the proposed optimal control. The re-

sults show that a 22% performance improvement is achieved by the optimal control over the logic-based hybrid VCC/TES system operation, even accounting for load preview. Fig. 10.25b shows that the proposed control system can regulate the container temperature around the set-point of 3 [°C] in spite of switching between the different modes of operation. Therefore, efficiency is improved without sacrificing temperature regulation performance.

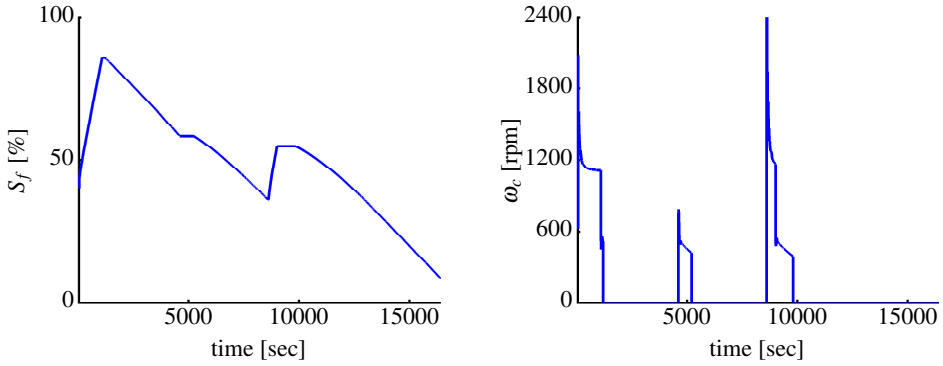

Figure 10.23: Optimal charge scheduling and model predictive control: (a) PCM solid fraction (state of charge); (b) compressor speed.

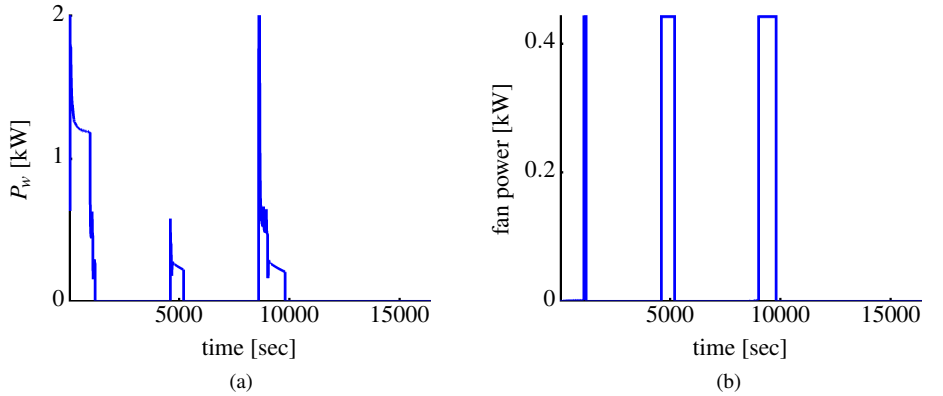

Figure 10.24: Optimal charge scheduling and model predictive control: (a) compressor power consumption; (b) power consumption of the evaporator fans.

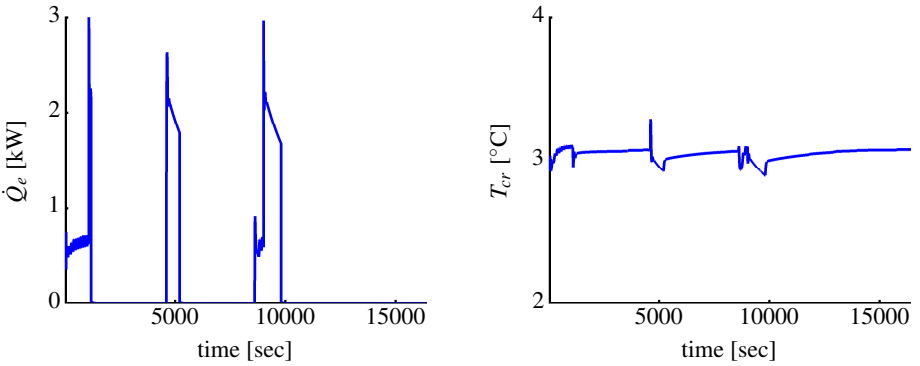

Figure 10.25: Optimal charge scheduling and model predictive control: (a) cooling capacity applied to the container; (b) container temperature.

7 Conclusion

In [Fasl, 2013, Fasl et al., 2014], the potential benefits of a hybrid thermal management system was introduced and shown to outperform a standalone VCS System. The management in the previous work was a simple logic-based approach. In this work, we investigate the optimal utilization of thermal energy storage units for transport refrigeration. A particular parallel-hybrid vapor compression system was considered where the TES unit can preserve the container temperature when discharging. A simplified model was introduced for the purpose of controller design and implementation and a more detailed nonlinear simulation model was employed for simplified model validation and controller simulations.

Initially, results showed that active TES charging and discharging corresponding to the traffic status was beneficial. For TES charging, a 17% energy saving can be achieved by performing the energy storage activity during light traffic vs heavy traffic. It was also shown that the use of load predictions could result in a more efficient overall utilization of TES operations with possible system design sizing implications.

Then, using the 17% advantage, a comparative study was performed between a simple logic-based controller and a proposed dual-stage controller containing an MPC to see if the traffic-relevant benefits could apply to an overall drive cycle management approach. A comparative study was performed between a simple logic-based controller and a proposed dual-stage controller containing an MPC using prediction to capture the traffic pattern. For ease of comparison between the two approaches, an integrated coefficient of performance, which applies to the whole drive cycle, was introduced. The results indicate that a 22% performance improvement can achieved by the proposed cascade optimal control approach over the type of logic based switching approach presented in [Fasl, 2013, Fasl et al., 2014].

To the knowledge of the authors, this work reports some of the earliest results on optimal hybridization and management of transport refrigeration systems. The reader should note that the numbers given here will obviously change depending on the particular op-

erating conditions and they should be interpreted as such. Additionally, the approach could be extended to include other types of modes (e.g boost) or operating characteristics (constraints of fixed speed compressors). However, from this investigation, the potential should be clear. There is significant value to be explored in (i) the hybridization of transport refrigeration systems, (ii) model-based optimization of these systems, and (iii) the use of preview information that is currently available in most vehicle systems.

A Simulation Parameters

In the following, informative details of the complex nonlinear simulation model represented in Fig. 10.16 are provided. More details such as dynamical equations, modeling assumptions, explanation of the physical structure and parameter descriptions are found in [Fasl, 2013].

Heat Exchanger Parameters

Heat exchangers are modeled using the moving boundary lumped parameter approach with mode switching capabilities [Fasl, 2013]. There are four possible modes of operation depending on the number and composition of fluid phase zones present: (i) three-zone (vapor, two-phase and liquid); (ii) two-zone (vapor and two-phase); (iii) one-zone (two-phase); and (iv) one-zone (vapor). The parameters for the heat exchangers (*i.e.,* condenser and evaporator) are provided by Table 10.6.

Table 10.6: Heat exchangers parameters.

Parameter	Condenser	Evaporator
Refrigerant	R404A	R404A
Hydraulic diameter [m]	7.3×10^{-3}	8.8×10^{-3}
Refrigerant length of one pass [m]	14.1	6
Number of parallel refrigerant passes	6	11
Air side cross sectional area of one pass [m^2]	0.070	0.028
Air side surface area of one pass [m^2]	5.47	0.80
Refrigerant side cross sectional area [m^2]	4.22×10^{-5}	6.03×10^{-5}
Refrigerant side surface area of one pass [m^2]	0.32	0.08
Wall mass of one pass [kg]	2.78	1.19
Wall specific heat [kJ/(kg.K)]	0.71	0.59

TES Parameters

The thermal energy storage unit is modeled as a coaxial tube arrangement using a fixed grid enthalpy approach [Fasl, 2013]. Table 10.7 gives the associated parameters.

Container Parameters and Environmental Conditions

The container model calculates the temperature dynamics associated with refrigerating an air filled mobile space interacting with ambient conditions [Fasl, 2013]. The container

Table 10.7: Thermal energy storage parameters.

Parameter	Thermal energy storage
Phase change material	Water
Number of nodes	10
Fin thickness [m]	1×10^{-3}
Number of fins	8
Tube length per parallel pass [m]	6
Number of parallel refrigerant passes	11
Inner tube diameter [m]	8×10^{-3}
Outer tube diameter [m]	0.032
Transverse pitch ratio	1.5
Longitudinal pitch ratio	1.25
Number of tube passes per plane	10
Wall material	Aluminum
Wall thickness [m]	1.58×10^{-3}

parameters and ambient conditions are given in Table 10.8.

Table 10.8: Container parameters and ambient condition.

Parameter	Value
Length [m]	7
Height [m]	2.5
Width [m]	2.4
UA value [W/K]	30
Wall capacitance [J/K]	1×10^{6}
Solar view factor [0-1]	0.25
Surface emissivity factor [0-1]	0.8

Other Component Parameters

The receiver and accumulator are modeled as a constant volume tank with assumption of lumped uniform thermodynamic properties throughout the entire volume of the tank [Fasl, 2013]. Here the receiver volume is 1.85×10^{-3} [m^3], and the accumulator volume is 1×10^{-3} [m^3].

The compressor is modeled as a fixed displacement unit with a variable speed allowing modulation of the mass flow rate by controlling the rotational speed. The dynamics associated with compressor shell heat capacitance are simulated by applying a first order low pass filter to the static outlet enthalpy [Fasl, 2013]. Here, the filter time constant is $\tau = 10$ [s].

The electronic expansion valve model calculates the mass flow using a static relationship depending on the stroke fraction value which is regulated by applying an electronic control signal. The valve coefficient described in [Fasl, 2013] is chosen here to be $C_v = 1 \times 10^{-4}$.

Acknowledgements

Work presented in this paper was supported by the Southern Denmark Growth Forum and the European Regional Development Fund under the project "Smart & Cool".

References

[Bellan et al., 2014] Bellan, S., Gonzalez-Aguilar, J., Romero, M., Rahman, M. M., Goswami, D. Y., Estefanakos, E. K., and Couling, D. (2014). Numerical analysis of charging and discharging performance of a thermal energy storage system with encapsulated phase change material. *Applied Thermal Engineering*, 71:481–500.

[Candanedo et al., 2013] Candanedo, J. A., Dehkordi, V. R., and Stylianou, M. (2013). Model-based predictive control of an ice storage device in a building cooling system. *Applied Energy*, 111:1032–1045.

[Cole et al., 2012] Cole, W. J., Edgar, T. F., and Novoselac, A. (2012). Use of model predictive control to enhance the flexibility of thermal energy storage cooling systems. In *Proceedings of the American Control Conference*, Montréal, Canada.

[Dincer, 2002] Dincer, I. (2002). On thermal energy storage systems and applications in buildings. *Energy and Buildings*, 34:377–388.

[Dincer and Rosen, 2010] Dincer, I. and Rosen, M. A. (2010). *Thermal Energy Storage Systems and Applications*. John Wiley & Sons, New York.

[Fasl, 2013] Fasl, J. (2013). Modeling and control of hybrid vapor compression cycles. Master's thesis, University of Illinois at Urbana-Champaign, Department of Mechanical Engineering.

[Fasl et al., 2014] Fasl, J. M., Briscoe, C. R., Mohs, W. F., and Alleyne, A. G. (2014). Dynamic model of a refrigeration system with active thermal energy storage. *ASHRAE Transactions*, 120(1):1–8.

[Javani et al., 2014] Javani, N., Dincer, I., Naterer, G. F., and Yilbas, B. S. (2014). Exergy analysis and optimization of a thermal management system with phase change material for hybrid electric vehicles. *Applied Thermal Engineering*, 64:471–482.

[Kim, 2013] Kim, S. H. (2013). Building demand-side control using thermal energy storage under uncertainty: An adaptive multiple model-based predictive control (mmpc) approach. *Building and Environment*, 67:111–128.

[Ma et al., 2012a] Ma, Y., Borrelli, F., Hencey, B., Coffey, B., Bengea, S., and Haves, P. (2012a). Model predictive control for the operation of building cooling systems. *IEEE Transactions on Control Systems Technology*, 20(3):796–803.

[Ma et al., 2012b] Ma, Y., Kelman, A., Daly, A., and Borrelli, F. (2012b). Predictive control for energy efficient buildings with thermal storage. *IEEE Control Systems Magazine*, 32(1):44–64.

[Rasmussen, 2002] Rasmussen, B. (2002). Control oriented modeling of transcritical vapor compression systems. Master's thesis, Department of Mechanical Engineering, University of Illinois at Urbana-Champaign, IL, USA.

[Rasmussen and Alleyne, 2006] Rasmussen, B. P. and Alleyne, A. G. (2006). Dynamic modeling and advanced control of air conditioning and refrigeration systems. Technical report, ACRC, University of Illinois at Urbana-Champaign.

[Shafiei et al., 2013] Shafiei, S. E., Rasmussen, H., and Stoustrup, J. (2013). Modeling supermarket refrigeration systems for demand-side management. *Energies*, 6(2):900–920.

[Shafiei et al., 2014] Shafiei, S. E., Stoustrup, J., and Rasmussen, H. (2014). Model predictive control for flexible power consumption of large-scale refrigeration systems. In *Proceedings of the American Control Conference*, pages 412–417, Portland, OR, USA.

[Tassou et al., 2009] Tassou, S. A., De-Lille, G., and Ge, Y. T. (2009). Food transport refrigeration – approaches to reduce energy consumption and environmental impacts of road transport. *Applied Thermal Engineering*, 29:1467–1477.

[Walkowicz et al., 2014] Walkowicz, K., Kelly, K., Duran, A., and Burton, E. (2014). Fleet DNA project data. Technical report, National Renewable Energy Laboratory.

[Walsh et al., 2013] Walsh, B. P., Murray, S. N., and O'Sullivan, D. T. J. (2013). Free-cooling thermal energy storage using phase change materials in an evaporative cooling system. *Applied Thermal Engineering*, 59:618–626.

[Wang et al., 2007] Wang, F., Maidment, G., Missenden, J., and Tozer, R. (2007). The novel use of phase change materials in refrigeration plant. part 1: Experimental investigation. *Applied Thermal Engineering*, 27:2893–2901.